Formulation and Evaluation of Advanced Buccal Mucoadhesive Systems for Cannabinoid Delivery: In-Situ Gels and 3D-Printed Films

Anushree Nagaraj

A thesis submitted to Auckland University of Technology in fulfilment of the requirement for the degree of Doctor of Philosophy (PhD).

School of Science

Biomedical Sciences

Faculty of Health and Environmental Sciences

Auckland University of Technology

Abstract

The resurgence of interest in plant-derived therapeutics has positioned cannabinoids, particularly Δ^9-tetrahydrocannabinol (THC) and cannabidiol (CBD), as promising pharmacological agents with demonstrated analgesic, anti-inflammatory, antiemetic, and neuroprotective effects. However, their clinical translation remains hindered by low aqueous solubility, extensive hepatic first-pass metabolism, and poor oral bioavailability (<10–20%). Conventional oral and oromucosal dosage forms, including oils, capsules, and sprays such as Sativex, often yield variable absorption and unpredictable pharmacokinetics, leading to inconsistent therapeutic responses and unwanted psychoactive effects. These limitations underscore the need for alternative delivery systems capable of bypassing hepatic metabolism, enhancing cannabinoid absorption, and ensuring controlled drug release. This thesis aimed to develop and optimize buccal cannabinoid delivery systems, including thermoresponsive mucoadhesive in-situ gels, ion-activated in-situ gels, and extrusion-based 3D bioprinted mucoadhesive films to address the abovementioned shortcomings. Buccal delivery offers a non-invasive and patient-friendly route that enables direct absorption into the systemic circulation, allowing for rapid onset of action and improved bioavailability.

Two distinct in-situ gelling mechanisms were employed in the development of cannabinoid formulations, with the gelling polymers combined with either hydroxypropyl methylcellulose (HPMC) or Carbopol 934 to produce mucoadhesive in-situ gels. The first approach involved the formulation of thermoresponsive in-situ gels using Poloxamer 407, optimized through factorial design to achieve ideal sol–gel transition temperatures, appropriate viscosity, and mucoadhesive strength. These formulations exhibited reversible sol–gel behaviour, transitioning from a free-flowing liquid at room temperature to a cohesive semi-solid gel at 37°C. The second formulation platform focused on ion-activated in-situ gels, utilizing gellan gum, κ-carrageenan, and a novel κ/ι-carrageenan blend that gelled upon exposure to salivary cations. The κ/ι-carrageenan system formed a synergistic polymeric network balancing rigidity and flexibility, resulting in enhanced gel strength, elasticity, and mucoadhesion compared to single-polymer systems. Both thermoresponsive and ion-activated gels demonstrated prolonged mucosal residence, with Carbopol-based formulations exhibiting superior mechanical strength, mucoadhesion, and physicochemical properties compared to HPMC-based gels. The systems displayed biphasic release profiles, characterised by an initial lag phase (~15–30 minutes) followed by sustained cannabinoid release over 4 hours.

To further improve stability and storage properties, ion-induced in-situ gels containing Carbopol were developed into freeze-dried formulations that could be readily rehydrated before administration These lyophilized systems retained their gelling capacity and preserved over 94% of cannabinoid content after six months, offering improved storage stability and eliminating the need for strict cold-chain conditions.

The third approach involved using 3D bioprinting to fabricate extrusion-based mucoadhesive films composed of HPMC and Carbopol matrices, enabling precise control over geometry, thickness, and cannabinoid loading. HPMC-based films demonstrated excellent mechanical integrity, uniform drug distribution, and sustained cannabinoid release over 2 hours. This work demonstrated the feasibility of employing bioprinting techniques for producing individualized cannabinoid dosage forms with enhanced pharmacokinetic predictability.

This work also introduced a novel formulation strategy integrating multiple terpenes as permeation enhancers with hydroxypropyl-β-cyclodextrin inclusion complexes of cannabinoids within the developed buccal systems, providing a complementary mechanism to enhance both solubility and buccal absorption.

This thesis provided a comprehensive foundation for buccal delivery of cannabinoids by integrating formulation optimization, physicochemical and rheological characterization, ex vivo permeation, and stability evaluation. The findings underscore the potential of mucoadhesive buccal systems to overcome the pharmacokinetic limitations of oral cannabinoids, reduce required doses, enhance patient compliance, and support the clinical translation of cannabinoid therapies for conditions such as chemotherapy-induced nausea, appetite stimulation, chronic pain, and multiple sclerosis.

Contents

List of figures

List of Tables

Attestation of Authorship

I hereby declare that this submission is my own work and that, to the best of my knowledge and belief, it contains no material previously published or written by another person (except where explicitly defined in the acknowledgements), nor used artificial intelligence tools or generative artificial intelligence tools (unless it is clearly stated, and referenced, along with the purpose of use), nor material which to a substantial extent has been submitted for the award of any other degree or diploma of a university or other institution of higher learning.

Signed: 

Date: 31/10/2025

Acknowledgments

I would first like to express my deepest gratitude to my supervisor, Dr. Ali Seyfoddin, for his exceptional mentorship, support, and encouragement throughout my PhD journey. His remarkable expertise, dedication to research excellence, and inspiring enthusiasm for scientific discovery have been the foundation of my growth as a researcher. Dr. Ali's patience, kindness, and constructive feedback guided me through every stage of this work, from the earliest concepts to the final stages of writing. His insightful perspective and consistent encouragement motivated me to approach challenges with curiosity and resilience. Beyond his academic guidance, his compassion, and optimism have been truly inspiring. Working under his supervision has been a privilege that has profoundly shaped both my scientific and personal development. I would also like to sincerely thank my secondary supervisor, Dr. Ghada Zidan, for her motivation, valuable insights, and continuous encouragement.

I would also like to express my sincere appreciation to Auckland University of Technology (AUT) for providing the facilities, resources, and a supportive environment to carry out this research. My heartfelt thanks go to Callaghan Innovation and Helius Therapeutics for their financial and technical support through the scholarship program. Their commitment to advancing research in cannabinoid science has been instrumental in making this project possible.

My warm thanks go to Adrian Owens and Tony Chen for their invaluable technical assistance and unwavering willingness to help. Their expertise, patience, and problem-solving skills were essential throughout the experimental work. Whether it was troubleshooting instruments, offering practical insights, or ensuring smooth lab operations, their support made a tremendous difference.

I am also deeply grateful to my friends and colleagues in the Drug Delivery Research Group (DDRG) for their constant encouragement, collaboration, and friendship. The shared discussions, teamwork, and laughter made the lab a place of learning and belonging, enriching both the scientific and personal dimensions of this journey.

To my parents, I owe my deepest gratitude. My mother, Poorna, whose strength, love, and selflessness have been my greatest source of inspiration, has taught me perseverance and compassion in all aspects of life. My father, Nagaraj, whose unwavering faith in me and constant encouragement have guided me through every challenge, has been my moral compass and source of wisdom. To my brother, Achyuta, thank you for keeping me grounded and motivated throughout. This achievement stands as a testament to the sacrifices, love, and guidance of my family.

To my husband, Ajay Srinivas, I express my appreciation for your patience and understanding. Your encouragement during moments of doubt, your willingness to shoulder responsibilities, and your

constant reassurance have been my greatest strength. To my in-laws, I extend my heartfelt gratitude for their kindness and encouragement.

This thesis is dedicated to all of you for your love, faith, and endless support.

Chapter 1: General Introduction and Thesis Format

1.1. Introduction

1.1.1 History of medicinal Cannabis

Plant of Genus Cannabis belongs to the family Cannabaceae, and primarily comprises of three species: Sativa, indica, and ruderalis with varying phytochemical constituents. Cannabis is also known as marijuana and hemp, with marijuana containing higher levels of the psychoactive compound tetrahydrocannabinol (THC), while hemp has lower levels of it. Morphologically, cannabis is a dioecious flowering plant with separate male and female individuals, possessing a fibrous root system, erect branching stems, and palmately compound leaves with serrated edges. The flowers differ by sex: male plants produce pollen, whereas female plants develop pistillate flowers rich in glandular trichomes, which synthesize cannabinoids and terpenes that underlie the plant's psychoactive and therapeutic effects (Figure 1.1). Hemp boasts a long history of varied applications, both in the past and today. It has been utilized for textiles and clothing, industrial products, and in the manufacturing industry (Baron, 2015). Cannabis, widely known for its psychoactive effects, is among the oldest drugs, with medicinal use dating back to 4000 BC in China (Aldrich, 1997). The plant was advocated as a surgical analgesic when in combination with alcohol as well as to treat a variety of ailments such as rheumatic pains, bouts, beriberi, malaria, and sleep disorders (Aldrich, 1997). Successive records show its medicinal use in India, Middle East, Central Asia, South America, Greece, Rome, and South Africa (Aldrich, 1997). In the early 19th century, cannabis use expanded into Britain and European countries when an Irish physician, Dr. William Brooke O'Shaughnessy, studied the plant's medicinal properties when in India. His research revealed its potential benefits, including anti-convulsant, anti-emetic, anxiolytic, and relaxant effects (Ben Amar, 2006; Kalant, 2001; Robson, 2001).

By the late 19th and early 20th centuries, cannabis had become a widely available medicine in western countries' dispensaries and pharmacies. The early 20th century highlighted the therapeutic use of cannabis in three main categories: sedative/hypnotic, analgesic, and various other applications, including appetite stimulation, diarrhoea, dyspepsia, and digestion (Zuardi, 2006). However, the prohibition on Cannabis came in accordance with the 1971 Misuse of Drugs Act, and the plant was placed in the same group with heroin and cocaine as a Schedule 1 class drug. This was largely due to growing concern over its psychoactive effects, perceived potential for abuse, and lack of recognized medical value at the time. Additionally, issues regarding the plant's inconsistent potency, variable effects when taken orally, and poor storage stability were noted during this time. This resulted in the replacement of medicinal use of cannabis with pure opiates, and modern synthetic drugs developed (Mikuriya, 1969; Robson, 2001). The classification of cannabis as an illegal substance stemmed from a lack of scientific understanding of the plant. Unfortunately, this prohibition also hindered research into the evidence of its potential benefits, despite being used for treatment of various illness and disorders since ancient times (Baron, 2015).

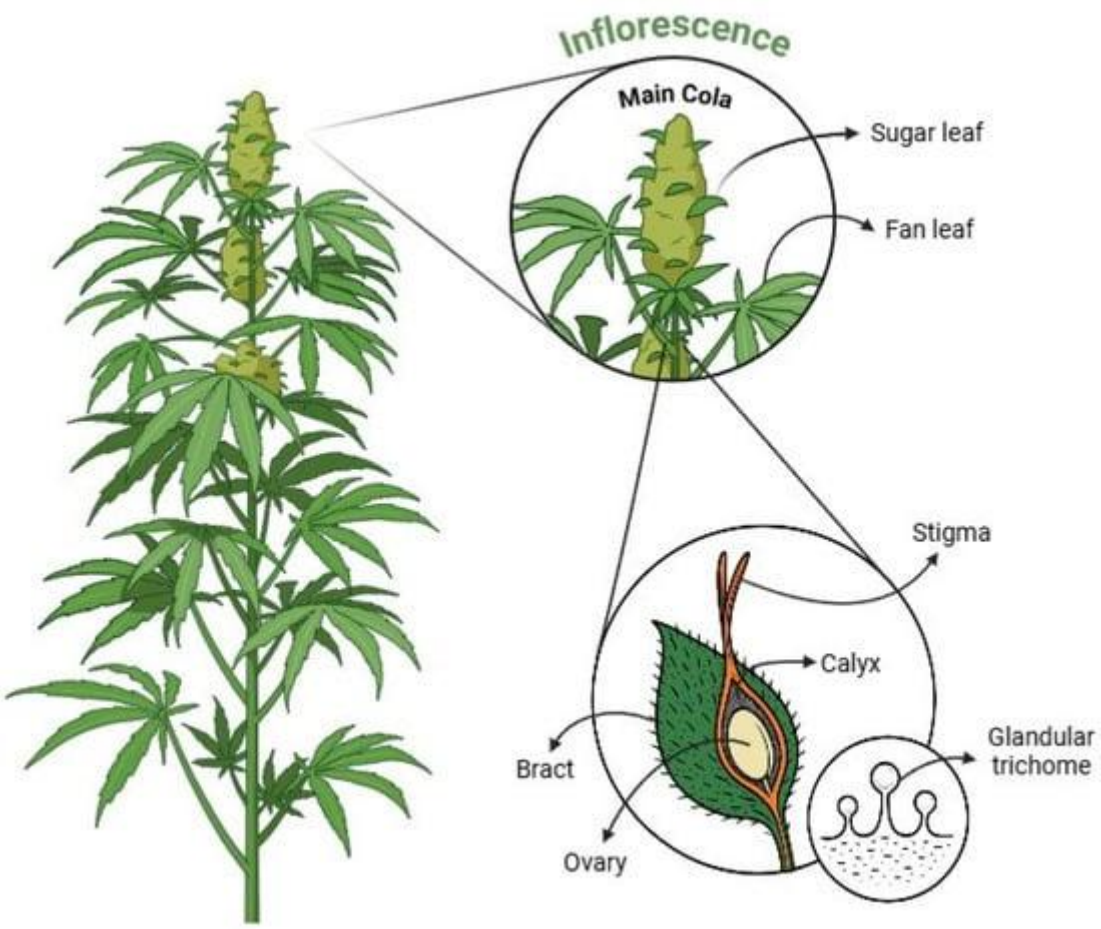

Figure 1.1 Morphology of the cannabis plant showing key structural features, including the main cola, sugar leaves, fan leaves, bracts, stigma, ovary, calyx, and trichomes (Adopted from (Alberti et al., 2025)).

Research on cannabis saw a resurgence in the early 1990s following the identification of cannabinoid receptors in the nervous system and the discovery of endocannabinoids, naturally occurring cannabinoids produced by the body (Zuardi, 2006). These discoveries were advanced by several research groups, including the pioneering work of Israeli chemist Raphael Mechoulam and colleagues, who identified the endogenous cannabinoid anandamide in 1992 (Mechoulam & Parker, 2013). Use of isolated compounds from the cannabis plant as therapeutics with scientifically proven clinical indices, along with their safety and efficacy, are gaining rapid attention worldwide (Baker et al., 2003; Zuardi, 2006). Due to the growing medicinal properties of the plant's phytochemicals, an increasing number of countries are approving the administration of regulated cannabis products for various conditions, including spasticity associated with multiple sclerosis (MS), rare epileptic disorders Lennox-Gastaud and Dravet syndromes, chronic pain, chemotherapy-induced emesis and nausea, and reviving appetite in patients affected by human immunodeficiency virus (HIV) (Stella et al., 2021).

However, with the recent ease of government restrictions worldwide, research on the therapeutic potential of cannabis is blooming. Nevertheless, significant challenges continue to exist despite the recognized benefits of cannabinoid therapies. In many countries, the plant remains illegal even for medicinal purposes, creating a substantial barrier to access for patients who could benefit from such treatments. In other countries where medical use is legal, the regulatory landscape can be highly restrictive, often imposing stringent regulations

that limit research and clinical trials involving cannabinoids and their therapeutic applications (Bifulco & Pisanti, 2015).

1.1.2 Phytochemical constituents of the cannabis plant

The cannabis plant is complex in terms of its chemical composition. It has over 600 chemical compounds, and they vary depending on the plant's genotype, soil and climatic conditions in which they are grown, and different cultivation techniques (Barrales-Cureño et al., 2020; Yadav et al., 2023). The cannabis phytochemicals are classified as either major or minor depending on the amount found in the plant.

Cannabinoids

Among the most prevalent, cannabinoids include Δ-9-tetrahydrocannabinolic acid (THCA) and cannabidiolic acid (CBDA). When subjected to heat, these acids transform into their active forms: Δ-9-tetrahydrocannabinol (THC) and cannabidiol (CBD). The Δ9- tetrahydrocannabinol (THC) and cannabidiol (CBD) account as widely investigated major phytochemicals that are formulated into various dosage forms to treat medical conditions (Andre et al., 2016; Sampson, 2021). The chemical structures of THC and CBD are represented in Figure 1.2 below.

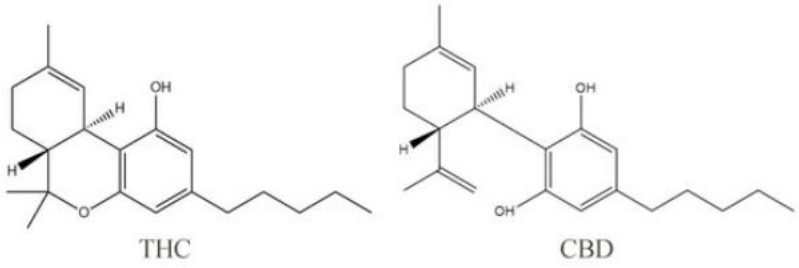

Figure 1.2 Chemical structures of THC and CBD (Adopted from (Ma et al., 2024)).

Cannabinoids are classified into two types based on the presence or absence of a carboxyl group as acids or neutral cannabinoids, respectively. Although present in much smaller amounts than THC and CBD, research into minor cannabinoids and other phytoconstituents has uncovered various medicinal properties that enhance the effects of the more thoroughly studied THC and CBD. Cannabinoids are synthesized on the trichomes, which are small dome-like structures prevalent on the bud and leaves of the cannabis plant. Cannabis used in commercial products is generally grouped according to the ratios of THC to CBD. The main classifications are "THC-dominant," which has minimal CBD, "CBD-dominant," characterised by low THC and high CBD levels, and "balanced THC/CBD," where THC and CBD are present in similar amounts (El Oihabi et al., 2024; ElSohly & Slade, 2005; Smith et al., 2022).

In addition to minor cannabinoids, the plant contains over 140 phytochemicals present in smaller quantities, such as flavonoids, phenolic compounds, terpenes, and alkaloids. These compounds have also been recognized for their individual therapeutic properties (Sampson, 2021).

Terpenes

Terpenes are hydrocarbons that contribute to the distinctive aroma of the cannabis plant and are composed of isoprene units. Terpenes are usually involved with protecting the plant from predators and attracting pollinators. They are categorized into several types, hemiterpenes, monoterpenes, sesquiterpenes, and diterpenes, depending on the number of isoprene units present. Currently, more than 50 distinct chemical phenotypes of terpenes have been identified in the cannabis plant, with each plant exhibiting variations in these compounds. Terpenes prominent across cannabis plant species include d-limonene, pinene, caryophyllene, camphene, and terpinol (Eric Fordjour et al., 2023; Lowe et al., 2021). Research has revealed a wide range of health benefits associated with terpenes, some of which enhance the effects of cannabinoids. While prevalent only in a few strains of the cannabis plant, terpenes like menthol are recognized in pharmaceuticals for their suitability for patients and are also noted for their health advantages (Kamatou et al., 2013).

Flavonoids

Flavonoids are polyphenolic compounds that occur in a diverse array of fruits, teas, chocolates, and vegetables, playing a key role in imparting both flavour and vibrant colour to these foods. In the cannabis plant, they have been isolated from leaves, seeds, and flowers. The cannabis plant contains over 20 identified flavonoids, which are categorized into six classes: anthocyanidins, flavonols, isoflavones, flavan-3-ols, flavanones, and flavones. These flavonoids can vary based on environmental conditions, as their main function is to protect the plant (Bautista et al., 2021; Lowe et al., 2021).

Alkaloids

Alkaloids are heterocyclic compounds that are usually found in plants, but microorganisms and other animals also produce them. Common examples of alkaloids include caffeine, nicotine, and morphine. Endogenous alkaloids of the plant include cannabisativine and anhydrocannabisativine. Extracted from stems, leaves, and roots of the plant, the cannabis alkaloids were used in traditional medicine to treat various ailments (Eric Fordjour et al., 2023; Radwan et al., 2021).

Research has demonstrated that both cannabinoid and non-cannabinoid phytochemicals possess diverse biological activities. Investigating the mechanisms by which these phytochemicals interact with the human body can elucidate their therapeutic effects, providing insights into potential clinical applications.

1.1.3 The endocannabinoid system

The therapeutic effects of the cannabinoid phytochemicals are brought about through the up/downregulation of the signalling mechanisms via cannabinoid receptors present in various regions of the body. The endocannabinoid system refers collectively to these endogenous receptors, ligands also referred to as the endocannabinoids, and the enzymes responsible for their synthesis in the human body (De Petrocellis & Di Marzo, 2009).

The cannabinoid receptors 1 and 2 (CB1 and CB2) were discovered in the latter half of the 20th century (Robson, 2001). These receptors belong to a family of transmembrane domain receptors called G-protein coupled receptors, which get activated upon binding of specific molecules and further signal the intercellular G-protein, which regulates several downstream pathways. The agonists of the receptors result in inhibiting the secondary messenger systems, c-AMP cyclic adenosine monophosphate messenger, triggering several mitogen-activated protein (MAP) kinases and resulting in cellular and physiological changes. These consequences can be essential drug targets affecting disease mechanisms (Howlett et al., 2002; Trzaskowski et al., 2012). The discovery of these receptors brought about a need for extensive research to further understand the biological activities governing the endocannabinoid system in the body. This further brought to light two endogenous ligands, anandamide and 2-arachidonoylglycerol (2-AG).

Anandamide, derived from the Sanskrit word “ananda”, which means bliss, joy, or happiness, acts as a partial agonist of both receptors with higher binding affinity to the CB1 receptor, whereas 2-AG is a complete agonist with lower binding affinities to both receptors (Rodríguez de Fonseca et al., 2005). The levels of these ligands can be controlled by prominent enzymes that deactivate endocannabinoids, with fatty acid amide hydrolase (FAAH) responsible for anandamide and monoacylglycerol lipase (MEG) for 2-AG (Vemuri & Makriyannis, 2015). Besides CB1 and CB2 receptors, the endogenous ligands also bind to transient receptor potential (TRP) ion complexes, peroxisome proliferator-activated (PPA) nuclear receptors, and were recently discovered as new cannabinoid G-protein receptors, GPR55 and GPR119 (Shahbazi et al., 2020).

CB1 receptors are usually expressed in large quantities in the central nervous system, and when activated, it mediates psychoactive, neurological, and pain suppressing functions in addition to maintaining the body’s homeostasis. Whereas CB2 receptors are involved closely with our immune system, especially with modulating anti-inflammatory effects suggesting significance in disorders such as rheumatoid arthritis and atherosclerosis (Lu & Mackie, 2016; Turcotte et al., 2016). The initial concept introduced by research regarding the expression of CB1 and CB2 receptors has evolved into a more nuanced understanding of their roles in regulating a diverse array of cellular and physiological functions. Figure 1.3 elaborates on the presence and roles of CB1 and CB2 receptors on different organs of the body (An et al., 2020).

THC is a partial agonist of the CB1 receptor, where it mediates most of its biological and psychoactive effects. CBD, however, allosterically brings about conformational changes to CB1 receptors, which causes negative modulation, balancing the “feeling high” effects of THC when administered together in similar quantities. Furthermore, CBD was found to interact with CB2, ion channels, serotonin and opioid receptors explaining wide pharmacological benefits of this molecule (Laprairie et al., 2015; Pertwee, 2008). Research is still growing to uncover several mechanisms and pathways associated with the endocannabinoid systems.

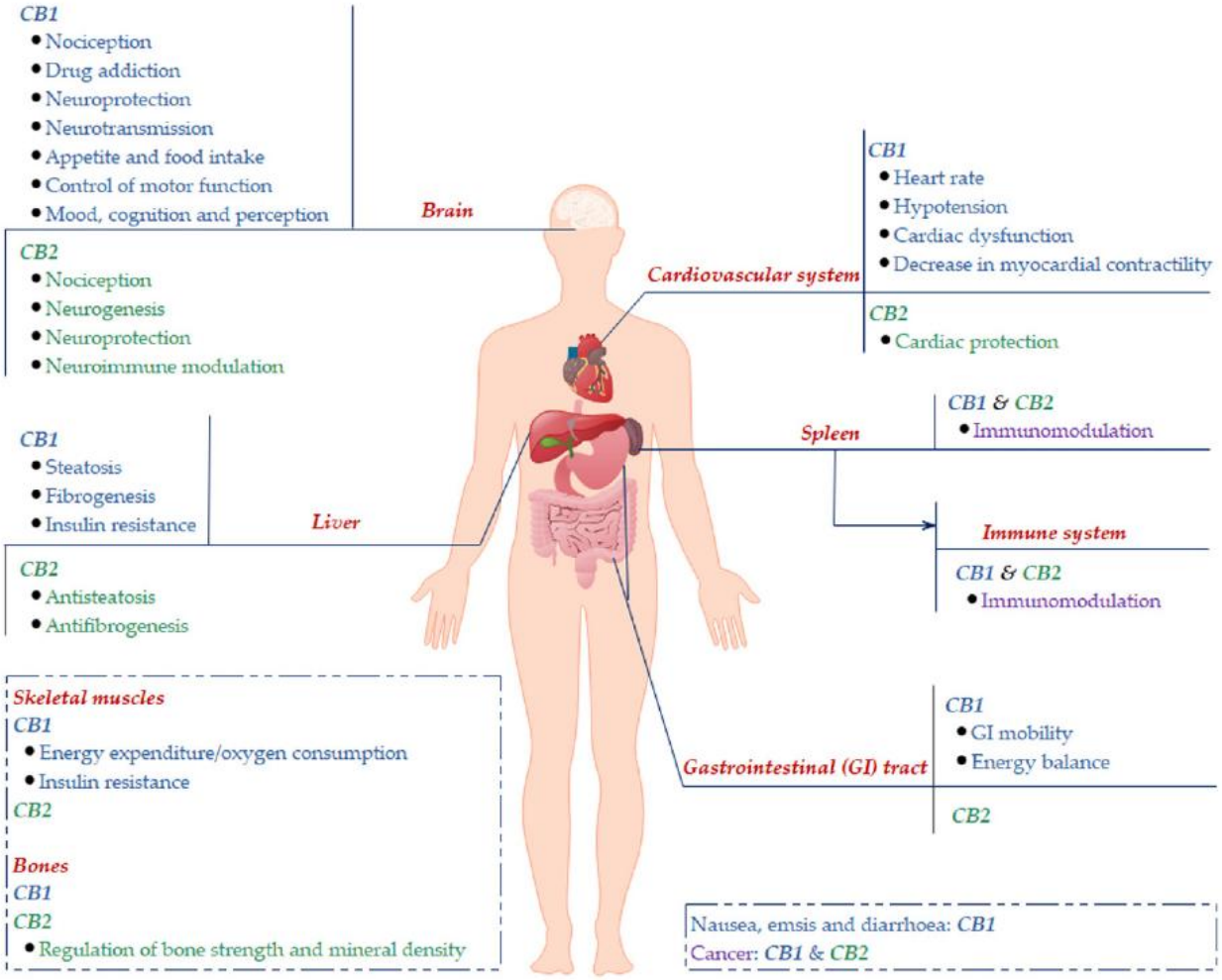

Figure 1.3. Physiological distribution and major functions of cannabinoid receptors CB_1 and CB_2 in various organs and systems of the human body. Note that this schematic does not include receptor presence or activity in the skin, buccal mucosa, or other peripheral tissues (Adopted from (An et al., 2020)).

1.1.4 Therapeutic potential of the phytoconstituents of the Cannabis plant

The therapeutic effects of the plant span various medical conditions. Research has illustrated the potential benefits of cannabinoids in pain management, mental health, seizure control, nausea relief, appetite stimulation, neuroprotection, and inflammation.

Chronic pain

Cannabis has been utilized as an analgesic for thousands of years and remains one of the most prevalent medicinal applications in contemporary practice. Cannabinoids have been shown to effectively manage chronic pain by interacting with endocannabinoid receptors, demonstrating efficacy comparable to that of synthetic drugs. This modulation of pain pathways highlights the potential of cannabinoids as a viable alternative or adjunct to traditional pain management therapies (Vučković et al., 2018). Johal et al. (2020), in a systematic review, showed that cannabis was more effective against non-cancerous neuropathic pain, when compared to other types of pain. Treatment of neuropathic pain associated with HIV and multiple sclerosis using cannabinoid products has shown particularly promising results (Turcotte et al., 2010). Many studies have also shown enhanced analgesic effects of cannabis when used in conjunction with opioids for managing

pain and migraines (Safi et al., 2024). However, there is a lack of data regarding the comparative efficacy and safety of cannabis or cannabinoids in relation to existing pain treatments, including opioids.

Clinical trials investigating the effectiveness of cannabinoids for the management of rheumatic pain, postoperative pain, and cancer-related pain have produced inconsistent findings. The discrepancies in trial results can be attributed to several factors, including short study durations, small sample sizes, inconsistent dosing and routes of cannabinoid administration, and variations in the evaluation of different pain aspects. These issues highlight the necessity for further research to clarify the therapeutic potential of cannabinoids in managing these pain syndromes (Safi et al., 2024; Schmidt, 2024; Vučković et al., 2018). Research has also identified cannabis terpenes to influence ion channels, which affect neuron signalling, thereby inhibiting pain (Anand et al., 2023).

Seizure disorders

The effectiveness of smoked cannabis in controlling seizures compared to synthetic medications has led to the development of oral alternatives, such as oils and extracts that encompass a full range of phytochemicals. Research has demonstrated that THC, CBD, and cannabidivarin exhibit anti-convulsant properties. THC's effects are primarily mediated through CB1 receptors, but studies have shown that CBD and cannabidivarin also operate through signalling pathways that do not involve endocannabinoid receptors. Notably, THC has been associated with both anti-convulsant and pro-convulsant effects, leading to concerns about its psychoactive side effects and reducing its appeal as a standalone treatment for epilepsy. This has shifted focus toward CBD, particularly due to its promising potential in seizure management, which has resulted in the development of CBD-enriched products (Perucca, 2017; Ružić Zečević et al., 2018).

Stockings et al. (2018) conducted a systematic review of clinical trials examining the use of CBD for treating seizures associated with various conditions. The findings revealed significantly positive outcomes, particularly in paediatric and adolescent populations. Epidiolex, an oral solution, was the first approved pharmaceutical grade CBD for the treatment of epilepsy associated with Lennox-Gastaud and Dravet syndromes. Researchers are also developing formulations of CBD to be administered via alternatives routes in order to maximize its bioavailability (Gaston & Szaflarski, 2018; Stockings et al., 2018). Cannabidivarin showed strong anti-convulsant properties in preclinical studies. However, it did not yield the same results in phase II clinical trials. One potential reason for this discrepancy could be the heightened placebo response observed in participants during these trials (Morano et al., 2020).

Mental health

Cannabis has been negatively associated with mental health, largely due to the psychoactive effects of THC. However, with the ease of the cannabis ban, a substantial amount of research is focusing on its positive influences on mental health. Research has specifically focused on smoked or oral cannabis products for combating sleep disorders and PTSD. Studies showed that patients had a significantly large reduction of

symptoms associated with PTSD, such as anxiety, poor sleep, avoidance, and re-experiencing related trauma (Bonn-Miller et al., 2014; Greer et al., 2014). There are divergent perspectives on cannabis, with some research suggesting that it may act as a gateway drug, potentially leading to the use of more harmful substances. Conversely, other studies propose that cannabis can serve as an exit drug, assisting individuals in reducing or substituting their use of alcohol and other drugs. Furthermore, evidence indicates that cannabis may provide a beneficial alternative for those seeking to mitigate their dependence on these substances (Lucas et al., 2016). However, large-scale clinical trials are necessary to validate the efficacy of cannabis as a treatment for substance use disorders.

Cannabis administration has been shown to elevate mood for both medical and recreational purposes. Earlier studies identified cannabis use as a risk factor for depression, apathy, and lethargy. It has been proposed that social factors and adverse conditions, such as unemployment, family issues, and lower educational attainment, may contribute to the development of depression in cannabis users, factors that were often overlooked in many studies. However, several cross-sectional reviews indicate that cannabis may have positive effects on reducing depression and could be beneficial in treating bipolar disorders (Haller, 2024; Walsh et al., 2017).

Neurodegenerative disease

Neurodegenerative diseases, such as Alzheimer’s, Parkinson’s, multiple sclerosis, and Huntington’s disease, are characterised by significant damage to motor neurons, resulting in impaired motor function and cognitive decline. Recent research suggests that the phytochemical constituents of the cannabis plant may offer therapeutic benefits for these conditions due to their anti-inflammatory and neuroprotective properties. The pathogenesis of these neurological disorders often involves the aggregation of specific protein molecules, which contributes to the progression of symptoms. Understanding these underlying mechanisms is crucial for developing effective treatments. Emerging evidence points to cannabinoids as potential modulators of these processes, potentially alleviating inflammation and promoting neuronal health (Sharon et al., 2024; Stasiłowicz-Krzemień et al., 2024). THC and CBD, two key cannabinoids, have shown the ability to prevent protein aggregation by influencing the endocannabinoid system and engaging with cannabinoid receptors. This interaction highlights their potential to help alleviate the protein accumulation observed in neurodegenerative disorders. CBD has also shown the ability to restore locomotor function in Parkinson's disease models (Kaszyńska, 2024).

Preclinical and invitro studies show CBD’s potential in Alzheimer's disease to improve cognition and reduce agitation (Marques & Campos, 2024). Randomized placebo-controlled trials have demonstrated the benefits of Nabiximol (Sativex), an oro-mucosal spray containing CBD and THC in similar ratios, to reduce spasticity and pain associated with multiple sclerosis, and were found useful as an adjunct therapeutic in combating severity of the symptoms (Bethoux et al., 2024). Beyond cannabinoids, terpenes, flavonoids, and other non-

cannabinoid complexes might also synergistically act to enhance the effects (Stasiłowicz-Krzemień et al., 2024).

Cancer and associated symptoms

Cannabis and cannabinoids have been extensively studied for their potential to alleviate a range of cancer-related symptoms. These include pain, nausea, insomnia, anxiety, and anorexia. Additionally, they are considered beneficial in palliative care for cancer patients, enhancing overall quality of life. Numerous studies have also demonstrated the efficacy of cannabinoids in managing chemotherapy-induced nausea, showing comparable effectiveness to synthetic alternatives (Shalata et al., 2024; Wardill et al., 2024). Muscle wasting, or cachexia, along with anorexia, are prevalent symptoms that affect over 50% of patients with terminal or late-stage cancer. Research indicates that cannabinoids can help alleviate cachexia through their interaction with CB1 receptors, which influence both muscle and fat tissue (Seymour-Jackson et al., 2023).

In-vitro studies and animal models have uncovered that cannabinoids repress proliferation and instigate programmed cell death in breast cancer by acting on the cannabinoid receptors in the affected cells. Researchers have also shown the ability of synthetic cannabinoid JWH-133, CBD, and THC to be effective in inhibiting the growth of breast tumours and limiting metastasis in mice models. Preclinical data showed that cannabinoids also hindered proliferation and metastasis, angiogenesis, and decreased the progression of chemotherapy resistant cells in colorectal cancer (Alsalamat et al., 2024). However, studies indicate that the activation of CB2 receptors by low doses of cannabinoids may promote cellular proliferation, which could pose a risk for the development of certain cancers. This response is influenced by dosage, as higher concentrations of cannabinoids tend to exert inhibitory effects on cancer progression. Thus, the relationship between cannabinoid dosage and its impact on cancer biology is complex, requiring careful consideration in therapeutic contexts (H.-S. Lee et al., 2022). Epidiolex, a medication developed by GW Pharmaceuticals, contains cannabidiol (CBD) and is primarily known for its use in treating certain types of epilepsy. However, it has also been explored as an adjuvant treatment for glioma, a type of brain tumour. In this context, Epidiolex may help enhance the effects of other therapies and alleviate symptoms associated with glioma. The incorporation of CBD in treatment regimens aims to leverage its potential anti-inflammatory and neuroprotective properties, potentially improving patient outcomes when used alongside traditional cancer therapies (Hu et al., 2024). Blasco-Benito et al. (2018) noted that herbal preparations of cannabis flowers containing an array of cannabinoids and terpenes were more effective in their antitumor effects when compared to pure isolated THC, emphasizing on the synergistic or entourage effects of the phytocompounds from the cannabis plant.

Fibromyalgia and chronic fatigue syndrome

Skeletal and muscular pain, along with physical and psychological impairment, marks the disease fibromyalgia, a chronic fatigue syndrome. Conventional pharmacological therapies alleviate the disease to a

certain extent but have severe adverse effects and might consequentially worsen the condition. A pilot study done by Giardina et al. (2024) concluded that a full spectrum cannabis formulation, marketed under the name Bedrocan, could serve as an alternative therapeutic regimen for patients suffering from this condition. A systematic review of previous clinical trials also revealed that *Cannabis* successfully improved the quality of life of patients suffering from fibromyalgia by alleviating symptoms such as sleep deprivation and poor appetite (Giardina et al., 2024). A growing body of clinical evidence indicates that cannabis may enhance sleep quality, mitigate fatigue, and reduce chronic pain, while also addressing psychiatric comorbidities linked to fibromyalgia. These findings point out the potential of cannabis as a therapeutic option for managing the multifaceted symptoms of this condition (Wang et al., 2024).

Other potential health benefits

Skin disorders

The anti-inflammatory properties of CBD have been demonstrated to significantly enhance the wound healing process. Cannabis oils, which comprise of a wide range of the plant's phytoconstituents, have demonstrated antimicrobial properties attributed to the presence of THC and CBD, as well as antioxidant and anti-inflammatory effects. Several recent studies have explored the use of cannabis oils alongside biomaterials as a promising strategy for enhancing wound healing (Israni et al., 2024).

The skin's endogenous ligands and its endocannabinoid system provide a basis for utilizing cannabinoids in the treatment of various dermatological conditions, such as psoriasis, dermatomyositis, and dermatitis. By modulating pro-inflammatory cytokines, cannabinoids play a vital role in maintaining homeostasis within the skin, thereby promoting overall skin health and recovery. Clinical trials utilizing oral synthetic cannabinoids indicated improvements in autoimmune skin disorders at certain endpoints. However, these positive effects were not maintained in the later stages of the trial, possibly due to the co-administration of immunosuppressive medications, which may have influenced the outcomes. In contrast, topical administration of cannabinoids has proven to be an effective treatment for dermatitis and psoriasis (Kuzumi et al., 2024).

Ocular health

Since the early 1970s, cannabis has been investigated as a potential treatment for glaucoma. Research has identified endocannabinoid receptors in various ocular tissues, including the retinal epithelium, ciliary body, and retina. Cannabinoids can modulate intraocular pressure through their action on these receptors by both reducing the production of aqueous humour and facilitating its outflow. This dual action contributes to the lowering of intraocular pressure, a significant pathological feature of glaucoma. However, clinical studies remain limited, even when considering the plant as an adjunct therapy, and the studies encounter challenges associated with formulations that offer only a short duration of cannabinoid activity (Fava et al., 2024; Joshi et al., 2024).

Corneal hyperalgesia, a condition characterised by heightened sensitivity to pain resulting from damage to nerve endings in the cornea, can be provoked by normal air, light, or even minimal stimuli. The topical application of cannabinoids has demonstrated efficacy in managing this condition, especially with higher concentrations of THC and CBD, either individually or in combination. However, there have yet to be any clinical trials investigating this therapeutic approach (Fava et al., 2024).

Gut Health

Cannabinoids have been recognized for their role in supporting gastrointestinal function and maintaining homeostasis, largely due to the presence of the endocannabinoid system within the gut. This system plays a crucial role in regulating various physiological processes, including appetite, digestion, and gut motility. By interacting with CB2 receptors, cannabinoids can modulate the effects of inflammation and stress on the gastrointestinal tract. Specifically, they have been shown to control heightened gastrointestinal motility, which can be exacerbated by inflammatory conditions or stress responses. This modulation can lead to a reduction in symptoms such as diarrhoea and abdominal discomfort, promoting overall gut health. Furthermore, the ability of cannabinoids to influence the gut microbiome and the immune response in the gastrointestinal system adds another layer to their therapeutic potential. As research continues to uncover the complexities of the endocannabinoid system, cannabinoids may offer promising avenues for treating various gastrointestinal disorders, including irritable bowel syndrome (IBS) and inflammatory bowel disease (IBD) (Al-Khazaleh et al., 2024; Wardill et al., 2024).

Oral health

Cannabinoid receptors CB1 and CB2, along with TRPV receptors, are found throughout the oral cavity, including the tongue, periodontal tissue, oral mucosa, and salivary gland tissue. Pre-clinical studies have proven cannabinoids to be beneficial for various diseases affecting the oral cavity by mediating their action via these receptors. In animal models of periodontal disease, which is an inflammatory oral disease caused by plaque formation and could lead to tooth loss, CBD was found to inhibit plaque formation and reduce inflammation, thereby hinder the progression of the disease. Research has also shown CBD and CBG to be effective in inhibiting biofilm formation owing to their anti-microbial activity, highlighting their potential in treating mucosal inflammation and ulcers in the mouth. Cannabinoids were found to reduce inflammation and promote vascularization in dental pulp and periodontal stem cells, highlighting their potential for treating dental pulp regeneration and dentin repair. Research suggests that CBD may offer potential benefits for treating temporomandibular disorders and addressing bone tissue defects. However, further studies are needed to validate its clinical efficacy in these areas (Hu et al., 2024).

1.1.5 The pharmacokinetic effect from different routes of cannabinoid administration

Historically, cannabis use has involved smoking or various other methods of inhaling the dried flowers of the plants. However, recent research has expanded to process raw cannabis or isolated cannabinoids into

various dosage forms. The pharmacokinetic effects vary depending on the route that they are administered (Spindle et al., 2019).

Smoking/inhalation

Smoking cannabis is a primary route of drug consumption. Studies show that the effect of smoking on the pharmacokinetics of cannabinoids is similar to the intravenous route in terms of fast onset of action. Smoking leads to the absorption of 25% of the cannabinoids present (Peters & Chien, 2018). Benefits derived from smoking cannabis include rapid delivery, quick onset of pharmacological actions and freedom for individuals to titrate their dose. However, smoking cannabis with tobacco or vaporizing with e-liquids has been associated with poor health outcomes and harmful consequences not yet understood in the case of some e-liquids (Fairman, 2015; Giroud et al., 2015). Furthermore, the stigma associated with "cannabis smoking" (Bottorff et al., 2013), THC's psychoactive actions (Huestis, 2007), and the potential of producing toxic compounds at high temperatures (Czégény et al., 2021), in addition to the high THC concentrated strains cultivated today, limits this route in terms of medical administration (Peters & Chien, 2018).

Oral route

The oral route is recognized for its preference by most patients, excluding unconscious patients and patients with swallowing obstructions. Edibles of cannabinoids have been used widely for recreational purposes due to associated durable effects combined with a lack of difficulty in administration. However, this route of administration is hindered by the first-pass metabolism effects, where THC is broken down into psychotropic 11-OH-THC, further metabolized to 11-COOH-THC (Catherine J Lucas et al., 2018; Poyatos et al., 2020). When consumed by the oral route, the bioavailability of the cannabinoids is reduced significantly to one third compared to smoking, while there is also an increase in its psychoactive effect. The average bioavailability (considering inter-and intra-individual variability) of CBD and THC is identified as 31% when smoked/inhaled, was significantly higher than the bioavailability of the oral route, where less than 20% of THC and CBD reached systemic circulation following ingestion (Catherine J Lucas et al., 2018; Millar et al., 2018). In addition to the first-pass metabolism effects, variation in absorption from the gut due to inconsistent dosing across different oral formulations and the effects of body composition (presence of higher fat mass) and the degradation in the stomach also contributes to poor bioavailability of the oral route (Huestis, 2007; Williams et al., 2021). An exceptionally low proportion of studies considering the impacts of consuming food and drinks could also add to the absorption variation effects (Vandrey et al., 2017).

Approaches to enhance the bioavailability of oral cannabinoids include using oil-based cannabinoid formulations and developing delivery systems that emulsify under the acidic conditions of the GI tract. However, such self-emulsifying methods are associated with low economic feasibility and limited stability and safety (Brunetti et al., 2020; Cherniakov et al., 2017; Knaub et al., 2019).

Routes to avoid first pass effects.

Alternative routes of cannabinoids' administration to avoid first-pass metabolism effects such as transdermal, rectal, intranasal, and oro-mucosal are currently under investigation. There is, however, a lack of information regarding the pharmacokinetic parameters, such as the bioavailability of cannabinoids via these routes. The transdermal route is an attractive option with the potential to treat dermatological conditions and even skin cancers due to the different cannabinoid receptors present on the skin, which are actively involved in skin cell activities (Tijani et al., 2021). Research on delivery via the transdermal route is now focused on developing carrier systems for the highly lipophilic cannabinoids and also enhancing diffusion and penetration into deeper layers of the skin to reach the blood circulation. The low stability of cannabinoids, their susceptibility to degradation under light and heat, and impaired delivery in patients with wasting syndrome need to be addressed to successfully deliver cannabinoids via this route (Catherine J Lucas et al., 2018). Mucosal sites offer good alternatives to oral routes for systemic drug delivery. Although rectal routes offer two times higher cannabinoid bioavailability compared with the oral route, and a lower amount of THC metabolized, lack of patient acceptance and defecation involved with impaired absorption limits delivery of cannabinoids via this route (Geshtakovska & Stefkov, 2016). Intranasal delivery of several drugs such as propranolol, progesterone, and anti-convulsants has successfully circumvented the fist-pass effects and enhanced drug bioavailability. Delivery of cannabinoids via this route is restricted due to their highly lipophilic nature in addition to the limited area of absorption and low water activity of mucin in the nasal cavity (Al-Ghananeem et al., 2011; Valiveti et al., 2007).

The oral mucosa or the oro-mucosal route is a popular choice for delivering a wide range of drugs, as it offers a larger surface area through which significant volume of drugs can be delivered. The formulations offering higher mucoadhesion allows for retention and the ability to dissolve slowly at the site of administration (Goyal et al., 2018). However, bioavailability and absorption of highly lipophilic molecules such as cannabinoids via this route face challenges such as saliva flow, stability in a physiological environment, and residence time of the formulation which need to be tackled to develop superior formulations (Hua, 2019; Millar et al., 2018).

1.1.6 Approved formulations of *Cannabis* products

Formulations of *Cannabis* approved for use include synthetic preparation of THC and its analogue, or pure CBD, including Dronabinol, Nabilone, Epidiolex, and oro-mucosal Sativex for a few clinical indications (Kocis & Vrana, 2020; Schrot & Hubbard, 2016); the clinical indications of these drugs are shown in Table 1.1, along with their bioavailability and onset of action. The use of synthetic THC in oral formulations was a significant cause of concern for adverse CNS effects (Badowski, 2017); although Nabilone, an analogue of synthetic THC, was reported to have higher bioavailability compared with Dronabinol (synthetic THC), it had more severe drowsiness, dizziness, and psychoactive effects (Ben Amar, 2006).

Table 1.1. Clinical indications of FDA-approved Cannabis products, their onset of action and bioavailability identified.

Drug	Formulation name & dose	Approved clinical indications	Formulation	Average Onset of action	Bioavailability	References
Dronabinol-synthetic THC	Marinol 5 mg	Chemotherapy-induced nausea, appetite stimulant in AIDS	Soft gelatine oral capsule	1.5 h	10 to 20%	(Badowski & Yanful, 2018; FDA, 2021; Smith et al., 2015)
	Syndros 4.25 mg	Chemotherapy-induced nausea, chronic pain	Oral solution	1 hr		
Nabilone-synthetic analogue of THC	Cesamet 2 mg	Chemotherapy-induced nausea	Oral capsules	1-1.5 h	60%- studies not conclusive	(Bedi et al., 2013; FDA, 2021; Smith et al., 2015; Tsang & Giudice, 2016)
THC and CBD	Sativex 5 and 15 mg THC	Spasticity in multiple sclerosis (MS), Clinical trial phase III for cancer pain.	Oro-mucosal Spray	Up to 40 min	5 and 15 mg oral THC- relative bioavailability was 92.6% (13.1%) and 98.8% (11.0%) respectively. Buccal – 93.9% relative bioavailability higher compared to sublingual - 87.2%	(FDA, 2021; Karschner et al., 2011; Tanasescu & Constantinescu, 2013)
CBD	Epidiolex	Lennox-Gastaud and Dravet syndromes - epileptic disorders	Oral solution	Not determined	13-19%	(Bruni et al., 2018; Millar et al., 2018)

1.1.7 The need for novel formulations

Cannabinoid oral formulations that are currently available in the market have poor bioavailability, as drugs administered orally suffer from extensive biotransformation due to the first pass metabolism effects. These approved oral cannabinoid formulations can further cause adverse effects because of the presence of synthetic or analogues of synthetic cannabinoids (Badowski, 2017; Catherine J Lucas et al., 2018). The alternative oromucosal route of delivery has the potential to improve the bioavailability of cannabinoids by avoiding the first-pass metabolism. Sativex, an approved oromucosal spray containing *Cannabis* extracts, fails to completely deliver the cannabinoids into oral mucosa as the formulation is prone to being accidentally swallowed and thus possesses poor bioavailability. The formulation is also needed to be frequently administered, and its high ethanol content causes lesions in the mouth after long-term use (Karschner et al., 2011; Scully, 2007). Furthermore, there is a lack of focus on the drug release characteristics of potential oromucosal cannabinoid formulations under research. Formulations with sustained-release properties can provide prolonged therapeutic effects without the need for frequent administration by maintaining effective levels of cannabinoids in the systemic circulation. Such prolonged-release formulations with improved bioavailability can be used for treating chemotherapy-induced nausea/emesis, chronic pain, spasticity

associated with multiple sclerosis, and sleep disturbances. It could also improve the care and quality of life of palliative patients.

1.1.8 Need for 3D printing

The technique of constructing objects through the sequential addition of materials in a layer-by-layer manner is termed additive manufacturing, commonly referred to as 3D printing. It has been utilized in multiple medical fields, including the development of advanced medical tools and equipment that enhance surgical precision and patient care. Additionally, in tissue engineering, this technology plays a crucial role by allowing for the fabrication of complex biological structures, including scaffolds that support cell growth and tissue regeneration. Three-dimensional printing is also growing successfully as an alternative tool for designing and developing pharmaceutical products. The technique offers the ability to develop dosage forms with improved quality and tailored release profiles (Paccione et al., 2024). 3D printed products are highly valued as personalized drug delivery vehicles offering the ability to provide customizable doses to patients with varying requirements, wherein traditional formulations are lacking in this aspect. Several 3D printing techniques have been employed in drug manufacturing, including fused deposition modelling, extrusion printing, selective laser sintering, and binder jetting. Each of these methods offers distinct advantages and disadvantages, making them suitable for different applications within pharmaceutical production (Wang et al., 2023). Extrusion printing has been used for printing a wide range of oral and oromucosal formulations comprising of both immediate and extended-release delivery forms (Park et al., 2019; Zhu et al., 2020). 3D printing has been demonstrated to be effective in fabricating buccal films, which facilitate controlled release and enhance bioavailability through direct absorption across the oral mucosa. Using this technique, films can also be customized in terms of thickness, shape, and drug content, enhancing patient compliance and therapeutic effectiveness (Jovanović et al., 2021).

1.2 Thesis aims.

The main aim of this thesis is to formulate and develop buccal formulations with cannabinoids possessing sustained release properties and improved bioavailability. Two types of dosage forms were developed for this purpose, mucoadhesive in-situ gels, which are formulations that transition from liquid to gel once in contact with the buccal mucosa, and 3D printed mucoadhesive films. Both types of formulations were loaded with CBD and THC in a similar (1:1) ratio, consistent with the oromucosal formulation Sativex. In the formulation process, various combinations and concentrations of in-situ gelling and mucoadhesive polymers are optimized to achieve the desired properties. The mechanical and physicochemical characteristics of the formulations are extensively analysed, along with their in-vitro release profiles and ex-vivo permeation capabilities, to ensure effective delivery of cannabinoids through the buccal mucosa. Both types of buccal formulations are specifically designed to release cannabinoids in a sustained manner, aiming to improve patient compliance and enhance therapeutic outcomes.

Specific objectives of this thesis are:

i. To enhance the solubility and permeation profiles of cannabinoids, by incorporating cyclodextrins to form inclusion complexes and terpenes, respectively in the developed formulations.
ii. To investigate various in-situ gelling mechanisms, polymer concentrations, and excipients, while studying sol-gel transitions to establish optimal formulation parameters
iii. To utilize 3D printing extrusion technique to develop mucoadhesive buccal films with sustained release properties.
iv. To compare the mucoadhesive polymers HPMC and Carbopol incorporated into the in-situ gelling and 3D printed formulations.
v. To evaluate the characteristics of the developed formulations in terms of their physicochemical and mechanical properties, release profiles, permeation capabilities, and stability.

1.3 Thesis structure

This thesis is structured with an introductory chapter 1, followed by a literature review forming Chapter 2. It contains five experimental Chapters 3 to 6, culminates in a final discussion and conclusion in Chapter 7, and is accompanied by a thorough reference list.

1.4 Thesis overview

Chapter 2 Literature review on cannabinoid buccal delivery: approaches to formulation, fabrication, and permeation enhancement

Buccal formulations deliver active compounds through the mucosal membranes of the mouth, providing an effective route for cannabinoid administration. This method bypasses first-pass metabolism, enhancing bioavailability and offering rapid onset of action. This chapter has explored potential buccal delivery systems for cannabinoids, focusing on strategies to overcome poor oral bioavailability, first-pass metabolism, and variable absorption. Different formulation strategies, including mucoadhesive polymers, lipid-based systems, inclusion complexes, nanoformulations, and terpene-enhanced platforms has been discussed to improve solubility, stability, and mucosal permeation. The chapter also analysed mechanisms of release, including controlled, immediate, and targeted delivery. Dosage forms such as sprays, solid mucoadhesive films, and in-situ gels have been compared in terms of release profiles, residence time, and patient acceptability. Advanced fabrication technique has been identified for producing personalized, sustained-release formulations Finally, has highlighted future directions for research and innovation in buccal cannabinoid formulations, providing a comprehensive overview of the factors influencing their design and effectiveness.

Chapter 3 Pre-formulation approaches to improve solubility and permeation of cannabinoids.

This chapter explored the properties of cannabinoids and polymers suitable for developing in-situ gels and 3D printed films. The information obtained from this chapter have been used for formulating these dosage

forms and analysing them under appropriate conditions. Isolated cannabidiol and THC dominant distilled oil were analysed for their physical and chemical properties, including solubility studies, and the drug's in-vitro permeation profiles, which was essential for developing stable and effective formulations. In terms of solubility, β-cyclodextrin and hydroxypropyl β-cyclodextrin were used to develop inclusion complexes and were compared for their effectiveness to form such complexes with both the cannabinoids based on their in-vitro dissolution profiles. Furthermore, various concentrations and combinations of terpenes were investigated for their permeation-enhancing effects on cannabinoids across porcine buccal mucosa. Previously validated analytical method high performance liquid chromatography (HPLC) was confirmed by determining the limit of quantitation in this chapter.

Chapter 4 Development of thermoresponsive mucoadhesive in-situ gels for buccal cannabinoid delivery

In chapter 4, temperature induced in-situ gelling polymers such as poloxamers were utilized as cannabinoid delivery vehicles, as they are known for their wide range of mucosal applications and prolonged release properties. They possess the ability to self-aggregate into micelles at certain temperatures, allowing them to transition from liquid to gel like states and vice versa when reverting the temperatures. To achieve gelling above 35 °C, which is ideal for the buccal cavity, and to enhance the mechanical properties of poloxamer gels, various concentrations of poloxamers were optimized alongside different mucoadhesive polymers, such as HPMC and carbopol, in varying concentrations. Additionally, the suitability of other excipients in the formulations was assessed. Optimizations were carried out using the design expert software, where parameters identified include sol-gel transition temperatures, time, and gelling capacity by measuring viscosity at room temperature and at 37 °C. Formulations were incorporated with either only CBD or both CBD and THC in 1:1 ratio. Optimized formulations with either HPMC or carbopol were then compared for their mucoadhesive strength, mechanical, physicochemical, in-vitro release, and ex-vivo permeation profiles. Six-month stability of the formulations in 4°C conditions was determined.

Chapter 5 Mucoadhesive ion-responsive in-situ gels for buccal drug delivery of cannabinoids

In this chapter, ion induced gelation mechanisms were explored for the development of buccal in situ gels using gellan gum and carrageenans as the primary gelling polymers. Gellan gum and carrageenans, specifically kappa and iota types, were investigated for their cation induced gelling ability when combined with cannabinoids, either CBD alone or in combination with THC in similar ratios. For both gellan gum and carrageenan systems, various polymer concentrations were optimized along with appropriate cationic salts, and mucoadhesive polymers, HPMC or Carbopol, by assessing sol gel transition time, fluidity at room temperature, and gelling capacity. Optimized formulations were evaluated for mechanical strength, mucoadhesive performance, in vitro drug release profiles, and ex vivo buccal permeation to ensure efficient and sustained cannabinoid delivery. Additionally, stability studies were conducted at 37 °C over periods of one, three, and six months, focusing on sol gel transition behaviour, pH, drug content, and visual appearance, to assess the robustness of the formulations. The incorporation of previously identified excipients was

maintained throughout to ensure consistency in formulation performance. These ion-induced in situ gels demonstrate a promising strategy for buccal cannabinoid delivery. By providing controlled release at the site of administration, these novel formulations have the potential to enhance bioavailability, prolong mucosal residence time, and improve the overall therapeutic efficacy of cannabinoid-based treatments. The study highlights the versatility of gellan gum and carrageenan-based gels as non-invasive, patient friendly delivery platforms with broad clinical potential. By ensuring that cannabinoids are released in a controlled manner at the buccal mucosa, these innovative delivery systems can significantly enhance the effectiveness of cannabinoid therapies.

Chapter 6 Development and characterization of 3D-printed mucoadhesive buccal films of cannabinoids

In this chapter, optimized concentrations of mucoadhesive polymers HPMC and carbopol were used to prepare bioinks incorporated with inclusion complexes of cannabinoids and terpenes, along with other selected excipients. The bioinks were printed using Allevi 2 3D printer with optimized printing parameters. Printed films were then characterised for their mechanical and physicochemical properties, ex-vivo permeation, and in-vitro release profiles. Films remained stable and adhesive to the porcine buccal mucosa for over an hour, indicating their effectiveness for prolonged drug delivery. Overall, 3D-printed films developed have the potential to serve as a promising delivery system for cannabinoids, improving patient compliance and therapeutic outcomes through effective buccal administration.

Chapter 7 General discussion

This chapter will comprise an in-depth analysis of the results from the previous chapters. This will be done by interpreting the obtained results, determining their significance, and exploring this research done in context with previous studies identified from the literature. A critical discussion will also be done on the benefits and limitations of this research while pointing towards future studies such as in-vivo pharmacokinetics for the formulation with optimal excipients and desired properties.

Chapter 2: Literature review: Cannabinoid Buccal Delivery: Approaches to Formulation, Fabrication, and Permeation Enhancement

Abstract

Cannabinoids such as cannabidiol (CBD) and tetrahydrocannabinol (THC) have garnered significant interest for their broad-spectrum pharmacological activity in managing chronic pain, neurological disorders, and cancer-associated symptoms. Despite their therapeutic promise, clinical translation remains hindered by poor aqueous solubility, extensive first-pass metabolism, and inconsistent systemic exposure following oral administration. Buccal drug delivery systems offer a viable alternative by enabling transmucosal absorption, bypassing hepatic metabolism, and facilitating both rapid and sustained drug release. This review examines the evolution and design of buccal dosage forms, including fast-dissolving films, mucoadhesive matrices, in-situ gels, and particulate systems and highlights the critical role of formulation strategies in enhancing cannabinoid bioavailability. Fabrication techniques such as solvent casting, hot melt extrusion, and emerging 3D printing methods are also discussed, with a focus on their potential to enable personalized dosage forms. Furthermore, the integration of permeation enhancers like terpenes, and novel systems such as inclusion complexes and lipid-based carriers, presents new opportunities for improving the solubility and stability of lipophilic cannabinoids. Together, these innovations provide a framework for the development of stable, effective, and patient-centric buccal cannabinoid delivery platforms with improved pharmacokinetic and therapeutic profiles.

2.1 Introduction

Cannabinoids are being increasingly harnessed for their medicinal properties in various dosage forms, with the most common routes of administration being oral and pulmonary. Smoking/inhaling cannabis is the most common and preferred route for both recreational and medical uses because it provides rapid effects and efficient delivery (Eisenberg et al., 2014; Huestis, 2007). Despite the advantages, smoking/vaporization of cannabis is associated with side effects due to mixed tobacco/E-liquids, the possibility of toxic compounds that are formed at high temperatures, unregulated doses in some cases, and it still remains stigmatized by many (Bruni et al., 2018; Czégény et al., 2021; Tijani et al., 2021). Also, cannabis administered via the pulmonary route faces fluctuation of absorption and bioavailability due to inter- (between individuals) and intra-individual (within individuals across varying observations) variabilities arising from differences in frequency and depth of inhalation and titration of dose (Badowski, 2017; Millar et al., 2018). This variation is also observed with the most frequently used oral route due to factors such as food or drinks consumed. Furthermore, the bioavailability of cannabinoids remains a significant limitation in developing oral formulations (Thomas & Pollard, 2016), which is mainly due to its degradation in the gastrointestinal tract (GIT), inadequate absorption in GIT, and first-pass metabolism in the liver (Catherine J Lucas et al., 2018; Millar et al., 2018). Moreover, once subjected to first-pass metabolism, the metabolites such as 11-OH-THC (11-OH-Tetrahydrocannabinol) can be four times more psychoactive than THC, posing more side effects (Poyatos et al., 2020). Hence, research is focused on developing formulations for delivery via routes not affected by first-pass effects such as oral mucosa (oro-mucosal), including buccal, sublingual, transdermal, rectal, and intranasal routes.

Constraints for the oro-mucosal delivery of the currently approved product, Sativex, are mainly related to the stability of the dosage form in the oral cavity and poor bioavailability since most of the formulation is accidentally swallowed rather than being absorbed into the mucosa, which leads to oral delivery rather than oro-mucosal (Karschner et al., 2011). Limitations also include the need for frequent administration (Duran et al., 2010), slow onset of action (Tanasescu & Constantinescu, 2013), and long-term adverse effects of mouth lesions due to the use of excipient ethanol (Scully, 2007). Limitations of Sativex highlight another essential consideration for developing cannabis formulations, which is the release characteristics of the dosage form. Most of the research done so far with oro-mucosal delivery of cannabinoids remains constrained to revamping Sativex in terms of its dosage form for targeted delivery into the oral mucosa failing to address the dosage form's drug release properties.

Medications can be formulated in either conventional or sustained-release dosage forms. Traditional fast-release formulations face severe adverse effects as a result of requiring frequent administration of high doses of therapeutics. However, sustained/extended-release systems can provide prolonged release of medication, eliminating the need for repeated administration, and are generally of lower cost. Furthermore, the slow expulsion of the active ingredient from sustained-release formulations avoids severe effects from the sudden

release of high doses into the system seen with conventional drugs (Laffleur & Keckeis, 2020). Sustained release of therapeutics from dosage forms largely depends on the increased resident time of the formulation in the region of application/administration, which can be achieved by modifying the type of dosage form developed and by using excipients that prolong the release of the drug (Vlachou et al., 2018).

The bioavailability and controlled release of active ingredients, particularly cannabinoids, are critical factors affecting their therapeutic efficacy. Thus, the careful selection of excipients and their concentrations is crucial for achieving optimal formulation performance (Peera Tabboon et al., 2022). Moreover, increasing the residence time of the formulation in the oromucosal space can significantly enhance drug absorption through the buccal mucosa, providing higher systemic availability compared to conventional formulations such as Sativex (Karschner et al., 2011). By prolonging contact with the mucosal surface, mucoadhesive systems not only facilitate more efficient drug permeation but also allow for controlled, sustained release, improving therapeutic outcomes while reducing dosing frequency and potential side effects.

This review will explore drug delivery of cannabinoids (CBD and THC) via the buccal route, comparing it with other oro-mucosal routes of administration. It will discuss suitable polymers and excipients for buccal delivery, fabrication techniques for various dosage forms, and strategies to enhance bioavailability and prolong the release of cannabinoids. Additionally, the review will examine current research on oromucosal cannabinoid products.

2.2 Drug delivery through the oral mucosa

Oro-mucosal drug delivery systems mitigate the challenges associated with the limited bioavailability of conventional oral routes and provide a more convenient alternative to intravenous administration (Zhang et al., 2002). There are different routes available for administering drugs within the oral mucosa, including buccal, gingival, sublingual, and soft-palatal mucosa (Figure 2.1) (Shery Jacob et al., 2021). The selection of the delivery route within the oral mucosa is determined by whether the drug is intended for local or systemic effects. Delivery into the gingival regions, encompassing sites near the teeth and negligible areas of the alveolar bone, is limited for local drug requirements and not feasible for systemic delivery. While the soft-palatal sites, consisting of the soft tissues on the roof of the mouth, provide an optimal pH of 7.34 ± 0.38 for stable drug delivery and produce minimal saliva, they are also susceptible to risks associated with the inadvertent swallowing of the medication (Liang et al., 2020; Shakya et al., 2011). Furthermore, the keratinized epithelial layers of the gums and soft palate display permeation rates comparable to those of the skin, which are significantly lower than the higher absorption rates observed in the non-keratinized buccal and sublingual mucosal tissues (Montero-Padilla et al., 2017). Therefore, buccal and sublingual mucosa are commonly chosen for systemic drug delivery because they offer enhanced absorption rates and improved bioavailability compared to other oral mucosal sites.

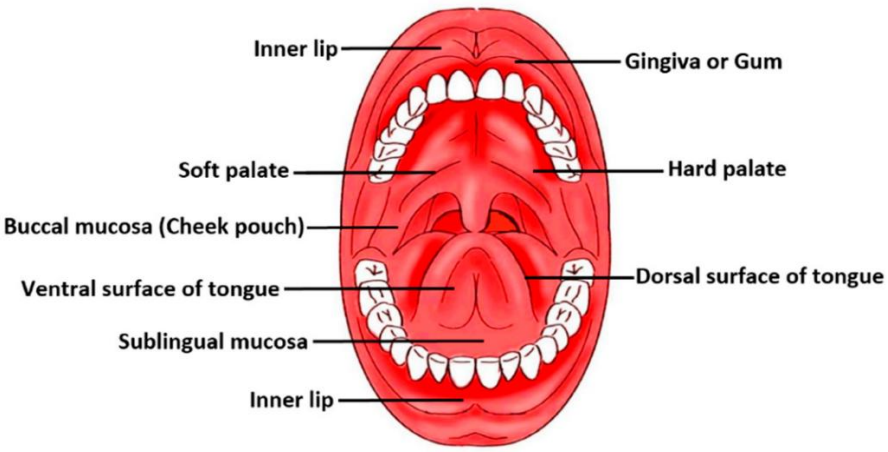

Figure 2.1. Regions of the oral cavity (Adopted from (Shery Jacob et al., 2021)).

2.2.1 Buccal and Sublingual mucosa

The buccal and sublingual mucosa, comprising the inner cheek lining and the floor of the mouth (under the tongue), respectively, are popular routes for delivering systemic drugs; comparisons of these regions are represented in Figure 2.2 (Hua, 2019). The buccal region has a relatively larger surface area (around 53 cm^2) and thicker stratified squamous (SS) epithelial layer of cells (500–800 µm) compared to the sublingual region having a surface area of 27 cm^2 and SS epithelial layer of cells comprising 100–200 µm thickness. Under this SS epithelial layer lies a mesh of blood vessels, capillaries, and smooth muscles forming the connective tissue, through which the drugs administered enter systemic circulation (Gilhotra et al., 2014; Hua, 2019). The transport of drugs within the layers of the buccal and sublingual regions involves concentration gradient dependent, transcellular and paracellular pathways. Essential characteristics of the drug governing transport across these regions include lipophilicity, molecular size, and degree of ionization (pKa). Lipophilicity of the drug plays a crucial role in transport, as lipophilic drugs can easily travel through the transcellular route to cross the phospholipid layers of the cells. However, despite paracellular paths being available for hydrophilic drugs, their movement is limited by the tight junctions present. Small-sized drug molecules (<500 Da) can efficiently permeate, even via tight junctions. High logP values (>2) and non-ionizable drugs are found to be preferable (Lam et al., 2020). Drug bioavailability and stability in formulations, in addition to absorption and transport features of the medicine, are also dependent on factors such as saliva flow, pH of the oral cavity, and the residence time of the formulation (Hua, 2019).

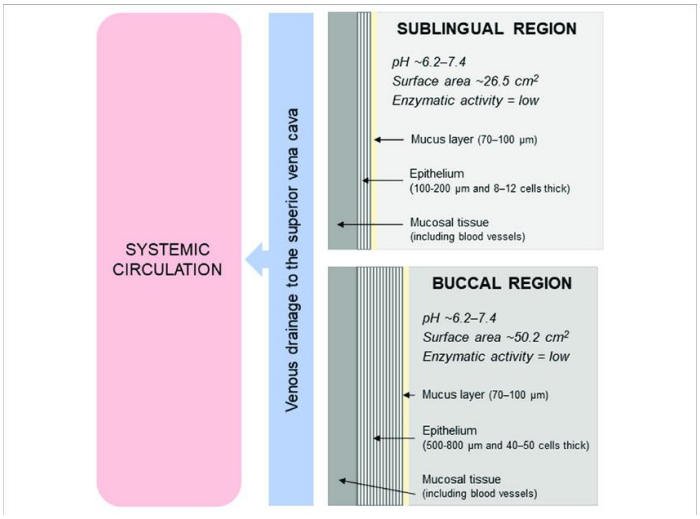

Figure 2.2 Comparison of the buccal and sublingual regions for systemic drug delivery (Adopted from (Hua, 2019)).

Both the sublingual and buccal routes offer advantages in terms of ease of drug delivery and patient compliance. The sublingual route provides the added benefit of faster drug absorption due to its ability to quickly penetrate the mucosal membranes, whereas the buccal region experiences slower penetration due to the presence of a larger number of smooth muscles. However, the sublingual region is generally not suitable for sustained drug release systems as it is constantly affected by saliva secretion and movement of the tongue. Furthermore, buccal mucosa has the lowest enzyme activity in the oral mucosa and an intermediate turnover time of the cells (4-14 days) compared with rapid intestinal and prolonged skin cells. Thus, formulations that possess mucoadhesive properties can reside and act as controlled release systems dispensing the drug slowly (Narang & Sharma, 2011; Pather et al., 2008; Rao et al., 2013). Additional benefits of the buccal route include a lower risk of drug degradation due to enzymatic activity. Moreover, patient comfort is preserved through easy administration and the safe removal of dosage forms in cases of mucosal irritation (Barua et al., 2016).

2.3 Release characteristics of buccal formulations

Various types of dosage forms have been developed to deliver active ingredients/drugs across the buccal mucosa, depending on the clinical indication for which they are used. These include hydrogels, mucoadhesive carrier systems, bioadhesive wafers and lozenges, thin films, in-situ gels, tablets/capsules, carrier oils, extracts, sprays, and particulate systems. Each type of dosage form offers distinct advantages depending on the drug's characteristics and the required pharmacokinetic profile (Barua et al., 2016). Drugs can either be required to provide rapid and immediate complete effects within a few minutes of administration or prolonged effects, where the drug is released gradually over an extended period.

2.3.1 Conventional fast dissolving immediate release dosage forms

Conventional buccal drugs are formulated using excipients that wholly and quickly dissolve and release the medicine in a burst effect, making it immediately available for pharmacological action. It should however be

noted that this burst effect is only ideal for drugs to be used in low concentrations, such that there are no toxic effects seen with high concentrations of the administered drugs (Costa et al., 2019). These therapeutics are issued for conditions of pain and nausea after acute migraine, anti-epileptic, and anti-histaminic effects in paediatric and geriatric patients (Bala et al., 2013). Fast-dissolving polymer matrices can be developed in various dosage forms, including thin films, orally disintegrating tablets, and lyophilized (freeze-dried) wafers. Soluble hydrophilic polymers, with or without mucoadhesive properties, are used for developing these fast-dissolving compositions (Mahajan et al., 2011).

2.3.2 Sustained release formulations

Sustained-release formulations can be developed as either slow or fast-dissolving dosage forms. Approaches to developing such formulations include using excipients such as mucoadhesive polymers that release the active pharmacological ingredient (API) in a sustained fashion, developing in-situ gels, fabricating micro/nanoparticulate dosage forms with or without a pharmacological base, and controlling the type of dosage form produced– bi/multi-layered (Vlachou et al., 2018).

2.3.2.1 Mucoadhesive polymeric formulations

Mucoadhesive polymers are the most commonly used excipients for developing various dosage forms, including gels, lozenges, solutions, wafers, microparticles, films, and tablets, and are often used along with or as a base of dosage forms such as in-situ gels or nanoparticles, respectively (Chinna Reddy et al., 2011). Different theories govern the adhesion of these polymers to the buccal mucosa, creating the contact and consolidation stages. The contact stage is when the formulation encounters the soluble mucins, swells, and is wetted. After this, various noncovalent bonds interconnect the formulation with bound mucins, which diffuse and further form both non-covalent and covalent bonds (Rao et al., 2013). Ideally, a mucoadhesive polymer is required to have a molecular weight > 100 kDa, long and flexible polymer chains with lower crosslinking density, presence of charges and groups involved with strong hydrogen bonding, and favourable surface properties for good adhesion onto the mucosa. They are usually classified into first-generation and new second-generation polymers. However, the classification can also be based on factors such as their charge (anionic or cationic), origin (natural, synthetic, or semisynthetic), water solubility, and mucoadhesive interactions (including electrostatic, covalent, or hydrogen bonding) (Khutoryanskiy, 2011). Different properties of polymers such as degree and rate of swelling influence their muco-adhesiveness. Insoluble mucoadhesive polymers have been employed to help the drugs slowly diffuse into the target environment, even for longer than 20 hours. However, to avoid mucosal irritation and provide better patient compliance, formulations are required to have a maximum residence time of 4-6 hours in the buccal mucosa (Russo et al., 2016).

Mucoadhesive polymeric dosage forms with sustained-release properties can be slow or fast dissolving. Formulations that dissolve slowly usually employ a slowly dissolving polymer layer to provide uni-directional

sustained release of the API (Shery Jacob et al., 2021). Fast dissolving sustained-release formulations are developed with drug-particulate systems in a fast-dissolving polymer base. Rapid dissolution of the pharmacological base helps to eliminate formulation discomfort at the buccal cavity. It ensures that the drug-particulate system is released completely in a short period of time into the mucosal layers, where the particulate system can slowly release the drug (Allam & Fetih, 2016).

2.3.2.2 Particulate systems

Research by Jelvehgari et al. (2016) showed that particulate dosage forms exhibit slower release characteristics when compared with mucoadhesive films. However, these micro/nanoparticles succumb to easy washout in the mouth or accidental swallowing. Hence, stable formulations are developed with these particulate systems incorporated into hydrophobic mucoadhesive polymers for slow/fast dissolving and release properties (Barua et al., 2016). Despite this, the success of such drug-particulate systems is limited by their ability to remain in the mucosal layers without being displaced by saliva. While multi-layered formulations, featuring layers designed for uni-directional flow, mucoadhesive particulate systems, and penetration enhancers, help mitigate this issue to some extent (Patel et al., 2007; Rana & Murthy, 2013), concerns persist regarding the potential toxicity and side effects of these particulate systems accumulating in various organs, particularly in cases of unintended swallowing.

2.3.2.3 In-situ gels

In-situ gels are smart formulations that can transition from liquid to gel or powder to gel once in contact with the physiological environment of the human body. These gels can be fabricated to provide both local and systemic drug effects. In-situ formulations provide the benefits of intimate adherence to the mucosa layer with increased residence time and ease of applying evenly distributed formulations (Shery Jacob et al., 2021; Forouhe Zahir-Jouzdani et al., 2018). Physiological/physical mechanisms that form the gel inside the body include temperature-induced, pH-induced, and ion-induced (A. M. Prasannan et al., 2018). Polymers that gel upon stimulation by temperature changes are further classified into negatively activated, positively stimulated, and reversible polymers. Negatively induced polymers possess lower critical solution temperatures (LCST), above which they gel and exist as a flowable liquid below these temperatures. Positively induced polymers holding upper critical solution temperature (UCST) present as a liquid and gel above and below this temperature, respectively (Huang et al., 2019). Thermoreversible polymers show reversible gelation by harnessing the ability to convert into a liquid again upon cooling (Jain et al., 2016). Table 2.1 presents the advantages and disadvantages of various physiological mechanisms of gelation, along with the commonly used polymers associated with each mechanism.

Chemical methods include enzymatic crosslinking, irradiation, click-reaction, genipin, and thiol oxidation stimulated gelling reactions (Forouhe Zahir-Jouzdani et al., 2018). Chemical methods of gelation involve chemical reactions crosslinking the polymer chains. Although crosslinking is known to develop hydrogels with

improved mechanical strength, chemical reactions producing side products or even the crosslinkers used, have the potential to be toxic to cells. Chemical reactions such as click-reactions, enzymatic reactions, and other crosslinking strategies have been developed to provide with non-toxic side products. However, instability of gelation or of the enzymes/crosslinkers used and weak mechanical properties of the product gels remain significant constraints (Bi & Liang, 2016).

Table 2.1 Benefits and limitations of physiological mechanisms of gelation.

Physiological mechanism of gelation	Commonly used polymers	Benefits	Limitations	References
Temperature-induced	- Negatively induced-poly-N-isopropyl Acrylamide, Chitosan, cellulose, PEG, PLGA - Positively induced-Gelatine, amylose, polyacrylamide, Polyacrylic acid (PAA), agarose, amylopectin - Reversible - poloxamers	- Easy adjusting of LCST and UCST by combinations/varying concentrations of polymers - Absence of any significant irritation with poloxamers at mucosal sites - Transition at body temperature is safe - Does not require any harmful crosslinkers	- Storage issues - Low mechanical strength - Rapid erosion - Poor mucoadhesion -Slow gelling time	(Budumuru et al., 2020; Huang et al., 2019; Wu et al., 2019; Forouhe Zahir-Jouzdani et al., 2018)
Ion-induced	Gellan gum, Sodium alginate, Carrageenan, pectin	- Non-irritant in nature - Use of natural polymers - Non-cytotoxic	- Weak mechanical properties - Formation of heterogeneous gels in some cases	(Wu et al., 2019; Forouhe Zahir-Jouzdani et al., 2018)
pH-induced	PAA derivatives such as carbopol's and polycarbophils, and chitosan.	- Good stability with drugs not sensitive to pH changes. - Some polymers such as carbopol are found to be sufficiently mucoadhesive.	-Requires acidic/basic conditions to maintain low viscosity in solution state - Limited in their ability to deliver pH-sensitive actives - Can cause discomfort at the site of application	(HB N & Pawar, 2010; Wu et al., 2019; Forouhe Zahir-Jouzdani et al., 2018)

Physiologically responsive in-situ gels are known to have weak mechanical attributes, require extended time to gel, and in case of thermoresponsive poloxamers even lack mucoadhesion (Huang et al., 2019; Forouhe Zahir-Jouzdani et al., 2018). Incorporating mucoadhesive polymers such as carbopol, HPMC, and hyaluronic acid have been shown to reverse the limitations of these gels and develop sustained-release formulations (Elmowafy et al., 2019; Mayol et al., 2008; P. Ravi et al., 2015; Barbara Vigani et al., 2019).

2.4 Mucoadhesive polymers used in buccal formulations.

Polymers that are widely utilized in buccal drug delivery systems and possess mucoadhesive properties due to strong hydrogen bonding include a range of natural, synthetic, and semisynthetic materials. These polymers are particularly effective in enhancing the adhesion of drug formulations to the buccal mucosa, improving the retention time and thus the therapeutic efficacy of the drug (Asane et al., 2008; Chatterjee et al., 2017). Commonly used mucoadhesive polymers for buccal drug delivery applications include polyacrylates, cellulose derivatives, alginate, chitosan, pectin, and hyaluronic acid.

2.4.1 Polyacrylates

Synthetic polymers like polycarbophils and carbomers (e.g., carbopol) are polymers of acrylic acid (polyacrylates). These polymers are able to form hydrogen bonds with the mucosal surface, allowing them to adhere strongly to the buccal tissue. Their ability to swell in water and form gels further enhances their adhesive strength, making them ideal for controlled or sustained drug release applications in buccal systems (Chatterjee et al., 2017). A systematic review conducted by Mohammad Hamdi, Azmi, Mohd Sabari, et al. (2023) highlighted carbopol's effectiveness as a mucoadhesive polymer, demonstrating its ability to provide strong mucoadhesion, extend residence time in the oro-mucosal cavity, and enhance the permeation of active ingredients.

2.4.2 Cellulose derivates

Cellulose derivates like hydroxypropyl cellulose (HPC) and hydroxypropyl methyl cellulose (HPMC) adhere to mucosa by the strong hydrogen bonds coupled between the carboxylic group and glycoproteins found in mucin, contributing to a stable and prolonged adhesion to the buccal mucosa. These polymers are commonly used in the formulation of buccal tablets, films, and gels, offering advantages like easy fabrication and the ability to control drug release (Chatterjee et al., 2017). The concentration of HPMC plays a significant role in modulating the drug release profile in mucoadhesive formulations. In a study by Jaipal et al. (2015) involving buccal discs, it was found that increasing the concentration of HPMC led to a slower release of mannitol. This was attributed to the more substantial gel formation at higher concentrations, which created a more rigid structure, reducing the rate at which the drug was released. However, the higher concentration of HPMC also improved mucoadhesion, leading to an extended residence time of the formulation in the oro-mucosal cavity.

2.4.3 Alginate

Alginate, a natural polysaccharide extracted from seaweed, contains both hydroxyl and carboxyl functional groups capable of forming hydrogen bonds with the mucosal surfaces. These interactions contribute to its mucoadhesive properties, making alginate an effective material for buccal drug delivery systems. The mucoadhesive strength of alginate is pH-dependent, with lower pH levels leading to reduced chain entanglement of the alginate polymer. This decrease in chain entanglement results in a smaller surface area

of contact between the alginate and mucin, thereby reducing its mucoadhesive properties (Chatterjee et al., 2017). In addition to its mucoadhesive properties, the use of alginate as a single polymer in drug delivery systems presents some limitations. One significant drawback is its relatively low gel strength, which leads to the formation of soft gels that may not provide adequate mechanical support for sustained mucoadhesion (Ahmad Raus et al., 2021). Additionally, alginate's in vivo degradation is typically slow and can be unpredictable, which may compromise its effectiveness in drug release applications. These challenges can be mitigated by combining alginate with other mucoadhesive polymers, such as chitosan, carbopol, or HPMC, which can enhance its mucoadhesive strength, improve gel integrity, and optimize the degradation rate (Bouhadir et al., 2001). Alternatively, the formation of alginate microparticles can address these issues by increasing the surface area available for interaction with mucosal tissues, thereby enhancing mucoadhesion (Ahmad Raus et al., 2021; Chatterjee et al., 2017).

2.4.4 Chitosan

Chitosan, a cationic polymer derived from chitin (typically sourced from crustaceans), is extensively studied and commonly used in mucoadhesive formulations, particularly in drug delivery. Its solubility in weak acids, such as acetic acid, results from the protonation of its amino groups (-NH2) at low pH, which enhances its mucoadhesive properties in acidic environments. Chitosan's mucoadhesion is driven by hydrogen bonding, electrostatic interactions, and conformational flexibility, which enable strong adhesion to mucin. The extent of adhesion varies with mucin composition, particularly sialic acid content. In buccal drug delivery applications, chitosan faces limitations such as inadequate mechanical strength and excessive swelling, which can impair the controlled release of drugs. However, studies have demonstrated that these issues can be moderated through chemical modification or derivatization of chitosan, enhancing its stability and extending its release profile (Arpa et al., 2023; Chatterjee et al., 2017).

2.4.5 Pectin

Pectin, a biodegradable polysaccharide extracted from cell walls of plants, exhibits mucoadhesion through hydrogen bonding and electrostatic interactions with mucin. The carboxyl groups in pectin facilitate H bonding, while increased pectin concentration in aqueous solutions can cause electrostatic repulsion, leading to polymer chain uncoiling and enhanced adhesion. Although hydrogen bonding and electrostatic repulsion mechanisms appear contradictory, both contribute to mucoadhesion. As a hydrophilic polymer, pectin is highly susceptible to water, which can limit its effectiveness in sustained-release buccal formulations by promoting rapid swelling and degradation. However, research has demonstrated that crosslinking pectin can mitigate these water-sensitive limitations by enhancing its structural integrity and reducing its solubility in aqueous environments. While crosslinking improves the stability of pectin in sustained-release applications, it has been observed to reduce its mucoadhesive properties (Szekalska et al., 2023).

2.4.6 Hyaluronic acid

As a biodegradable and biocompatible polymer, hyaluronic acid is another common polymer extensively researched for its mucoadhesive properties. Its bioadhesive properties are primarily attributed to its random coil structure, which allows entanglement with the mucosal layer by formation of hydrogen bonds, enhancing mucoadhesion. Previous research has demonstrated that by structurally modifying the compound by introducing thiolation or by lowering its molecular weight, its mucoadhesive properties can be enhanced. Such modifications allow for sustained release and improved drug absorption, making hyaluronic acid a versatile material for buccal drug delivery systems (Chatterjee et al., 2017).

2.5 Techniques for fabricating buccal formulations

Developing buccal formulations requires a focus on creating dosage forms that can be administered through the mucosal lining of the mouth. Fabrication techniques involved depend on the choice of dosage form being developed. The choice of formulation directly influences the manufacturing method, which must ensure the proper release profile, drug stability, and patient acceptability.

2.5.1 Solid dosage forms

Typical solid dosage forms include tablets and films/patches, with each involving different fabrication techniques (Chinna Reddy et al., 2011).

2.5.1.1 Buccal tablets

Buccal tablets are one of the most common solid dosage formulations, which dissolve or disintegrate in the buccal mucosa allowing the drug to be absorbed. These are typically formulated using direct compression, a process that begins by ensuring the drug and excipient particles have a consistent size, either by mixing them directly or using a mortar and pestle. Next, binders and lubricants are added to the blend. The final mixture is then compressed into the desired shape and size, usually using a tablet compression machine (Çelik, 2017). Tablets are formulated with the ability to release the drug to be absorbed directly into the buccal mucosa or in the saliva, wherein they may face the constraint of being accidentally swallowed. Furthermore, tablets are usually found to cause patient discomfort, especially when fabricated for sustained release of active ingredients (Chinna Reddy et al., 2011).

2.5.1.2 Buccal films and patches

Buccal films and patches are among the most widely preferred dosage forms by patients due to the comfort provided by their flexibility and are ideal for delivering active ingredients in a sustained fashion. They are generally fabricated using either solvent casting or hot melt extrusion. Hot melt extrusion technique involves heating a mixture of drug and other excipients and extruding the molten substance through an orifice or mould to form homogeneous films. This technique is suitable for drugs that are poorly soluble, as they can be easily dispersed in the dosage forms. However, it is limited for active ingredients, polymer, and other

excipients that are temperature sensitive (Chinna Reddy et al., 2011; Shipp et al., 2022). Solvent casting is a process where the drug and excipients are dissolved in a solvent, which is then poured onto a flat surface to form a thin layer. Afterward, the solvent is allowed to evaporate, leaving behind a thin film. While solvent casting is an effective method for producing buccal films, several factors can impact the quality and safety of the final product, such as drug stability, solvent residues, and film uniformity. Some drugs may degrade during the process, and residual solvents, particularly organic ones, can pose toxicity risks or cause irritation. Achieving consistent film thickness and drug distribution is also challenging, which can affect drug release and efficacy (Shipp et al., 2022). Other methods for fabricating films include electrospinning and spray drying. The former includes the application of high voltage to create polymer fibres that are then collected, while the latter involves atomizing a drug-polymer solution into a fine mist, which is subsequently dried to form films. Both electrospinning and spray drying have limitations in developing buccal films, including challenges with achieving uniform drug distribution and controlling the mechanical properties of the films (Łyszczarz et al., 2021; Wang et al., 2022).

2.5.2 3D printing techniques for fabricating solid dosage forms

Three-dimensional printing is a type of additive manufacturing fabrication method that involves depositing material in a layer-by-layer fashion. 3D printing provides the ability to achieve consistent drug distribution within the material, ensuring uniformity throughout the dosage form. This technology also enables the creation of personalized dosages tailored specifically to individual patient needs. By customizing the shape, size, and drug release profile, 3D printing allows for more precise control over the therapeutic dose, accommodating variations in patient-specific factors such as age, weight, and disease conditions (Siamidi et al., 2020; Zhu et al., 2020). There are several 3D printing techniques, with fused deposition modelling (FDM) and extrusion-based printing being among the most widely used for the development of buccal formulations (Shipp et al., 2022).

2.5.3.1 Fused deposition modelling (FDM)

In FDM, the material, typically a polymer or drug-loaded composite, is heated and extruded to form thermoplastic filaments. These filaments are then used to build up the desired structure layer by layer. When combined with Computer-Aided Design (CAD), specific design models with precise shapes and dimensions can be created. This technique is particularly suited for creating complex geometries and can be used to print mucoadhesive buccal formulations that provide localized drug release. This technique has several limitations when applied to pharmaceutical formulations, including a restricted range of suitable materials, particularly for heat-sensitive drugs, as the high temperatures involved can degrade certain active ingredients. Nozzle clogging and filament quality are critical factors that often compromise the quality and dose consistency of the dosage form developed (Elkanayati et al., 2022; Shipp et al., 2022).

2.5.3.2 Extrusion-based printing

This technique involves the continuous extrusion of a material through a syringe-based nozzle to build up the desired shape layer by layer. It is commonly used in the pharmaceutical industry for creating oral dosage forms, including buccal patches and films, as it allows for the integration of multiple components (e.g., drugs, excipients, and polymers) into a single printed object with high precision. Extrusion-based 3D printing of polymers, especially natural mucoadhesive polymers, has been found to be beneficial to fabricate controlled drug release systems (Aguilar-de-Leyva et al., 2020; Azad et al., 2020; Park et al., 2019). Bioprinting, a technique used to print scaffolds and cells into functional biomaterials, is being popularly used for 3D printing pharmaceuticals. Allevi 3D extrusion bioprinter has been widely used for printing oromucosal films. The use of extrusion-based bioprinters in pharmaceutical applications offers significant benefits, such as the ability to develop films with higher doses. Additionally, this method allows for the printing of thermolabile active ingredients and polymers without degradation, due to the lower temperatures required for printing compared to the higher temperatures needed in fused deposition modelling and hot melt extrusion techniques (Tian et al., 2019). Research by E. Sjöholm and N. Sandler (2019) used Allevi 3D extrusion bioprinter to print orodispersible films containing hydroxypropyl cellulose polymer combined with warfarin sodium as the active ingredient to provide paediatric and geriatric patients with personalized doses. Another study utilized a bioprinter to fabricate mucoadhesive oromucosal films in various shapes and sizes, considering the potential of these films to be tailored to meet specific patient needs for treating mouth ulcers (Shipp et al., 2022).

A significant example of 3D printing's capability to produce personalized pharmaceutical doses was seen in 2015, when the FDA approved Spritam® (levetiracetam). This orodispersible tablet, created through 3D printing, highlighted the potential of additive manufacturing in developing tailored drug formulations (Fitzgerald, 2015). Patient-specific personalization of drugs such as cannabinoids can be achieved through 3D printing techniques. The technology could transform how cannabis products are made, allowing for not just personalization but also precision and new forms of consumption. However, it's an emerging area that is still under research. Paraskevi Kyriaki Monou et al. (2022) 3D printed films with polymers such as alginate, along with cannabinoids encapsulated in nanoparticles intended for promoting topical wound healing. Research is ongoing into oral food-grade formulations of cannabidiol. In a study by Andriotis et al. (2020) , cannabinoid-based inks were developed using pectin and honey. These inks, when 3D printed and dried, resulted in the formation of solid structures suitable for potential oral delivery. Research by Abdella et al. (2023) demonstrated the potential of 3D printed mucoadhesive films incorporating nanocarriers of cannabinoids to offer sustained release capabilities while also enabling personalized dosing. This highlights the flexibility and precision of 3D printing technology in creating tailored cannabinoid formulations with controlled release profiles. Highly lipophilic drugs like cannabinoids, coupled with their poor solubility, present significant

formulation challenges. To overcome these issues and improve the bioavailability of the dosage forms, careful selection of excipients is crucial, especially when designing buccal delivery systems.

2.5.3 Semi-solid dosage forms

Semi-solid buccal formulations, including gels, ointments, creams, and pastes, offer numerous advantages for localized and systemic drug delivery via the buccal mucosa. Gels are widely favoured, particularly when formulated with mucoadhesive polymers, due to their ability to sustain drug release into mucosal tissues. However, they often struggle to provide precise drug dosages, which limits their applicability (Barua et al., 2016). In-situ gels address this limitation by allowing for accurate dosage delivery through a solution-based formulation (B. Vigani et al., 2020). Semi-solid dosage forms are typically prepared by either mixing the drug and excipients at room temperature (cold-method gelation), evaporating the solvent, or creating emulsions by combining oil and aqueous phases, particularly in the formulation of creams (K. Garala et al., 2013; Siemiradzka et al., 2020).

2.6 Formulation strategies for enhanced buccal delivery of cannabinoids

Cannabinoids such as cannabidiol (CBD) and tetrahydrocannabinol (THC) are highly lipophilic compounds, with their logP < 5 values reflecting their significant hydrophobicity. This poor water solubility creates formulation challenges, making it difficult to incorporate them into conventional dosage forms (Gallardo et al., 2024). Additionally, their low bioavailability upon administration can further hinder the development of effective cannabinoid-based therapies. The buccal route, however, offers a promising alternative to enhance the bioavailability of cannabinoids. To optimize cannabinoid delivery via this route, formulation strategies must focus on integrating these lipophilic active ingredients effectively into dosage forms. This involves careful selection of excipients as well as the use of compounds that enhance the permeation of cannabinoids into the buccal cavity, ensuring efficient absorption and improved therapeutic outcomes. To address the physicochemical challenges of cannabinoids, researchers are exploring innovative dosage forms and advanced delivery mechanisms.

2.6.1 Development of lipid-based formulations

Cannabinoids such as CBD and THC are soluble in lipids and hence have been formulated as oral and oro-mucosal solutions using a wide range of oil carriers. Studies have consistently shown that lipid-based dosage forms exhibit superior bioavailability compared to lipid-free formulations. This advantage can be attributed to several key factors that work synergistically to enhance drug absorption and improve therapeutic outcomes. First, lipid-based formulations significantly improve the solubility of drugs, especially those that are poorly soluble in water, by incorporating the drug into lipid carriers such as emulsions, micelles, or liposomes. This increases the drug's availability for absorption in the gastrointestinal tract. In addition, lipid-based systems enhance membrane permeability, facilitating the passage of drugs through the intestinal walls

and into the bloodstream. The lipid molecules interact with cell membranes, allowing for more efficient passive diffusion of the drug, particularly for lipophilic compounds that have difficulty crossing aqueous environments. Moreover, lipid-based formulations promote drug absorption via the lymphatic system. Researchers have also proven the ability of medium-chain triglyceride oils to significantly improve the delivery of CBD (O'Sullivan et al., 2024). However, oil-based formulations delivered via the buccal route face the issue of being unintentionally swallowed. Johnson et al. (2024) found that the bioavailability of oral CBD capsules and sublingual CBD oils was similar, indicating that the CBD was likely swallowed before any absorption could occur through the oro-mucosal membrane.

2.6.2 Inclusion complexes of cannabinoids

Inclusion complexes are non-covalent molecular associations where a smaller guest molecule is encapsulated within the cavity of a larger host molecule, offering benefits like enhanced solubility, stability, and controlled release. Cannabinoids can be encapsulated within the cavity of a host molecule, typically a cyclodextrin or a polymer. Cyclodextrins, which are cyclic oligosaccharides, are commonly used as host molecules due to their unique ability to form inclusion complexes with a wide variety of substances, including hydrophobic compounds like cannabinoids. The host molecule's cavity allows the guest (the cannabinoid) to be trapped within, often improving its solubility, stability, and bioavailability. By forming inclusion complexes, the water solubility of cannabinoids is enhanced, making them more suitable for oral, sublingual, or topical administration. Additionally, these complexes can help protect cannabinoids from environmental factors like oxidation and degradation, improving their shelf life and stability (Adriana Ribeiro et al., 2024). Studies have shown that incorporating cannabinoids as inclusion complexes developed with cyclodextrins or chemically modified cyclodextrins can improve the permeation, release, and bioavailability of cannabinoids in buccal formulations (Mannila et al., 2007; Mannila et al., 2005; Mannila et al., 2006).

2.6.3 Cannabinoids in nano-formulations

Nanoformulations, including nanoemulsions, nano-lipid carriers, and nanoparticles, are advanced dosage forms that improve cannabinoid stability, enhance absorption through oro-mucosal membranes, and increase bioavailability. These nanoformulations improve bioavailability through several mechanisms, such as altering surface characteristics, minimizing particle size, optimizing drug distribution, and safeguarding poorly soluble compounds. By reducing particle size, these formulations increase the surface area for absorption, leading to more efficient uptake by the body. Surface modifications can also enhance interactions with biological membranes, facilitating better penetration and absorption. Additionally, nanoformulations help protect sensitive, poorly water-soluble drugs from degradation, ensuring greater stability and more effective delivery to target sites. These strategies collectively enhance the therapeutic potential of cannabinoids by ensuring they are absorbed more efficiently and effectively in the body (Banerjee et al., 2024; Provenzano et al., 2024). Various nanoformulations of CBD are currently being developed, with preclinical evidence suggesting they

effectively alleviate the symptoms they are designed to treat. However, nanoformulations face the challenge of limited understanding regarding their long-term in vivo toxicity, making it essential to fully assess their safety and potential for adverse effects (Sharma et al., 2024).

2.6.4 Incorporating terpenes into dosage forms.

The incorporation of terpenes into cannabis-based dosage forms not only enhances the flavour profile but also amplifies the therapeutic effects of cannabinoids through synergistic interactions. Both terpenes alone and in combination with cannabinoids have demonstrated a range of beneficial effects, including anti-inflammatory, analgesic, neuroprotective, and other therapeutic properties, as evidenced by numerous in-vitro, animal, and clinical studies. These studies suggest that the presence of terpenes may optimize the medicinal potential of cannabis by potentiating the biological activity of cannabinoids, offering a broader spectrum of health benefits (Hanuš & Hod, 2020). Furthermore, terpenes are found to improve the permeation capability of cannabinoids. Terpenes are recognized for their safety by the U.S. Food and Drug Administration (FDA), and studies have found that naturally occurring terpenes are less toxic than synthetic permeation enhancers like laurocapram (Azone). This underscores the potential of terpenes as safer alternatives in various formulations, offering both therapeutic benefits and a lower risk of adverse effects (Chen et al., 2016; Sapra et al., 2008).

2.7 Cannabinoid formulations developed for oro-mucosal routes.

2.7.1 Sprays

Formulations comprising cannabinoids as active ingredients for oro-mucosal delivery are being researched. Sativex, an oro-mucosal spray, is approved by the FDA for treating spasticity in multiple sclerosis (MS) patients and contains 70% of CBD and THC in similar ratios (1:1), 5% minor cannabinoids, and other phytochemicals of two standardized cannabis plant extracts. It is also currently under phase III clinical trial for the treatment of cancer pain and is being investigated for therapeutic effects in polyneuropathy, HIV-associated neuropathy, and palliative care (FDA, 2021; Itin et al., 2019; Kocis & Vrana, 2020). However, formulation limitations of the spray include the need for repeated administration to achieve desired effects (Duran et al., 2010), varying onset of action (15-40 mins) (Tanasescu & Constantinescu, 2013), and excipients such as ethanol causing ulcers and lesions due to frequent use (Scully, 2007). Furthermore, similar 11-OH-THC/THC ratios were observed with both Sativex and oral formulations, indicating failure to evade first-pass effects, as it was found that a larger amount of the dose administered was accidentally swallowed (Itin et al., 2019; Karschner et al., 2011).

Pilot studies of NanaBis™, a buccal spray containing aqueous soluble nanoparticle solutions of CBD and THC, demonstrated that it was two times higher in bioavailability when compared with Sativex. The formulation comprises of strategic delivery of cannabinoids using nanoparticles, which enhance their absorption from

mucous membranes. More than 40% of the patients with progressive cancer experiencing severe pain (total number of participants, n = 25) reported amelioration from pain, measured by their mean pain scores upon administering up to 3 sprays every 4 hours. This spray is currently under clinical trial phase III for opioid management in metastatic cancer patients. It was noted that 72% of the patients reported mild or moderate drowsiness, nausea, and vomiting (Clarke et al., 2020). Similarly, Provenzano et al. (2024) formulated a solution of cannabinoid nano-emulsion with the ability to self-assemble. The in-vivo bioavailability of the formulation was found to be higher when compared with oral formulations of cannabinoids. Such formulations of nanoparticles and nanoemulsions require frequent administration and are lacking in evidence on the effectiveness of the drug penetrating the buccal mucosa.

2.7.2 Solid dosage forms

Alternative to sprays, research has also explored formulation of solid dosage forms to deliver cannabinoids through the oro-mucosal routes. Solid formulations containing complexes of THC/CBD with cyclodextrins, which are cyclic oligosaccharides known to improve the lipophilicity of the API, were developed as either compressed tablets or as gelatine capsules to enhance the bioavailability of the cannabinoids (Mannila et al., 2005; Mannila et al., 2006). Mannila et al. (2006) identified in their later research that naturally available β cyclodextrin could be added at lower bulk masses compared with randomly methylated cyclodextrins. These complexes were found to have quicker dissolution than when using plain cannabinoids in capsules and superior bioavailability compared with oral administration of ethanolic cannabinoids (Mannila et al., 2007). However, the formulation faces disadvantages of low residence time in the sublingual region, which might lead to the cannabinoids being swallowed rather than penetrating the mucosal area. Cannabinoid lozenges (Trokie® Lozenges) as alternative formulations to Sativex for treating chronic pain and palliative care are being researched. These Lozenges are susceptible to accidental swallowing, have reported late-onset of action, and lack validated pharmacokinetic data in humans (Crowley et al., 2018). Monton et al. (2024) developed tablet wafers containing cannabis extracts that disintegrate in saliva, enabling the immediate release of cannabinoids into the oro-mucosal cavity for fast absorption. However, the wafers can be unintentionally swallowed and require in-vivo studies to validate their effectiveness and safety.

2.7.3 Mucoadhesive formulations

As understood previously, the use of excipients that can adhere to the mucosa might be suitable for carrying the active ingredient stably. Itin et al. (2020) fabricated a mucoadhesive shell by compressing mucoadhesive polymers carbopol and hydroxypropyl cellulose of high molecular weight (Klucel) and other excipients. Upon completion of adhesion of the shell to the porcine buccal mucosa in both ex-vivo and in-vivo studies, CBD in 1:1 ethanol: propylene glycol was administered orifice of the mucoadhesive shell facing away from the mucosa, and the shell was able to hold the solution without any leakages from inside. The entire formulation was removed within 8 hours. The researchers were able to show in their in-vivo study, slow and controlled

permeation of CBD in the oral mucosa, upon measuring the plasma levels. However, there was a lack of correlation between their in-vivo and ex-vivo permeation studies, as no permeation occurred when using a diffusion chamber. The researcher's attribute this to the ineffectiveness of the organic solvents used to facilitate CBD release into the receiver chamber. Furthermore, the formulation composition used was similar to Sativex, thus not eliminating the long-term adverse effects associated (Itin et al., 2020).

Taha et al. (2024) employed hot melt extrusion to develop buccal films containing CBD, utilizing various mucoadhesive polymers. Among these, carbopol was found to exhibit superior mucoadhesive strength compared to hydroxypropyl cellulose and other polymers tested. Their work successfully demonstrated the effectiveness of these films for the immediate release of cannabinoids within the buccal cavity. Buccal bi-layered thin films of CBD were fabricated by Laoasoke et al. (2024) using solvent casting technique. Such films demonstrated excellent mucoadhesive strength attributed to HPMC incorporated, and was able to sustain the release of CBD over 4 hours. Abdella et al. (2023) 3D printed buccal films containing nano-lipid carriers of CBD to enhance the delivery and bioavailability of cannabinoids. These films were made mucoadhesive by incorporating polymers like hydroxyethyl cellulose and polyethylene glycol, which help the films adhere to the buccal mucosa for prolonged release. The research demonstrated the feasibility of creating personalized dosage forms for CBD, as well as the potential for developing sustained-release cannabinoid formulations. However, the safety, efficacy, and in-vivo performance of these nanoparticle-based systems still need to be validated through clinical studies to ensure their effectiveness and suitability for therapeutic use.

Söpper et al. (2021) created buccal dosage forms with mucoadhesive polymers, namely carbopol, chitosan, and HPMC, and incorporated CBD in mesoporous silica (carrier) into it. Mucoadhesion with carbopol surpassed other polymers used. Although the use of carbopol also led to lower muco-penetration, which was found to be enhanced by using 5% propylene glycol as the penetration enhancer, it was not superior to the other polymers. The study was able to show the ability of mucoadhesive polymers to counteract the poor residence time of cannabinoid formulations and help achieve controlled release. However, identifying suitable combinations of polymers and excipients is required to improve cannabinoid buccal formulations.

2.8 Conclusions

The buccal mucosa is ideal for bypassing first-pass metabolism, providing sustained effects, and ensuring good patient compliance. However, cannabinoid formulations developed for buccal delivery face several challenges, including poor dosage form stability, the need for frequent administration, susceptibility to washout and accidental swallowing, and a lack of sustained cannabinoid delivery with reliable in vivo and ex vivo permeation correlations. Therefore, there is a critical need to develop sustained-release cannabinoid formulations by identifying suitable excipients and their combinations. The use of mucoadhesive polymers such as HPMC and carbopol has been found to enable the sustained release of drugs. These polymers enhance drug retention at the mucosal site, allowing for prolonged therapeutic effects and improved

bioavailability. Previous studies are strongly evidenced for hybrid physiologically induced in-situ gelling polymers and mucoadhesive polymers to provide sustained effects of drugs, along with ease of administration, good patient compliance, and providing lower costs of large-scale manufacturing. This research will aim to develop sustained-release in-situ gels for buccal delivery with THC and CBD in similar ratios, which has not yet been done in any previous research. Further, in this research extrusion-based bioprinting, a 3D printing technique, will be utilized for developing mucoadhesive films for sustained delivery of cannabinoids. By using such fabrication techniques, precise control over the structure, drug uniformity, and composition of the films can be achieved. Additionally, these methods offer the potential for personalized drug dosing, allowing for the development of tailored formulations that meet the specific needs of individual patients.

These novel buccal formulations developed could possess a wide range of systemic therapeutic benefits, including curbing chemotherapy-induced nausea and vomiting, chronic pain, sleep disturbances, and insomnia, and as an appetite stimulant especially in patients with HIV (Human Immunodeficiency Virus). It could also promote the quality of life of patients in palliative care. Additionally, these formulations have the potential for localized benefits, such as relief from dental pain, inflammation, and mouth ulcers, supported by growing evidence of cannabinoids' effectiveness in addressing these conditions.

Chapter 3: Pre-Formulation Approaches to Improve Solubility and Permeation of Cannabinoids

Abstract

Pre-formulation studies are essential for developing effective pharmaceutical dosage forms, especially for lipophilic compounds like cannabidiol (CBD) and tetrahydrocannabinol (THC), which have significant therapeutic potential due to their anti-inflammatory, analgesic, and neuroprotective properties. However, their low aqueous solubility and high lipophilicity present major challenges in creating effective and patient-friendly formulations. This study aimed to optimize buccal delivery of CBD and THC through a pre-formulation strategy focused on enhancing solubility and mucosal permeation. Surfactants such as Tween 20 significantly improved solubility, with 3% Tween-PBS identified as the optimal medium for in vitro release and diffusion studies. Cyclodextrin-based inclusion complexes using hydroxypropyl-β-cyclodextrin (HP-β-CD) enhanced aqueous solubility up to 388.8-fold for CBD and 450-fold for THC, achieving nearly 100% release within 4 hours. FTIR and SEM confirmed molecular encapsulation and morphological changes. In vitro release studies using Franz diffusion cells highlighted the effects of donor solvent selection, receptor volume, and orifice diameter, with aqueous surfactants outperforming lipophilic vehicles such as MCT oil. To improve mucosal permeation, terpenes including 1,8-cineole, d-limonene, α-pinene, and L-menthol were evaluated individually and in combination, with combinations significantly surpassing individual terpenes and synthetic enhancers like Azone in ex vivo porcine buccal studies. This research establishes a comprehensive pre-formulation framework addressing poor solubility and limited permeability of cannabinoids. The combined use of cyclodextrin complexation and terpene-based permeation enhancers offers a promising platform for novel buccal delivery systems, potentially improving bioavailability, patient compliance, and therapeutic outcomes in cannabinoid-based therapies.

3.1 Introduction

Pre-formulation studies encompass a wide range of experiments and tests to understand physicochemical characteristics of the active ingredients, which are tetrahydrocannabinol (THC) and cannabidiol (CBD) used in this research. Prior to the development of dosage forms, pre-formulation studies are carried out to evaluate the physicochemical properties of the active pharmaceutical ingredient (API) and excipients. These studies guide formulation strategies and influence the stability, bioavailability, and overall performance of the final dosage form. Pre-formulation research addresses key factors such as solubility, dissolution rate or drug's in vitro release, and stability, which are critical in designing a robust, effective, and reproducible pharmaceutical product (Chaurasia, 2016). In addition, pre-formulation studies involve the selection of appropriate excipients, including permeation enhancers and solubility enhancers, which facilitate effective delivery and bioavailability of the active pharmaceutical ingredient (API) in the developed dosage forms. These studies also focus on identifying other excipients, such as flavouring agents, sweeteners, and preservatives, which are crucial for improving the patient acceptability, stability, and shelf-life of the final product. (Chalamaiah & Sharma, 2016). Determining the permeation and release of the active ingredients, which are cannabinoids in this study, is done by in vitro studies using Franz diffusion cell. In vitro buccal permeation studies of the drug involve using an artificial membrane and are usually performed to determine experimental conditions for ex vivo permeation analysis. In-vitro techniques are helpful for pre-formulation studies as they provide quick predictions regarding the fate of the drug (cannabinoids) (Wang et al., 2021). Furthermore, validation of analytical methods used to assess formulation parameters is carried out before the preparation of the formulation, ensuring the reliability and consistency of the techniques to achieve the intended results (Kailash & Rahul, 2023).

Pharmacokinetic effects of cannabinoids are dependent on the route of administration. In the buccal cavity, cannabinoids CBD and THC are absorbed directly into the bloodstream through the oral mucosa, bypassing the gastrointestinal tract and first-pass metabolism in the liver. This results in potentially higher bioavailability and faster onset of effects compared to oral administration. However, as Class II drugs in the biopharmaceutical classification system, CBD and THC exhibit low solubility and high permeability. These properties contribute to challenges in their disintegration and absorption within the body (Qian et al., 2024; Samineni et al., 2022). Hence, solubility studies are crucial to identify the drug/solvent reaction at the site of administration. The analysis for determining solubility includes identifying intrinsic solubility, partition coefficient, and pKa. The API's solubility is affected by temperature, pH, physical agitation, pressure applied, and physicochemical properties (Chaurasia, 2016). Knowing the API's solubility is crucial, as it affects the results of further studies, including in-vitro release experiments, where to maintain sink conditions, the concentration of the drug is required to not exceed 30% of the drug's solubility (Pinto et al., 2020; Seyfoddin et al., 2010). CBD has a logP value of 6.3, indicating its partitioning between n-octanol and water, and a water solubility of 12.6 µg/ml. It exhibits weak acidic properties with a pKa of 9.1. THC has a slightly higher logP

value of 6.97, a low water solubility of 1-2 µg/ml, and a pKa of 10.6 (Adelli et al., 2017; Patilea-Vrana & Unadkat, 2019; Stella et al., 2021).

3.1.1 Enhancing water solubility of cannabinoids.

Improving the water solubility of hydrophobic drugs like CBD and THC facilitates their dissolution, enhances absorption, and may lead to a quicker therapeutic response. Various approaches, including physical modifications, chemical alterations, and other techniques, are commonly employed to improve solubility (Savjani et al., 2012; Zhou et al., 2022). Physical modifications to improve solubility involve changing the drug's form or structure to enhance its dissolution and absorption (Savjani et al., 2012). Techniques such as reducing particle size (development of micro or nanoparticles) increase surface area for faster dissolution. Polymorphism, where different crystal forms of a drug are used, can also impact solubility, with some forms dissolving more readily. Converting drugs to amorphous forms or creating solid dispersions in hydrophilic matrices have been used to boost solubility of various drugs (Savjani et al., 2012). Chemical modifications to improve solubility involve altering a drug's chemical structure to enhance its dissolution in water or other solvents. One common approach is salt formation, where a drug is converted into its salt form, which is typically more water-soluble. Solubility can also be improved by introducing hydrophilic functional groups, such as hydroxyl or amino groups, and PEGylation, which involves attaching polyethylene glycol chains (Makharadze et al., 2025; Savjani et al., 2012). Research has also identified other methods wherein solubilizers, excipients, and surfactants are used in formulation development to aid the solubility of active ingredients (Savjani et al., 2012). The most widely used method for enhancing the solubility of lipophilic drugs involves formation of inclusion complexes where the non-polar region of the drug, referred to as the guest molecule, is physically entrapped within the cavity of a host molecule such as cyclodextrins (Esteso & Romero, 2024; Zhou et al., 2022).

Cyclic oligosaccharides such as cyclodextrins have a non-symmetrical structure with a hydrophobic cavity from the orientation of glycoside bonds, a hydrophilic surface and hydroxyl groups towards the end, as highlighted in Figure 3.1 below. These non-toxic units are barrel-shaped and comprised of glucopyranoside units joined by α-1,4-glycosidic bonds. These naturally occurring molecules were first isolated in 1891, with three different forms of α-, β-, and γ-cyclodextrins differing in their number of glucose units, size, and solubility. Cyclodextrins are utilized in various fields, including pharmaceuticals, agriculture, and textiles. They can form inclusion complexes with poorly soluble compounds, thereby enhancing the solubility and bioavailability of formulations. In these complexes, the hydrophobic region of the cyclodextrin binds to a non-polar drug through electrostatic interactions or van der Waals forces, typically in a 1:1 or 1:2 ratio (Esteso & Romero, 2024; Adriana Ribeiro et al., 2024; Savjani et al., 2012). To further enhance solubility, chemically modified cyclodextrins, such as hydroxypropyl-β-cyclodextrin (HP-β-CD) and randomly methylated-β-cyclodextrin, have been developed. These modifications effectively increase the solubility and bioavailability of poorly soluble drugs by forming inclusion complexes. HP-β-CD, recognized as generally safe by the

European Pharmacopoeia, is commonly used in pharmaceutical formulations to improve the dissolution rates of active pharmaceutical ingredients (APIs). Additionally, they help stabilize sensitive compounds, reduce toxicity, and enable controlled release, making these cyclodextrins vital in drug formulation, especially for oral and injectable dosage forms (Adriana Ribeiro et al., 2024).

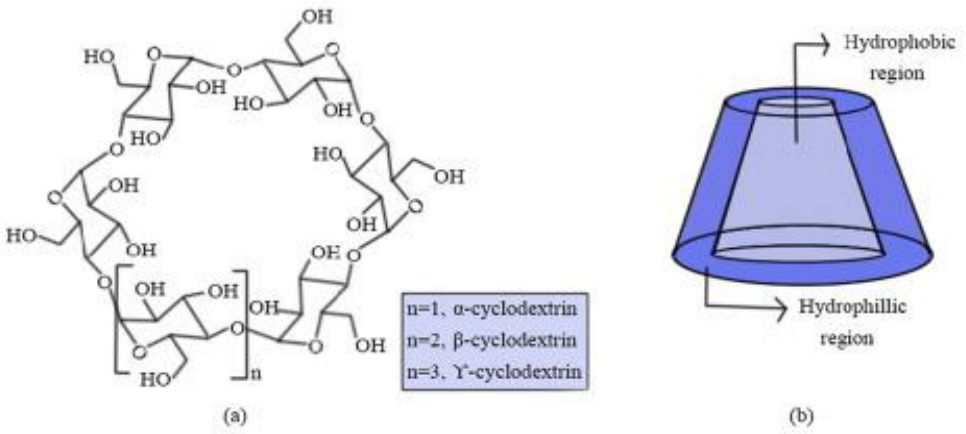

Figure 3.1.Structure of cyclodextrin (Adopted from (Gandhi & Shende, 2021)).

Cyclodextrin inclusion complexes can be formed through several methods, including saturated aqueous solution, kneading, spray-drying, freeze-drying, colloid-grinding, and the supercritical fluid method. Each technique involves the interaction of cyclodextrin and a drug molecule to encapsulate the drug within the cyclodextrin's hydrophobic cavity, improving solubility and stability (Zhou et al., 2022). Among these methods, freeze-drying offers distinct advantages, such as preserving the molecular integrity of both the cyclodextrin and the drug, while avoiding heat degradation. It also enhances the solubility and dissolution rate of the drug by creating a porous structure, improves stability through reduced moisture content, and eliminates solvent residues. These benefits make freeze-drying a highly effective and preferred method for preparing stable, bioavailable cyclodextrin-drug formulations (Zhou et al., 2022). Various cyclodextrins have been explored for their ability to form inclusion complexes with individual cannabinoids, such as THC and CBD, as well as whole-spectrum cannabis extracts, to enhance their solubility. These complexes help overcome the poor water solubility of cannabinoids, improving their bioavailability in pharmaceutical and nutraceutical formulations (Jarho et al., 1998; H. Li et al., 2021; Li et al., 2022; Adriana Ribeiro et al., 2024). Studies have shown that inclusion complexes formed with β-cyclodextrin or HP-β-CD and either THC or CBD enhance their anti-inflammatory and antinociceptive effects (Agabio et al., 2017; Grijó et al., 2023). Lipophilic drugs that are complexed with cyclodextrins have demonstrated improved permeation across biological membranes. In an in vitro permeation study conducted by Park et al. (2023), cyclodextrin complexed with cannabinoid acids were shown to improve the permeation of these compounds across a synthetic membrane by improving cannabinoid solubility (Park et al., 2023).

3.1.2 Boosting permeability of cannabinoids through the buccal mucosa.

The buccal route offers significant potential for cannabinoid delivery, but cannabinoids face challenges in permeating the buccal membrane. The lipophilic nature, molecular size, and low membrane partitioning of cannabinoids, as indicated by their solubility in the mucosal layers and formulation, impede their permeation (Stella et al., 2021). To overcome these barriers, permeation enhancers are essential. These compounds are usually involved in increasing the quantity of active ingredient reaching the buccal epithelium or altering the drug-epithelial interactions. Various chemical permeation enhancers work through different mechanisms to improve drug absorption. Surfactants like sodium dodecyl sulfate and bile salts enhance permeability by extracting intercellular lipids from the buccal mucosa; however, they may compromise the barrier properties of the tissue. Fatty acids have been shown to increase drug permeability, likely by enhancing the partitioning of the drugs into the buccal tissue. While ethanol is an effective permeation enhancer, it can cause mouth ulcers and increase the risk of oral cancer. Laurocapram (Azone) disrupts the lipid bilayer structure, facilitating drug permeation, but it can also cause mucosal irritation and may have potential cytotoxic effects on buccal cells (Meher et al., 2012; Nicolazzo et al., 2005; Sohi et al., 2010).

Terpenes are effective permeation enhancers, known for their ability to increase the absorption of various compounds across biological membranes. They achieve this by interacting with the lipid layers of cell membranes, disrupting their structure, and enhancing the fluidity of the membrane. This disruption creates temporary openings or makes the membrane more permeable, allowing drugs to pass through more easily (Chen et al., 2016). They are naturally occurring, less toxic than chemical enhancers and have been reported to produce effects with minimal and reversible irritation to the tissue when used in low concentrations of 1% to 5%. They are also recognized as generally safe by the US FDA (Chen et al., 2016; Kang et al., 2013; Sapra et al., 2008). When applied to the buccal membrane, terpenes can facilitate the penetration of lipophilic compounds, such as cannabinoids, which typically struggle to cross the buccal mucosa due to their low solubility in aqueous environments (P. Tabboon et al., 2022). Terpenes are hydrocarbons responsible for the distinctive aroma and flavour of cannabis, with over 50 different types identified across various cannabis species (E. Fordjour et al., 2023). In addition to their permeation-enhancing properties, terpenes can also have synergistic effects with cannabinoids. They have the ability to enhance the therapeutic effects of cannabinoids by improving their absorption and increasing their bioavailability (Hanuš & Hod, 2020). Cyclodextrins can improve cannabinoid solubility in aqueous environments, facilitating better interaction with the buccal mucosa. Terpenes, on the other hand, act as membrane disruptors, temporarily altering the lipid bilayer to enhance the penetration of cannabinoids. Together, these enhancers may improve the overall delivery of cannabinoids, leading to improved bioavailability, faster onset, and more controlled therapeutic effects while minimizing side effects.

Previous research has demonstrated that various terpenes possess permeation-enhancing properties. Menthol, a cyclic monoterpene commonly used as a flavouring agent in many oral formulations and found in

the cannabis plant, particularly in Kush strains, has demonstrated the ability to enhance the permeation of hydrophobic drugs. An ex-vivo study utilizing porcine buccal mucosa identified that L-menthol effectively enhanced the permeation of the lipophilic drug dideoxycytidine through the buccal cavity, with the enhancement increasing in a dose-dependent manner as the concentration of L-menthol was elevated (Shojaei et al., 1999). However, the impact of menthol on the permeation of cannabinoids requires further investigation. In a different study, the ex-vivo buccal permeation of the slightly lipophilic drug ropinirole was found to be significantly enhanced by limonene, a terpene with a citrus scent, which is also present in the cannabis plant (De Caro et al., 2012). Sharma et al. (2019) demonstrated that natural terpenes, including d-limonene, cineole, and eugenol, individually enhance the in-vitro drug release of lornoxicam when incorporated into patches, with 4% d-limonene yielding the highest drug release. Similarly, another research found that the transbuccal delivery of benznidazole was significantly enhanced with limonene, when compared to the use of other terpenes such as eugenol and carvacrol (Amaral et al., 2020). P. Tabboon et al. (2022) showed that oleic acid and nerolidol caused either insignificant or retardation of buccal mucosal permeation effects of CBD when combined with lipid-based vehicles such as medium-chain triglycerides (MCT). MCT was used as the vehicle in this study due to its ability to effectively solubilize lipophilic cannabinoids and provide a suitable medium for evaluating terpene-mediated permeation enhancement. This suggests that certain terpenes, like limonene, may be more effective in improving the permeation of drugs through the buccal mucosa, highlighting the importance of selecting the right terpene for optimizing drug delivery.

Essential oil of plant S. desoleana containing specific proportions of terpenes β-pinene, cineole, linalool and α-terpineol were found to permeate the buccal mucosa effectively when formulated into hydrogels and micro-emulsions by Ceschel et al. (2000). This suggests that the terpenes play a crucial role in facilitating the absorption through the mucosal barrier. Using a combination of terpenes, rather than relying on a single terpene, could have the potential to increase the absorption rate of drugs through the buccal mucosa. Numerous studies have established combinations of terpenes in various concentrations to be effective in transdermal permeation of lipophilic drugs (Aqil et al., 2007). The ability of combined terpenes to enhance the permeation of lipophilic drugs through the buccal mucosa remains limited, necessitating further research to better understand their potential.

3.1.3 High performance liquid chromatography (HPLC)

HPLC is an analytical technique used to separate and quantify compounds according to their dispersion due to the interaction between a solid stationary phase and a liquid mobile phase. For detection and quantification of cannabinoids, the most commonly used mobile phase comprises of either methanol or acetonitrile with 0.1% formic acid and a C18 column as the stationary phase (Pourseyed Lazarjani et al., 2020). Method validation is a pre-formulation parameter where the analytical method is validated by determining accuracy, precision, limit of detection (LOD), limit of quantification (LOQ), and linearity. HPLC validation for

cannabinoids has been previously established in our drug delivery research group by Lazarjani et al. (2024). Limit of detection refers to the lowest concentration of a substance that can be detected but not quantified, and LOQ refers to the lowest concentration that can both be detected and quantified. For confirmation, these parameters are re-evaluated and compared with the previously validated HPLC-UV method (Shrivastava, 2011).

This chapter aims to determine the solubility and in vitro release characteristics of cannabinoids THC and CBD. To improve their water solubility for development as in-situ gels or bioinks for 3D printed films, inclusion complexes of both cannabinoids will be formed with beta-cyclodextrin (β-CD) and hydroxypropyl-beta-cyclodextrin (HP-β-CD), which will be further confirmed. Additionally, various combinations and concentrations of terpenes will be evaluated to enhance the ex-vivo permeation of cannabinoids using porcine buccal mucosa. The chapter will also include the reconfirmation of the validated HPLC method as previously established by Lazarjani et al. (2024).

3.2 Materials and methods

3.2.1 Materials

D-Limonene was purchased from Thermo Fisher, New Zealand, 1,8- cineole, α-Pinene from Sigma-Aldrich, New Zealand, laurocapram 95% from AK Scientific, and l-Menthol from Chem express supplied by Focus Bioscience, Australia. Medium chain triglyceride (edible oil) purchased from local store, Auckland. Phosphate buffered saline (PBS) tablets (pH 7.4, Tween-20%, β-CD, HP-β-CD, acetonitrile, Bovine Serum Albumin (BSA), methanol, and MCT oil were purchased from Sigma-Aldrich, New Zealand. Pure isolated CBD and distilled oil of THC was provided by Helius Therapeutics Ltd, New Zealand. Dimethyl sulfoxide from Scharlab S.L., Barcelona, Spain. All other reagents used were of analytic grade.

3.2.2 Solubility Measurements

The solubility of CBD and THC in PBS containing 0.5, 2, 3, and 4% Tween 20 was determined experimentally using the shake-flask method. An excess amount of cannabinoids was added to 1 mL of each PBS solution, which was placed in separate glass vials. The vials were then incubated on a magnetic stirrer at 37 °C for 24 hours. After incubation, the samples were centrifuged at 10,000 rpm for 20 minutes to separate the supernatant. The supernatant was subsequently filtered using a 0.45 µm PVDF syringe filter, diluted appropriately, and analysed by HPLC. The solubility measurements were performed in triplicate for each concentration of Tween 20 in PBS solution (Casiraghi et al., 2020; Tiago et al., 2022).

3.2.3 In-vitro drug release studies

In vitro release of CBD through cellulose membranes (MWCO 14,000 Da) was evaluated using Franz diffusion cell apparatus (Orchid Scientific, India). Use of cellulose membrane was not intended to serve as a rate-limiting barrier, but rather to ensure separation between the donor and receptor compartments. The

cellulose membranes were cut to the required size and hydrated for 24 hours before the commencement of the experiment to ensure proper swelling and functionality. Two Franz diffusion cell configurations were employed to assess the influence of receptor cell volume and membrane diffusion area on CBD release behaviour: one with a 12 mL receptor volume and 15 mm orifice diameter, and another with a 20 mL receptor volume and 20 mm orifice diameter. The donor solutions consisted of CBD (25 mg/mL) dissolved either in medium-chain triglyceride (MCT) oil or in a water: Tween-20 (1: 1 v/v) mixture. For the receptor phase, the compartments were filled with either phosphate-buffered saline (PBS) containing 3% Tween-20 or a methanol: water (1: 1 v/v) solution to evaluate the effect of receptor medium composition on drug solubilisation.

Prior to the experiment, the Franz cells were pre-equilibrated at 37 ± 0.5 °C for one hour to maintain a physiologically relevant and constant temperature. After assembly, 20 mL (for the larger configuration) or 12 mL (for the smaller configuration) of the designated receptor medium was added to each receptor compartment. The pre-hydrated cellulose membrane was carefully mounted between the donor and receptor chambers, ensuring no air bubbles were trapped, and the units were securely clamped. Subsequently, 1 mL of the donor solution was added to each donor compartment. The donor openings were sealed with Parafilm to prevent solvent evaporation and maintain sink conditions throughout the 4-hour study period. Samples were withdrawn at predetermined time intervals (0.5, 1, 2, 3, and 4 hours) from the receptor compartments and immediately replaced with an equal volume of freshly pre-warmed receptor medium (maintained at 37 °C). All experiments were conducted in triplicate, and the collected samples were analysed for CBD concentration using high-performance liquid chromatography (HPLC) (Casiraghi et al., 2020; Kirk et al., 2022).

3.2.4 Synthesis of cannabinoid-cyclodextrin inclusion complexes

3.2.4.1 Preparation of physical mixtures and inclusion complexes

Inclusion complexes of CBD and THC with β-CD and HP-β-CD were formed using a freeze-drying technique. The cannabinoids and cyclodextrins were weighed in a precise 1:1 molar ratio. A 40% (v/v) ethanol solution (40 ml) was used to dissolve the cyclodextrins, with stirring until fully dissolved. Separately, 500 µl of ethanol was used to dissolve the cannabinoids, which were then gradually added to the cyclodextrin solution. The resulting mixture was heated on a hot plate at 30°C and stirred magnetically for 6 hours. Afterward, the mixture was filtered, and the filtrate was solidified in a freeze dryer (Christ alpha series freeze dryer, Osterode am Harz, Germany) for 48 hours. The procedure was adapted from established protocols (H. Li et al., 2021; Park et al., 2023).

Physical mixtures of cannabinoids and cyclodextrins were prepared by thoroughly blending them in a 1:1 molar ratio at room temperature for 5 minutes, followed by storage in a dryer for later use (H. Li et al., 2021).

3.2.4.2 CBD and THC's complexation and loading efficiency in inclusion complexes and solubility studies.

To assess the quantity of cannabinoids (guest molecules) encapsulated within the cyclodextrins (host molecules), it is necessary to determine the complexation and loading efficiency. An accurately weighed amount of the developed inclusion complex (10 mg) was dissolved in 10 mL of methanol and subjected to sonication using an ultrasound probe (UP100H; Hielcher, Germany) at room temperature for 40 minutes to ensure the release of trapped cannabinoids into the solution. The samples were then centrifuged (model 1580R; Gyrozen, Korea) at 4000 rpm for 5 mins and analysed using HPLC to determine the cannabinoid content.

Mass of CBD or THC entrapped (Me), total weight of cannabinoid initially added (Mt), and weight of cyclodextrin used (Mc) are used to calculate the complexation and loading efficiency as shown in equations 1 and 2 below (H. Li et al., 2021).

Equation 3.1 $\text{Complexation effeciency } (\%) = \left(\frac{\text{Me}}{\text{Mt}}\right) \times 100$

Equation 3.2 $\text{Loading effeciency } (\%) = \left[\frac{\text{Me}}{\text{Me+Mc}}\right] \times 100$

The aqueous solubility of the cannabinoids in inclusion complexes was evaluated by dissolving an excess of the prepared inclusion complex, containing approximately 10 mg of CBD or THC, in a conical flask with 20 mL of distilled deionized water. The mixture was magnetically stirred at 37°C for 24 hours, then centrifuged at 4000 rpm for 20 minutes. The resulting supernatant was analysed for cannabinoid content using HPLC (H. Li et al., 2021).

3.2.4.3 Fourier transform infrared (FTIR) spectroscopy of physical mixtures and inclusion complexes of cannabinoids and cyclodextrins.

FTIR spectra of the prepared inclusion complexes, physical mixtures, CBD, THC, β-CD and HP-β-CD were carried out on an FTIR spectrometer (Thermo Scientific, model: Nicolet iS10, USA). Samples were positioned on a monolithic diamond crystal cell, and spectra were acquired in the 4000–500 cm^{-1} range with a 4 cm^{-1} resolution over 32 scans. A background spectrum, captured from the clean empty cell at room temperature (25°C), served as a reference.

3.2.4.4 Characterization by scanning electron microscopy (SEM) of physical mixtures and inclusion complexes of cannabinoids and cyclodextrins.

Schottky field emission SEM (Thermos scientific, HITACHI, SU-70) was used to view the structure of the inclusion complexes, after they were coated using ion sputter (Hitachi E-1045 coater) with platinum for 20 seconds.

3.2.4.5 In-vitro dissolution profiles of the inclusion complexes

In vitro dissolution profiles of the inclusion complexes were determined experimentally using PBS as the dissolution medium. Following the procedure outlined by H. Li et al. (2021), cannabinoids (CBD or THC), each equivalent to 1.5 mg, were added separately to beakers containing 100 mL of PBS, either in their raw form or as inclusion complexes. The solution was magnetically stirred, and the temperature was maintained at 37°C. At predetermined time intervals, 1 mL aliquots were withdrawn and replaced with fresh buffer to maintain a consistent volume of the medium. The samples were centrifuged at 10,000 rpm for 20 minutes to obtain the supernatant, which was then filtered through a 0.45 µm PVDF syringe filter. The filtrate was suitably diluted and analysed using HPLC to determine the cannabinoid concentration.

3.2.5 Ex-vivo penetration studies of CBD with terpenes

3.2.5.1 Porcine buccal mucosa preparation

Fresh pig heads were purchased from a local butcher shop, Auckland. Within an hour of slaughter, inner regions of the cheek were excised carefully uniformly below 0.5 mm thickness with a scalpel and rinsed with saline.

Figure 3.2 below, highlights the porcine buccal mucosa excised. All experiments were performed with porcine mucosa obtained from three different pigs.

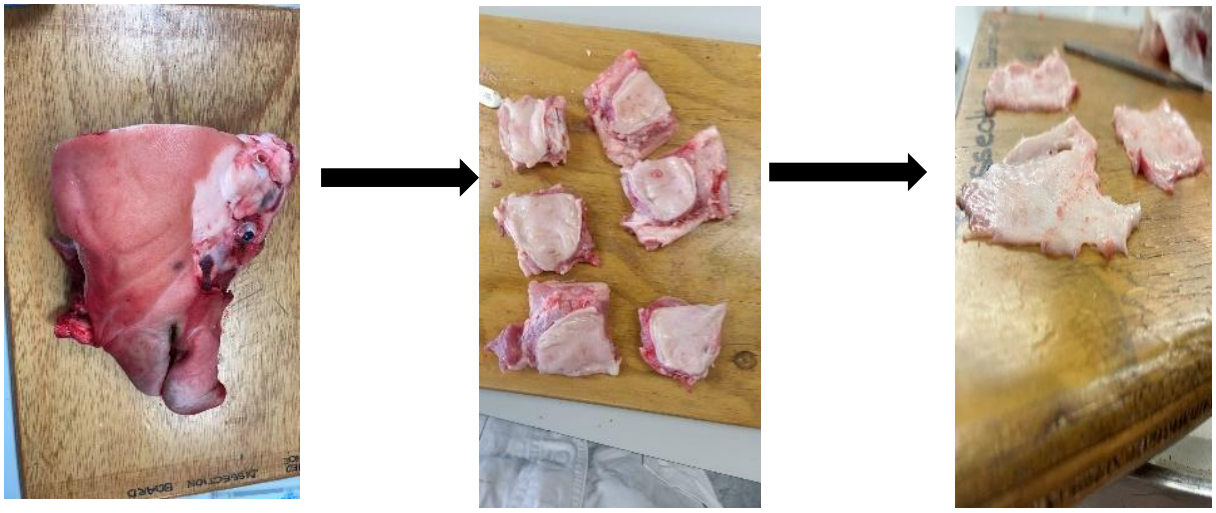

Figure 3.2. Stepwise preparation of buccal porcine mucosa tissue showing (from left to right): freshly obtained porcine cheek tissue, sectioning into smaller pieces, and removal of underlying connective and adipose layers to isolate the mucosal membrane for experimental use.

If required, the tissues were frozen in a standard freezer (-15°C to -25°C) in freshly prepared PBS with 2% DMSO or 10% BSA, added as cryoprotectants (Franz-Montan et al., 2016).

3.2.5.2 Preparation of cannabinoid solutions with permeation enhancers

Donor solutions were prepared by mixing CBD (25 mg/ml) in MCT oil, to which different concentrations and combinations of the terpenes d-limonene, l-menthol, α-pinene, and 1,8-cineole or synthetic enhancer

laurocapram (Azone) were added as listed in Table 3.1 below. The concentrations of permeation enhancers were selected based on literature reports indicating that terpene concentrations up to approximately 5% are generally considered safe for mucosal applications. Therefore, a maximum concentration of 5% was used for individual enhancers, while combinations of enhancers were formulated so that the total concentration did not exceed 5%.

Table 3.1. Formulation codes and concentrations of permeation enhancers in donor CBD solutions.

Solution code	**Concentration of permeation enhancer(s) added % v/v**
CBD	nil
C5l	CBD + 5% limonene
C5M	CBD + 5% Menthol
C5P	CBD + 5% Pinene
C5C	CBD + 5% Cineole
C5A	CBD + 5% Azone
C1.25MCLP	CBD + 1.25%mclp
C3.12L0.6MCP	CBD+3.125%L, 0.625%MCP
C2.5LC	CBD+2.5%L,2.5%C
C2.5MP	CBD+2.5%M,2.5% P
C3.12M0.62LCP	CBD+3.125%M, 0.625%LCP
C3.12P0.62LCM	CBD+3.125%P, 0.625%LCM
C2.5MC	CBD+2.5%M, 2.5%C
C2.5PC	CBD+2.5%P, 2.5%C
C2.5LP	CBD+2.5%L, 2.5%P
C2.5LM	CBD+2.5%L, 2.5%M
C3.12C0.6LPM	CBD+3.125%C, 0.625%LPM

3.2.5.3 Ex vivo penetration with Franz cells

The receptors were filled with 20 mL of phosphate-buffered saline (PBS) containing 3% Tween-20 while maintaining sink conditions, and the cells were pre-warmed to 37°C for one hour to ensure proper temperature equilibration. A piece of porcine buccal mucosa, carefully cut to match the diameter of the cell compartments, was positioned between the donor and receptor sections, and securely clamped in place to create a stable barrier. Subsequently, 1 mL of the prepared donor solution was introduced into the corresponding donor chamber, the openings were sealed with parafilm to prevent any solvent evaporation during the course of the experiment, and it was set up as highlighted in the Figure 3.3 below. After a two-hour period, the porcine buccal mucosa was carefully removed from the setup. The tissue was then gently wiped with absorbent tissue to remove any residual donor solution from the surface of the mucosa. Following this, the CBD that had penetrated through the mucosal layers was extracted for further analysis. This experiment was done with triplicates of each of the above prepared solutions.

Figure 3.3. Set up of the ex vivo penetration using Franz cell.

3.4.5.3 Extracting the cannabinoids deposited in the mucosa.

The porcine buccal mucosa, after permeation, was washed thrice with deionized water, following which it was cut into small pieces. The mucosa was frozen with liquid nitrogen and ground into a powder. A homogenizer (IKA T25 ULTRA-TURRAX, Germany) was used at 8000 rpm for 5 minutes to homogenize the powder dissolved in acetonitrile/water (1:1 v/v) solution. The homogenized solution was then centrifuged at 4000 rpm for 20 mins, supernatant filtered, and filtrate analysed by HPLC. The penetration was calculated by determining the amount of CBD per surface area (μg/cm^2) (P. Tabboon et al., 2022).

3.2.6 Validation of the analytical method

HPLC analysis was performed by injecting 5 µL of the prepared samples into a Shimadzu LC-20 series HPLC system, equipped with a UV detector set at 280 nm for cannabinoid quantification. An Agilent Zorbax Eclipse Plus C-18 column was used for separation, employing an isocratic method with a mobile phase consisting of 84% acetonitrile, 0.1% formic acid, and 16% Milli-Q water. The cannabinoids were eluted and partitioned over a 26-minute run time.

3.2.6.1 Limit of detection (LOD) and Limit of Quantification (LOQ)

The previously validated method was reassessed to confirm its sensitivity by determining the Limit of Detection (LOD) and Limit of Quantification (LOQ). The LOD represents the smallest amount of cannabinoids that can be detected but not quantified, while the LOQ is the lowest amount that can both be detected and accurately quantified. To prepare the external standards, cannabinoids were serially diluted, and six calibration standards were analysed, with six repetitions for each concentration level. The LOD and LOQ were determined by identifying the lowest concentrations that produced a signal-to-noise ratio of 3 and 10, respectively.

3.3 Statistical analysis

Statistical analysis of the data obtained was done using R-programming and GraphPad Prism software (version 10.2.3). Significance was identified by performing one-way Anova (when parametric data was obtained) and Kruskal–Wallis test for non-parametric alternatives followed with post hoc multiple comparisons by Turkey's test. The level of statistical significance was set at $P<0.05$.

3.4 Results and discussion

3.4.1 Solubility of cannabinoids

Cannabinoids are lipophilic in nature, with poor water solubility of 12.6 and 2.8 µg/mL for CBD and THC, respectively (Adelli et al., 2017; Stella et al., 2021). Previous research has determined that the addition of solubilizers such as surfactants or organic solvents can improve their aqueous solubility. However, these solubilizers can impact the penetration of compounds by affecting the barrier tissue and should be used in minimal concentrations (Som et al., 2012). Surfactants like Tween 20 are known to enhance the solubility of lipophilic compounds in aqueous solutions, especially when compared to other surfactants (Kirk et al., 2022; Park et al., 2020). Solubility of cannabinoids CBD and THC in PBS with 0.5, 2, 3 and 4% tween experimentally determined by the shake-flake method was as highlighted in

Table 3.2 below. An increase in solubility of both CBD and THC was observed with increasing concentrations of the surfactant. Similarly, a study by Yang et al. (2021) showed that increasing concentrations of solubilizers such as tween 80, increased the solubility of anthracene, a chemical used as a base for several

chemotherapeutic drugs. Solubility plays a crucial role in establishing appropriate receptor media for in-vitro release and ex-vivo permeation studies. Previous studies have shown that sink conditions are achieved when the drug concentration in the receptor medium does not exceed 30% of the drug's saturation solubility (Seyfoddin et al., 2010). This ensures that the concentration gradient between the donor and receptor compartments is maintained, which is essential for accurate release and permeation measurements. Maintaining sink conditions is critical to avoid saturation, which could alter the release profile and affect the interpretation of permeation data (Ng et al., 2010; Siepmann & Siepmann, 2020). PBS containing 3% Tween 20 was selected as the receptor medium to ensure sink conditions. Although PBS with 2% Tween 20 was sufficient based on calculated solubility thresholds, 3% Tween 20 was employed to provide a greater solubility margin and minimise the risk of receptor saturation during the experiment.

Table 3.2. Solubility of cannabinoids in PBS with different concentrations of tween 20 (n = 3; mean ± SD).

Cannabinoid	**PBS + 0.5% tween**	**PBS + 2% tween**	**PBS + 3% tween**	**PBS + 4% tween**
CBD	2 ± 0.3 mg/ml	8.2 ± 0.43 mg/ml	9.1 ± 0.56 mg/ml	12.82 0.7 mg/ml
THC	0.9 ± 0.22 mg/ml	4.72 ± 0.51 mg/ml	6.625 ± 0.08 mg/ml	8.012 ± 0.15 mg/ml

3.4.2 In-vitro drug release studies

In-vitro release of CBD was conducted using Franz diffusion cells with various receptor media for 4 hrs, including PBS containing 3% tween-20 and a 1:1 mixture of methanol and water. The donor solutions consisted of CBD dissolved in either MCT oil or a water-tween solution in similar ratios. Additionally, two different receptor cell volumes, 12 ml and 20 ml, were tested to assess any potential variations when MCT oil was used as the carrier. Notably, no CBD permeated when MCT oil was employed as the carrier and PBS with 3% tween served as the receptor medium. Research by P. Tabboon et al. (2022) showed that a high affinity of CBD for the carrier vehicle decreases its ability to partition into the membrane. When MCT oil was used as the donor solution, only approximately 0.5–0.6% of CBD was released over 4 hours into the methanol/water (1:1) receptor medium, as shown in Figure 3.5. The limited release is likely due to the strong affinity of CBD for the MCT oil phase, which restricts its partitioning into the receptor medium. In contrast, when water/Tween 20 (1:1) was used as the donor solution, a higher release of CBD was observed. Approximately 6% CBD release was detected in the methanol/water receptor medium after 4 hours, as illustrated in Figure 3.4. Under the same donor conditions, using phosphate-buffered saline (PBS) containing 3% Tween-20 as the receptor medium resulted in a slightly lower release of approximately 4% over the same period

Figure 3.5 presents a comparison of CBD release profiles using different receptor cell volumes. In this study, higher initial release was observed when using smaller 12 mL receptor cells with a 15 mm orifice diameter compared to larger 20 mL cells with a 20 mm orifice. This is likely due to the lower receptor volume in the smaller cells, which results in reduced dilution of the permeated drug and therefore higher detectable concentrations at early time points. However, after the first two hours, the release rate was greater in the

larger receptor cells. This may be attributed to the larger orifice diameter, which provides a greater effective diffusion area and facilitates increased drug transport across the membrane over time. Consequently, receptor cell geometry, including both volume and diffusion area, can influence the observed release kinetics of CBD. Similar observations have been reported in previous studies demonstrating that receptor cell dimensions can affect drug release and permeation behaviour (Maver & Maver, 2022). Smaller receptor cells make it easier to detect the initial concentrations of a drug, as they involve smaller volumes that are less prone to dilution (Finnin et al., 2012), while larger receptor cells with higher orifice diameter have larger membrane surface area and allow for higher drug diffusion, leading to a higher release rates over time (M. L. Hossain et al., 2023). However, the relatively low overall release of CBD across all configurations emphasizes the necessity for additional permeation-enhancing strategies, such as the incorporation of terpenes.

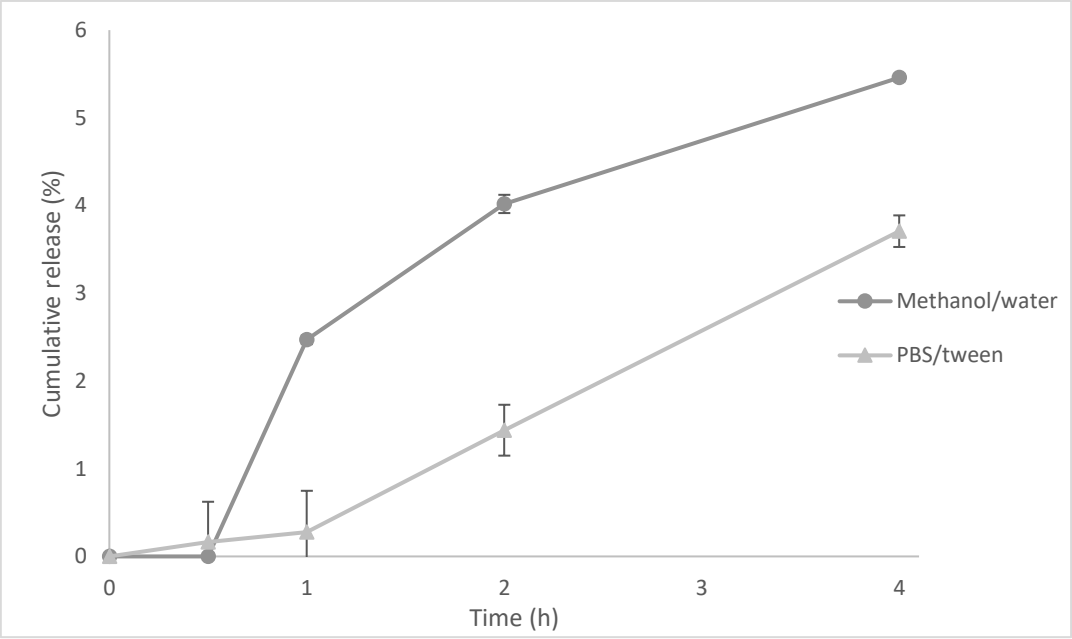

Figure 3.4 In-vitro release profile of CBD using water/Tween 20 (1:1) as the donor phase. The figure compares two receptor media: methanol/water (1:1) and PBS containing 3% Tween-20. Higher CBD release was observed in the methanol/water receptor system, likely due to its greater solubility and partitioning capacity for CBD (n = 3; mean ± SD).

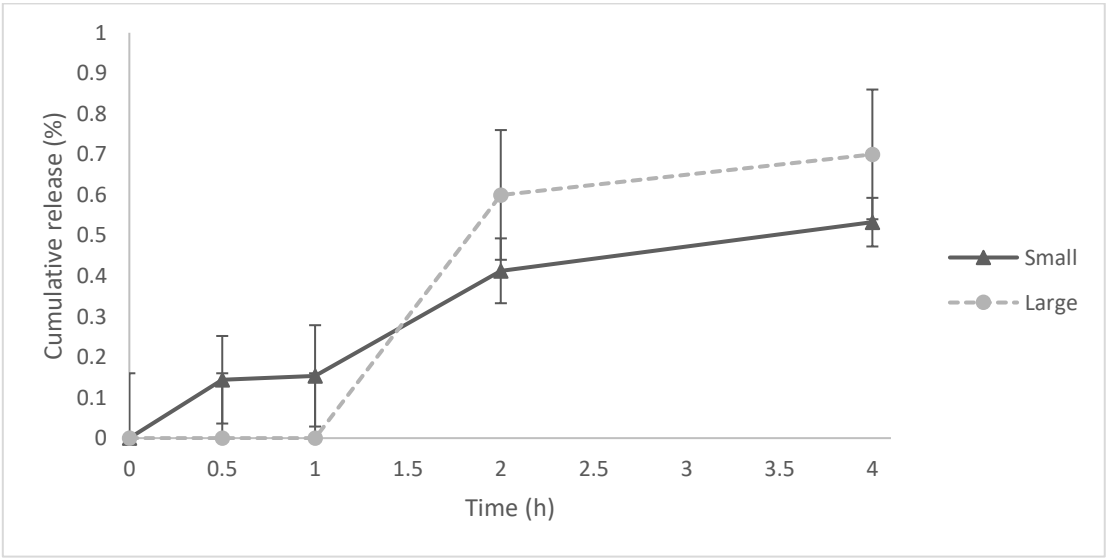

Figure 3.5. In-vitro release profile of CBD using Franz diffusion cells with MCT oil as the donor phase and methanol/water (1:1) as the receptor medium. The figure compares cumulative CBD release (%) over 4 hours using receptor cells with different volumes (12 mL and 20 mL) (n = 3; mean ± SD).

3.4.3 Cannabinoid-cyclodextrin inclusion complexes

3.4.3.1 Complexation and loading efficiency, and solubility enhancement.

The amount of cannabinoids THC and CBD (guest molecules) trapped inside the cyclodextrin (host) inclusion complex is measured by its loading efficiency. Complexation efficiency, on the other hand, represents the percentage of host molecules (cyclodextrins) that participate in forming inclusion complexes with the cannabinoids. In this study, both CBD and THC exhibited complexation efficiencies exceeding 90% w/w with β-CD and HP-β-CD, demonstrating highly effective encapsulation. The loading efficiencies for CBD with both cyclodextrins were consistent with those previously reported by H. Li et al. (2021). Furthermore, the aqueous solubility of CBD and THC increased by 388-fold and 450-fold, respectively, when complexed with HP-β-CD, compared to increases of 16.2-fold and 20.6-fold with β-CD. These findings underscore the superior solubilizing potential of HP-β-CD over β-CD. The detailed values for complexation and loading efficiencies, along with solubility improvements, are summarized in Table 3.3 below.

Table 3.3 Complexation efficiency (CE), loading efficiency (LE), and aqueous solubility of the inclusion complexes developed (n = 3; mean ± SD).

Complex	CE (%)	LE (%)	Solubility
IC β-CD and CBD	95 ± 0.56%	26 ± 0.29%	204.4 ± 0.39 µg/ml (16.2 folds higher than the solubility in water)
IC HP-β-CD and CBD	92.6 ± 0.43%	22.8 ± 0.37%	4.90 ± 0.22 mg/ml (388.8 folds higher than the solubility in water)
IC β-CD and THC	91 ± 0.16%	20 ± 0.08%	57.68 ± 0.87 µg/ml (20.6 folds higher than the solubility in water)
IC HP-β-CD and THC	90.8 ± 0.08%	15.6 ± 0.02%	1.26 ± 0.57 mg/ml (450 folds higher than the solubility in water)

3.4.3.2 Fourier transform infrared (FTIR) spectroscopy of physical mixtures and inclusion complexes of cannabinoids and cyclodextrins.

FTIR analysis was employed to examine the interactions between cannabinoids and cyclodextrins by detecting shifts in the positions of peaks and changes in the frequency of functional group vibrations. Figure 3.6 displays the FTIR spectra of CBD, β-CD, HP-β-CD, their physical mixtures (PM), and the corresponding inclusion complexes, while Figure 3.7 illustrates the spectra of THC, β-CD, HP-β-CD, the PM of THC and the cyclodextrins, and the developed inclusion complexes. In the CBD spectrum, characteristic peaks were observed at 2828 cm−1, 2854 cm−1, 2924 cm−1, and 2964 cm−1, corresponding to the stretching vibrations of -CH3 and -CH2 groups. A peak at 3073 cm−1 was attributed to C-H stretching vibrations from the benzene ring, while the 1600 cm−1 to 1400 cm−1 range corresponded to benzene ring vibrations. The peak at 1214

cm−1 was associated with C-O stretching vibrations. In the FTIR spectrum of the distilled THC oil, a peak at 3074 cm−1 was observed, corresponding to C-H stretching vibrations from the benzene ring. The peaks between 2900 cm−1, and 2800 cm−1 were associated with the stretching of -CH3 and -CH2- groups, common to both CBD and THC. The peaks at 1629 cm−1, 1585 cm−1, 1518 cm−1, and 1444 cm−1 corresponded to benzene ring skeleton vibrations. Meanwhile, the peaks at 1377 cm−1 and 1216 cm−1 were attributed to the bending vibration of -CH3 and the stretching vibration of C-O, respectively.

In the β-CD spectrum, peaks at 2900 cm−1 were linked to C-H stretching vibrations, and additional peaks at 1158 cm−1 and 1031 cm−1 were indicative of C-O and C-O-C stretching vibrations. The HP-β-CD spectrum showed similar features to β-CD, with an additional peak around 3400 cm−1, corresponding to hydroxyl group stretching. FTIR spectra of the physical mixtures of CBD and THC with the cyclodextrins showed a complete overlap of the spectra of the pure cannabinoids and cyclodextrins, suggesting that no interactions occurred between CBD or THC and either β-CD or HP-β-CD. In contrast, the spectra of the inclusion complexes were more similar to those of the cyclodextrins, with prominent cannabinoid peaks such as 1214 cm−1, 1623 cm−1, and 3073 cm−1 significantly reduced or absent. This suggests that CBD and THC was effectively encapsulated within either β-CD or HP-β-CD, forming stable inclusion complexes. Confirmation of inclusion complexes by FTIR are further supported by similar results from previous research (H. Li et al., 2021; Patil & Pandey, 2024; Upadhye et al., 2010).

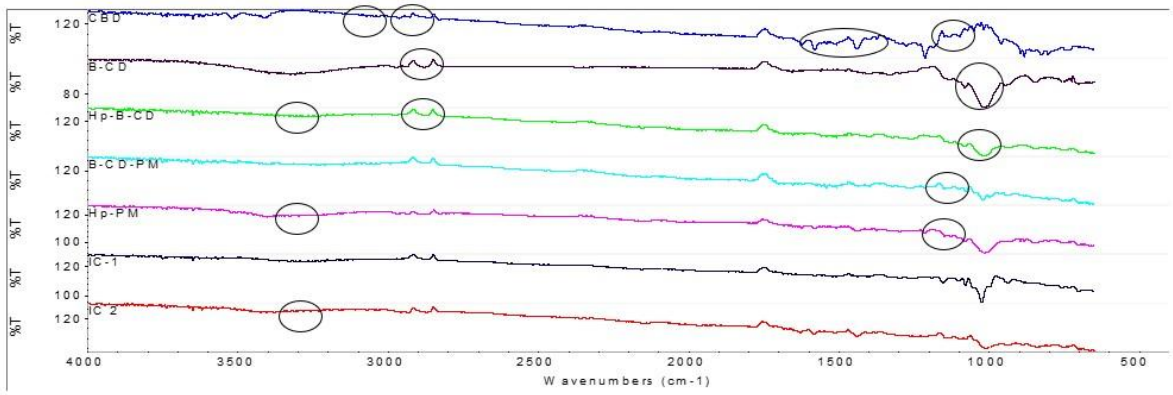

Figure 3.6 FTIR spectra of CBD, β-CD, HP- β-CD, β-CD physical mixtures (PM), HP- β-CD PM, IC1 (inclusion complex of CBD with β-CD), and IC2 (inclusion complex of CBD with HP- β-CD).

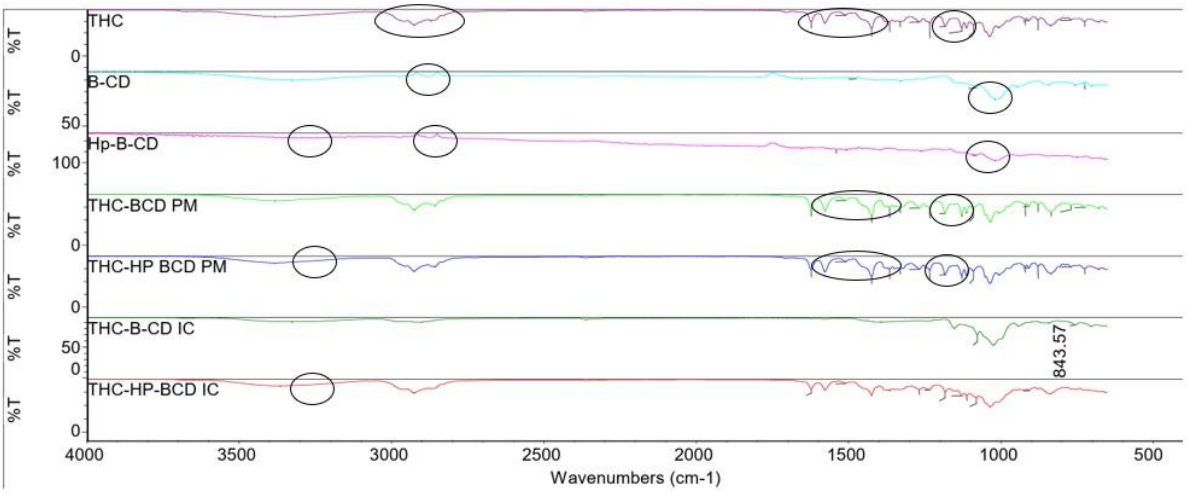

Figure 3.7. FTIR spectra of THC, β-CD, HP- β-CD, β-CD physical mixture (PM), HP- β-CD PM, THC β-CD inclusion complex (IC), and THC HP- β-CD IC.

3.4.3.3 SEM of physical mixtures and inclusion complexes of cannabinoids and cyclodextrins

Scanning electron microscopy (SEM) is commonly used to confirm the formation of inclusion complexes by comparing the morphological differences between pure cannabinoids, cyclodextrins, and their inclusion complexes. Figure 3.8 illustrates the structure of pure CBD, β-CD, and HP-β-CD, as well as their physical mixtures and inclusion complexes developed with both CBD and THC. Cannabidiol (CBD) shows a distinct crystalline structure, while β-CD is depicted with a prismatic crystalline form. HP-β-CD, on the other hand, has a spherical shape with fragmented cavities. These morphological differences help in verifying the formation of inclusion complexes. In the physical mixtures of CBD and the cyclodextrins, the individual structures, some of which were fragmented, were observed without any evident interactions between the components. In contrast, the inclusion complexes exhibited a complete disappearance of the characteristic structures of the individual compounds, indicating successful interactions between the host molecules (β-CD or HP-β-CD) and the guest molecules (CBD or THC). This observation is consistent with previous studies and is further supported by confirmation through FTIR analysis (H. Li et al., 2021).

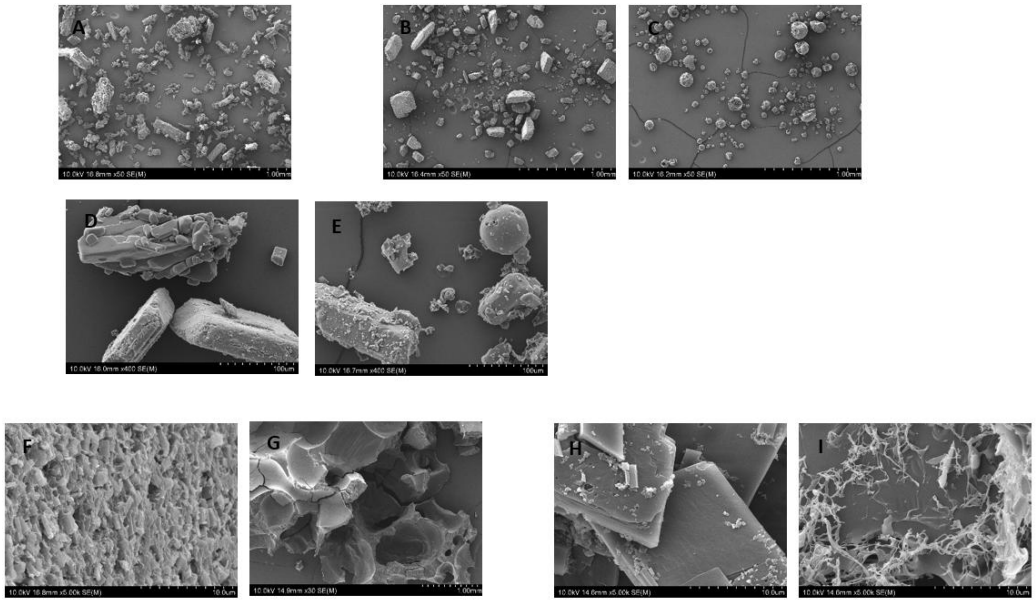

Figure 3.8. SEM images of A) CBD, B) β-CD, C) HP- β-CD, D) PM of CBD and β-CD, E) PM of CBD and HP- β-CD, F) Inclusion complex of CBD and β-CD, G) Inclusion complex of CBD and HP- β-CD, H) Inclusion complex of THC and β-CD, I) Inclusion complex of THC and HP- β-CD (scale bars as indicated in each micrograph).

3.4.3.4 In-vitro dissolution profiles

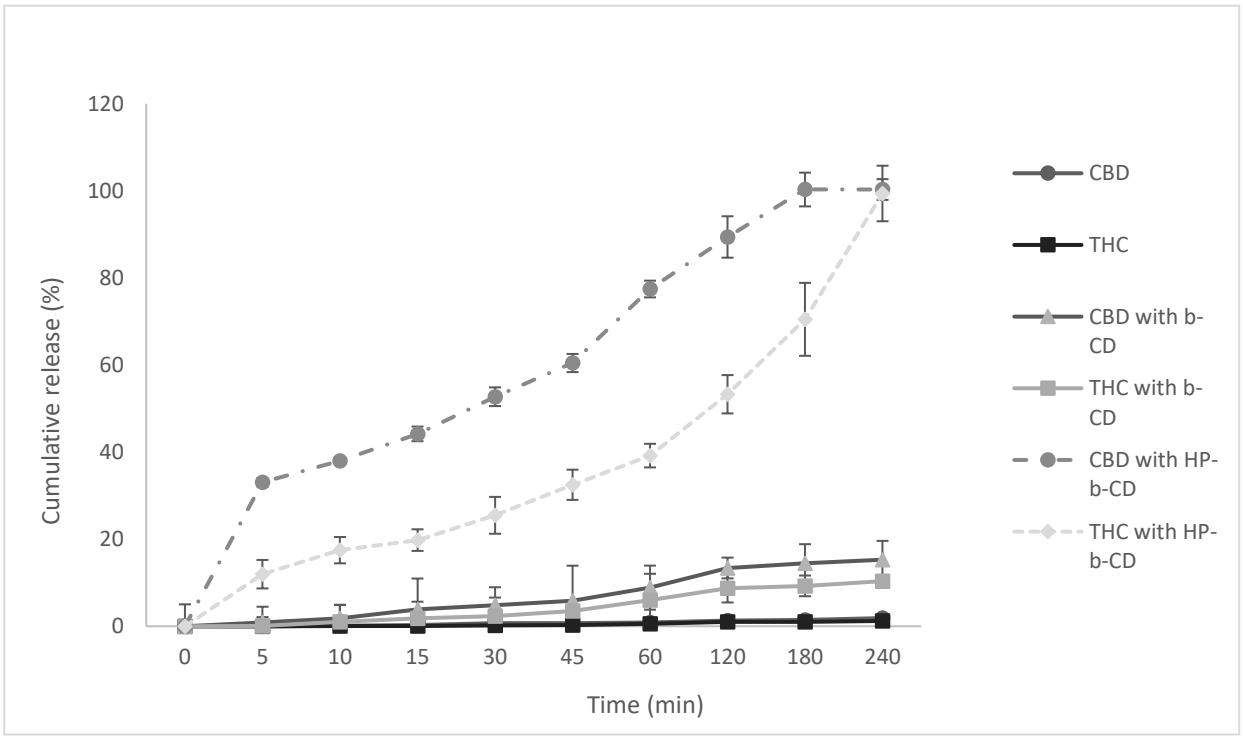

Figure 3.9. Comparison of in-vitro dissolution profiles between inclusion complexes and raw cannabinoids (CBD/THC). Data represent (n = 3; mean ± SD).

The dissolution profiles obtained reflect the release of cannabinoids from the inclusion complexes at various time points, shown in Figure 3.9 For raw CBD and THC, the dissolution was minimal, with less than 5% of the cannabinoids released after 4 hours. When the cannabinoids were included in complexes with β-CD, the dissolution rate increased, but it remained relatively low, with less than 20% of the cannabinoids released within the same 4-hour period. In contrast, the inclusion complexes formed with HP-β-CD exhibited a

significantly higher dissolution rate, achieving complete (100%) release of the cannabinoids within 4 hours. The enhanced dissolution rate observed with HP-β-CD can be attributed to its increased water solubility compared to β-CD. As revealed by previous SEM analysis, HP-β-CD displayed a spherical morphology, which likely contributes to its rapid release profile. The spherical structure of HP-β-CD may facilitate a burst release mechanism, likely due to swelling upon contact with the dissolution medium, allowing for faster dissolution of the encapsulated cannabinoids. The in-vitro release profiles obtained corroborate previous results of SEM and solubility studies done (Li et al., 2021).

This research successfully demonstrated the formation of cannabinoid-cyclodextrin inclusion complexes. These complexes significantly enhanced the solubility of CBD and THC, confirming that the interaction between the host (cyclodextrins) and guest molecules (CBD/THC) improved their dissolution properties.

3.4.4 Ex-vivo penetration of CBD in presence of terpene

Table 3.4. Log P and boiling point values of terpenes used in this study.

Terpene	Log P	Boiling point (°C)	Reference
1,8-Cineole	2.82	174 °C	(Furuishi et al., 2013)
L-Menthol	3.20	215.4 °C	(Furuishi et al., 2013)
α -Pinene	2.11	188.6 °C	(Furuishi et al., 2013)
D-limonene	4.45	175.4 °C	(Aissou et al., 2017)

Previous ex-vivo studies conducted within our research group demonstrated that the amount of CBD permeating through the mucosal tissue into the receptor compartment was minimal or negligible. Additionally, analysis of the donor compartment revealed that the residual concentration of CBD was also low, indicating that the compound was not simply retained in the donor media. Given these findings, it was hypothesized that CBD may be predominantly localizing within the mucosal tissue itself rather than undergoing full transmembrane diffusion. Hence, CBD penetration was evaluated by quantifying the extent of CBD that partitioned into and diffused throughout the mucosal layers. Ex-vivo penetration of CBD in the presence of different concentrations and combinations of terpenes d-limonene, l-menthol, α-Pinene, and 1,8-cineole were compared with a chemical permeation enhancer Azone and pure CBD dissolved in MCT vehicle (carrier), as shown in Figure 3.10. Among all the terpenes tested at a 5% concentration, 1,8-cineole demonstrated the greatest enhancement of CBD penetration into the mucosal tissue. This was followed, in decreasing order of effectiveness, by d-limonene, l-menthol, and α-pinene. None of the terpenes exhibited any inhibitory effect on CBD penetration.

Previous studies have suggested that the lipophilicity and boiling point (BP) of terpenes are critical physicochemical parameters influencing their ability to act as permeation enhancers. Generally, lipophilic terpenes are more effective in facilitating the permeation of hydrophobic drugs like CBD due to their effectiveness in penetrating lipid-rich layers of the skin or mucosa (Prasanthi & Lakshmi, 2012). Longgos et al. (2024) investigated the permeation-enhancing effects of various terpenes on lipophilic drugs and found that limonene exhibited greater enhancement compared to menthol, primarily due to its higher lipophilicity.

Another key factor influencing drug permeation was the boiling point of the terpenes. Terpenes with higher boiling points tended to show reduced enhancement potential, likely because their increased cohesiveness limited their interaction with biological membranes (Vlaia et al., 2014). Although 1,8-cineole has low lipophilicity, its boiling point is the lowest which might have contributed to higher permeation of CBD. A previous study by P. Tabboon et al. (2022) reported either negligible or inhibitory effects on mucosal CBD permeation when highly lipophilic terpenes such as nerolidol and oleic acid were used in combination with lipophilic carriers like MCT oil. This was attributed to CBD's strong affinity for the vehicle, which hindered its partitioning into the buccal mucosa.

Table 3.4 summarizes the log P values (indicating lipophilicity) and boiling points of the studied terpenes. While the synthetic enhancer Azone showed greater enhancement effects compared to individual terpenes, almost all combinations of terpenes outperformed Azone significantly. The most effective formulation consisted of 3.125% 1,8-cineole, 0.625% d-limonene, 0.625% L-menthol, and 0.625% α-pinene, which produced the greatest enhancement in CBD permeation.

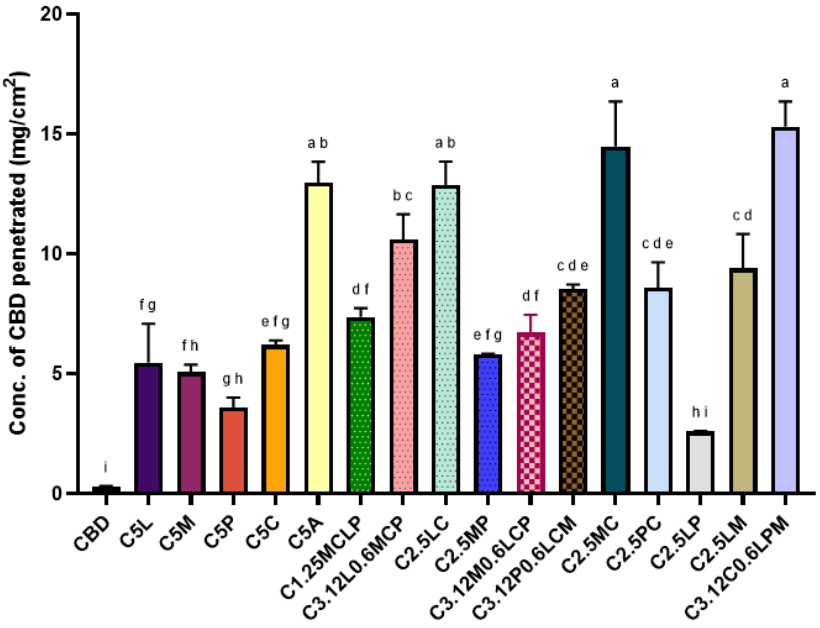

Figure 3.10. Ex-vivo buccal penetration effects of permeation enhancers on CBD (n = 3; mean ± SD). Bars annotated with different letters (a–i) indicate statistically significant differences between formulations ($p < 0.05$), while bars sharing the same letter are not significantly different.

3.4.5 HPLC validations

Calibration curves of CBD and THC were developed using prepared external standards of the cannabinoids in different concentrations. Method validation was carried out by running six concentrations of each cannabinoid six times (N=6). Calibration curves obtained were straight and linear. The correlation coefficient (R^2) of the CBD and THC were identified to be 0.9992 and 0.9998, respectively, with standard concentrations ranging from 0 to 100 µg/ml, highlighted in Figure 3.11.

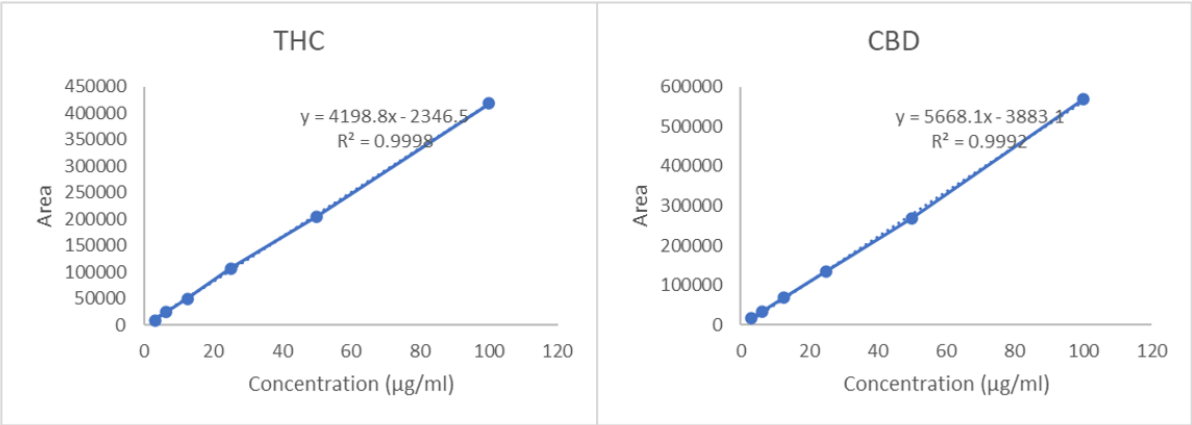

Figure 3.11. Calibration curves of THC and CBD using HPLC-UV.

LOD and LOQ values for the cannabinoids, as presented in Table 3.5 are consistent with those reported in earlier validation studies conducted by Lazarjani et al. (2024). The lowest concentration of both the cannabinoids used was 1.56 µg/ml. Notably, the determined LOD and LOQ values for both analytes were below this concentration, indicating the method's high sensitivity. Highly sensitive analysis can help ensure the accurate measurement of cannabinoids even in dilute samples or during early-stage permeation.

Table 3.5. LOD and LOQ of CBD and THC (n = 6).

Cannabinoid	LOD (µg/ml) (n = 6)	LOQ (µg/ml) (n = 6)
CBD	0.162245	0.540817
THC	0.255451	0.851502

3.5 Conclusions

This study successfully evaluated multiple strategies to improve the solubility, release, and mucosal penetration of lipophilic cannabinoids CBD and THC. Solubility studies revealed 3% Tween-PBS solution was found to provide sufficient solubility while maintaining sink conditions, making it an optimal receptor medium for in-vitro and ex-vivo studies. In-vitro drug release studies confirmed that CBD exhibits limited release when formulated in MCT oil, due to its strong affinity for the lipophilic carrier. Significant improvements in release were observed when using aqueous Tween-based donor solutions. Franz cell design parameters such as receptor volume and orifice diameter were also shown to influence the release profile, with larger receptor cells enhancing CBD diffusion over time. The formulation of cannabinoid-cyclodextrin inclusion complexes, especially with HP-β-CD, significantly improved aqueous solubility and dissolution rates. FTIR and SEM analyses confirmed successful complexation, while dissolution studies demonstrated nearly 100% release of cannabinoids from HP-β-CD complexes within 4 hours. These findings confirm the formation of stable host-guest complexes that enhance drug performance. Ex-vivo penetration studies revealed that individual terpenes such as 1,8-cineole, d-limonene, and L-menthol can enhance CBD permeation through buccal tissue. Notably, combinations of terpenes yielded even greater enhancement, with a specific blend of 3.125% 1,8-

cineole, 0.625% d-limonene, 0.625% L-menthol, and 0.625% α-pinene outperforming all other combinations, and the synthetic enhancer Azone. This suggests a synergistic effect among terpenes in promoting penetrating enhancing effects. Finally, the HPLC-UV analytical method used for quantifying cannabinoids was revalidated. It demonstrated excellent sensitivity, with obtained LOD and LOQ values below the minimum concentrations of cannabinoid standards used. This ensures its reliability for detecting cannabinoids in trace amounts during permeation and release studies. Overall, the combination of solubilizers, optimized donor/receptor systems, cyclodextrin complexation, and terpene-based permeation enhancers presents a comprehensive strategy for improving cannabinoid delivery via mucosal routes. These findings provide a strong foundation for the development of effective, non-invasive cannabinoid formulations with the potential for enhanced bioavailability through buccal administration.

Chapter 4: Development of Thermoresponsive Mucoadhesive In-Situ Gels for Buccal Cannabinoid Delivery

Abstract

Thermoresponsive in-situ gels are liquid formulations that undergo a sol–gel transition at body temperature, forming a semi-solid gel upon administration. Among the thermosensitive polymers, poloxamer 407 (P407) is widely used due to its reversible sol–gel transition, ease of formulation, biocompatibility, and ability to control drug release. This study aimed to develop and optimize thermosensitive mucoadhesive in-situ gel formulations for buccal delivery of cannabinoids using P407 in combination with either Carbopol 934P or hydroxypropyl methylcellulose (HPMC). To enhance solubility and ensure homogeneous gel incorporation, cannabidiol (CBD) and Δ^9-tetrahydrocannabinol (THC) were complexed with hydroxypropyl-β-cyclodextrin (HP-β-CD). A three-level factorial design was employed to optimize polymer concentrations, targeting viscosity, sol–gel transition temperature, and gelation time. Comprehensive characterization of the formulations included assessment of sol–gel transition behaviour, viscosity profiles, textural properties, ex-vivo mucoadhesive strength, drug release kinetics, ex-vivo penetration of cannabinoids, and long-term formulation stability. Carbopol-based gels demonstrated higher viscosity, stronger mechanical integrity, and superior mucoadhesive properties compared to HPMC-based formulations, resulting in prolonged mucosal residence. Gelation studies, in-vitro release and ex-vivo penetration indicated that HPMC-based gels transitioned more rapidly at 37°C and released cannabinoids more rapidly than Carbopol counterparts. Physicochemical analyses confirmed stable drug encapsulation without chemical interactions, while stability studies indicated superior cannabinoid retention in Carbopol-based gels. Overall, these findings highlight the potential of Poloxamer 407–based thermoresponsive in-situ gels as effective carriers for buccal cannabinoid delivery. Among all formulations, PC5C (Poloxamer with Carbopol and CBD) showed the best performance with strong adhesion, stability, and controlled release.

4.1 Introduction

Sustained-release dosage formulations play a critical role in improving the effectiveness of cannabis-based therapies, particularly when administered via the oro-mucosal route. They offer a promising solution by allowing the gradual release of active cannabinoids, maintaining more consistent drug levels, improving bioavailability, and minimizing dosing frequency. In-situ gel systems have gained considerable attention as sustained release formulations, particularly for alternative routes of administration such as oro-mucosal, nasal, ocular, and vaginal delivery. These systems are initially formulated as low-viscosity liquids, allowing for easy and precise administration to the target site, and transform into gels either via physiological or chemical mechanisms (B. Vigani et al., 2020). This ensures that the formulation remains fluid during storage and administration but solidifies after application, enhancing drug retention. Chemical methods for gelation include enzymatic crosslinking, irradiation, click-reaction, genipin, and thiol oxidation-stimulated gelling reactions (A. Prasannan et al., 2018; Zeng et al., 2014). Physiological mechanisms of gelation involve stimuli such as changes in temperature, pH, or the presence of ions that promote the liquid formulation to undergo a sol-to-gel transition, forming a semi-solid gel in situ. This transformation enhances the formulation's ability to remain at the site of application, prolonging drug residence time, minimizing wash-out, and facilitating controlled drug release. Physiologically triggered in-situ gels have received considerable attention in recent decades due to their ability to form gels without the need for organic solvents or co-polymerizing agents (Ruel-Gariépy & Leroux, 2004; B. Vigani et al., 2020).

Temperature-sensitive gelation relies on thermo-responsive polymers that respond to body temperature. Ideally, these polymers remain in a liquid state at room temperature and undergo a phase transition to form a gel at physiological temperatures (~37°C). This behaviour is due to their phase separation characteristics; some polymers gel when heated above their lower critical solution temperature (LCST), while others solidify upon cooling below their upper critical solution temperature (UCST). In certain cases, these transitions are reversible, allowing the polymers to switch between sol and gel states depending on the temperature (Ruel-Gariépy & Leroux, 2004; Taylor et al., 2017). Thermally induced gel-forming polymers include but are not limited to polymers such as pectin, carrageenan, cellulose derivatives, chitosan, xyloglucan, and poloxamers (Forouhe Zahir-Jouzdani et al., 2018). Natural polymers such as carrageenan exhibit thermo-reversible gelation, forming gels at lower temperatures and returning to a liquid state at higher temperatures. In contrast, certain cellulose derivatives can gel at elevated temperatures, but these temperatures are often too high for practical biomedical applications. Therefore, chemical or physical modifications are typically required to adjust their gelation properties to allow for transition at more suitable, physiologically relevant temperatures. Both xyloglucan and chitosan require enzymatic modification to achieve gelation at physiological temperatures, and they tend to have low mechanical gel strength. Additionally, chitosan is highly

pH-sensitive, remaining soluble only in acidic environments, which limits its use in neutral or alkaline conditions (Ruel-Gariépy & Leroux, 2004).

Commonly used thermo-responsive in-situ gelling polymers are poloxamers (also known as Pluronic's). They are inexpensive and have been found especially useful in various drug delivery systems, as well as wound dressing and cell culture applications. Thermo-sensitive poloxamers are a class of triblock copolymers composed of a central hydrophobic block of polypropylene oxide (PPO) attached by two hydrophilic blocks of polyethylene oxide (PEO). These polymers exhibit temperature-dependent sol-to-gel transitions, making them highly suitable for in-situ gelling applications. At certain concentrations known as critical micelle concentration (CMC) and above their lower critical solution temperature (LCST), poloxamers self-assemble into micelles. This self-assembly is primarily driven by hydrophobic interactions between the PPO blocks, which interact with each other via Van der Waals forces to form the core of the micelle. The hydrophilic PEO blocks then form the outer shell, which stabilizes the micelle in aqueous environments through hydrogen bonding with water molecules. As the temperature increases, the hydrophobic interactions between the PPO segments are enhanced, promoting more extensive micelle formation. Beyond a certain threshold temperature, these micelles begin to pack closely and organize into a three-dimensional network, leading to the formation of a semi-solid gel. This sol-to-gel transition is reversible; when the temperature is reduced, the hydrophobic interactions weaken, micelles dissociate, and the system reverts to its original liquid state. This mechanism is highlighted in Figure 4.1. The gelation behaviour of poloxamers is highly dependent on both concentration and temperature. Gel formation typically occurs only above a certain concentration referred to as the critical gelation concentration (CGC) and within a specific temperature range. The LCST of these polymers can be easily modified upon using a combination of different poloxamers in variations or by incorporating other polymers (Singh et al., 2013; Soliman et al., 2019).

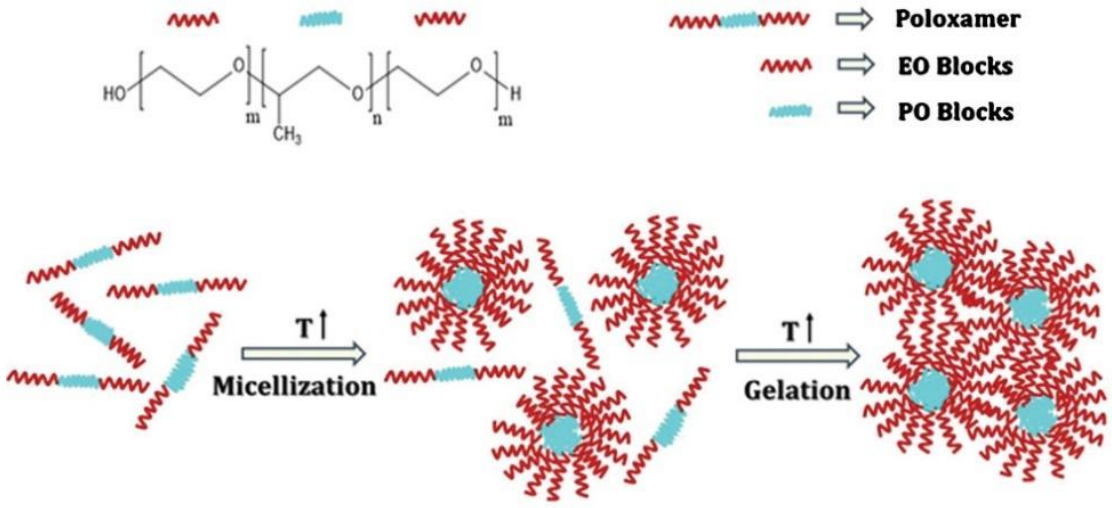

Figure 4.1. Thermo-reversible self-assembly of poloxamers into micelles and gels (Adopted from (Zarrintaj et al., 2020)).

Variations in the lengths of PEO and PPO groups allow for the synthesis of a wide range of poloxamers with specific properties. Among the various poloxamers, Poloxamer 407 (P407) (also known as PF-127), Poloxamer

188 (P188), and Poloxamer 338 (P338) are frequently researched for pharmaceutical applications, each offering distinct characteristics. Poloxamer 188, with an average molecular weight of 8400 Da, forms small micelles and has a lower gelation temperature. This characteristic makes it suitable for rapid drug release applications. However, when compared with P407, it exhibits lesser mucoadhesive strength. Although P338 has superior mechanical and mucoadhesive strength, its higher gelation temperature of 57°C at 20% (w/v) concentration limits its use in various drug delivery applications (Deiringer et al., 2025). P407, with an average molecular weight of 12,600 Da, is widely used in mucosal applications with its ability to remain completely fluid below 20-25°C, and forms a clear gel at physiological temperatures of 30-35°C. The sol-gel temperatures of P407 can be modified by combinations with other poloxamers, polymers, additives, and drugs. This poloxamer is chemically stable and is approved by the US FDA in various pharmaceuticals in the market. However, P407 also faces limitations such as poor mechanical properties, rapid degradation, and inadequate mucoadhesive strength (Diaz-Salmeron et al., 2021; Ruel-Gariépy & Leroux, 2004; F. Zahir-Jouzdani et al., 2018; Zeng et al., 2014).

Mucosal drug delivery systems require strong mucoadhesion to enhance residence time, improve bioavailability, and achieve sustained drug release. Poloxamer-based gels often incorporate mucoadhesive polymers such as Carbopol, hydroxypropyl methylcellulose (HPMC), xanthan gum, or chitosan to improve adhesion, mechanical strength, and stability. For instance, Carbopol enhanced mucoadhesion and bioavailability in ophthalmic and intranasal P407 formulations, with each increase in Carbopol content significantly improving gel cohesion(Qi et al., 2007; P. R. Ravi et al., 2015). Similarly, HPMC improved mucoadhesion and sustained release in ocular P407 gels (Chen et al., 2023). In addition the incorporation of these mucoadhesive polymers has also been shown to improve the mechanical strength of poloxamer-based gels, resulting in more robust and stable formulations suitable for prolonged mucosal application (F. Zahir-Jouzdani et al., 2018). However, inclusion of drugs or excipients can slightly lower the gelation temperature, highlighting the need to optimize formulations to maintain appropriate sol–gel transition for effective delivery (Choi et al., 2014).

Numerous studies have explored the development of P407-based in-situ gels for buccal drug delivery, targeting both local and systemic therapeutic effects. Rençber and Karavana (2020) developed mucoadhesive P407 gels with dexamethasone, achieving enhanced rheological properties and sustained drug release. Zeng et al. (2014) formulated P407–P188–xanthan gum gels for systemic delivery of salbutamol, improving mucoadhesion, controlled release, and bypassing first-pass metabolism. Chaudhary and Verma (2014) combined P407 with HPMC and Carbopol to sustain acyclovir release for both local antiviral action and systemic absorption. Similarly, Ferreira et al. (2019) developed P407–Carbopol 974P gels with curcumin, demonstrating effective ex-vivo buccal mucosal penetration and potential for systemic delivery.

Research on the application of cannabinoids through poloxamer-based in-situ gels for oro-mucosal routes remains limited. Changsan et al. (2023) formulated aqueous solutions of cannabidiol (CBD) complexed with

cyclodextrins into P407-based intranasal in-situ gels. This formulation was explored for its potential to modulate immune responses and treat cytokine storms induced by coronavirus infection. In another study, combinations of poloxamers were utilized to develop intranasal in-situ gels containing nanostructured lipid carriers loaded with CBD. These gels were designed with enhanced mucoadhesive properties to prolong nasal residence time for treatment of neuropathic pain (Matarazzo et al., 2021). The studies demonstrate the promise of poloxamer-based in-situ gels as effective delivery systems for cannabinoids, particularly through mucosal routes where sustained therapeutic effects are desirable.

Leveraging the demonstrated potential of P407-based in-situ gels for enhancing mucoadhesion, mechanical strength, and sustained drug release, and considering the limited application of such systems for cannabinoid delivery, this chapter aimed to develop poloxamer-based in-situ gelling formulations for buccal delivery incorporating CBD and THC complexed with hydroxypropyl-β-cyclodextrin (HP-β-CD). The study focused on evaluating the impact of incorporating mucoadhesive polymers HPMC or Carbopol 934P on gelation behaviour, mechanical strength, mucoadhesive performance, in vitro drug release, and ex vivo mucosal penetration, to identify formulations that provide an optimal balance of these properties. This formulation strategy is expected to not only enhance the bioavailability of cannabinoids by prolonging their residence time at the buccal mucosa but also to provide a non-invasive, patient-friendly delivery platform. By systematically evaluating the interplay between polymer composition and gel performance, the study intended to lay the groundwork for future preclinical and clinical investigations of P407-based cannabinoid delivery systems.

4.2 Materials and methods

Pluronic F-127 (Poloxamer 407) and (Hydroxypropyl)methyl cellulose (HPMC) was purchased from Sigma-Aldrich, New Zealand. Carbopol 934P (Serva) from DKSH LabShop, New Zealand, D-Limonene from Thermo Fisher, New Zealand, 1,8- cineole, α-Pinene from Sigma-Aldrich, New Zealand, laurocapram 95% from AK Scientific, and l-Menthol from Chem express supplied by Focus Bioscience, Australia. Medium chain triglyceride (edible oil) purchased from local store, Auckland. Phosphate buffered saline (PBS) tablets (pH 7.4, Tween-20%, β-CD, HP-β-CD, acetonitrile, and Bovine Serum Albumin (BSA) were purchased from Sigma-Aldrich, New Zealand. Pure isolated CBD and distilled oil of THC were provided by Helius Therapeutics Ltd, New Zealand. All other reagents used were of analytic grade.

4.2.1 Preparation and optimizations of P407 in-situ gels

4.2.1.1 Preliminary optimizations

Preliminary optimization studies were conducted using P407-only gels to determine the appropriate concentration range for inclusion in the final formulations. The visual appearance, fluidity at room

temperature, and gelling capacity of the prepared P407 solutions were initially assessed through simple visual observation.

To evaluate the sol–gel transition time, the formulations were transferred into glass vials and placed on a magnetic stirrer maintained at 37 °C. The gelation time was recorded as the point at which the magnetic stir bar ceased to rotate completely, indicating the formation of a gel. The gel formed was also confirmed by tube-inversion method (Galocha-León et al., 2023).

In addition, sol–gel transition temperatures were determined by measuring the viscosity of the formulations at gradually increasing temperatures, ranging from 10 to 50°C, using a rheometer (RST-SST, Brookfield) equipped with a rotating ramp measuring block. Viscosity values were recorded at a fixed shear rate of 100 s^{-1}, and the sol–gel transition temperature was identified as the temperature at which a pronounced increase in viscosity was observed, corresponding to the formation of a gel-like structure. These evaluations helped establish the ideal P407 concentration to ensure efficient gelation at physiological temperatures while maintaining suitable handling properties at room temperature (Harish et al., 2009).

4.2.1.2 Preparation of cannabinoid incorporated in-situ gels of P407s with mucoadhesive polymers.

For preparation of P407 only in-situ gelling solutions, the required amount of P407 (15 to 22% w/v) was gradually added to deionized water under mild stirring for approximately 5 minutes, followed by refrigeration at 4 °C for up to 12 hours to ensure complete dissolution. For the preparation of cannabinoid-loaded in-situ gels with mucoadhesive polymers, Carbopol or HPMC (0.1 to 0.5% w/v) were first dissolved in deionized water. Once the polymers were fully hydrated, P407 (20% w/v) was incorporated into the solution with gentle stirring and refrigerated for 12 hours to allow proper mixing. The previously prepared HP-β-CD inclusion complexes of cannabinoids were then introduced into the mixture to achieve a final cannabinoid concentration of 20 mg/ml. Additional excipients, including sweetener 2% (w/v) mannitol and 0.05% (w/v) preservative propyl paraben, were added and the mixture was stirred until all components were fully dissolved. The pH of the developed formulations was adjusted to 7 using triethanolamine. All formulations were subsequently stored at 4°C for a minimum of 24 hours before undergoing further evaluation (Choi et al., 2014; Ferreira et al., 2019; Rençber & Karavana, 2020).

4.2.1.3 Three-level factorial optimization of P407 with HPMC/Carbopol in situ gels

A 3^2 factorial design was employed to systematically optimize the concentrations of P407 and mucoadhesive polymers, either HPMC or Carbopol, using Design Expert software. Two independent formulation variables were selected, which were P407 concentration ranging from 18 to 22% (w/v) and polymer (HPMC or Carbopol) concentration ranging from 0.1 to 0.5% (w/v). The impact of these variables on characteristics of the in-situ gels was evaluated by monitoring three dependent variables, including viscosity at room temperature (cps), viscosity at 37°C (cps), and gelation time (s). The primary goals were to minimize viscosity at room temperature for ease of administration, maximize viscosity at 37°C to ensure stable gel formation,

and minimize gelation time to enable rapid transition at physiological conditions. The coded levels of independent variables and the constraints applied to the dependent variables are summarized in Table 4.1. Optimized formulations were further subjected to physicochemical and mechanical characterizations.

Table 4.1. Independent variables and corresponding levels used in the factorial design, and the constraints applied to the dependent (response) variables for optimization of thermoresponsive in-situ gels.

Independent variables			
		Levels	
	-1	0	+1
P407 % (w/v)	18	20	22
HPMC/Carbopol % (w/v)	0.1	0.3	0.5
Dependent variables			
		Constrains	
Viscosity at room temperature (cps)		Minimize	
Viscosity at 37°C (cps)		Maximize	
Gelation time (s)		Minimize	

4.2.2 Appearance, pH, and drug content of developed formulations

The appearance of the formulations was assessed visually for clarity, colour, and homogeneity. pH measurements were conducted by transferring 5 mL of the optimized in-situ gelling solution into a beaker and recording the pH at room temperature using a calibrated bench-top pH meter (Interlab, NZ), ensuring measurements were taken prior to gelation.

For drug content analysis, an amount of each optimized formulation equivalent to 20 mg of cannabinoids was accurately measured and diluted in a 1:1 mixture of acetonitrile and water. The resulting solutions were centrifuged, then filtered through a 0.45 µm membrane filter and analysed using a validated HPLC method as described in the previous chapter.

4.2.3 Sol-gel transition temperature and gelation time of the optimized formulations

The gelation time of the optimized formulations was determined by placing the samples on a hot plate with magnetic stirring. The temperature was maintained at 37 °C and monitored using a digital thermometer, and the time required for gel formation was recorded, as described previously in Section 4.2.1. Gelation was confirmed when the magnetic stir bar ceased to rotate, indicating the transition from sol to gel at physiological temperature.

Sol–gel transition temperatures were determined by measuring the viscosity of the formulations using a Brookfield RST-SST rheometer equipped with a rotating ramp measuring block while gradually increasing the temperature, with the transition temperature identified from the change in viscosity, as described in Section 4.2.1.

4.2.4 Mechanical properties of the P407 in-situ gels

Hardness, cohesiveness, and springiness of the optimized gels were assessed using a texture analyser (Stable Micro Systems, UK) fitted with a 50 N load cell. Gel samples (from 1 ml of in-situ gelling solutions) were placed in individual wells of a 12-well plate and positioned on the analyser platform. A stainless-steel spherical probe (5 mm diameter) was used to compress each sample to a depth of 1 mm at a test speed of 0.8 mm/s, with a 5-second relaxation period between two compression cycles (n = 3). The results were analysed using TA.XT Exponent software to quantify the mechanical parameters. The procedure was adapted from a previously employed method by De Souza Ferreira et al. (2017). Although the software allows additional parameters such as adhesiveness, consistency, and gel strength to be obtained, the present study focused on hardness, cohesiveness, and springiness as the primary indicators of gel mechanical behaviour.

4.2.5 Mucoadhesive strength of developed in-situ gels.

Experiments were performed by adapting the previously employed method by Patlolla et al. (2020). The mucoadhesive strength of the optimized in-situ gel formulations was evaluated ex vivo using a texture analyser (Stable Micro Systems, UK) equipped with a 50 N load cell and a 10 mm cylindrical probe. Fresh porcine buccal mucosa was obtained from a local butcher shop (Auckland, New Zealand), cleaned with phosphate-buffered saline (PBS, pH 7.4), and used within 2 hours of excision. The mucosal tissue was trimmed to a suitable size and securely attached to the upper probe of the texture analyser using double-sided adhesive tape to ensure stable positioning during the measurement, as shown in Figure 4.2 below.

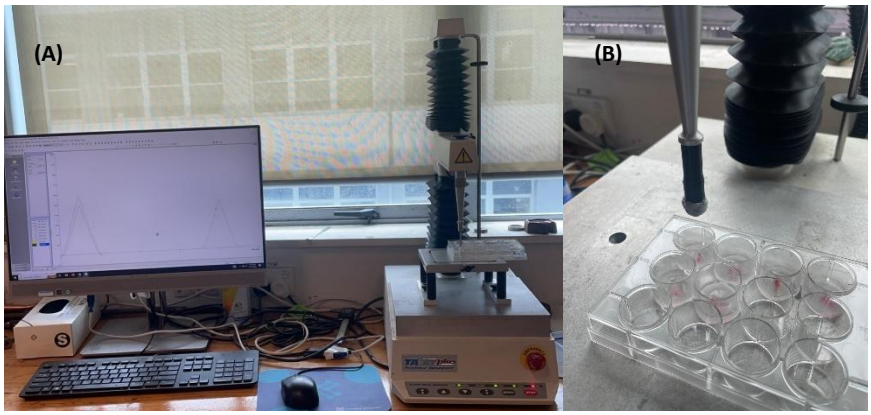

Figure 4.2 (A) Texture analyser used, (B) testing mucoadhesive strength with porcine buccal mucosa attached to the probe. The plate is attached to the platform using double sided tape.

Gel samples (from 1 ml of in-situ gelling solutions) were placed in individual wells of a 12-well plate and positioned on the analyser platform, below the probe. Prior to measurement, the samples were equilibrated

on a hot plate maintained at 37 °C. The probe was then lowered until it contacted the gel surface and maintained a constant contact pressure for 60 seconds to allow adhesive bonding between the formulation and the mucosa. After this contact period, the probe was withdrawn vertically at a speed of 0.8 mm/s, and the maximum detachment force (N) required to separate the probe (with attached mucosa) from the gel was recorded. Following each measurement, the samples were returned to the hot plate maintained at **37 °C** to preserve the gel state. Each experiment was conducted in triplicate (n = 3). The mean peak force value was used as an indicator of the mucoadhesive strength of the formulation.

4.2.6 In-vitro drug release studies

In-vitro release studies were conducted using a Franz diffusion cell apparatus (Orchid Scientific, India) equipped with dialysis membranes (MWCO 14,000 Da) to evaluate cannabinoid release from optimized formulations over a 4-hour period. Prior to use, the membranes were hydrated for 24 hours. The Franz cells were maintained at 37 °C and allowed to equilibrate for one hour before the experiment commenced. Each receptor chamber was filled with 20 ml of phosphate-buffered saline (PBS) containing 3% Tween 20, which was continuously stirred at 300 rpm. The pre-soaked cellulose membrane was then placed between the donor and receptor compartments and securely clamped. Subsequently, 1 mL of the thermoresponsive in-situ gelling formulation was placed directly into the donor chamber with 0.5 ml of artificial saliva added as the donor solution, and all openings were sealed with parafilm to minimize evaporation. At specified time intervals of 5, 10, 15, 30, 60, 120, and 240 minutes, 1 ml samples were withdrawn from the receptor chamber and immediately replaced with fresh medium pre-warmed to 37 °C. The inclusion of 3% Tween 20 and periodic replacement of withdrawn samples with fresh pre-warmed medium ensured that the drug concentration remained below 10% of its saturation solubility at all times, thereby maintaining sink conditions. The collected samples were analysed using HPLC to quantify the amount of cannabinoid released. All experiments were performed in triplicate for each optimized formulation. Several studies on poloxamer-based thermoresponsive mucoadhesive in-situ gels have utilized dialysis membranes in combination with Franz diffusion cells, either in standard or modified setups, to investigate the in-vitro release profiles of drugs (M.A. Fathalla et al., 2017; Raknam et al., 2022; Shivam U et al., 2020).

4.2.6.1 Drug release kinetics

Release kinetics of CBD and THC were analysed using KinetDS software 3.0 (rev. 2010). To characterise the drug release mechanisms from the formulations, several mathematical models were applied, including Zero-order, First-order, Higuchi, Korsmeyer-Peppas, and Hixson-Crowell models. The experimental release data were fitted to each of these models within the software to determine which model best describes the release behaviour of the cannabinoids. The goodness-of-fit for each model was assessed by the correlation coefficient (R^2) of the linear regression plot generated for each kinetic model. An R^2 value of 1.00 indicates a perfect fit between the model and the experimental data. Therefore, the closer the R^2 value is to 1.00, the better the

model describes the release kinetics of the drug from the formulation (Mendyk et al., 2012). This comparative analysis allows for a more comprehensive understanding of the release mechanisms governing the behaviour of CBD and THC in the thermoresponsive in-situ gel systems.

Zero Order

The zero-order kinetic model assumes that drug release occurs at a constant rate, independent of the drug's concentration within the formulation. This model is typically applied to systems where the formulation does not disaggregate or degrade rapidly and where the drug is released in a controlled, sustained manner over time. It is particularly relevant for drug delivery systems designed to maintain steady plasma concentrations.

The zero-order release can be mathematically described by the following equation:

$Qt = Q_o + K_o t$

Where Qt is the amount of drug released at time t, Q_o is the initial amount of drug in solution (usually zero for most controlled-release formulations), and K_o is the zero-order release rate constant (with units of concentration/time) (Askarizadeh et al., 2023; Dash et al., 2010).

First Order

The first-order kinetic model describes a drug release mechanism where the rate of release is directly proportional to the concentration of the drug remaining in the formulation. In other words, as the drug concentration decreases over time, the rate of release also decreases. This model is commonly associated with formulations where the release is diffusion-controlled and follows an exponential decline.

The mathematical expression for the first-order model is:

$\log C = \log C_0 - K_t / 2.303$

Where K is the first order rat constant (unit $time^{-1}$), t is the time, C represents concentration at t, and C_0 is the initial concentration of the drug (Askarizadeh et al., 2023; Dash et al., 2010).

Hixon-Crowell

The Hixon-Crowell cube root law describes drug release mechanisms influenced by changes in particle size and surface area of release. It is represented by the following equation:

$W_0^{1/3} - W_t^{1/3} = k*t$

Where W_0 is the initial drug amount in the formulation, W_t represents drug amount at a specific time (t), and k is the Hixon-Crowell release rate constant (Askarizadeh et al., 2023; Dash et al., 2010).

Korsmeyer-Peppas

The Korsmeyer-Peppas power law is used to describe drug release based on the mechanisms of drug transport, either by diffusion through the formulation or by swelling of the formulations or formulation dissolution, expressed through the equation:

$M_t / M_\infty = Kt^n$

Where, M_t / M_∞ represents drug release fraction at specific time "t", K is the release constant of Korsmeyer-Peppas, and n represents the release exponent used for characterizing release from different matrix (formulation) geometries (Askarizadeh et al., 2023; Dash et al., 2010).

Higuchi

It was the first model developed to determine drug release mechanisms from matrix, now extended to explain formulations of different geometries and porosities based on formulation swelling, diffusion, and dissolution.

$Q = K_H * t^{1/2}$

Where K_H is the dissolution constant, and Q represents the amount of drug released per unit area at specific time t (Askarizadeh et al., 2023; Dash et al., 2010).

4.2.7 Fourier Transform Infrared Spectroscopy (FTIR) of optimized thermoresponsive formulations.

FTIR analysis was conducted to characterise the pure drug, P407, HPMC and Carbopol and the developed in-situ gels. The in-situ gels were freeze dried using a Christ alpha series freeze dryer (Osterode am Harz, Germany) for 24 hours prior to FTIR. The spectra were recorded using a Thermo Scientific FTIR spectrometer (Nicolet iS10, USA). Samples were placed directly onto a monolithic diamond crystal cell, and spectra were collected over the wavenumber range of 4000–500 cm^{-1}. Each spectrum was obtained at a resolution of 4 cm^{-1} with 32 scans to ensure accuracy and reproducibility. A background spectrum was recorded using a clean, empty cell at room temperature (25 ± 2°C) and served as a reference.

4.2.8 Scanning Electron Microscopy (SEM) of thermoresponsive in situ gels

The optimized in-situ gel formulations, previously subjected to freeze-drying (as detailed in the preceding section), were prepared for morphological analysis. The lyophilized samples were coated with a thin layer of platinum using an ion sputter coater (Hitachi E-1045) for 20 seconds to enhance conductivity. Surface morphology was then examined using a Schottky field emission scanning electron microscope (FE-SEM) (Thermo Scientific, HITACHI SU-70). The images were captured to evaluate structural characteristics of the formulated gels.

4.2.9 Ex-vivo drug penetration

Ex-vivo drug penetration from in-situ gels was carried out using a Franz diffusion cells with porcine buccal mucosa, as previously mentioned (section 3.2.5.3).

4.2.10 Stability studies

Stability studies of the in-situ gel formulations were conducted under refrigerated storage conditions at 4 ± 2°C to evaluate their long-term stability. Samples were periodically withdrawn at defined intervals of 1, 3, and 6 months. At each time point, the formulations were assessed for changes in key physicochemical parameters, including pH, physical appearance (e.g., colour, clarity, presence of any precipitation or phase separation), drug content, and gelling capacity. These evaluations were performed to ensure the integrity, consistency, and performance of the formulation over time under refrigerated conditions (S M et al., 2018).

4.3 Statistical analysis

Statistical analysis of the experimental data was performed using R programming and GraphPad Prism software (version 10.2.3). For datasets exhibiting normal distribution and homogeneity of variance, one-way analysis of variance (ANOVA) was employed to determine statistical significance. In cases where the data did not meet parametric assumptions, the non-parametric Kruskal–Wallis test was used as an alternative. Where significant differences were identified, post hoc multiple comparisons were conducted using Tukey's test. A p-value of less than 0.05 ($P < 0.05$) was considered indicative of statistical significance.

4.4 Results and discussion

4.4.1 Preliminary evaluations

4.4.1.1 Optimizations of P407-only in-situ gels

Initial formulation development focused on evaluating P407 only in-situ gels across a concentration range of 15 to 22% (w/v) to determine their suitability as thermoresponsive drug delivery systems. All prepared formulations appeared clear and homogeneous with no signs of phase separation or precipitation. At room temperature (20°C), the solutions exhibited good fluidity, making them appropriate for ease of administration before gelation. The sol–gel transition behaviour was observed to be highly dependent on the concentration of P407. As reported in previous studies, concentrations above 15% typically result in gel formation at temperatures exceeding room temperature, with the gelation temperature decreasing progressively as P407 concentration increases (Fakhari et al., 2017). This trend was confirmed in the present study. Formulations containing 15 and 16% P407 remained low-viscosity liquids even when heated above 40°C. These concentrations did not demonstrate gelation within the observed 1-minute time frame and were classified as no gel (NG) formulations under the given test conditions. In contrast, formulations with higher P407 concentrations exhibited distinct thermoresponsive gelation behaviour. Specifically, gels formulated with 18, 20, and 22% P407 demonstrated sol–gel transition temperatures of approximately 28, 24, and 22°C, respectively, with corresponding gelation times of 84.6 ± 0.92, 55.8 ± 0.73, and 42.98 ± 0.12 s at 37°C. Table 4.2 summarizes the visual characteristics, fluidity, gelling capacity, sol–gel transition temperatures, and transition times at 37 °C for formulations ranging from 15 to 22% w/v P407.

It was noted that the subsequent inclusion of mucoadhesive polymers (HPMC or Carbopol) with drug-inclusion complex in later formulations led to an upward shift in the gelation temperature. Therefore, to compensate for this increase and maintain gelation close to physiological temperature, further formulation optimization efforts were confined to P407 concentrations between 18 to 22%. This concentration range offered a suitable balance between pre-administration fluidity and rapid sol–gel transition at mucosal temperatures, forming the foundation for subsequent studies involving polymeric blends and drug incorporation.

Table 4.2. Evaluation of P407 in-situ gelling formulations (n = 3; mean ± SD).

Conc. of P407 (W/V)	Visual appearance	Fluidity	Gelling capacity	Sol-gel transition temperature	Sol-gel transition time at 37 °C
15%	Clear	+++	+	Slightly viscous above 40°C. (NG)	>1mins
16%	Clear	+++	++	Slightly viscous above 40°C. (NG)	>1min
18%	Clear	+++	++	Viscosity increased from 28°C. Indicated by slow magnetic movement.	84.6± 0.92 s
20%	Clear	+++	++	Viscosity increasing from 24°C.	55.8 ± 0.73 s
22%	Clear	+++	++	Viscosity increasing from 22°C.	42.98 ± 0.12 s

Note: NG = No Gel formation within 1 minute, +++= high fluidity; ++ = moderate gelling; + = low gelling.

The effect of P407 concentration on gelation time was assessed using formulations containing 18, 20, and 22% (w/v) P407. As shown in Figure 4.3, an increase in P407 concentration resulted in a significant decrease in gelation time. The 18% formulation exhibited the longest gelation time (~85 seconds), while the 20 and 22% formulations demonstrated shorter gelation times of approximately 55 and 40 seconds, respectively. These differences were statistically significant across all groups (****, $p < 0.0001$), indicating a strong inverse relationship between P407 concentration and gelation time. Previous research by Gábor et al. (2021) has also confirmed this by showing that gelation time decreases with increasing concentrations of P407, with the behaviour attributed to the increased formation and densification of micelles at higher concentrations, which facilitates faster gelation through enhanced hydrophobic interactions and micellar packing. Such findings are particularly relevant for the development of thermoresponsive drug delivery systems, where rapid sol–gel transition is often essential for effective in situ application.

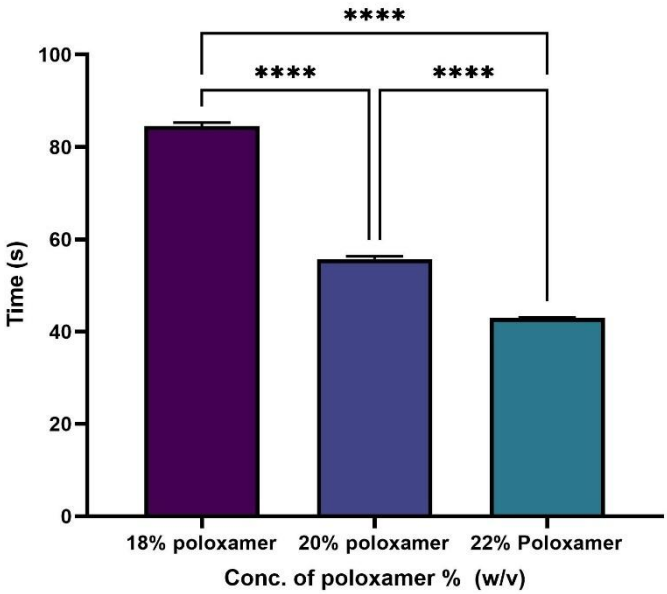

Figure 4.3. Effect of P407 concentration on gelation time (n = 3; mean ± SD). Statistically significant differences are denoted as ****p < 0.0001.

Figure 4.4 illustrates the relationship between temperature and viscosity for three different concentrations of P407 solutions (18, 20, and 22% w/v). As temperature increases from 10 to approximately 50°C, all formulations show a non-linear increase in viscosity, indicative of a thermoresponsive sol–gel transition. Among these, the 22% P407 solution displayed the highest viscosity at all temperatures, followed by 20% and then 18%, indicating that higher concentrations enhance the gel strength and responsiveness of the system. The viscosity increase is attributed to the formation of micellar structures and their progressive packing into a gel network upon heating. These findings are consistent with previous studies, such as Xia et al. (2019), who observed a similar concentration-dependent increase of viscosity in P407-based systems. Their work reported that at higher concentrations, P407 undergoes micellization and gels at lower temperatures, accompanied by a steeper viscosity rise, confirming the results observed in the present study.

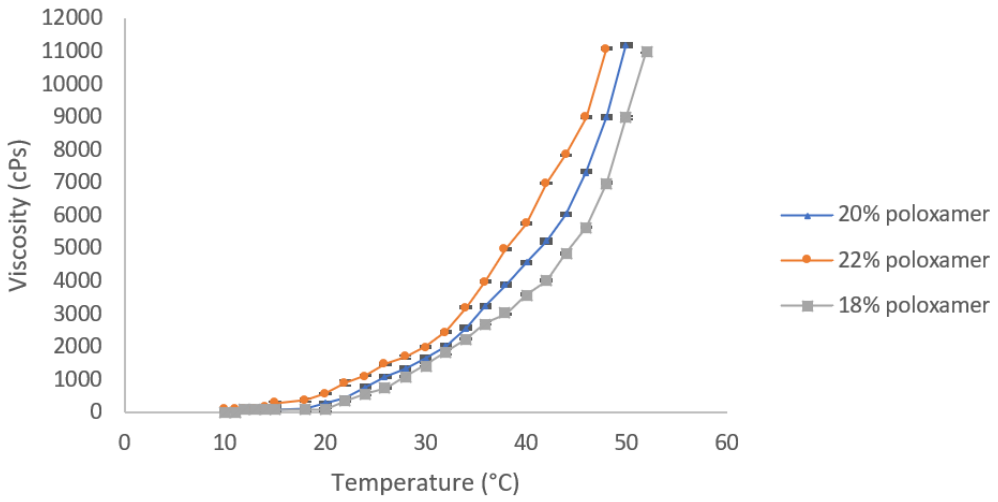

Figure 4.4. Temperature-dependent viscosity profiles of 18, 20, and 22% (w/v) P407 formulations (n = 3; mean ± SD).

4.4.1.2 Optimization of P407-HPMC/Carbopol in-situ gels via Factorial Design

This study employed a three-level factorial design to optimize temperature responsive in situ gelling formulations using P407 in combination with either HPMC or Carbopol. The key responses measured included viscosity at room temperature, viscosity at 37°C, and gelation time. The data were analysed using quadratic regression models, and the results were visualized through ANOVA tables, predicted vs. actual plots, and 3D surface response plots.

Viscosity at room temperature

The viscosity at room temperature was significantly influenced by both the polymers HPMC or Carbopol combined with P407. ANOVA results, as highlighted in Table 4.3 for both types of formulations developed, showed statistically significant quadratic models ($p < 0.0001$), confirming the relevance of the fitted models. The predicted vs. actual plots (Figure 4.5) indicated strong agreement with minimal deviation from the ideal line. The 3D surface plots shown in Figure 4.6 revealed that increasing concentrations of both HPMC/Carbopol and P407 increased viscosity at room temperature.

Table 4.3 ANOVA results summary of viscosity at room temperature for P407–Carbopol and P407–HPMC systems.

Response	**Model Type**	**Significant Factors**	**p-value (Model)**	**Lack of Fit p-value**
Viscosity at room temperature	Quadratic (P407–Carbopol)	A–P407 ($p < 0.0001$), B–Carbopol ($p < 0.0001$), AB ($p = 0.0072$), A^2 ($p < 0.0001$)	< 0.0001	0.037
Viscosity at room temperature	Quadratic (P407–HPMC)	A–P407 ($p < 0.0001$), B–HPMC ($p < 0.0001$), AB ($p = 0.0216$), A^2 ($p = 0.0047$)	< 0.0001	0.0357

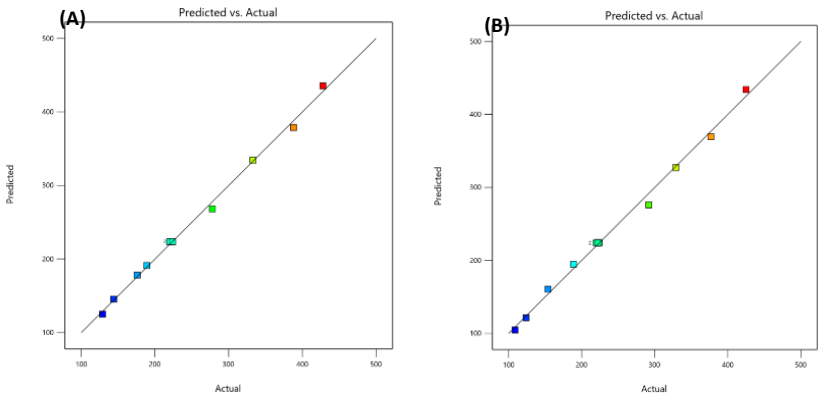

Figure 4.5. Predicted vs actual plots of viscosity at room temperature for (A) P407-Carbopol formulations and (B) P407-HPMC formulations.

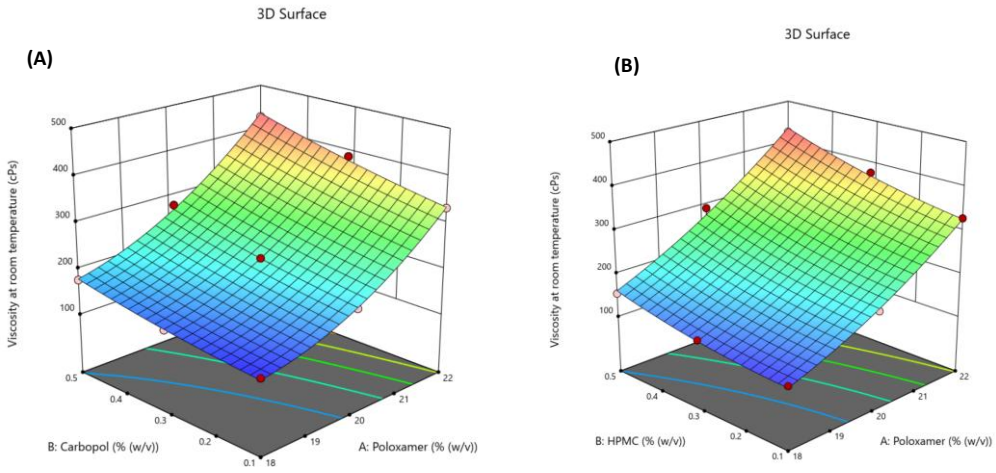

Figure 4.6. 3D surface plots of viscosity at room temperature for (A) P407-Carbopol formulations and (B) P407-HPMC formulations.

The viscosity at room temperature was significantly influenced by both P407 and polymer type (HPMC or Carbopol), exhibiting a strong positive linear and quadratic dependency. The fitted quadratic model for the P407-Carbopol and P407-HPMC are highlighted in Equation 4.1 and Equation 4.2, respectively.

Equation 4.1. $\text{Viscosity at room temp} = 223.69 + 116.67A + 38.50B + 12.00AB + 38.59A^2 + 6.09B^2$

Equation 4.2. $\text{Viscosity at room temp} = 224.21 + 124.00A + 40.67B + 12.75AB + 21.28A^2 + 11.28B^2$

Viscosity at 37°C

The viscosity at physiological temperature (37°C) followed trends consistent with room temperature viscosity, though the magnitudes were significantly higher due to thermoresponsive behaviour of P407 (ANOVA results highlighted in Table 4.4). The response surface plots of P407-based gels showed increased viscosity with both Carbopol and HPMC, as indicated in Figure 4.8. The predicted vs. actual values (Figure 4.7) were nearly ideal, suggesting accurate prediction of the model.

Table 4.4. ANOVA results summary of viscosity at 37 °C for P407–Carbopol and P407–HPMC systems.

Response	Model Type	Significant Factors	p-value (Model)	Lack of Fit p-value
Viscosity at 37 °C	Quadratic (P407–Carbopol)	A–P407 ($p < 0.0001$), B–Carbopol ($p < 0.0001$), A^2 ($p < 0.0001$)	< 0.0001	0.112
Viscosity at 37 °C	Quadratic (P407–HPMC)	A–P407 ($p < 0.0001$), B–HPMC ($p < 0.0001$), AB ($p = 0.0216$), A^2 ($p = 0.0047$)	< 0.0001	0.093

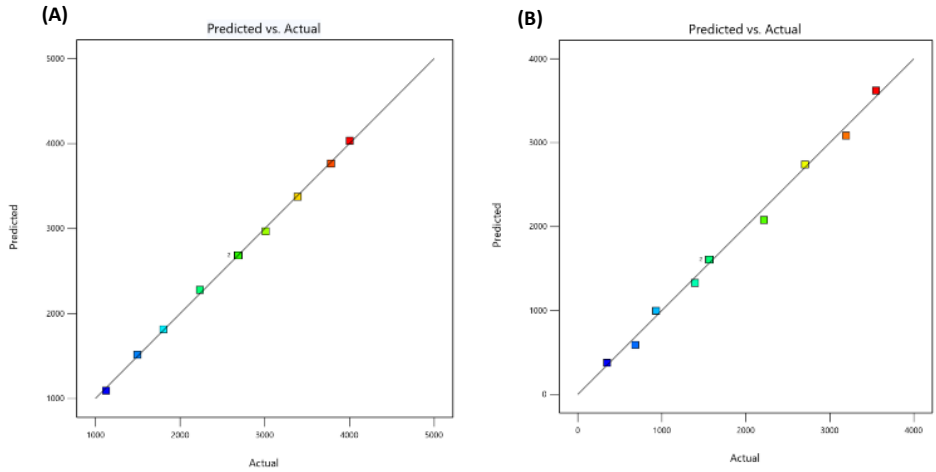

Figure 4.7. Predicted vs actual plots of viscosity at 37°C for (A) P407-Carbopol formulations and (B) P407-HPMC formulations.

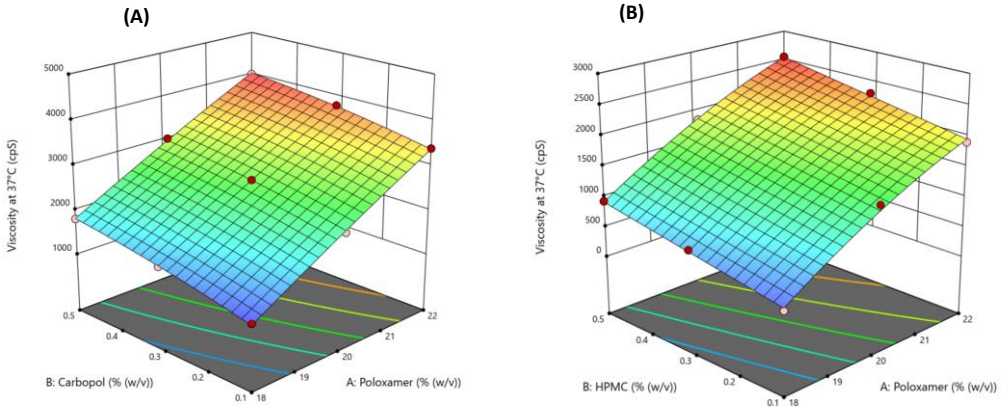

Figure 4.8. 3D surface plots of viscosity at 37°C for (A) P407-Carbopol formulations and (B) P407-HPMC formulations.

At physiological temperature (37°C), both P407-HPMC and P407-Carbopol in situ gel systems demonstrated a substantial increase in viscosity, primarily influenced by the concentration of P407. Regression modelling revealed non-linear behaviour in both systems, characterised by significant quadratic effects, which indicated that viscosity increases up to an optimal concentration before declining. The fitted quadratic equations for viscosity at 37°C for P407 with Carbopol and P407 with HPMC are represented in equation 3 and equation 4, respectively.

Equation 4.3. Viscosity at 37°C = 2787.413 + 576.5A + 176.33B + -43.249AB + -254.948A^2 + -21.448B^2

Equation 4.4. $\text{Viscosity at } 37°\text{C} = 1606.793 + 1247.166\text{A} + 375.00\text{B} + 65.25\text{AB} + 230.224\text{A}^2 + 96.724\text{B}^2$

Gelation time

Gelation time, a critical parameter for sol-gel transitions in in-situ gelling formulations, was primarily influenced by P407 concentration in both formulations (ANOVA results shown in Table 4.5). In both the models, the 3D surface plot indicated that increasing P407 concentration led to a marked decrease in gelation time, while HPMC and Carbopol had minimal influence. Surface plots referencing gelation time are highlighted in Figure 4.10. The predicted vs. actual plots (Figure 4.9) for gelation time show strong agreement, indicating high model accuracy for both P407-HPMC and P407-Carbopol systems. Minor deviations were

observed in the Carbopol formulation at higher concentrations, but overall predictive reliability remains strong.

Table 4.5. ANOVA results summary of gelation time for P407–Carbopol and P407–HPMC systems.

Response	Model Type	Significant Factors	p-value (Model)	Lack of Fit p-value
Gelation time	Quadratic (P407–Carbopol)	A–P407 ($p < 0.0001$), A^2 ($p = 0.0010$)	0.0002	0.2013
Gelation time	Quadratic (P407–HPMC)	A–P407 ($p < 0.0001$), B–HPMC ($p < 0.0001$), A^2 ($p < 0.0001$)	< 0.0001	0.1686

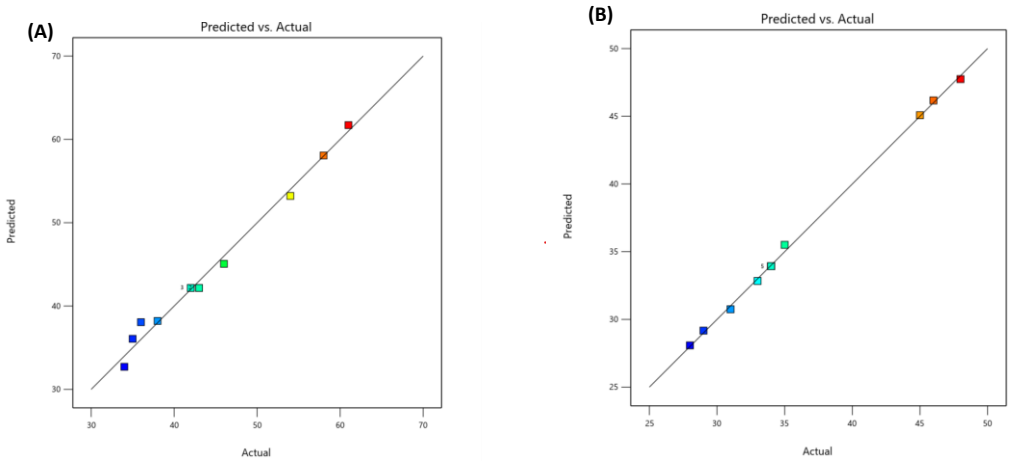

Figure 4.9. Predicted vs actual plots of gelation time for (A) P407-Carbopol formulations and (B) P407-HPMC formulations.

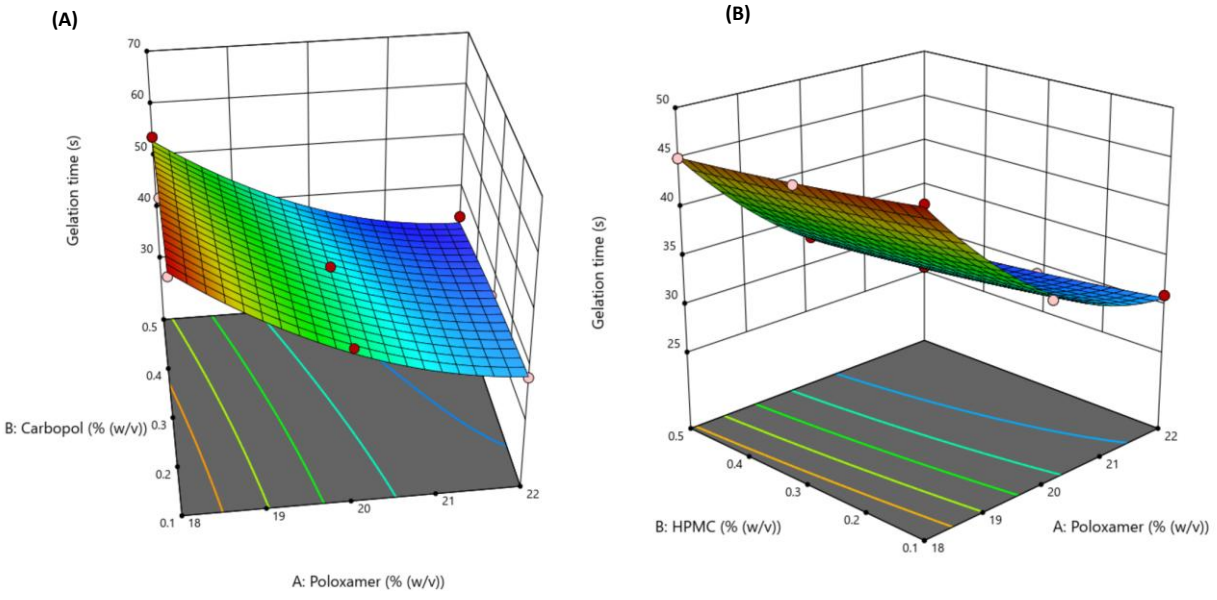

Figure 4.10. 3D surface plots of gelation time for (A) P407-Carbopol formulations and (B) P407-HPMC formulations.

Both P407-Carbopol and P407-HPMC systems exhibit decreasing gelation time, with poloxamer having a dominant influence on gelation time. The quadratic equation 5 represents gelation time for P407-Carbopol and equation 6 for P407-HPMC formulations.

Equation 4.5. Gelation time = $42.17 + -11A + -3.50B + +0.75AB + 4.90A^2 + -0.6034B^2$

Equation 4.6. Gelation time = $33.931 + -8.5A + -1.33B + 3.741A^2 + 0.241B^2$

The desirability function identified optimal compositions for both types of formulations, as shown in Table 4.6. The desirability values, ranging from 0 to 1, indicate how close the formulation responses are to the ideal targets; values closer to 1 reflect optimal outcomes for viscosity at room temperature, viscosity at 37°C, and gelation time (Paul et al., 2025). Both types of formulations exhibited good overall desirability, with values exceeding 0.7, suggesting favourable rheological and gelation properties. However, Carbopol-based formulations were found to be slightly superior in terms of viscosity at 37°C and desirability, suggesting better performance in sustained drug delivery applications.

Table 4.6 Optimized formulation parameters and responses for P407–Carbopol and P407–HPMC systems.

Formulation Type	Formulation Code (Description)	P407 (%)	Co-polymer (%)	Viscosity at Room Temperature (cP)	Viscosity at 37 °C (cP)	Gelation Time (s)	Desirability
P407–Carbopol	PC5TC / PC5C (CBD + THC / CBD only)	20.265	0.500	286.001	2538.477	36.797	0.745
P407–HPMC	PH5TC / PH5C (CBD + THC / CBD only)	20.064	0.500	264.276	2080.757	32.572	0.706

The optimized formulations were further characterised with either CBD only or with both CBD and THC added as inclusion complexes. Terpenes were excluded from formulations, as preliminary optimization trials showed that their inclusion markedly increased viscosity at room temperature, compromising the sol state and ease of administration. This finding is consistent with Rhee et al. (2007), who observed that terpenes increase the viscosity and reduce the sol–gel transition temperature of poloxamer systems. Such effects likely arise from hydrophobic interactions between terpenes and the micellar cores of Poloxamer, promoting tighter micelle packing and premature gel formation. As a result, the addition of terpenes could interfere with thermoresponsive behaviour and drug release consistency; hence, formulations were developed without terpenes to maintain desirable gelation properties and stability.

4.4.2 Appearance, pH, and drug content of developed formulations

All formulations were prepared using 20% w/v P407 in combination with either 0.5% Carbopol (PC5TC and PC5C) or 0.5% HPMC (PH5TC and PH5C) as the mucoadhesive polymer. Formulations PC5TC and PH5TC incorporated 10 mg/ml (total cannabinoid content 20 mg/ml) of both cannabidiol (CBD) and

tetrahydrocannabinol (THC), previously complexed in a 1:1 ratio with hydroxypropyl-β-cyclodextrin (HP-β-CD). Whereas formulations PC5C and PH5C contained only CBD complexed with HP-β-CD (20 mg/ml). This enabled comparison of the effect of polymer type and drug composition on the physicochemical characteristics of the in-situ gels. Table 4.7 highlights the pH, visual appearance, sol-gel transition time, and drug content of these formulations.

All formulations exhibited a homogenous creamish appearance, with no phase separation or precipitation, suggesting efficient solubilization and uniform dispersion of drug-cyclodextrin complexes. The drug content was consistent across all formulations, confirming uniform incorporation of cannabinoids within the P407-based in situ gel matrix. pH values in the range of 4.70 to 6.34, which were adjusted to 6.4 using triethanolamine to ensure physiological compatibility. Average pH of the oral mucosa was found to be around 6.7, with pH of the buccal mucosa around 6.3 (Aframian et al., 2006; He & Mu, 2023). Ideally, buccal formulations should be within the salivary pH range of 5.5 – 7.5 to minimize any discomfort at the site of application (Li & Castillo, 2020).

Table 4.7. Appearance, pH, and drug content of poloxamer-based buccal in-situ gels (n = 3; mean ± SD).

Formulation	pH	Appearance	Drug Content (mg/mL)	Sol- Gel Transition Temperature	Sol–Gel Transition Time at 37 °C (s)
PC5TC	4.92 ± 0.05	Homogenous, Cream coloured	10.11 ± 0.50 (CBD); 10.20 ± 0.07 (THC)	26 °C	36.2 ± 0.9
PC5C	4.70 ± 0.12	Homogenous, Cream coloured	20.30 ± 0.44 (CBD)	26 °C	38.2 ± 1.9
PH5TC	5.94 ± 0.22	Homogenous, Cream coloured	10.80 ± 0.12 (CBD); 10.07 ± 0.50 (THC)	28 °C	29.2 ± 1.2
PH5C	6.34 ± 0.10	Homogenous, Cream coloured	20.60 ± 0.23 (CBD)	28 °C	32.65 ± 2.6

4.4.3 Sol-gel transitions and gelation time of optimized formulations

Sol-gel transitions were measured by determining the viscosity profiles of the various formulations across a temperature range of 0 to 40°C. Results demonstrate that the viscosity of the in-situ gels is significantly influenced by both the type of mucoadhesive polymer and the drug composition. Formulations containing Carbopol (PC5TC and PC5C) exhibited higher viscosities across the temperature range compared to those with HPMC (PH5TC and PH5C), indicating that Carbopol enhances gel viscosity more effectively. It is well-documented that the addition of mucoadhesive polymers can influence the gelation temperature of poloxamer-based systems. Several studies have shown Carbopol/HPMC to lower gelling temperatures of poloxamer formulations (Balakrishnan et al., 2015; Jones et al., 2009; Silva et al., 2020). Additionally, formulations incorporating both CBD and THC (PC5TC and PH5TC) showed higher viscosities than their CBD-only counterparts (PC5C and PH5C), suggesting that the presence of THC contributes to increased gel consistency. The temperature-dependent increase in viscosity observed in all formulations confirms their

thermosensitive behaviour, with gelation occurring at physiological temperatures. These findings imply that both the choice of mucoadhesive polymer and the specific drug complex composition play crucial roles in modulating the physicochemical properties of the gels. These trends are illustrated in Figure 4.11. Figure 4.12 highlights confirmation of sol-gel transition of thermoresponsive formulation by the inversion method (Galocha-León et al., 2023).

Previous research has identified that acceptable in-situ gelling buccal formulations are required to exhibit gel like behaviour between 30°C and 37°C, and remain as liquids at room temperatures (Alhamdany et al., 2020). In-situ gels developed with mucoadhesive polymers and drugs CBD and THC increased gelation temperature. Research by Mohananaidu et al. (2022) have demonstrated that the addition of lipophilic drugs contributes to this increase, as their presence disrupts the self-assembly of hydrophobic groups into the micelle core, which can delay or reduce the extent of micelle packing required for gelation. All formulations developed remained liquids below 25°C. Overall, the findings emphasize the critical role of polymer type and cannabinoid presence in influencing the viscosity of the formulations, which is vital for optimizing drug delivery systems utilizing poloxamer-based in situ gels. Further investigations into mechanical properties and drug release kinetics are required to refine these formulations for clinical application.

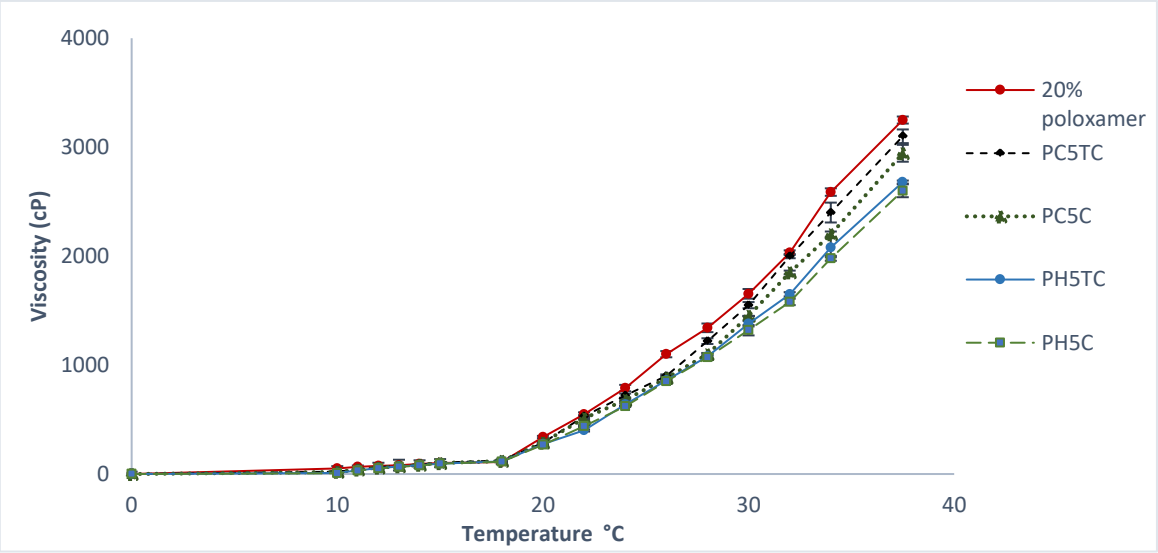

Figure 4.11. Viscosity profiles of 20% P407 and optimized in situ gel formulations (PC5TC, PC5C, PH5TC, PH5C) across a temperature range of 0°C to 37.5°C (n = 3; mean ± SD).

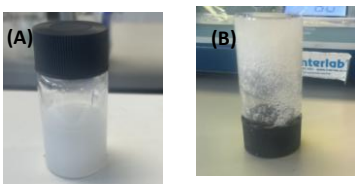

Figure 4.12. Confirmation of gel formation by inversion method (A) Formulation remaining at solution state in room temperature, (B) Formulation gelled at 37°C.

Evaluations of sol-gel transition time revealed that although P407–Carbopol formulations (PC5TC and PC5C) exhibited stronger gel structures, as demonstrated by their higher viscosity in the temperature-dependent

profiles (Figure 4.11), the HPMC-containing formulations (PH5TC and PH5C) transitioned to a gel state more rapidly. Gelation time, defined as the period required for the in-situ solution to form a coherent gel network upon exposure to physiological temperature, is influenced significantly by the viscosity of the formulation. Higher viscosities typically result from stronger intra- and intermolecular interactions within the polymer matrix, which can impede molecular rearrangement and thus delay gel formation (Ali & Al-Shohani, 2024). This relationship between viscosity and gelation speed was also evident in PC5TC and PH5TC (containing both CBD and THC) having higher viscosities than their CBD-only counterparts (PC5C and PH5C) and exhibiting slower gelation time. The sol-gel transition times for all formulations are presented in Table 4.8, supporting the observed relationship between viscosity and gelation rate.

Table 4.8. Sol-gel transition times of P407-based in situ gel formulations (n = 3; mean ± SD).

Formulation	**Sol-gel transition time at 37°C**
PC5TC	38.2 ± 1.9 s
PC5C	36.2 ± 0.9 s
PH5TC	32.65 ± 2.6 s
PH5C	31.2 ± 1.2s

4.4.4 Mechanical properties of optimized formulations

Texture analyser was used to measure the mechanical properties and mucoadhesive strength of the optimized formulations. The mechanical properties measured included hardness, cohesion and springiness reflected in Table 4.9. Hardness reflects the force required to deform the gel, which is important for assessing its resistance to mechanical stress during application, retention at the site of administration (buccal mucosa), and overall user experience. Gels that are too soft may not remain in place long enough to release the drug effectively (Gratieri et al., 2010). Springiness, also referred to as elasticity, is measured in in-situ gels to assess their ability to recover their original structure following deformation (Agossa et al., 2020). Appropriate elasticity ensures better retention at the site of application. It allows the formulations to resist washout from the site of application, ensuring sustained drug release (Gratieri et al., 2010). Cohesion refers to how well the gel holds together under deformation of stress. A highly cohesive gel resists fragmentation and maintains consistency under mechanical stress, ensuring uniform drug distribution and prolonged residence time at the site of administration (Durgun et al., 2022; Thapa et al., 2024).

The addition of mucoadhesive polymers has been shown to enhance the mechanical properties of in-situ gels, with improvements in viscosity often correlating with increased gel strength. This enhancement is attributed to the formation of a more structured polymeric network, which contributes to greater resistance to

deformation and improved textural integrity under physiological conditions (Fathalla et al., 2022; Swain et al., 2019). Thermosensitive formulations with Carbopol required higher forces to deform and had higher springiness and cohesiveness than those formulated with HPMC. Carbopol-based gels generally exhibit higher mechanical strength and cohesiveness than HPMC gels, owing to their greater crosslinking density and more cohesive polymer network Patel et al. (2011). Formulations containing both CBD and THC (PC5TC and PH5TC) demonstrated higher hardness and springiness values compared to their respective CBD-only counterparts (PC5C and PH5C). However, the opposite trend was observed for cohesiveness. This indicates that while the combination of CBD and THC contributes to a firmer and more elastic gel structure, it may reduce cohesiveness, possibly due to changes in polymer and cannabinoid interactions within the gel matrix.

Table 4.9. Mechanical properties of optimized thermosensitive formulations (n = 3; mean ± SD). Values in each column bearing different superscript letters are significantly different ($p < 0.05$), whereas those sharing at least one common letter are not significantly different (one-way ANOVA with Tukey's post hoc test).

Formulations	Hardness (N)	Springiness (%)	Cohesiveness
PC5TC	0.74 ± 0.06^{a}	99.140 ± 4.34^{ac}	0.784 ± 0.03^{ab}
PC5C	0.68 ± 0.05^{ab}	96.210 ± 2.35^{ab}	0.878 ± 0.13^{a}
PH5TC	0.53 ± 0.07^{bc}	94.790 ± 3.42^{bd}	0.732 ± 0.01^{ab}
PH5C	0.46 ± 0.06^{c}	91.626 ± 1.23^{cd}	0.759 ± 0.09^{b}

4.4.5 Mucoadhesive strength of thermoreversible formulations

The ex vivo mucoadhesion results (Figure 4.13) reveal significant differences in detachment forces, indicating varying mucoadhesive strengths among the four formulations. Formulations containing Carbopol (PC5TC and PC5C) exhibited significantly higher detachment forces compared to the HPMC-based counterparts (PH5TC and PH5C), indicating stronger adhesive interactions with the mucosal tissue. According to previous research, the superior mucoadhesive strength of Carbopol can be attributed to its higher molecular weight and greater capacity for hydrogen bonding. In contrast, HPMC, being non-ionic, exhibits weaker hydrogen bonding interactions with the mucosal membrane, which may explain its comparatively lower mucoadhesive performance (Dhawale et al., 2018).

It has been reported that dosage forms with higher mucoadhesive strength, which reflects greater attractive forces to the mucosal surface, tend to exhibit higher cohesiveness (Bassi da Silva et al., 2018). In this study, PC5C demonstrated the highest mucoadhesive force (~3.2 N), which corresponded with its highest cohesiveness value, suggesting that a well-organized internal gel structure may enhance adhesive performance. Similarly, PC5TC exhibited slightly lower mucoadhesive force (~2.5 N) but maintained relatively high cohesiveness, reinforcing this correlation. In contrast, formulations PH5TC and PH5C showed the lowest detachment forces (~1.7–1.8 N), which were consistent with their lower cohesiveness values. These findings

indicate that reduced internal structural integrity may compromise both gel cohesion and mucoadhesive potential.

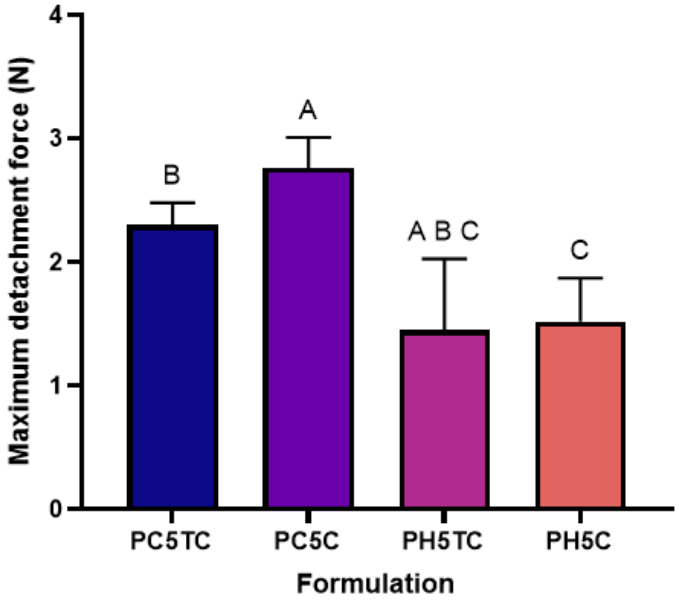

Figure 4.13. Ex vivo mucoadhesion of in situ gel formulations measured as maximum detachment force (N) (n= 3; mean ± SD). Different letters (A, B, C) above the bars indicate statistically significant differences between formulations ($p < 0.05$), bars sharing the same letter indicate no significant difference.

4.4.6 In-vitro drug release

The in vitro release profiles of the optimized in situ gel formulations are depicted in Figure 4.14. Both polymer type and drug composition were found to influence the release behaviour of the developed thermosensitive in-situ gels. Carbopol-based in-situ gel formulations (PC5TC and PC5C) demonstrated slower cumulative drug release compared to HPMC-based counterparts (PH5TC and PH5C). At 240 minutes, PH5C (CBD-only, HPMC) showed the highest release (97.5%), followed by PH5TC (88.6%), while PC5TC and PC5C reached 61.1% and 50.6%, respectively. Previous studies have demonstrated that although both Carbopol and HPMC help facilitate sustained release of drugs, release from Carbopol-based gels are slower than HPMC-based gels likely due to their higher viscosity, which can impede drug diffusion by forming a denser gel matrix (E. D. Özyılmaz et al., 2024). Furthermore, formulations containing both CBD and THC (PC5TC and PH5TC) exhibited slower release than their respective CBD-only variants (PC5C and PH5C), suggesting that the simultaneous presence of both cannabinoids impedes diffusion. This reduced release could be attributed to increased formulation viscosity, a factor previously highlighted by Ali and Al-Shohani (2024) and Zema et al. (2007), who reported that higher viscosity can limit drug mobility within gel matrices. Minimal release was observed from the carrier oils of CBD and THC alone. Further examination of individual cannabinoid release from Formulations PC5TC and PH5TC (Figure 4.14 (B) and (C)) revealed that both CBD and THC were released at similar rates from each gel, though CBD exhibited slightly higher cumulative release in both formulations. All formulations demonstrated an initial lag time of 30 minutes, which may be attributed to the time required for drug diffusion through the gel matrix, dissociation from cyclodextrin complexes, and subsequent partitioning into and across

the membrane before reaching the receptor compartment. This is expected be minimal or absent in vivo, where continuous salivary flow, and intimate contact with the buccal mucosa has the potential to accelerate gel hydration, network relaxation, and drug diffusion, allowing faster onset of release. Sundararaj et al. (2016) confirm that in vivo conditions for formulations yield different release rates than in vitro, with initial drug release faster and total gel erosion prolonged.

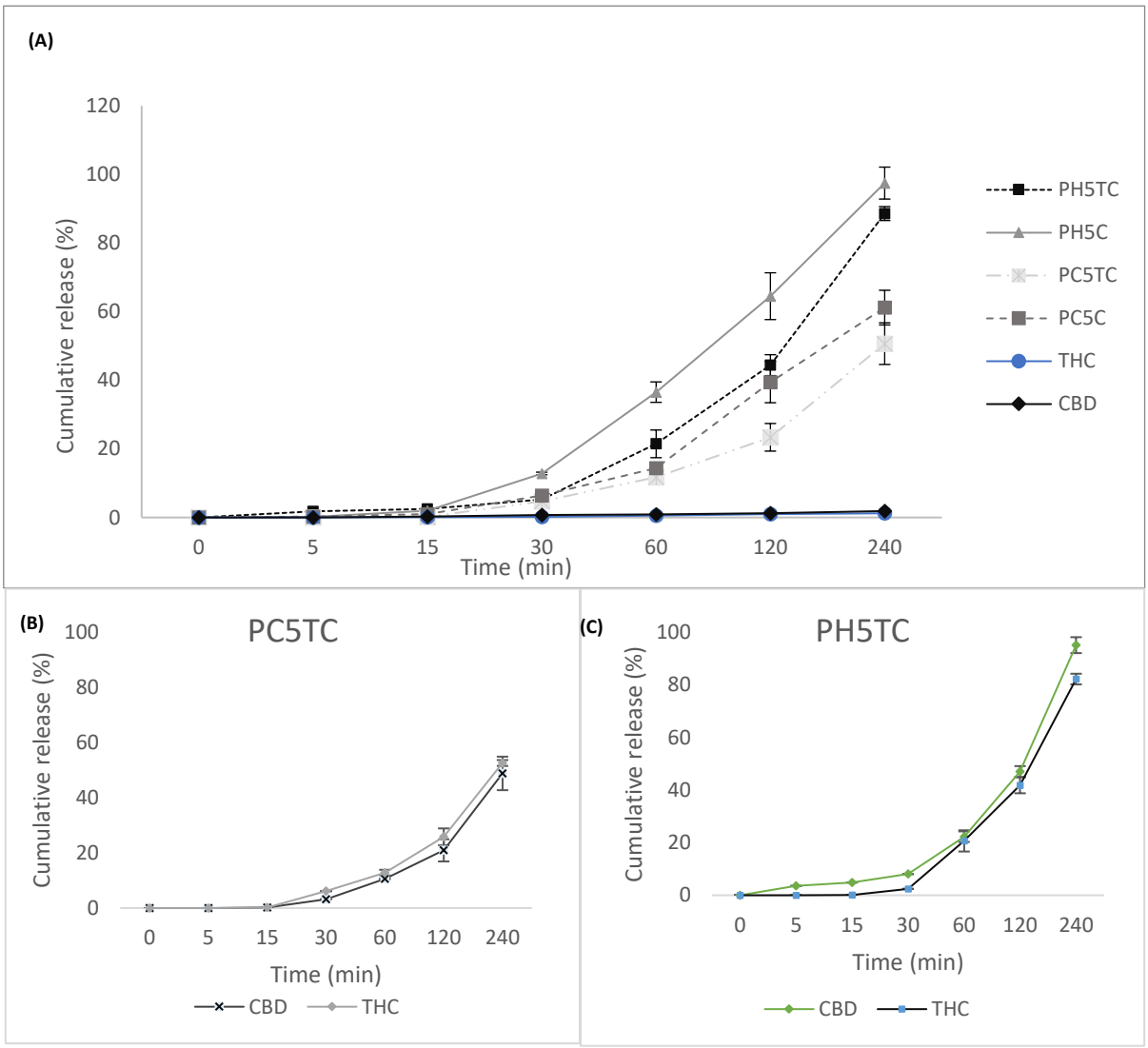

Figure 4.14. In vitro release profiles of cannabinoid-loaded thermosensitive in-situ gel; (A) comparison of gel formulations with pure CBD and THC distillates, (B) individual release profiles of CBD and THC from PC5TC, (C) individual release profiles of CBD and THC from PH5TC (n = 3; mean ± SD).

To elucidate the release mechanisms of cannabinoids from the in-situ gel formulations, drug release data were fitted to various kinetic models, including zero-order, first-order, Higuchi, Korsmeyer–Peppas, and Hixson–Crowell models, as shown in table below. The best fit was observed with the zero-order model across most formulations, with high correlation coefficients ($R^2 > 0.99$) for both CBD and THC in formulations, PC5TC and PH5TC, indicating a constant release rate independent of concentration. Abdeltawab et al. (2020) reported that several studies have demonstrated poloxamer-based in-situ gels to predominantly follow zero-order release kinetics. The Korsmeyer–Peppas model also showed good correlation in CBD-only formulations, indicating possible anomalous transport mechanisms. The release of

THC is likely governed by multiple mechanisms, including matrix interactions, partitioning into hydrophobic domains, and cyclodextrin dissociation, which are not adequately described by the Korsmeyer–Peppas model.

Table 4.10. Correlation coefficients (R^2) for various kinetic models applied to in vitro drug release data from cannabinoid-loaded in-situ gel formulations.

Formulations	Zero- order	First order	Higuchi	Korsmeyer-Peppas	Hixon-Crowell
			R^2		
PC5TC-CBD	0.9957	0.6177	-0.209	0.9515	0.8374
PC5TC-THC	0.9979	0.2714	-0.7542	0.6772	0.7824
PC5C-CBD	0.9665	0.6489	-0.0439	0.8644	0.7886
PH5TC-CBD	0.998	0.5395	-0.2734	0.9265	0.8318
PH5TC-THC	0.9979	0.2694	-0.7535	0.6727	0.7828
PH5C-CBD	0.9443	0.5639	-0.0778	0.907	0.7425

4.4.7 FTIR of optimized thermoresponsive formulations

FTIR spectroscopy was employed to characterise molecular interactions within the cannabinoid-loaded mucoadhesive hydrogels and confirm inclusion complex formation (Figure 4.15). All formulations exhibited broad absorption bands around 3400-3500 cm^{-1}, characteristic of OH stretching from P407 (Figure 19 (A)) hydroxyl groups, incorporated water molecules, and hydrogen bonding between mucoadhesive polymers and other components (Yasser et al., 2019). Strong peaks at approximately 2850 and 2950 cm^{-1} corresponded to symmetric and asymmetric C-H stretching from P407's polyoxypropylene chains (Kevin Garala et al., 2013; Yasser et al., 2019), cannabinoid alkyl groups from the CBD-HP-β-CD complex (Figure 19 (D)) and the THC-HP-β-CD complex (Figure 19 (E)) (H. Li et al., 2021; Patil & Pandey, 2024; Upadhye et al., 2010). The characteristic peaks of the inclusion complexes indicated successful encapsulation of the cannabinoids within the cyclodextrin cavities. Prominent peaks were observed around 1650 cm^{-1} and 1450 cm^{-1} in all formulations, confirming the presence of the polymer matrix and successful integration of all formulation components.

Formulations containing Poloxamer 407, HPMC, or Carbopol displayed typical polymeric peaks, including broad O–H stretching (3200–3400 cm^{-1}), C–H stretching (2850–2950 cm^{-1}), and strong ether (C–O–C) vibrations between 1000–1300 cm^{-1} (Furqan et al., 2017; Mahmood et al., 2023; Yasser et al., 2019). Upon incorporation of the drugs into the gel matrices (all formulations), the characteristic peaks of CBD and THC remained visible without significant shifts or disappearance, indicating the absence of major chemical

interactions. Furthermore, no new peaks were observed in the gel spectra, suggesting that the drug was physically entrapped within the polymeric matrix rather than chemically bonded.

These findings support the chemical compatibility of CBD and THC with the chosen excipients, confirming the stability of the drugs within the in-situ gel formulations and validating the suitability of the system for buccal or mucosal drug delivery.

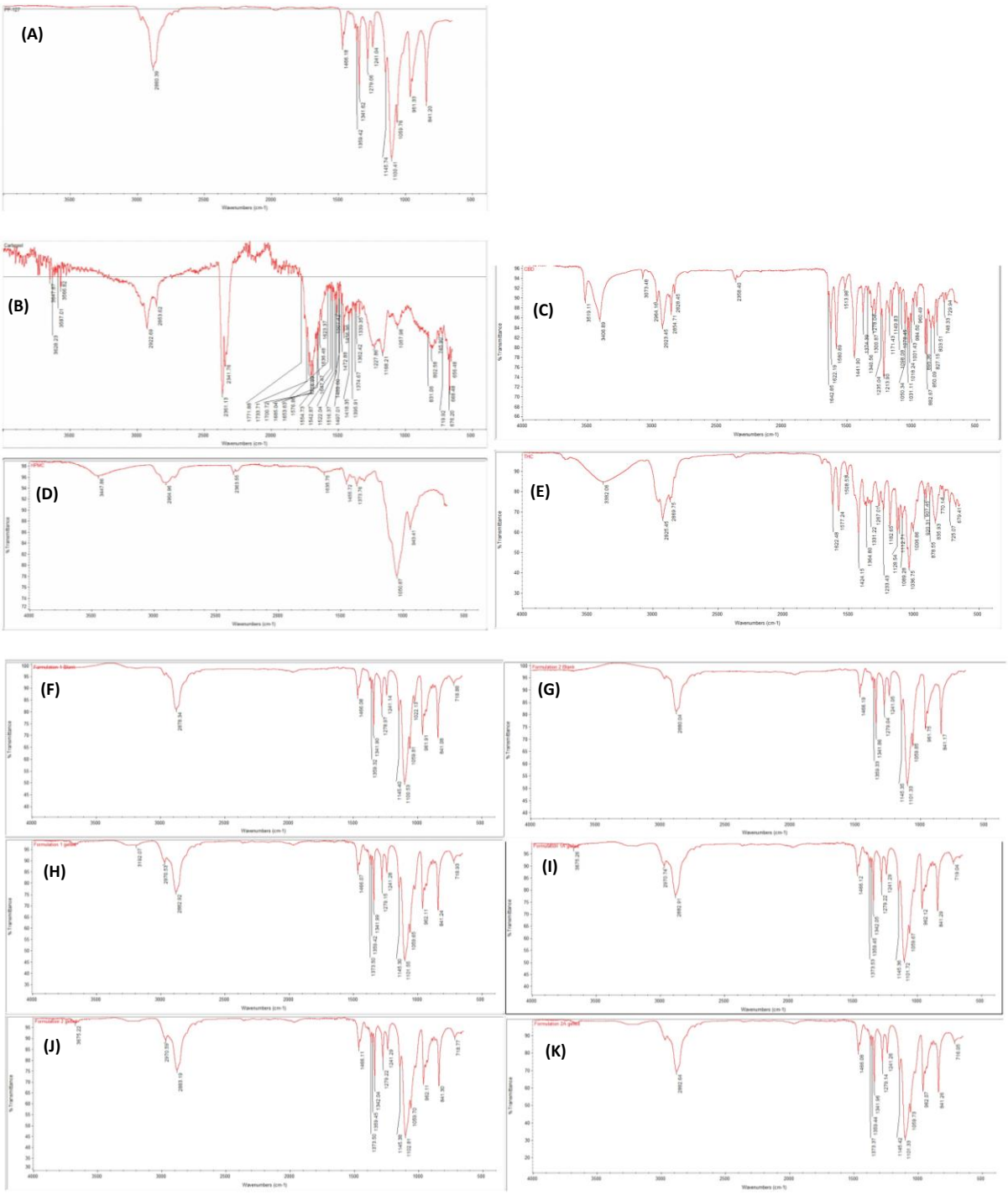

Figure 4.15. FTIR spectra of (a) Poloxamer 407, (b) Carbopol, (c) CBD, (d) HPMC, (e) THC, (f) blank Carbopol in situ gel, (g) blank HPMC in situ gel, (h) PC5TC, (i) PC5C, (j) PHCTC, and (k) PH5C.

4.4.8 SEM of thermoresponsive in situ gels

Scanning Electron Microscopy (SEM) was employed to assess the surface morphology of the freeze-dried in situ gel formulations prepared with 20% w/v Poloxamer 407 and either 0.5% Carbopol 934P (PC5TC and PC5C) or 0.5% HPMC (PH5TC and PH5C) as the mucoadhesive polymer, highlighted in Figure 4.16. No separation between the drug inclusion complexes and polymers was observed indicating successful incorporation of the drugs into the in-situ gels. Similar results were observed by Santos Akkari et al. (2016) when incorporating a drug complexed with HP-β-CD into poloxamer gels. Formulations with both CBD and THC (PC5TC and PH5TC) exhibited the smoothest and most organized surface morphology. In contrast, formulations with only CBD (PC5C and PH5C) displayed a more irregular and textured surface, indicating that the absence of THC compromised the structural integrity of the gel matrix. These observations suggest that the inclusion of THC contributes to the formation of a more cohesive and uniform microstructure, likely due to synergistic interactions between the cannabinoids and the polymeric matrix.

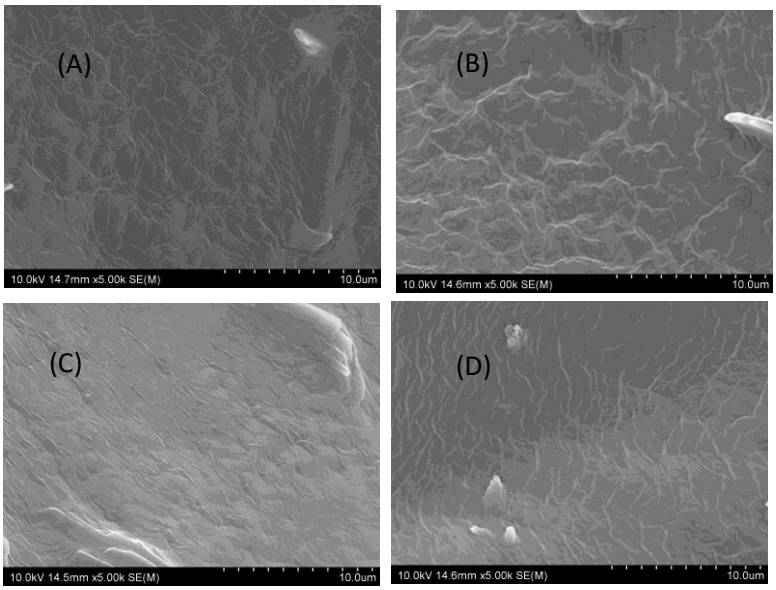

Figure 4.16. SEM captured at a magnification of ×5,000 with a scale bar representing 10 µm of optimized in-situ gels (A) PC5TC, (B) PC5C, (C) PH5TC, and (D) PH5C.

4.4.9 Ex vivo drug penetration

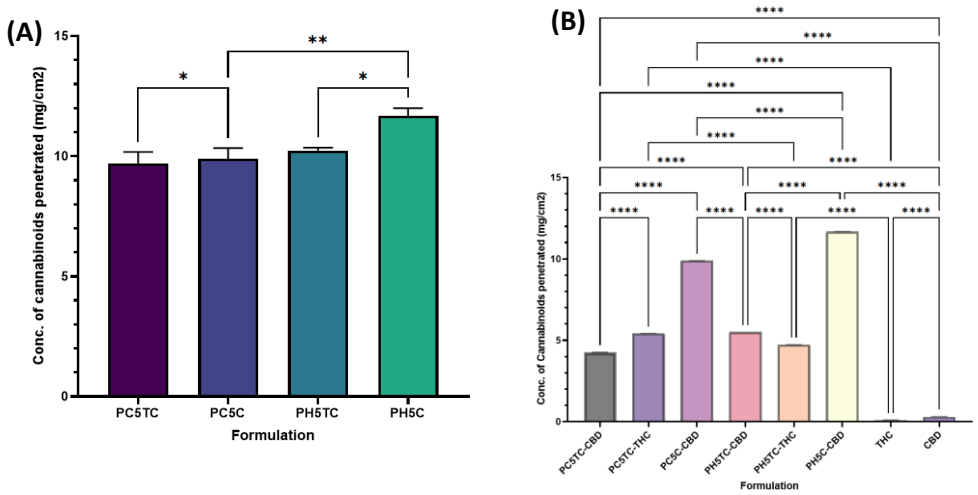

Figure 4.17. Ex-vivo penetration profiles of (A) Total cannabinoids from in-situ gelling formulations, (B) Individual permeation profiles of CBD and THC compared to pure CBD and THC distillate (n = 3; mean ± SD). Statistically significant differences are denoted as *p < 0.05 and **p < 0.01, ***p < 0.001, ****p < 0.0001.

The ex-vivo penetration study, as shown in Figure 4.17 (A), revealed that all thermosensitive in-situ gel formulations significantly improved the transmembrane delivery of cannabinoids within 2 hours. In contrast as shown in Figure 4.17 (B), pure CBD and THC distillate showed minimal penetration (<0.5 mg/cm²) into the porcine buccal mucosa. Among the formulations, PH5C (CBD-only, HPMC-based) exhibited the highest penetration (11.6 mg/cm²), followed by PH5TC (CBD and THC, HPMC-based) and PC5C (CBD-only, Carbopol-based), both achieving around 10 mg/cm². PC5TC (CBD and THC, Carbopol-based) showed slightly lower penetration (~9.6 mg/cm²). This suggests that HPMC-based gels were slightly more effective than Carbopol-based formulations in promoting drug permeation. This outcome aligns with previous findings that suggest the less cross-linked, more hydrophilic structure of HPMC forms a more permissive matrix for drug diffusion, particularly for solubilized or complexed molecules. In contrast, Carbopol's rigid and highly cross-linked gel network is known to restrict molecular mobility due to its tighter polymeric mesh, and its increased mucoadhesive strength improves residence time on the mucosal surface, providing sustained release effects (Ali & Al-Shohani, 2024; Mohammad Hamdi, Azmi, Sabari, et al., 2023; Zema et al., 2007).

When the permeation of individual cannabinoids was assessed (Figure 4.17 (B)), CBD permeated at higher concentrations than THC in both PC5TC and PH5TC formulations. THC's higher lipophilicity increases its affinity for the hydrophobic regions of the gel matrix, effectively reducing its free concentration and diffusion rate compared to CBD. Previous research has shown CBD to exhibit substantially higher permeability than THC in transdermal and mucosal systems. In vitro studies using human skin reported CBD permeability to be roughly 10 times greater than that of Δ^9-THC, attributed to its higher polarity and lower lipophilicity (C. J. Lucas et al., 2018; Varadi et al., 2023). The negligible permeation observed for unformulated CBD and THC emphasizes the need for formulation approaches that enhance solubility and diffusion, particularly for mucosal drug delivery systems. These results collectively demonstrate that both polymer type and drug composition strongly influence ex-vivo permeation, with CBD favouring better diffusion across the membrane compared to THC.

4.4.10 Stability studies

Table 4.11. Long-term Stability Profile of Cannabinoid-Loaded In-Situ Gels: pH, Appearance, Drug Content, and Gelling Capacity Over 6 Months at 4°C. Gelling capacity: +++ indicates excellent gel formation (n = 3; mean ± SD).

Formulation	**pH**			**Appearance**			**Drug content % drug remaining**			**Gelling capacity**		
	1m	**3m**	**6m**	**1m**	**3m**	**6m**	**1m**	**3m**	**6m**	**1m**	**3m**	**6m**
PC5TC	6.43± 0.02	6.32± 0.10	6.31± 0.2	Cream coloured	Cream coloured	Cream coloured	CBD 96.83± 0.19 THC 90.48± 0.23	CBD 95.41± 0.54 THC 90.99± 0.48	CBD 78.38± 0.73 THC 60.38± 0.92	+++	+++	+++

PC5C	6.72± 0.09	6.43± 0.02	6.40± 0.01	Cream coloured	Cream coloured	Cream coloured	CBD 95.23± 0.34	CBD 94.50± 0.38	CBD 76.84± 0.33	+++	+++	+++
PH5TC	6.70± 0.11	6.54± 0.01	6.50± 0.08	Cream coloured	Cream coloured	Cream coloured	CBD 94.39± 0.45 THC 85.64± 0.33	CBD 93.31± 0.33 THC 84.86± 0.023	CBD 70.32± 0.11 THC 58.38± 0.59	+++	+++	+++
PH5C	6.94± 0.01	6.77± 0.13	6.61± 0.02	Cream coloured	Cream coloured	Cream coloured	CBD 94.93± 0.48	CBD 92.34± 0.58	CBD 72.38± 0.33	+++	+++	+++

Stability studies were performed by storing the in-situ gels developed at 4 °C. Previous studies have shown that refrigerated conditions maintain rheological stability and preserves the integrity of cannabinoids. Furthermore, storage of thermosensitive in-situ gels at elevated temperatures have shown to trigger premature gelation, while prolonged storage at room temperature can cause shifts in sol–gel transition temperature, changes in viscosity, and altered drug release profiles (Akash et al., 2014; Chen et al., 2021). The stability data (Table 4.11) reveals several important trends across the four gel formulations over the 6-month storage period. All formulations demonstrated excellent physical stability, maintaining their cream-coloured appearance and optimal gelling capacity (+++) throughout the entire study duration, indicating formulation integrity regardless of polymer type or drug composition. Figure 4.18 highlights the formulation integrity after 6 months.

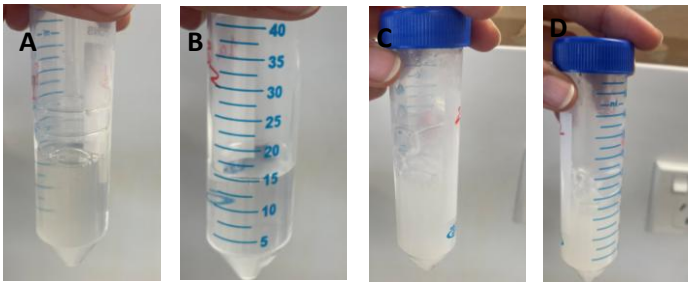

Figure 4.18. Appearance of formulations after 6 months (A) PC5TC, (B) PC5C, (C) PH5TC, and (D) PH5C.

Across all formulations, the pH values remained relatively stable and within the acceptable mucosal pH range (approximately 6.3–6.9), ensuring compatibility with the buccal environment and avoiding mucosal irritation. Visually, all formulations retained their cream colouration with no evidence of precipitation, phase separation, or discolouration, indicating good physical stability throughout the storage period. P407 based formulations generally show good stability (Giuliano et al., 2018). This was confirmed when the gelling capacity of the formulations was maintained as strong (+++), suggesting that both the thermoresponsive behaviour of P407 and the secondary polymers (Carbopol or HPMC) remained intact, with no major degradation or loss of gelation efficiency.

Drug content stability revealed significant differences between formulations. All formulations showed good drug retention up to 3 months of storage. PC5TC showed superior drug retention compared with other formulations, maintaining 96.83% and 90.48% of CBD and THC respectively at 1 month, with values declining

to 78.38% and 60.38% at 6 months. PC5C demonstrated comparable CBD stability (95.23% to 76.84%), while PH5TC and PH5C showed lower overall drug retention, with PH5TC particularly affected in THC stability (85.64% to 58.38%). Notably, THC consistently showed greater degradation than CBD across all formulations, and the dual drug formulations (PC5TC, PH5TC) generally exhibited lower drug stability compared to their CBD-only counterparts (PC5C, PH5C), suggesting potential drug-drug interactions or competitive degradation pathways. Both the cannabinoids are prone to degradation. Literature reports have shown significant instability in aqueous systems, with CBD experiencing up to 60% degradation within 7 days at 5°C and THC displaying even greater susceptibility to degradation. Oxidation of THC in the absence of light has been shown to result in the formation of CBD (Fairbairn et al., 1976; Fraguas Sánchez et al., 2020). However, inclusion complexation with cyclodextrins has been demonstrated to enhance cannabinoid stability by reducing exposure to environmental degradation factors (H. Li et al., 2021; A. Ribeiro et al., 2024).

Furthermore, Carbopol-based formulations demonstrated superior drug stability compared to HPMC formulations, likely due to better drug-polymer interactions and enhanced protection against degradation. This is supported by previous research which have identified poloxamer combined with HPMC to have lower stability (Giuliano et al., 2018).

4.5 Conclusions

This study successfully developed, optimized, and characterised thermosensitive mucoadhesive in-situ gel formulations for the buccal delivery of cannabinoids using P407 in combination with either Carbopol 934P or HPMC as mucoadhesive polymers. The main aim of this study was to design a drug delivery system capable of achieving sustained and controlled cannabinoid release at the buccal site, improving bioavailability and patient compliance while minimizing first-pass metabolism.

Initial formulation screening established that P407 concentrations of 18–22% w/v were suitable for achieving sol–gel transitions within the physiological temperature range. The incorporation of mucoadhesive polymers altered the gelation temperature and viscosity profile, necessitating further optimization through factorial design. The statistical models revealed that both polymer type and concentration, in combination with Poloxamer, significantly influenced viscosity at room and physiological temperatures and gelation time. Carbopol-based systems consistently exhibited higher viscosities and slower gelation, while HPMC-based systems transitioned more rapidly at 37°C.

Optimized formulations containing CBD alone (PC5C, PH5C) and CBD with THC (PC5TC, PH5TC) were successfully prepared using hydroxypropyl-β-cyclodextrin inclusion complexes. These gels demonstrated appropriate pH, appearance, and uniform drug content. Temperature-dependent viscosity analysis confirmed their thermoresponsive behaviour, while sol–gel transition times were inversely related to viscosity. Mechanical analysis showed that Carbopol-based formulations possessed superior hardness and springiness, while CBD-only formulations demonstrated higher cohesiveness. Mucoadhesion testing confirmed stronger

adhesive forces in Carbopol-based gels, particularly in PC5C, supporting their potential for prolonged buccal retention.

In-vitro release studies indicated that HPMC-based gels released cannabinoids more rapidly than Carbopol counterparts, with CBD-only systems outperforming those containing both CBD and THC. Ex vivo penetration studies further supported this, revealing significantly enhanced transmucosal penetration from all in-situ gel formulations relative to pure cannabinoid distillates. Notably, CBD penetrated more efficiently than THC, likely due to its greater aqueous solubility and less extensive interaction with the gel matrix. Drug release data followed zero-order kinetics, indicating a consistent and sustained release profile over time.

FTIR spectroscopy confirmed physical encapsulation of cannabinoids within the gels and absence of chemical interactions or degradation. SEM images supported the integrity of drug-polymer matrices, showing smoother and more homogeneous surfaces in formulations. Long-term stability testing over six months demonstrated that all formulations maintained acceptable pH, appearance, gelling ability, and physical integrity. Drug retention was excellent for up to 3 months in storage for all the formulations. However, degradation of cannabinoids, particularly THC, was more pronounced in HPMC-based formulations after 6 months. Carbopol-based formulations showed superior retention of both cannabinoids.

In conclusion, thermosensitive in-situ gels based on P407 with Carbopol or HPMC provide a promising platform for the buccal delivery of cannabinoids. The choice of polymer and drug composition substantially influenced formulation performance. Among the tested systems, PC5C (P407 with Carbopol and CBD) emerged as the most promising, combining optimal mucoadhesion, structural integrity, controlled release, enhanced mucosal permeation, and stability. The findings in this chapter offer a strong foundation for further preclinical and clinical development of non-invasive cannabinoid delivery systems targeting mucosal routes.

Chapter 5: Mucoadhesive Ion-Responsive In-Situ Gels for Buccal Drug Delivery of Cannabinoids

Abstract

Ion-induced in-situ gels are stimuli-responsive systems that undergo sol-to-gel transformation upon contact with physiological ions, offering a non-invasive platform for mucosal drug delivery. These gels exploit interactions with endogenous cations such as Ca^{2+} and K^{+} to form three-dimensional networks that sustain drug release and prolong mucosal residence. Anionic polysaccharides, including gellan gum and κ/ι-carrageenans, are particularly suitable due to their biocompatibility, ion-responsive gelation, and tuneable mechanical and mucoadhesive properties. This study aims to develop in-situ gels using gellan gum, κ-carrageenan, and mixture of κ/ι-carrageenans, incorporated with inclusion complexes of cannabinoids and hydroxypropyl-β-cyclodextrin (HP-β-CD) to enhance solubility and either Carbopol or HPMC to improve mucoadhesion. Formulations were characterised for gelation, rheology, mechanical strength, mucoadhesive strength, drug release, ex vivo buccal penetration of cannabinoids, and stability. Carbopol-based gels exhibited rapid gelation, higher viscosity, and superior mechanical and mucoadhesive properties, whereas HPMC-based gels facilitated faster cannabinoid release and higher penetration due to less dense networks. Mixed κ/ι-carrageenan systems provided an optimal balance of rigidity, elasticity, and mucoadhesive strength. Stability studies confirmed sustained gelation and pH maintenance, with cannabinoid degradation observed. Freeze-drying of Carbopol-based in situ gels preserved gelation properties and mucoadhesive strength upon rehydration, while improving long-term cannabinoid stability, demonstrating the feasibility of solid-state storage for enhanced shelf-life. Overall, Carbopol-based mixed κ/ι-carrageenan gels emerged as the most promising candidates for buccal cannabinoid delivery, offering controlled release, prolonged mucosal residence, and enhanced mucoadhesive strength. These findings highlight the potential of ion-activated in-situ gels as a patient-friendly platform for effective mucosal delivery of lipophilic therapeutics.

5.1 Introduction

Ion induced in-situ gels, which are a type of physiologically stimulated in-situ gelling formulations, undergo a solution-to-gel transformation in the presence of ions. These in-situ gels stand out for their high responsiveness, formulation simplicity, and compatibility with biological environments. These systems exploit ionic interactions with endogenous ions present in bodily fluids (e.g., Ca^{2+}, Na^{+}, K^{+}, Mg^{2+}) to induce gel formation. Such stimuli are especially abundant in oral, nasal, ocular, and gastrointestinal mucosa, making ion-induced gelling systems particularly suitable for non-invasive local and systemic drug delivery via mucosal routes. Ion-induced gels are typically formulated using anionic natural polymers that are sensitive to ionic crosslinking. Examples of such polymers include alginate, gellan gum, pectin, carrageenan, and xanthan gum. Their carboxylate or sulfate functional groups facilitate strong electrostatic interactions with cations, leading to rapid formation of a three-dimensional gel matrix upon contact with physiological fluids. The concentration and the type of ion used in combination with specific polymers influences gelling rate and extent of the formulations developed (Karavasili & Fatouros, 2016; Kolawole & Cook, 2023). In this study, gellan gum and carrageenans (kappa- and iota-types) are selected for the development of buccal in-situ gel formulations of cannabinoids due to their well-established ion-responsive gelling behaviour, mucosal compatibility, and regulatory acceptance.

Gellan gum is a linear anionic polysaccharide produced by the bacterium Sphingomonas elodea and is one of the most versatile polymers employed in in-situ gelling systems. Its gelation can be triggered by various stimuli, including pH, temperature, or ionic interactions. In response to temperature changes, gellan gum exhibits a reversible sol-to-gel transition. When dispersed in water at lower temperatures, polymer chains align and form double helices through van der Waals forces and hydrogen bonding, eventually leading to gel formation. Conversely, increasing the temperature disrupts these interactions, converting the gel back into a random coil configuration, thus returning to the sol state. This polymer also forms strong, brittle gels under acidic conditions, while at higher pH, it yields softer, more deformable gels due to reduced electrostatic repulsion between negatively charged carboxylate groups. The pH-dependent gel properties are attributed to the ionization state of the polymer, which influences intermolecular interactions and the overall rigidity of the gel network (Cassanelli, Prosapio, et al., 2018; Karavasili & Fatouros, 2016; Salunke & Patil, 2016).

Gellan gum exists in a random coil conformation in aqueous solution but can undergo ion induced gelation upon the introduction of monovalent or divalent cations. These cations serve as crosslinking agents, promoting the alignment of polymer chains into stable double helices and facilitating the formation of a three-dimensional gel network (Gomes et al., 2023; Salunke & Patil, 2016). The strength and mechanical properties of the resulting gels are strongly influenced by both the type and concentration of cations present, with divalent cations such as calcium capable of bridging directly between adjacent helices, thereby producing more rigid and robust gel matrices compared to monovalent ions (Coutinho et al., 2010). Complexing agents are added to gellan gum solutions in ion-induced formulations to control gelation,

enhance stability, and improve gel quality. By binding divalent cations like calcium or magnesium, agents such as sodium citrate or EDTA prevent premature gelation, ensuring uniform dispersion of gellan gum molecules. This results in smoother, more consistent gel textures and allows precise tuning of gel strength and elasticity. Complexing agents also stabilize solutions during processing, prevent aggregation, and facilitate handling by delaying gel formation until desired conditions, such as cooling or ion release, are achieved. This is particularly valuable in food, pharmaceutical, and cosmetic applications where consistent gel properties are critical (Morris et al., 2012).

Mucosal routes offer a non-invasive and effective pathway for both local and systemic drug delivery. Gellan gum-based ion-activated in-situ gels have been investigated for systemic drug delivery via the mucosal routes. For example, nasal formulations of scopolamine hydrobromide and other drugs have shown successful systemic absorption and therapeutic efficacy. These gels benefit from the rapid gelation and mucoadhesion provided by gellan gum, resisting mucociliary clearance and allowing prolonged drug release and absorption (Cao et al., 2007; Chen et al., 2020; Qian et al., 2025). Recent research has increasingly focused on the application of gellan gum-based ion-activated in-situ gels for buccal drug delivery, especially for the local treatment of oral conditions such as candidiasis, periodontal disease, and mucosal inflammation (Elmowafy et al., 2019; Garcia et al., 2024; Mahdi et al., 2014; Raja Kumar et al., 2011; Wojtyłko et al., 2024). These formulations offer several advantages, including improved patient compliance, ease of administration, and the ability to maintain therapeutic drug levels at the site of absorption. While the potential of these gels for systemic delivery via the buccal mucosa is considerable, particularly for lipophilic and poorly bioavailable drugs like cannabinoids, research in this area remains relatively limited.

Carrageenans are a family of natural, water-soluble sulfated polysaccharides extracted from red seaweeds (Rhodophyceae) and are recognized as safe by the US FDA. They are composed of alternating galactose units and 3,6-anhydrogalactose, with varying degrees of sulfation that determine their classification into three main types: kappa (κ-), iota (ι-), and lambda (λ-) carrageenan. Among these, κ- and ι-carrageenans are of particular interest in pharmaceutical applications due to their ion-sensitive gelling properties (Pacheco-Quito et al., 2020). The primary mechanism of gel formation in carrageenan in situ gels is driven by ionic interactions, particularly with monovalent or divalent cations such as potassium (K^+) or calcium (Ca^{2+}) present in physiological fluids. Kappa-carrageenan forms strong, rigid gels in the presence of potassium ions, while iota-carrageenan forms softer, more elastic gels with calcium ions. The sulfate groups on carrageenan chains interact with these cations, inducing a conformational change from a random coil to a double-helix structure, followed by helix aggregation, which creates a robust gel network. For instance, when carrageenan is administered in a liquid form for mucosal delivery, exposure to ions in bodily fluids triggers gelation, ensuring prolonged drug retention at the site (Liu et al., 2015). The gelation process results in a three-dimensional network that encapsulates therapeutic agents, controlling their release through diffusion or gel degradation. The liquid state of carrageenan in situ gels allows for easy administration via injection, sprays, or drops, while

the subsequent gelation at the target site ensures prolonged drug release. The structure of the gel, which depends on the type of carrageenan used and the ions that help form the gel, affects how fast or slow the drug is released (Necas & Bartosikova, 2013).

Carrageenan-based in situ gels are widely explored for mucosal drug delivery due to their biocompatibility, mucoadhesive properties, and ability to form gels in response to physiological stimuli like ions or temperature. These gels are particularly suited for delivering drugs to mucosal surfaces where they enhance drug retention, improve bioavailability, and provide controlled release. Such gels are effective for buccal drug delivery, providing prolonged contact with the buccal mucosa for local or systemic drug administration (Jabeen et al., 2025; Pacheco-Quito et al., 2020). Ion activated in situ gels of carrageenan's have been developed to treat oral conditions such as mucositis, gingivitis, or periodontal disease by delivering drugs for sustained drug release at the mucosa, maximizing local therapeutic effects (B. Vigani, A. Faccendini, et al., 2019). They have also been employed for systemic delivery of drugs. Li et al. (2020) developed a bupivacaine-loaded carrageenan-based in situ gel with poloxamer and Carbopol, which gelled in response to salivary ions, achieving enhanced mucoadhesion and sustained systemic release for pain management in oral mucositis, with improved bioavailability compared to oral routes. Similarly, Kianfar et al. (2013) formulated lyophilized carrageenan-poloxamer wafers loaded with paracetamol and ibuprofen, which converted to gels upon contact with saliva, achieving gradual systemic release over 2 hours, suitable for both soluble and insoluble drugs. Additionally, Kianfar et al. (2013) reported carrageenan-based films with indomethacin, where ion-induced gelation ensured sustained systemic release, ideal for chronic conditions requiring prolonged absorption.

As seen from previous literature, gellan gum and carrageenans have demonstrated considerable potential as ion-responsive polymers for mucosal drug delivery due to their biocompatibility, ability to undergo gelation in the presence of physiological ions, and capacity to sustain drug release. Their distinct gelation mechanisms and mechanical profiles make them suitable for tailoring in situ formulations specifically for the buccal environment. Building on this foundation, this chapter aims to develop ion-activated in situ gels for buccal delivery of cannabinoids, using gellan gum or κ- or ι-carrageenans as the primary gelling agents. To overcome the poor aqueous solubility, hydroxypropyl-β-cyclodextrin (HP-β-CD) inclusion complexes will be incorporated to enhance drug solubilization and stability, and mucosal penetration of cannabinoids will be enhanced by using previously determined combination of terpenes (3.125% 1,8-cineole, 0.625% d-limonene, 0.625% L-menthol, and 0.625% α-pinene). Additionally, either Carbopol or hydroxypropyl methylcellulose (HPMC) will be included as mucoadhesive polymers to improve adhesion to the buccal mucosa, prolong residence time, and support controlled drug release. This formulation strategy is expected to enhance the bioavailability of cannabinoids and provide a non-invasive, patient-friendly platform for effective delivery.

5.2 Materials and methods

Gellan gum, kappa-carrageenan, iota-carrageenan, and hydroxypropyl methyl cellulose (HPMC) were purchased from Sigma-Aldrich, New Zealand. Sodium citrate dihydrate from Fisher Scientific, Carbopol 934P (Serva) from DKSH LabShop, New Zealand, D-Limonene from Thermo Fisher, New Zealand, 1,8- cineole, α-Pinene from Sigma-Aldrich, New Zealand, laurocapram 95% from AK Scientific, and l-Menthol from Chem express supplied by Focus Bioscience, Australia. Phosphate buffered saline (PBS) tablets (pH 7.4), Tween-20%, β-CD, HP-β-CD, acetonitrile, and Bovine Serum Albumin (BSA) were purchased from Sigma-Aldrich, New Zealand. Pure isolated CBD and distilled oil of THC were provided by Helius Therapeutics Ltd, New Zealand. All other reagents used were of analytic grade.

Artificial saliva (AS) (pH 6.8) was prepared by dissolving 1.5% w/v potassium chloride (KCl), 0.43% w/v sodium chloride (NaCl), 0.22% w/v calcium chloride ($CaCl_2$), 0.42% w/v sodium bicarbonate ($NaHCO_3$), and an appropriate amount of sodium dihydrogen phosphate monohydrate ($NaH_2PO_4 \cdot H_2O$) in distilled water (B. Vigani, S. Rossi, et al., 2019).

5.2.1 Preparation and optimizations of ion induced in-situ gels.

5.2.1.1 Preparation and preliminary optimizations of cannabinoid loaded in-situ gels with gellan gum.

Preliminary Studies

Preliminary studies were carried out to determine the optimal concentration range of gellan gum and the required amount of calcium chloride necessary to facilitate ion induced gelation. Gellan gum was added to 0.15% w/v sodium citrate solutions and heated to 90°C under continuous stirring until fully dissolved. Various concentrations (0.1–0.5% w/v) of gellan gum were prepared and allowed to cool before different concentrations (0.06 to 0.1% w/v) of calcium chloride were introduced. Visual appearance and fluidity at room temperature were examined. To assess gelation behaviour, 0.5 ml of artificial saliva at 37°C, mimicking buccal conditions, was added to 1 ml of the prepared solutions with magnetic stirring. The onset of gelation was identified as the moment when the magnetic stir bar ceased rotating, indicating the transition of the formulation from a liquid to a semi solid state. Observations were made regarding gelling capacity, and gelation time. Gelling capacity was evaluated qualitatively. A score of (+) denoted weak or unstable gel formation that dispersed quickly; ++ indicated rapid gelation with the formation of a soft gel that retained its structure for a short duration typically less than 30 minutes; and +++ corresponded to immediate gelation with the formation of rigid gels. These observations were used to select the most suitable concentrations of gellan gum and calcium chloride for further formulation development (Belgamwar et al., 2009; Mahajan & Gattani, 2010).

Preparation of the in-situ gels

The in-situ gelling solutions were prepared by adding gellan gum and either HPMC or Carbopol, into a 0.15% w/v sodium citrate solution with continuous stirring at 90°C. After the polymers were fully dispersed, the solution was cooled to below 40°C. At this stage, calcium chloride and the cannabinoid, either CBD alone or a combination of CBD and THC in the form of inclusion complexes with HP-β-CD, were introduced into the solution at a final concentration of 20 mg/ml. The solution was subjected to continuous agitation using a magnetic stirrer to promote homogenous mixing of all constituents. Additional excipients, including sweetener 2% (w/v) mannitol, 0.05% (w/v) preservative propyl paraben, and natural permeation enhancer terpene combination (3.125% 1,8-cineole, 0.625% d-limonene, 0.625% L-menthol, and 0.625% α-pinene, as previously determined) were added and the mixture was stirred until all components were fully dissolved. The pH of the developed formulations was adjusted to 6.4 using triethanolamine. The resulting formulation was cooled to room temperature and stored at 4°C for further characterization (Harish et al., 2009; Xu et al., 2014).

5.2.1.2 Preparation and preliminary optimizations of cannabinoid loaded in-situ gels with carrageenan's.

Preliminary studies

Preliminary optimization studies were conducted to determine the optimal concentration κ-CG, ι-CG, and their combination (0.1 to 0.5% w/v), along with KCl and $CaCl_2$ (0.06 to 0.1% w/v), for ion-induced in situ gelation suitable for buccal applications. κ-CG and ι-CG were individually dispersed in distilled water, heated to 80°C, and stirred at 150 rpm until fully dissolved. After cooling to 40°C, KCl was added to κ-CG solutions and $CaCl_2$ to ι-CG solutions, with stirring until dissolution. Combined κ-CG/ι-CG solutions (0.3% w/v total) were prepared similarly with KCl added to the solutions. Visual appearance and fluidity at room temperature were examined. Gelation was assessed by adding 0.5 ml artificial saliva to 1 ml of the prepared solutions and gelling capacity was identified as described above (section 5.2.1.1).

Preparation of in-situ gels

Either κ-CG or a mixture of both κ-CG and ι-CG was dispersed in distilled water heated to 80°C and subjected to gentle magnetic stirring at 150 rpm until fully dissolved. After complete solubilization, solution was cooled below 40°C. HPMC or Carbopol was added, and the mixture was stirred continuously for 2 hours. Cannabinoids (CBD only or CBD and THC in 1:1) encapsulated in HP-β-CD inclusion complexes were then incorporated into the κ-CG or mixture of κ-CG and ι-CG polymer solution at a final concentration of 20 mg/ml. Finally, potassium chloride (KCl) was added to induce in situ gelation, with stirring maintained until the salt was completely dissolved. Additional excipients, including sweetener 2% (w/v) mannitol, 0.05% (w/v) preservative propyl paraben, and natural permeation enhancer terpene combination (3.125% 1,8-cineole, 0.625% d-limonene, 0.625% L-menthol, and 0.625% α-pinene, as previously determined) were added and the mixture was stirred until all components were fully dissolved. The pH of the developed formulations was

adjusted to 6.4 using triethanolamine. The resulting formulation was cooled to room temperature and stored at 4°C for further characterization (Thrimawithana et al., 2011; B. Vigani, S. Rossi, et al., 2019).

5.2.1.3 Design of experiments approach for optimizing ion responsive in situ gels

To optimize the formulation parameters of the ion activated in situ gels, a Box Behnken experimental design was employed. This response surface methodology was selected due to its efficiency in exploring quadratic response surfaces and its ability to minimize the number of experimental runs without compromising statistical reliability. Three independent formulation variables were selected based on preliminary studies, concentration of gellan gum or carrageenan ranging from 0.1 to 0.3% w/v, concentration of calcium chloride or potassium chloride ranging from 0.06 to 0.08% w/v and concentration of mucoadhesive polymer (HPMC or Carbopol) ranging from 0.1 to 0.5% w/v. Each factor was studied at three levels (low, medium, and high), and a total of 15 experimental runs were generated by the design. The dependent variables evaluated in the study included the viscosity of the formulation at room temperature as an indicator of fluidity, the gelling capacity, and the gelation time. Gelling capacity was assessed on a three-point scale, with a score of 1 representing a weak or unstable gel that dispersed quickly, 2 indicating a soft gel that formed rapidly but dissolved within a short time, and 3 corresponding to a firm gel with sustained structural integrity over an extended period. The coded levels of independent variables and the constraints applied to the dependent variables are summarized in Table 5.1. Optimized formulations were further subjected to physicochemical and mechanical characterizations.

Table 5.1 Box Behnken design: variable levels and constraints.

Independent variables			
		Levels	
	-1	0	+1
Gellan gum/ κ-CG/κ-CG and ι-CG % (w/v)	0.1	0.2	0.3
$CaCl_2$/KCl % (w/v)	0.06	0.07	0.08
HPMC/Carbopol % (w/v)	0.1	0.3	0.5
Dependent variables			
		Constrains	
Viscosity at room temperature (cps)		Minimize	
Gelling capacity		Maximize	
Gelation time (s)		Minimize	

5.2.2 Appearance, pH, and drug content of developed formulations

The appearance, pH, and drug content of the optimized formulations were evaluated as described in Section 4.2.2. Visual inspection was conducted to assess the clarity, uniformity, and absence of particulate matter in the formulations. The pH was measured using a using a calibrated bench-top pH meter (Interlab, NZ). Drug content was determined using high performance liquid chromatography to ensure accurate and consistent incorporation of the active compounds.

5.2.3 Sol-gel transition time and viscosity of the optimized formulations

Sol-gel transition time of the formulations were measured by tube inversion technique. Optimized solutions were transferred to a transparent test tube maintained at 37°C in a water bath to mimic buccal conditions. Gelation was initiated by adding 0.5 ml of artificial saliva. A stopwatch was started immediately, and the tube was gently inverted occasionally to assess flow behaviour. The sol-gel transition time was recorded as the duration (in seconds) from saliva addition until the formulation ceased to flow upon inversion, indicating complete gelation (Swain et al., 2019).

Viscosity of the solutions before and after gelling were measured using a Brookfield RST-SST rheometer equipped with a rotating ramp measuring block. Viscosity values were recorded at a fixed shear rate of 100 s^{-1}.

5.2.4 Mechanical properties of the ion induced in-situ gels.

Mechanical properties of the optimized gels were determined using a texture analyser (Stable Micro Systems, UK) fitted with a 50 N load cell, as described previously in section 4.2.4.

5.2.5 Mucoadhesive strength of the ion induced formulations.

Mucoadhesive strength of the optimized ion activated gels were evaluated using freshly prepared porcine buccal mucosa, and using a texture analyser (Stable Micro Systems, UK). Method previously detailed in section 4.2.5.

5.2.6 In-vitro drug release studies and drug release kinetics

In-vitro drug release studies were conducted with a Franz diffusion cell apparatus (Orchid Scientific, India) equipped with dialysis membranes (MWCO 14,000 Da), and drug release kinetics was analysed using KinetDS software 3.0 (rev. 2010), with the procedure outlined earlier in section 4.2.6.

5.2.7 Fourier Transform Infrared Spectroscopy (FTIR) of ion-induced formulations.

FTIR of the optimized ion induced in situ gels were recorded using a Thermo Scientific FTIR spectrometer (Nicolet iS10, USA) using samples freeze dried with Christ alpha series freeze dryer (Osterode am Harz, Germany), as highlighted in section 4.2.7.

5.2.8 Scanning Electron Microscopy (SEM) of ion-induced formulations

SEM of freeze dried in situ gels were coated with platinum using an ion sputter coater (Hitachi E-1045) and examined with a Schottky field emission scanning electron microscope (FE-SEM) (Thermo Scientific, HITACHI SU-70) in accordance with the method described in section 4.2.8.

5.2.9 Ex-vivo drug penetration

Ex-vivo penetration of cannabinoids from the optimized ion stimulated in situ gels was carried out using porcine buccal mucosa placed in the Franz diffusion cell apparatus ((Orchid Scientific, India), as outlined in the methodology section 3.2.5.3. The donor chamber was loaded with 1 mL of the optimized ion-induced in situ gel formulation containing (20 mg/ml of cannabinoids). Following application, 0.5 mL of artificial saliva was added to the donor compartment to initiate ion-triggered gelation at the mucosal interface.

5.2.10 Stability studies

Long term stability studies were carried out by incubating the ion induced gelling solutions at room temperature of 25°C. Samples were withdrawn periodically at 1, 3 and 6 months, and were assessed for changes in key physicochemical parameters, including pH, physical appearance (e.g., colour, clarity, presence of any precipitation or phase separation), drug content, and gelling capacity.

5.2.10.1 Freeze dried in-situ gels.

Carbopol-based ion-induced in situ gels were freeze-dried using Christ alpha series freeze dryer (Osterode am Harz, Germany) for 48 hours. The dried gels were stored at room temperature (25 °C) for six months. For rehydration, distilled water was added dropwise in a volume equivalent to the initial formulation volume prior to freeze-drying, after which the samples were evaluated for pH, drug content, and gelling capacity, followed by determination of their sol–gel transition behaviour using artificial saliva.

5.3 Statistical analysis

Experimental data were analysed using R programming and GraphPad Prism software (version 10.2.3). For datasets that satisfied the assumptions of normality and equal variances, statistical significance was evaluated using one way analysis of variance. When these assumptions were not met, the Kruskal Wallis test was applied as a non-parametric alternative. Where significant differences were observed, post hoc analyses were performed using Tukey's multiple comparison test. A probability value of $P < 0.05$ was considered statistically significant.

5.4 Results and discussion

5.4.1 Preliminary optimizations of ion-induced gels

5.4.1.1 Optimizing concentration range of ion induced gelling polymers and salts.

Preliminary optimization studies evaluated gellan gum (0.1–0.5% w/v) and κ-CG (0.1–0.5% w/v) with $CaCl_2$ (0.06–0.1% w/v) and KCl (0.06–0.1% w/v), respectively, for ion-induced in situ gelation. Spontaneous gelation occurred in the absence of artificial saliva when either the ion-responsive polymer concentration (≥ 0.5% w/v) or the corresponding salt concentration (≥ 0.1% w/v) exceeded critical thresholds, indicating that sufficient polymer or ionic content alone was capable of inducing gel formation. Results showing visual appearance, fluidity, gelling capacity, and time are highlighted in Table 5.2. Formulations containing ι-CG formed soft, crumbly gels upon artificial saliva addition, consistent with previous findings by Rungpetchanan et al. (2023) noting this behaviour when the ion induced gelling solutions were exposed to ionic environments. Therefore, a combination of ι-CG and κ-CG in varying ratios at a total polymer concentration of 0.3% w/v was selected for further optimization.

All formulations of gellan gum (0.1–0.5% w/v, 0.06–0.1% $CaCl_2$, 0.15% sodium citrate) exhibited a clear appearance, indicating complete dissolution and homogeneity. Formulations of κ-CG at 0.1–0.5% w/v with 0.06–0.1% KCl were clear. Gellan gum's fluidity decreased with increasing polymer and $CaCl_2$ concentrations, reflecting stronger Ca^{2+} induced cross-linking that reduces flowability before artificial saliva addition. At 0.1–0.3% w/v with 0.06–0.08% $CaCl_2$, high to moderate fluidity (+++/++) was observed. Premature gelation (non-flowing, -) at higher concentrations (0.4–0.5% w/v, ≥0.08% $CaCl_2$) indicated excessive cross-linking. For κ-CG, high fluidity (+++) at 0.1–0.3% w/v with 0.06–0.08% KCl was observed. Premature gelation at 0.4–0.5% w/v or 0.1% KCl suggests K^+ ions trigger rapid helix formation, reducing fluidity during preparation. These findings align with studies noting that low polymer concentrations maintain fluidity for in situ gels, while higher ion levels cause premature gelation (Mokhtari et al., 2021; Zia et al., 2018).

Gellan gum gelation times decreased with increasing polymer concentrations, from 67 s (0.1%, with 0.06% $CaCl_2$) to 42 s (0.4%, with 0.06% $CaCl_2$). 0.3% κ-CG showed fastest gelation when combined KCl, gelling at 15-8 s. Gellan gum exhibited robust ion-induced gelation with Ca^{2+} ions, consistent with its high sensitivity to divalent cations. At 0.1–0.3% w/v with 0.06–0.08% $CaCl_2$, Gellan gum's gelling capacity improved with increasing $CaCl_2$ and polymer concentrations, achieving optimal gelation (+++). For κ-CG, no gelation at 0.1% w/v with 0.06–0.08% KCl indicates inadequate polymer concentration for helix formation. Optimal (+++) and exceptional (++++) gelation was observed at 0.3% w/v with 0.06–0.08% KCl. However, research by Barbara Vigani et al. (2020) have noted that addition of other components/excipients such as mucoadhesive polymers are found to have an influence on the gelling capacity of ion-induced polymers. Premature gelation of both the polymers at 0.4–0.5% w/v limits their use, emphasizing the need for lower concentrations. Hence, for further optimizations 0.1-0.3% w/v of gellan gum, κ-CG (0.1–0.3% w/v), and a combined κ-CG/ι-CG

formulation (0.3% w/v total) were selected. Additionally, $CaCl_2$/ KCl concentrations of 0.06–0.08% w/v were chosen for these optimizations.

Table 5.2. Preliminary optimization of gellan gum and κ-CG In Situ Gels with $CaCl_2$ and KCl, respectively (n = 3; mean ± SD).

Concentration of ion induced gelling solution % (w/v)		Conc. of salt $CaCl_2$ or KCl % (w/v)	Visual appearance	Fluidity	Gelling capacity	Gelation time upon the addition of AS at 37 °C
Gellan gum	0.1%	0.06% $CaCl_2$	Clear	+++	+	67 s
		0.08% $CaCl_2$	Clear	++	++	60.5 s
		0.10% $CaCl_2$	Clear	-	--	-
	0.2%	0.06% $CaCl_2$	Clear	+++	++	57.4 s
		0.08% $CaCl_2$	Clear	++	+++	50 s
		0.10% $CaCl_2$	Clear	-	--	-
	0.3%	0.06% $CaCl_2$	Clear	++	+++	51 s
		0.08% $CaCl_2$	Clear	++	+++	48.3 s
		0.10% $CaCl_2$	Clear	-	--	-
	0.4%	0.06% $CaCl_2$	Clear	+	+++	42 s
κ-CG	0.1%	0.06% KCl	Clear	+++	-	-
		0.08% KCl	Clear	+++	-	-
		0.10% KCl	Clear	-	--	-
	0.2%	0.06% KCl	Clear	+++	+	49 s
		0.08% KCl	Clear	+++	++	32 s
		0.10% KCl	Clear	-	--	-
	0.3%	0.06% KCl	Clear	+++	+++	15 s
		0.08% KCl	Clear	+++	++++	8 s
		0.10% KCl	Clear	-	--	-

Note: Fluidity represented as +++ (highly fluid), ++ (moderately fluid), + (low fluidity), - (non-flowing, gelled). Gelling capacity represented as + (partial gelation, limited viscosity), ++ (moderate gelation, increased thickness), +++ (rapid, stable gelation), ++++ (exceptionally rapid/strong gelation), - (no gelation), -- (already gelled).

5.4.1.2 Optimization of ion induced in situ gels using design expert: effect of polymer and Ionic crosslinker concentrations.

5.4.1.2.1 Ion induced gels of gellan gum with HPMC/Carbopol

Box-Behnken Design was employed using Design Expert software to investigate systems comprised of either gellan gum, HPMC, and calcium chloride ($CaCl_2$), or formulations containing gellan gum, Carbopol, and $CaCl_2$.

For the gellan gum-HPMC formulations with $CaCl_2$, the ANOVA results, summarized in Table 5.3, confirmed statistical significance for all models ($p < 0.0001$), with quadratic models for fluidity and gelling capacity and a linear model for gelation time effectively capturing the relationships between independent variables, gellan gum (A), HPMC (B), and $CaCl_2$ (C) concentrations, and the responses. Non-significant lack of fit p-values ($p > 0.05$) validated the models' adequacy, aligning with response surface methodology (RSM) best practices. The equations representing the models are highlighted in Equation 5.1, Equation 5.2, and Equation 5.3. The optimized formulation (0.195% gellan gum, 0.4% HPMC, 0.07% $CaCl_2$) achieved a fluidity of 34.83 mPa·s, a maximum gelling capacity of 3, and a gelation time of 56.1 seconds, with a desirability score of 0.629, reflecting a balanced compromise. These results are visually supported by the 3D surface plots (Figure 5.1 (D), (E), and (F)) and predicted vs. actual plots highlighted (Figure 5.1 (A), (B), and (C)), which illustrate the response surfaces and model accuracy, respectively.

Equation 5.1. $Fluidity = 28.89 + 15.89A + 12.19B + 3.03C + 7.91AB + 0.60AC + 0.49BC – 6.10A^2 + 0.89B^2 – 0.35C^2$

Equation 5.2. $Gelling\ Capacity = 3.0 + 1.3A + 0.37B + 0.25C + 0.25AB + 7.02AC + 2.94BC – 1.12A^2 – 0.62B^2 – 0.37C^2$

Equation 5.3. $Gelation\ Time = 60.11 – 3.86A – 7.30B – 2.16C$

Fluidity was significantly influenced by gellan gum, HPMC, and their interaction (AB, $p = 0.0462$), with a negative quadratic term for gellan gum (A^2, $p = 0.0019$). The 3D surface plot (Figure 5.1) showed viscosity increasing synergistically with polymer concentration, peaking before declining. Gelling capacity was driven by gellan gum, HPMC, $CaCl_2$, and strong AC ($p < 0.0001$) and BC ($p = 0.0003$) interactions, reflecting the role of calcium ions in network crosslinking. Quadratic curvature indicated an optimal range, avoiding over-crosslinking. Gelation time decreased linearly with all factors, with HPMC showing the greatest effect. The moderate desirability score (0.629) meets RSM acceptability thresholds (Montgomery & St, 2022).

Table 5.3 Analysis of Variance (ANOVA) summary for the gellan gum-HPMC-$CaCl_2$ system.

Response	Model Type	Significant Factors	p-value (Model)	Lack of Fit p-value
Fluidity	Quadratic	A-Gellan gum (p<0.0001), B-HPMC (p<0.0001), C-CaCl2 (p<0.0001), AB (p=0.0462), A^2 (p=0.0019)	<0.0001	0.8360
Gelling capacity	Quadratic	A-Gellan gum (p<0.0001), B-HPMC (p=0.0016), C-CaCl2 (p=0.0062), AC (p<0.0001), BC (p=0.0003)	<0.0001	0.7521
Gelation time	Linear	A-Gellan gum (p<0.0001), B-HPMC (p<0.0001), C-CaCl2 (p=0.0037)	<0.0001	0.3360

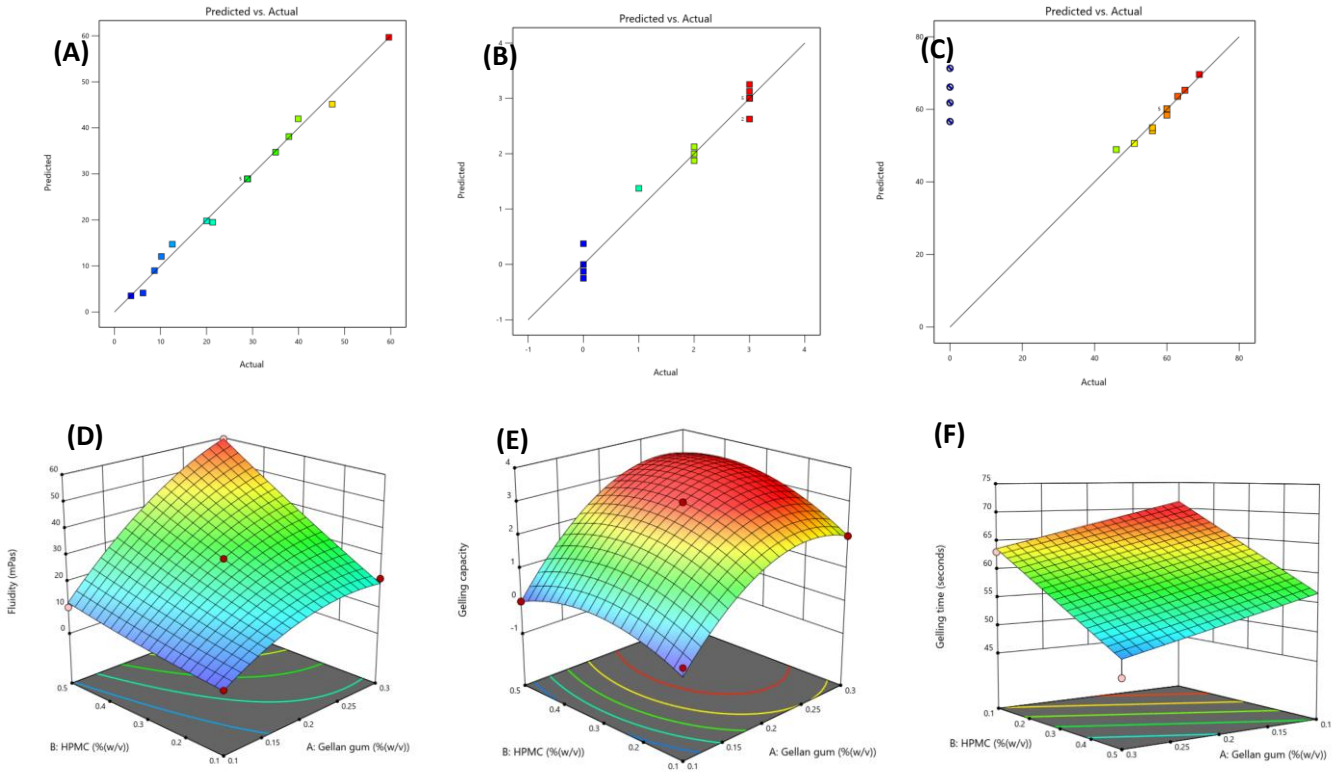

Figure 5.1 Response surface and predictive analysis for gellan gum-HPMC-$CaCl_2$ system, (A) predicted vs. actual plot for fluidity, (B) predicted vs. actual plot for gelling capacity, (C) predicted vs. actual plot for gelation time, (D) 3D surface plot for fluidity, (E) 3D surface plot for gelling capacity, (F) 3D surface plot for gelation time.

For the gellan gum-Carbopol formulations with $CaCl_2$, the ANOVA results presented in Table 5.4 establish a statistical basis for optimizing ion-induced gels using gellan gum, Carbopol, and calcium chloride ($CaCl_2$), with fluidity, gelling capacity, and gelation time as response variables. The highly significant p-values for all models ($p < 0.0001$) indicate that the quadratic models effectively capture the relationships between the independent variables, gellan gum (A), Carbopol (B), and $CaCl_2$ (C) concentrations, and the responses. The non-significant lack of fit p-values ($p > 0.05$ for all responses) further confirm the adequacy of these models, aligning with best practices in RSM as outlined by Montgomery and St (2022). The optimized formulation (0.187% gellan gum, 0.37% Carbopol, 0.080% $CaCl_2$) with a desirability score of 0.687 reflects a well-balanced optimization. Quadratic models are represented by Equation 5.4, Equation 5.5, and Equation 5.6.

Equation 5.4. $\text{Fluidity} = 27.81 + 23.06A + 21.15B + 4.81C + 1.53AB + 0.67AC + 0.44BC - 1.31A^2 - 0.36B^2 - 0.19C^2$

Equation 5.5. $\text{Gelling Capacity} = 2.74 + 1.14A + 1.12B + 0.62C + 0.25AB + 0.22AC + 0.19BC - 0.26A^2 - 0.23B^2 - 0.10C^2$

Equation 5.6. $\text{Gelation Time} = 45.98 - 7.17A - 6.89B - 3.62C - 1.83AB - 0.87AC - 0.45BC + 1.02A^2 + 0.88B^2 + 0.22C^2$

The fluidity model was quadratic and significantly influenced by gellan gum ($p < 0.0001$), Carbopol ($p < 0.0001$), their strong interaction AB ($p < 0.0001$), and the quadratic term A^2 ($p = 0.0001$). The 3D surface plot (Figure 5.2(D)) shows a pronounced viscosity peak with rising Carbopol content. Gelling capacity was also

quadratic, with significant contributions from gellan gum ($p < 0.0001$), Carbopol ($p = 0.0151$), $CaCl_2$ ($p = 0.0062$), and strong AC ($p < 0.0001$) and BC ($p < 0.0001$) interactions, highlighting robust ionic crosslinking, also seen in the 3D surface plot (Figure 5.2 (E)). Gelation time followed a quadratic model, significantly affected by all factors ($p < 0.0001$), interaction AB ($p < 0.0001$), and quadratic terms B^2 and C^2 ($p = 0.0001$). The 3D surface plot (Figure 5.2 (F)) shows a steep decline at higher concentrations, yielding rapid gelation (31.32 s). Accuracy was confirmed by the predicted vs. actual plots ((Figure 5.2 (A), (B) and (C)).

Table 5.4. Summary of ANOVA results for the Gellan gum–Carbopol–$CaCl_2$ system.

Response	Model Type	Significant Factors	p-value (Model)	Lack of Fit p-value
Fluidity	Quadratic	A–Gellan gum ($p<0.0001$), B–Carbopol ($p<0.0001$), C–$CaCl_2$ ($p<0.0001$)	<0.0001	0.3726
Gelling capacity	Quadratic	A–Gellan gum ($p=0.0011$), B–Carbopol ($p=0.0011$), C–$CaCl_2$ ($p<0.0001$), AC ($p<0.0001$), BC ($p<0.0001$)	<0.0001	0.5310
Gelation time	Quadratic	A–Gellan gum ($p<0.0001$), B–Carbopol ($p<0.0001$), C–$CaCl_2$ ($p<0.0001$), AB ($p<0.0001$), AC ($p<0.0001$)	<0.0001	0.0001

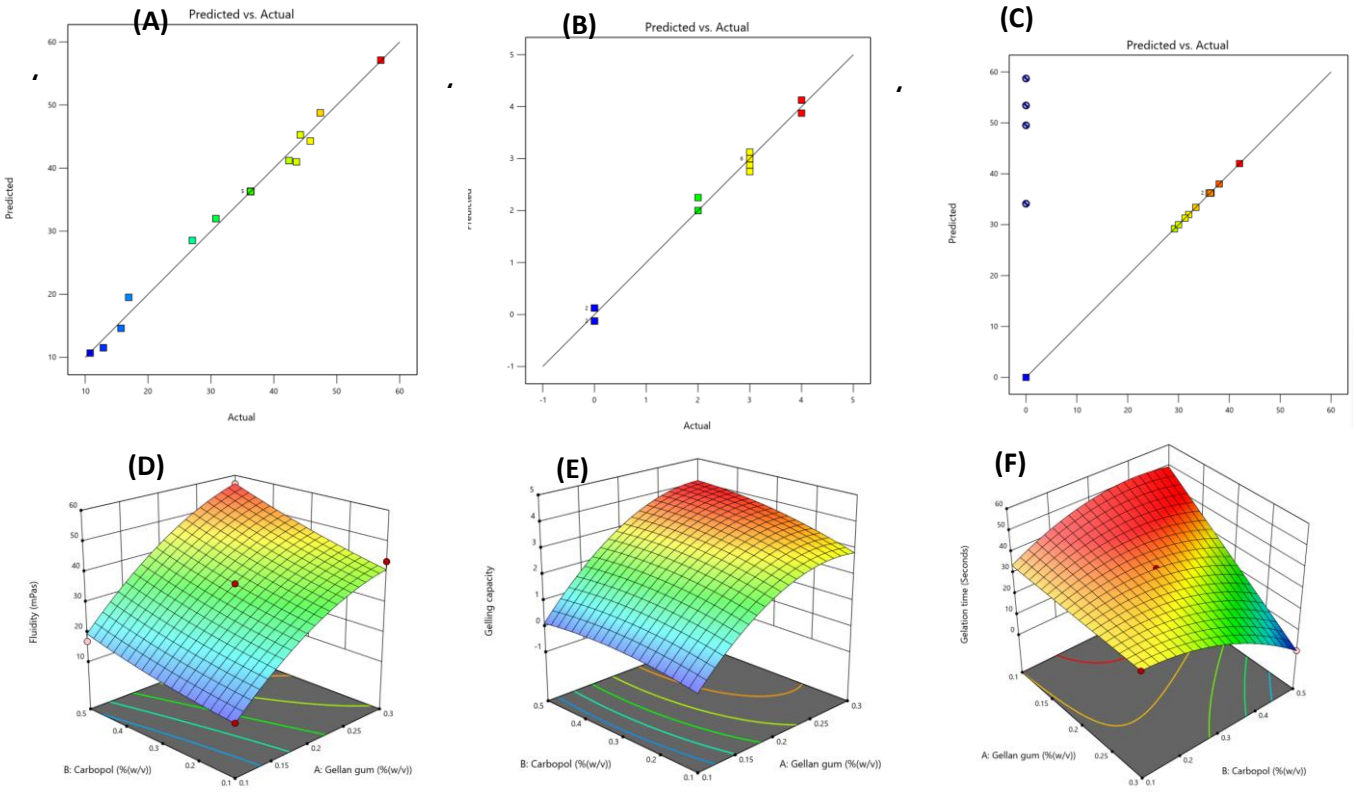

Figure 5.2. Response surface and predictive analysis for gellan gum-Carbopol-$CaCl_2$ system, (A) predicted vs. actual plot for fluidity, (B) predicted vs. actual plot for gelling capacity, (C) predicted vs. actual plot for gelation time, (D) 3D surface plot for fluidity, (E) 3D surface plot for gelling capacity, (F) 3D surface plot for gelation time.

5.4.1.2.2 Ion induced gels of κ-CG with HPMC/Carbopol

The κ-carrageenan–HPMC–KCl formulation was optimized using Box–Behnken Design (BBD), with fluidity, gelling capacity, and gelation time as response variables. ANOVA (shown in Table 5.5) confirmed that the models for all three responses were statistically significant ($p < 0.0001$), with quadratic models describing fluidity and gelling capacity, and a linear model fitting gelation time. KCl (0.06 to 0.08%) did not have a statistically significant effect on gelation time and fluidity ($p > 0.05$) but was found to have a moderate response on gelling capacity ($0.05>p>0.01$). Non-significant lack-of-fit values ($p > 0.05$) indicated that the models adequately captured the experimental trends. The optimized formulation contained 0.300% κ-carrageenan, 0.28% HPMC, and 0.08% KCl, producing an excellent balance of low viscosity, high gel strength, and rapid setting, reflected in the highest desirability score (0.759). Equation 5.7, Equation 5.8, and Equation 5.9 were found to represent the models.

Equation 5.7. $\text{Fluidity} = 18.55 + 10.11A + 11.05B + 1.35C + 4.28AB + 1.35AC + 0.43BC – 1.90A^2 + 5.14B^2 + 0.46C^2$

Equation 5.8. $\text{Gelling Capacity} = 3 + 1.375A + 0.75B + 0.375C + 2.13AB + 0.25AC – 6.15BC – 0.62A^2 – 0.37B^2 – 0.62C^2$

Equation 5.9. $\text{Gelation Time} = 10.36 – 2.63A – 1.09B + 0.18C$

Fluidity was significantly influenced by κ-carrageenan ($p < 0.0001$), HPMC ($p < 0.0001$), and the quadratic term for κ-carrageenan ($p = 0.0057$). The 3D surface plot in Figure 5.3 (D) showed an upward curvature, with fluidity increasing at higher polymer concentrations. Gelling capacity was also quadratic, with significant effects from κ-carrageenan ($p < 0.0001$) and HPMC ($p = 0.0026$). The 3D surface plot (Figure 5.3(E)) revealed a peak gelling capacity at moderate polymer concentrations, suggesting an optimal network density for gel strength. Gelation time followed a linear model, with κ-carrageenan and HPMC both significantly reducing setting time ($p < 0.0001$). The 3D plot Figure 5.3(F)) showed a steep linear decline in gelation time as polymer concentrations increased. Reliability of the models was confirmed by the predicted vs. actual plots highlighted in Figure 5.3 (A), (B), and (C) where data points closely followed the ideal correlation line.

Table 5.5 Summary of ANOVA results for the κ-carrageenan–HPMC–KCl system.

Response	**Model Type**	**Significant Factors**	**p-value (Model)**	**Lack of Fit p-value**
Fluidity	Quadratic	A–κ-cg ($p<0.0001$), B–HPMC ($p<0.0001$), C-KCl ($p=0.1955$), A^2 ($p = 0.0057$)	<0.0001	0.7837
Gelling capacity	Quadratic	A–κ-cg ($p<0.0001$), B–HPMC ($p = 0.0026$), C-KCl ($p=0.0716$)	0.0021	0.8013
Gelation time	Linear	A–κ-cg ($p<0.0001$), B–HPMC ($p<0.0001$), C-KCl ($p=0.5327$)	<0.0001	0.5327

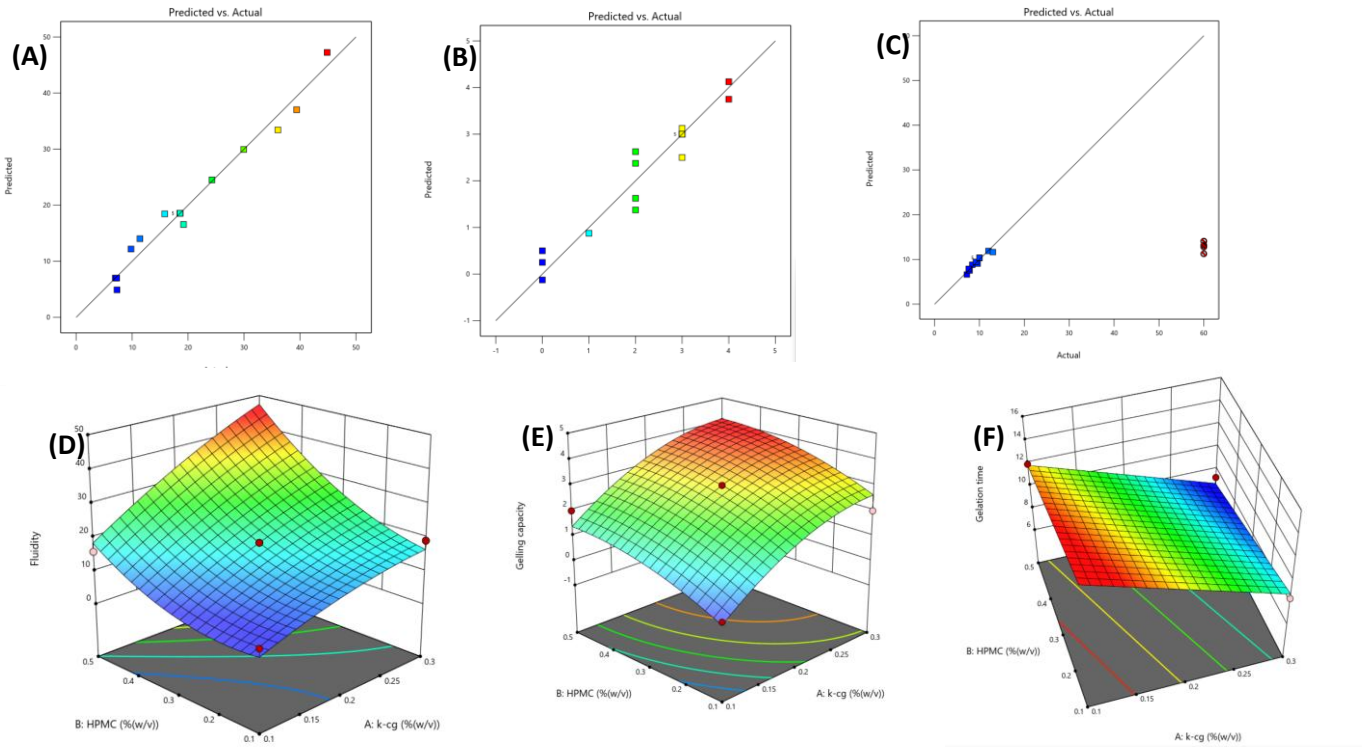

Figure 5.3 Response surface and predictive analysis for κ-CG-HPMC-KCl system, (A) predicted vs. actual plot for fluidity, (B) predicted vs. actual plot for gelling capacity, (C) predicted vs. actual plot for gelation time, (D) 3D surface plot for fluidity, (E) 3D surface plot for gelling capacity, (F) 3D surface plot for gelation time.

The κ-carrageenan–Carbopol–KCl formulation was optimized using RSM, with fluidity, gelling capacity, and gelation time as responses. ANOVA confirmed significant quadratic models for fluidity and gelling capacity ($p < 0.0001$) and a linear model for gelation time ($p < 0.0001$) (Table 5.6). KCl (0.06 to 0.08%) did not have a statistically significant effect on gelation time, gelling capacity, and fluidity. Non-significant lack-of-fit values ($p > 0.05$) indicated good model adequacy, with Equation 5.10, Equation 5.11, and Equation 5.12 representing the models. The optimized formulation (0.286% κ-carrageenan, 0.300% Carbopol, 0.074% KCl) achieved low viscosity (10.51 mPa·s), high gelling capacity (3.02), rapid gelation (6.39 s), and a desirability score of 0.650.

Equation 5.10. $\text{Fluidity} = 8.3 + 2.612A + 1.23B + 0.07C + 0.27AB + 0.3AC + 0.24BC + 1.612A^2 + 0.162B^2 + 0.28C^2$

Equation 5.11. $\text{Gelling Capacity} = 2 + 1.25A + 0.62B - 0.125C - 0.25AB + 0.25AC + 4.24BC - 0.25A^2 + 0.5B^2 - 5.41C^2$

Equation 5.12. $\text{Gelation Time} = 8.49 - 3.63A - 0.87B - 0.23C$

Fluidity was predominantly influenced by κ-carrageenan ($p < 0.0001$) and Carbopol ($p < 0.0001$), with a strong quadratic effect of κ-carrageenan (A^2, $p < 0.0001$). The 3D surface plot (Figure 5.4 (D)) showed a curvilinear decrease in viscosity at optimal polymer ratios. Gelling capacity was significantly affected by κ-carrageenan ($p < 0.0001$), Carbopol ($p < 0.0001$), and quadratic terms (A^2 and B^2, $p < 0.0001$), indicating a non-linear relationship with polymer concentration. The surface plot shown in Figure 5.4 (E) showed a distinct peak, suggesting optimal gel strength occurs at balanced polymer ratios. Gelation time was best described by a linear model, with κ-carrageenan ($p < 0.0001$) as the dominant factor, followed by Carbopol ($p = 0.0155$). The surface plot (Figure 5.4 (F)) illustrated a rapid decline in gelation time with increasing polymer concentrations. The predicted vs. actual plots. Figure 5.4 (A), (B), and (C) demonstrated a strong correlation, supporting model precision.

Table 5.6. Summary of ANOVA results for the κ-carrageenan–Carbopol–KCl system.

Response	Model Type	Significant Factors	p-value (Model)	Lack of Fit p-value
Fluidity	Quadratic	A–κ-cg ($p<0.0001$), B–Carbopol ($p<0.0001$), C-KCl ($p=0.526$), A^2 ($p<0.0001$)	<0.0001	0.1059
Gelling capacity	Quadratic	A–κ-cg ($p<0.0001$), B–Carbopol ($p<0.0001$), A^2 ($p<0.0001$), C-KCl ($p=0.1036$), B^2 ($p<0.0001$)	<0.0001	1.0000
Gelation time	Linear	A–κ-cg ($p<0.0001$), B–Carbopol ($p=0.0016$), C-KCl ($P=0.443$)	<0.0001	0.4435

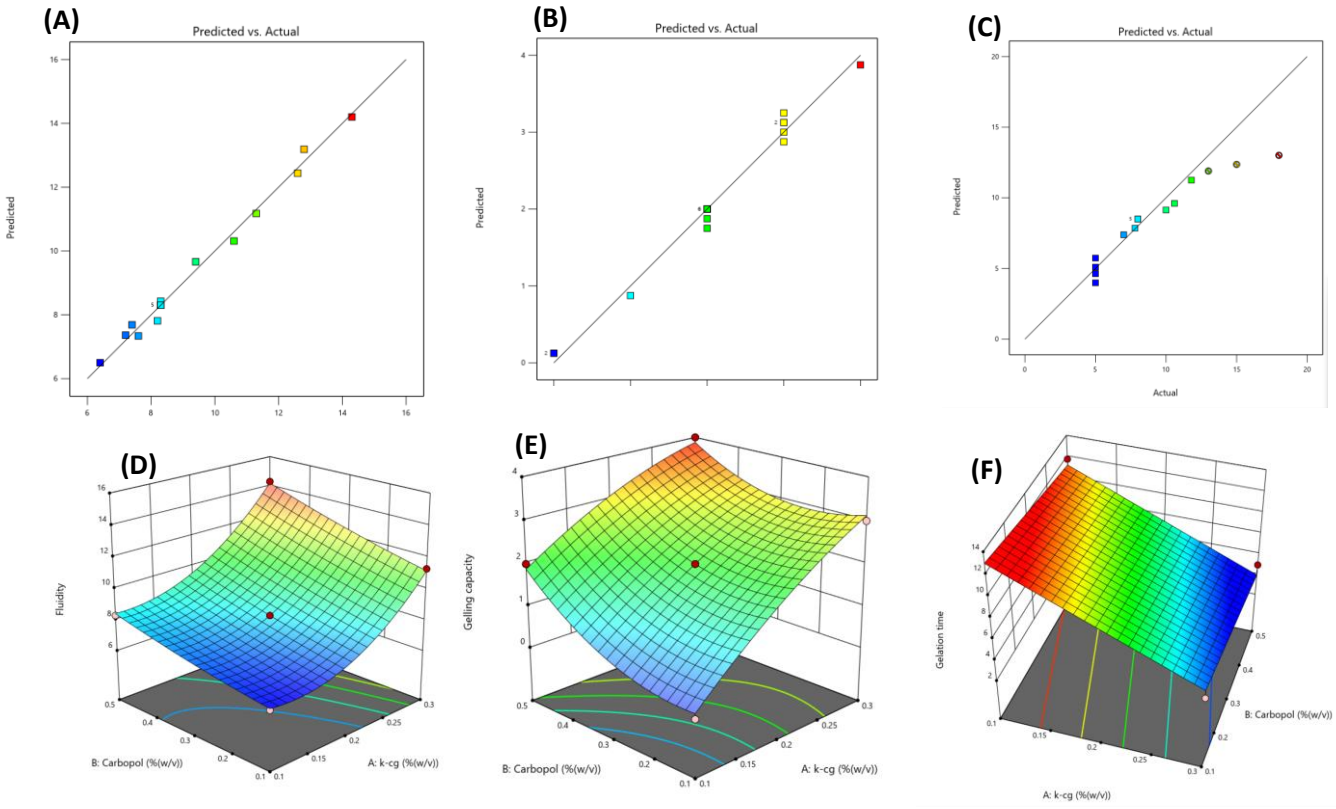

Figure 5.4. Response surface and predictive analysis for κ-CG-Carbopol-KCl system, (A) predicted vs. actual plot for fluidity, (B) predicted vs. actual plot for gelling capacity, (C) predicted vs. actual plot for gelation time, (D) 3D surface plot for fluidity, (E) 3D surface plot for gelling capacity, (F) 3D surface plot for gelation time.

5.4.1.2.3 Ion induced gels of combined κ-CG and ι-CG with HPMC/Carbopol

For combined κ-CG and ι-CG with HPMC systems, the ANOVA results (Table 5.7) indicated that fluidity and gelling capacity followed a quadratic model, while gelation time was best described by a linear model. Models are represented by Equation 5.13, Equation 5.14, and Equation 5.15. All models were statistically significant ($p < 0.0001$ for fluidity and gelling capacity; $p = 0.0002$ for gelation time) with non-significant lack of fit values, confirming model adequacy. The optimized formulation (0.100% ι-CG, 0.200% κ-CG, 0.481% HPMC) achieved a fluidity of 30.74 mPa.s, gelling capacity of 2.66, and gelation time of 21.50 s, with a desirability of 0.753.

Equation 5.13. $\text{Fluidity} = 20 + 5.71A + 4.56B + 3.827C – 2.247AB + 2.78AC + 2.94BC – 0.63A^2 – 0.66B^2 – 6.11C^2$

Equation 5.14. Gelling Capacity = $1 + 0.87A + 1.25B + 0.125C – 0.5AB + 0.24AC + 9.81BC + 0.37A^2 + 0.62B^2 – 0.125C^2$

Equation 5.15. Gelation Time = $14.39 + 0.18A – 1.30B – 0.67C$

For fluidity, significant effects were observed for ι-carrageenan (A, $p < 0.0001$), κ-carrageenan (B, $p < 0.0001$), and HPMC (C, $p < 0.0001$). The 3D surface plot in Figure 5.5 (D) shows that increasing κ-carrageenan and HPMC concentrations markedly enhanced viscosity. For gelling capacity, significant effects were noted for A ($p < 0.0001$), B ($p < 0.0001$), and C ($p = 0.0040$). The surface plot (Figure 5.5 (E)) revealed a peak in gel strength at intermediate κ-carrageenan levels, suggesting an optimal ionic network density that maximizes gel integrity without excessive rigidity. For gelation time, the linear model identified κ-carrageenan ($p < 0.0001$) and HPMC ($p = 0.0067$) as significant factors. The response surface highlighted in Figure 5.5 (F) indicated that higher κ-carrageenan levels reduced gelation time, likely due to increased availability of junction zones, while HPMC contributed to faster structural consolidation. The predicted vs. actual plots in Figure 5.5 (A), (B), and (C) demonstrated a strong correlation, supporting model precision.

Table 5.7. Summary of ANOVA results for the ι-carrageenan & κ-carrageenan–HPMC system.

Response	Model Type	Significant Factors	p-value (Model)	Lack of Fit p-value
Fluidity	Quadratic	A–ι-CG ($p<0.0001$), B–κ-CG ($p<0.0001$), C–HPMC ($p<0.0001$)	<0.0001	0.2992
Gelling capacity	Quadratic	A–ι-CG ($p<0.0001$), B–κ-CG ($p<0.0001$), C–HPMC ($p=0.0040$)	<0.0001	0.2641
Gelation time	Linear	B–κ-CG ($p<0.0001$), C–HPMC ($p=0.0067$)	0.0002	0.0913

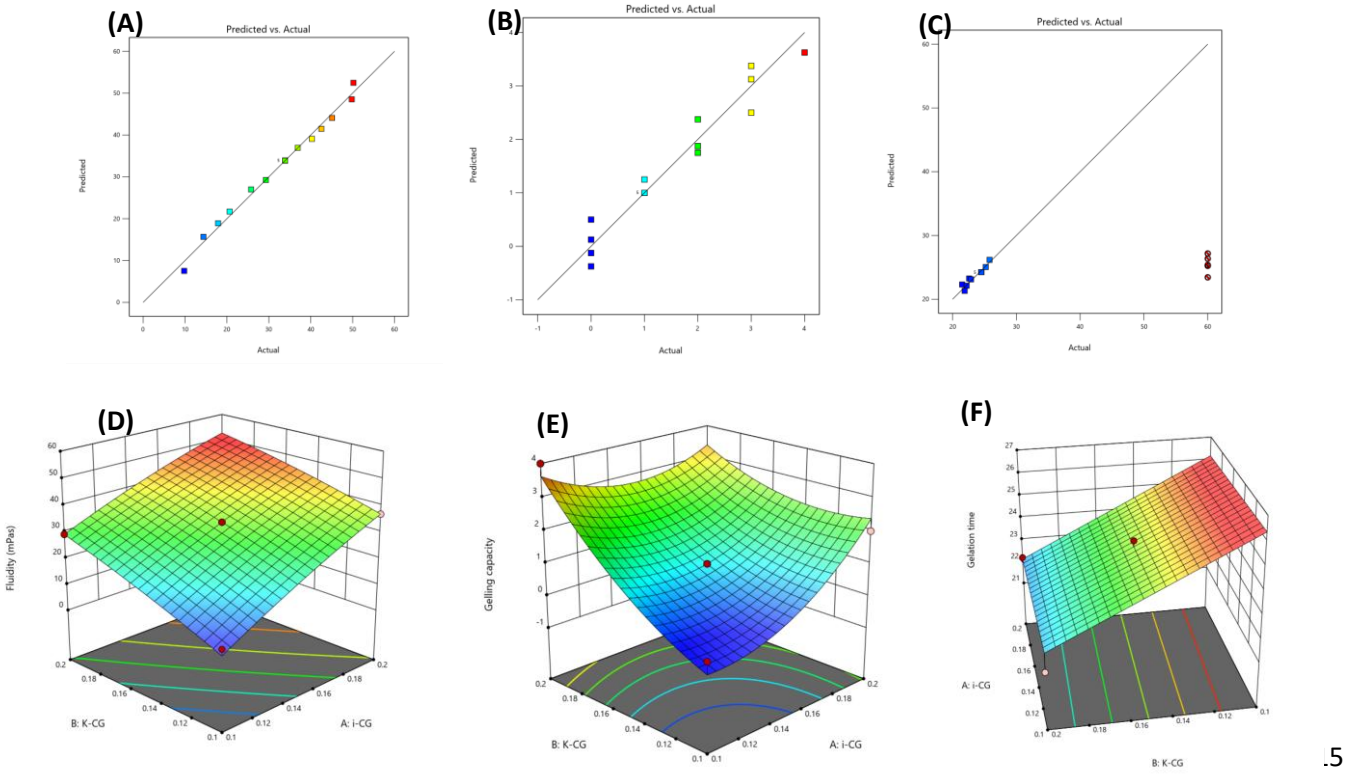

Figure 5.5 Response surface and predictive Analysis for κ-CG- ι-CG -HPMC systems, (A) predicted vs. actual plot for fluidity, (B) predicted vs. actual plot for gelling capacity, (C) predicted vs. actual plot for gelation time, (D) 3D surface plot for fluidity, (E) 3D surface plot for gelling capacity, (F) 3D surface plot for gelation time.

For combined κ-CG and ι-CG with Carbopol, ANOVA outcomes (Table 5.8) showed that fluidity and gelling capacity responses fitted best to quadratic models, whereas gelation time was adequately described by a linear model. All models were statistically significant ($p < 0.0001$), with non-significant lack-of-fit values, indicating that the selected models were appropriate and predictive. Models are represented by Equation 5.16, Equation 5.17, and Equation 5.18. The optimized formulation containing 0.100% ι-carrageenan, 0.200% κ-carrageenan, and 0.570% Carbopol exhibited a fluidity of 17.681 mPa·s, gelling capacity of 2.625, and gelation time of 12.238 s, achieving a high desirability value of 0.844.

Equation 5.16. $\text{Fluidity} = 33.89 + 13.162A + 9.316B + 3.27C – 1.54AB + 0.25AC – 0.76BC – 1.38A^2 – 0.96B^2 – 0.66C^2$

Equation 5.17. $\text{Gelling Capacity} = 0.9 + 0.625A + 1.25B + 0.37C – 0.75AB – 5.95AC + 0.25BC + 0.75A^2 + 0.5B^2 – 0.24C^2$

Equation 5.18. $\text{Gelation Time} = 24.25 – 0.0933A – 2.03B – 0.9C$

For fluidity, significant main effects were observed for all three factors: ι-carrageenan (A, $p<0.0001$), κ-carrageenan (B, $p<0.0001$), and Carbopol (C, $p<0.0001$). The 3D surface plot shown in Figure 5.6 (D) indicated that higher concentrations of κ-carrageenan and Carbopol led to a marked increase in viscosity, reflecting denser gel networks. For gelling capacity, all three factors significantly influenced the response (A, $p<0.0001$; B, $p<0.0001$; C, $p=0.0040$). The response surface highlighted in Figure 5.6 (E) revealed that intermediate κ-carrageenan levels maximized gel strength, suggesting an optimal polymer–ion network density that enhances gel integrity without causing brittleness. For gelation time, the linear model identified κ-carrageenan ($p<0.0001$) and Carbopol ($p=0.0011$) as significant contributors. The response surface (Figure 5.6 (F)) showed that higher κ-carrageenan concentrations reduced gelation time, likely due to the faster formation of crosslinks, while Carbopol promoted quicker structural stabilization. Predicted vs. actual plots highlighted in Figure 5.6 (A) (B) and (C) for all responses demonstrated strong correlation, indicating high model precision and reliability for formulation optimization.

Table 5.8. Summary of ANOVA results for the ι-carrageenan, κ-carrageenan, and Carbopol system.

Response	Model Type	Significant Factors	p-value (Model)	Lack of Fit p-value
Fluidity	Quadratic	A–ι-CG ($p<0.0001$), B–κ-CG ($p<0.0001$), C–Carbopol ($p<0.0001$)	<0.0001	0.2992
Gelling capacity	Quadratic	A–ι-CG ($p<0.0001$), B–κ-CG ($p<0.0001$), C–Carbopol ($p=0.0040$)	<0.0001	0.2641
Gelation time	Linear	B–κ-CG ($p<0.0001$), C–Carbopol ($p=0.0011$)	<0.0001	0.1463

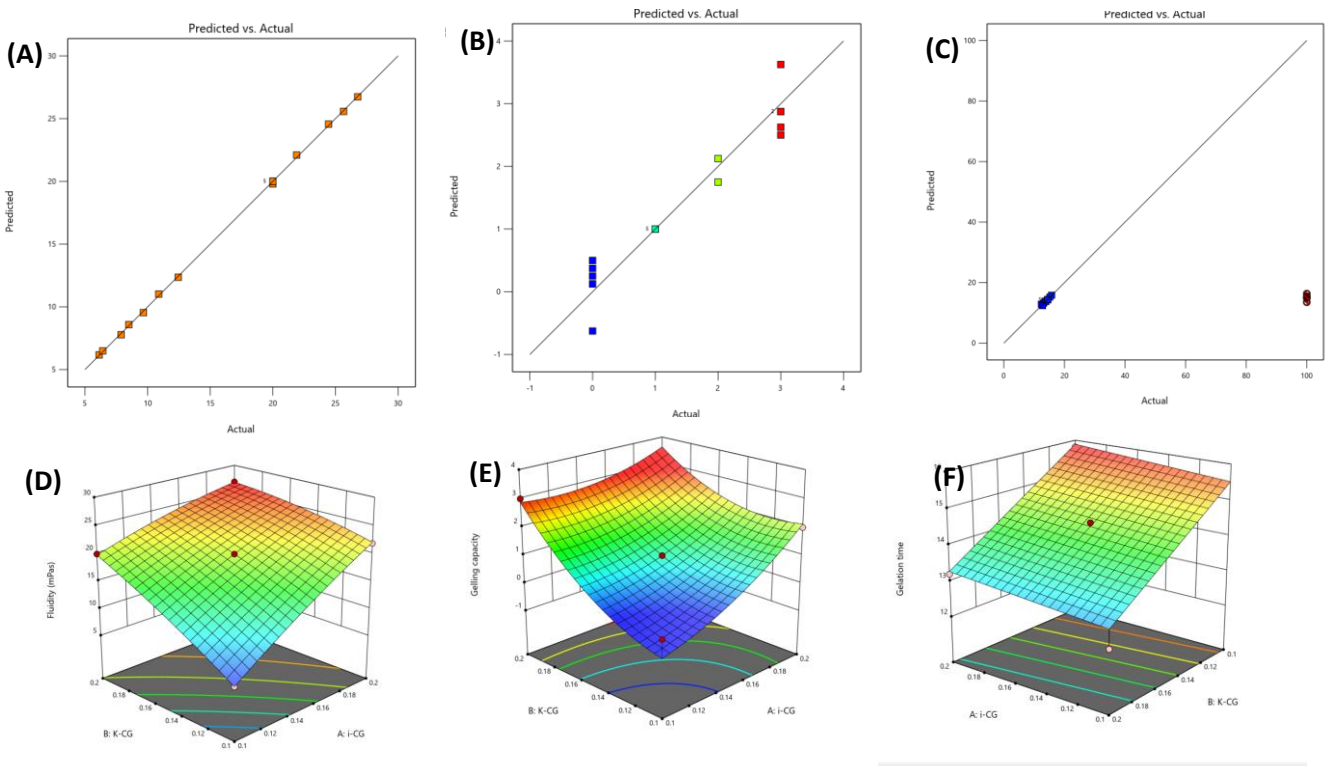

Figure 5.6. Response surface and predictive analysis for κ-CG- ι-CG -Carbopol systems, (A) predicted vs. actual plot for fluidity, (B) predicted vs. actual plot for gelling capacity, (C) predicted vs. actual plot for gelation time, (D) 3D surface plot for fluidity, (E) 3D surface plot for gelling capacity, (F) 3D surface plot for gelation time.

Further characterizations were carried out using the formulations optimized, with the polymer and salt concentration highlighted in Table 5.9 below.

Table 5.9 Optimized ion-Induced in-situ gel formulation parameters derived from design of experiments.

Formulation Code	Polymer (% w/v)	HPMC / Carbopol (% w/v)	Salt (% w/v)	Cannabinoid Composition
G-H4TC	0.197% Gellan gum	0.4% HPMC	0.077% $CaCl_2$	THC + CBD (1:1, 20 mg/ml total)
G-H4C	0.197% Gellan gum	0.4% HPMC	0.077% $CaCl_2$	CBD (20 mg/ml)
G-C37TC	0.18% Gellan gum	0.37% Carbopol	0.08% $CaCl_2$	THC + CBD (1:1, 20 mg/ml total)
G-C37C	0.18% Gellan gum	0.37% Carbopol	0.08% $CaCl_2$	CBD (20 mg/ml)
K-H28TC	0.3% κ-CG	0.28% HPMC	0.08% KCl	THC + CBD (1:1, 20 mg/ml total)
K-H28C	0.3% κ-CG	0.28% HPMC	0.08% KCl	CBD (20 mg/ml)
K-C3TC	0.28% κ-CG	0.3% Carbopol	0.074% KCl	THC + CBD (1:1, 20 mg/ml total)
K-C3C	0.28% κ-CG	0.3% Carbopol	0.074% KCl	CBD (20 mg/ml)
KI-H48TC	0.2% κ-CG, 0.1% ι-CG	0.48% HPMC	0.07% KCl	THC + CBD (1:1, 20 mg/ml total)

KI-H48C	0.2% κ-CG, 0.1% ι-CG	0.48% HPMC	0.07% KCl	CBD (20 mg/ml)
KI-C5TC	0.2% κ-CG, 0.1% ι-CG	0.5% Carbopol	0.07% KCl	THC + CBD (1:1, 20 mg/ml total)
KI-C5C	0.2% κ-CG, 0.1% ι-CG	0.57% Carbopol	0.07% KCl	CBD (20 mg/ml)

5.4.2 Appearance, pH, and drug content of developed formulations

Table 5.10 highlights the pH, visual appearance, and drug content of the optimized formulations. All formulations maintained a consistent cream-coloured appearance, indicating no visible instability or cannabinoid precipitation post-loading. Drug content was highly uniform, with dual-drug systems delivering approx. 10 mg/ml for each cannabinoid, with single-dose systems around 20 mg/ml of CBD, suggesting minimal loss during preparation and even drug dispersion.

The pH values ranged from 3.19 to 6.79, reflecting differences in polymer and salt combinations, and ion-exchange equilibria. The pH of required formulations was adjusted to 6.4 using triethanolamine to enhance compatibility with the buccal environment. The pH of buccal formulations should ideally be within 5.5–7.5 to match the oral mucosa and minimize irritation (Aframian et al., 2006; He & Mu, 2023; Li & Castillo, 2020).

Table 5.10. pH, appearance, and drug content of cannabinoid-loaded ion-induced in-situ gel formulations (n = 3; mean ± SD).

Formulation	pH (± SD)	Appearance	Drug content (mg/ml, ± SD)
G-H4TC	6.40 ± 0.38	Cream coloured	CBD: 10.04 ± 0.03 THC: 10.06 ± 0.97
G-H4C	6.79 ± 0.11	Cream coloured	CBD: 20.12 ± 0.70
G-C37TC	4.82 ± 0.54	Cream coloured	CBD: 10.01 ± 0.94 THC: 10.47 ± 0.67
G-C37C	4.92 ± 0.69	Cream coloured	CBD: 20.24 ± 0.29
K-H28TC	4.98 ± 0.06	Cream coloured	CBD: 10.23 ± 0.25 THC: 10.30 ± 0.60
K-H28C	5.28 ± 0.10	Cream coloured	CBD: 20.19 ± 0.29
K-C3TC	3.97 ± 0.05	Cream coloured	CBD: 10.23 ± 0.41 THC: 10.37 ± 0.73
K-C3C	3.19 ± 0.02	Cream coloured	CBD: 20.64 ± 0.86
KI-H48TC	5.78 ± 0.15	Cream coloured	CBD: 10.33 ± 0.72 THC: 10.25 ± 0.93

KI-H48C	5.80 ± 0.19	Cream coloured	CBD: 20.35 ± 0.39
KI-C5TC	3.70 ± 0.29	Cream coloured	CBD: 10.52 ± 0.14 THC: 10.35 ± 0.87
KI-C5C	3.50 ± 0.02	Cream coloured	CBD: 20.43 ± 0.57

5.4.3 Sol-gel transition time and viscosity of the ion-induced gelling formulations

Sol-gel transition time of formulations was measured using the tube inversion technique. Figure 5.7 highlights confirmation of gelation upon the addition of artificial saliva (AS) for gellan gum, κ-CG, and κ-CG/ι-CG mixed formulations.

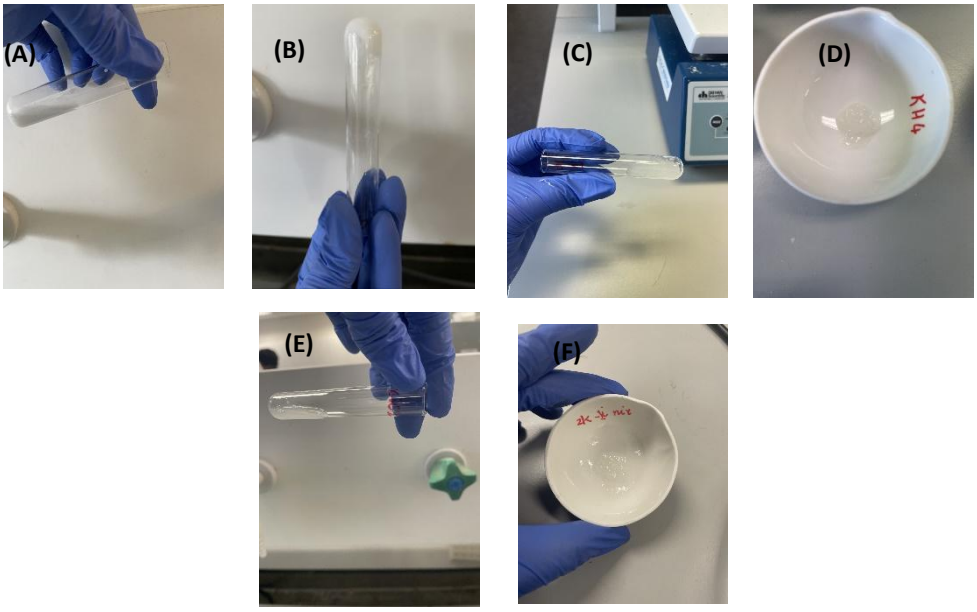

Figure 5.7 Confirmation of gel formation of ion induced gels (A) Gellan gum formulations before addition of AS, (B) Gellan gum formulations after addition of AS (C) κ-CG formulations before addition of AS, (D) κ-CG formulations after addition of AS (E) Combined κ-CG and ι-CG formulations before addition of AS, (F) Combined κ-CG and ι-CG formulations after addition of AS.

Sol-gel transition time of the optimized formulations are represented in Table 5.11. Gelation time is influenced by concentration of polymers, type of ions used, as well as viscosity of the formulation. Formulations with gellan gum (G-H4TC/G-H4C and G-C37TC/G-C37C) exhibited slower gelation times when compared with the other formulations of carrageenan. This may be attributed to the low gellan gum concentration used, resulting in weaker and slower gel network formation. Furthermore, in gellan gum–based formulations, sodium citrate was incorporated as a complexing agent. The presence of citrate ions can sequester divalent cations such as Ca^{2+}, needed to prevent premature gelation, which could have delayed the onset of gelation and prolonged the sol-to-gel transition time (Morris et al., 2012). Carbopol consistently reduced gelation times compared to HPMC across all ion-sensitive polymers, with κ-CG outperforming gellan gum formulations. The faster gelation times observed in Carbopol-containing formulations (G-C37TC, G-C37C, K-C3TC, K-C3C, KI-C5TC, KI-C5C),

ranging from 7.5 to 33 s, may be attributed to Carbopol's ability to facilitate stronger intermolecular interactions within gel networks compared to cellulose derivatives such as HPMC (Peppas & Sahlin, 1996). Although higher viscosities can generally slow gelation by restricting polymer chain mobility, Carbopol's rapid ionic interaction in ion-induced systems leads to faster gelation compared to HPMC-based systems (Mahajan et al., 2019). Mixed carrageenan systems (κ-CG + ι-CG; KI-H48TC/KI-H4C and KI-C5TC/KI-C5C) exhibited intermediate gelation times (12–26 s). The addition of ι-CG produces softer, more elastic gels, slightly delaying rigid network formation. However, when Carbopol was used (KI-C5TC/KI-C5C), gelation was accelerated compared to HPMC systems (KI-H48TC/KI-H48C), highlighting the synergistic effect of Carbopol in ion-responsive polymer matrices.

Table 5.11 Sol–gel transition times of cannabinoid-loaded ion-induced in-situ gel formulations (n = 3; mean ± SD).

Formulation Code	Sol–gel transition time (s, ± SD)
G-H4TC	57.0 ± 1.30
G-H4C	53.0 ± 2.28
G-C37TC	33.0 ± 2.60
G-C37C	32.0 ± 1.80
K-H28TC	15.2 ± 3.00
K-H28C	11.8 ± 2.40
K-C3TC	7.5 ± 1.30
K-C3C	9.0 ± 2.00
KI-H48TC	22.1 ± 1.60
KI-H48C	26.1 ± 0.90
KI-C5TC	12.2 ± 1.10
KI-C5C	19.6 ± 1.50

The viscosity analysis confirmed that all formulations underwent a marked increase in viscosity upon ionic gelation, demonstrating successful in-situ gel formation (highlighted in figure 5.8 below). All Carbopol-containing formulations (G-C37TC, G-C37C, K-C3TC, K-C3C, KI-C5TC, KI-C5C) produced the higher gel viscosities, significantly greater than HPMC-containing ones (G-H4TC, G-H4C, K-H28TC, K-H28C, KI-H48TC, KI-H48C). This consistent with previous studies that have demonstrated that Carbopol addition results in higher formulation viscosity than HPMC at the same concentration (E. Özyılmaz et al., 2024; Wu et al., 2007). Mixed

κ/ι-CG formulations exhibited the highest viscosities overall. The interactive gelation of κ-CG and ι-CG, where κ-CG contributes rigidity and ι-CG provides elasticity, resulted in a more cohesive and elastic gel matrix (Campo et al., 2009). Formulations containing both CBD and THC exhibited higher viscosities compared to their CBD-only counterparts, indicating that the inclusion of THC enhanced gel consistency.

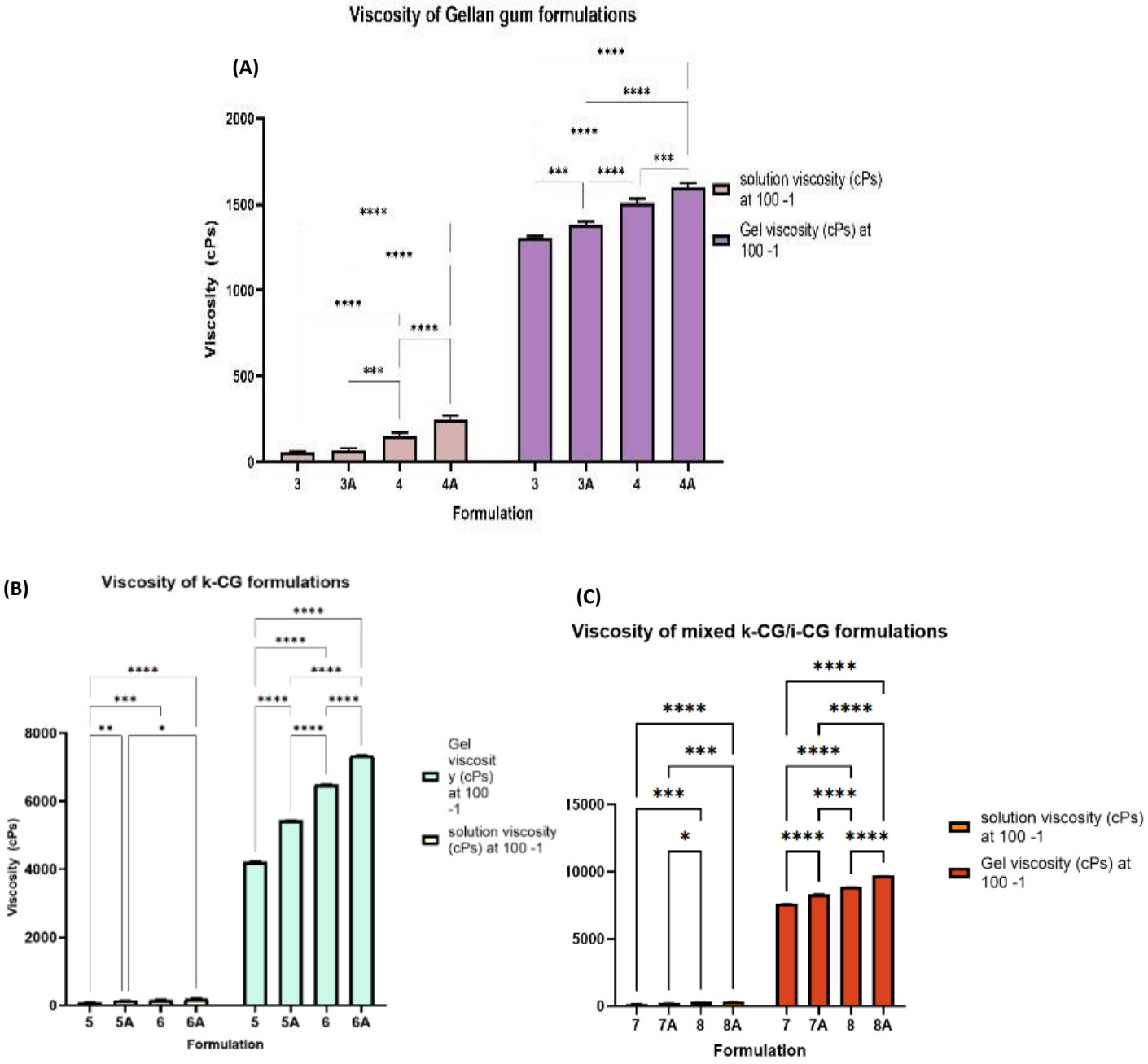

Figure 5.8 Viscosity profiles of (A) gellan gum formulations with HPMC or Carbopol in the presence of $CaCl_2$, (B) κ-CG formulations containing HPMC or Carbopol in the presence of KCl, (C) mixed κ-CG/ι-CG formulations with HPMC or Carbopol in the presence of KCl (n = 3; mean ± SD). Statistically significant differences are denoted as *p < 0.05 and **p < 0.01, ***p < 0.001, ****p < 0.0001.

5.4.4 Mechanical properties of the ion induced in-situ gels.

The mechanical and textural characteristics of the prepared formulations were evaluated in terms of hardness, springiness, and cohesion (Table 5.12). Significant differences were observed depending on the

polymer type, mucoadhesive co-polymer, salt system, and cannabinoid composition. Across all paired formulations, cannabinoid composition (THC and CBD vs. CBD) had only a minor influence on textural properties. CBD-only formulations tended to show slightly lower cohesion and hardness, though differences were not statistically significant in several formulations.

Among all formulations, those incorporating Carbopol showed higher hardness and elasticity relative to HPMC-based gels. This increase in mechanical strength is likely due to the higher viscosity of Carbopol-based, ion-triggered gels, which reinforces the gel network. Additionally, Carbopol-containing formulations (G-C37TC, G-C37C, K-C3TC, K-C3C, KI-C5TC, KI-C5C) exhibited slightly higher cohesion values compared to HPMC systems, suggesting the formation of stiffer gels with enhanced structural integrity under applied stress. Patel et al. (2011) have reported in their study that Carbopol-based gels generally demonstrate higher mechanical strength and cohesiveness than HPMC gels, due to their greater crosslinking density and cohesive polymer network.

Gellan gum formulations exhibited greater hardness and springiness overall, despite displaying comparatively lower viscosities. This indicates that while viscosity plays a role in determining mechanical characteristics (Fathalla et al., 2022; Swain et al., 2019), other factors such as strong crosslinking from the use of divalent cations could have contributed to the stronger mechanical properties. Prior studies have shown that hydrogels may exhibit low viscosity under shear yet maintain high hardness and elasticity due to strong ionic crosslinking and network formation (de Jong & van de Velde, 2007; Funami, 2011). Mixed carrageenan formulations also exhibited higher hardness and springiness when compared with κ-CG only in-situ gels. These findings are consistent with previous literature which suggest that κ-/ι-carrageenan mixtures yield gels with greater strength and elasticity compared to individual carrageenan. Furthermore, κ-CG based gels have been demonstrated to be prone to syneresis, where liquid separates from the gel, when subjected to mechanical stress/deformation (Campo et al., 2009), which explains the lower hardness, and springiness of κ-CG based gels.

Table 5.12 Textural properties (hardness, springiness, and cohesion) of gellan gum- and carrageenan-based in situ gels with HPMC or Carbopol (n = 3; mean ± SD). Values in each column bearing different superscript letters are significantly different ($p < 0.05$), whereas those sharing at least one common letter are not significantly different (one-way ANOVA with Tukey's post hoc test).

Formulations	Hardness (N)	Springiness (%)	Cohesion
G-H4TC	4.383 ± 0.028^{b}	99.230 ± 1.23^{bd}	0.474 ± 0.02^{acgj}
G-H4C	4.271 ± 0.031^{cde}	99.630 ± 2.12^{ce}	0.467 ± 0.09^{beg}
G-C37TC	4.945 ± 0.02^{c}	99.580 ± 2.11^{bef}	0.478 ± 0.01^{bcegh}
G-C37C	4.408 ± 0.03^{e}	100.000 ± 3.21^{ce}	0.475 ± 0.06^{bceh}
K-H28TC	3.383 ± 0.28^{h}	75.510 ± 2.19^{ade}	0.406 ± 0.018^{hi}
K-H28C	3.346 ± 0.38^{h}	74.720 ± 1.29^{af}	0.402 ± 0.029^{hijkl}

K-C3TC	3.518 ± 0.01^{g}	78.380 ± 1.73^{acd}	0.441 ± 0.021^{efl}
K-C3C	3.827 ± 0.55^{ab}	78.995 ± 3.22^{bcef}	0.433 ± 0.091^{dfgi}
KI-H48TC	3.956 ± 0.21^{d}	99.492 ± 0.19^{bcef}	0.454 ± 0.092^{adeh}
KI-H48C	3.887 ± 0.32^{f}	98.974 ± 0.39^{bcf}	0.452 ± 0.031^{adeh}
KI-C5TC	4.977 ± 0.07^{g}	99.497 ± 0.99^{bc}	0.463 ± 0.02^{bdk}
KI-C5C	3.994 ± 0.09^{a}	98.753 ± 1.67^{bcef}	0.461 ± 0.01^{cdf}

5.4.5 Mucoadhesive strength of ion induced gels.

The ex-vivo mucoadhesion study revealed distinct differences in maximum detachment force among the tested formulations (Figure 5.9). Although formulations containing both cannabinoids exhibited higher mucoadhesive strength than their CBD-only counterparts, likely due to the greater cohesiveness observed earlier, however these differences were not statistically significant. Carbopol-based formulations (G-C37TC, G-C37C, K-C3TC, K-C3C, KI-C5TC, KI-C5C) consistently demonstrated significantly higher mucoadhesive strength compared to HPMC-based systems (G-H4TC, G-H4C, K-H28TC, K-H28C, KI-H48TC, KI-H48C). This finding agrees with previous reports that Carbopol exhibits superior mucoadhesive properties due to the presence of abundant carboxylic functional groups, which facilitate strong hydrogen bonding and electrostatic interactions with mucin glycoproteins. HPMC is a non-ionic polymer and interacts with mucin primarily through secondary interactions such as hydrogen bonding, which are inherently weaker compared to the ionic and hydrogen bonding potential of Carbopol (Dhawale et al., 2018; Smart, 2005).

In this study, gellan gum formulations exhibited higher mucoadhesive strength than κ-carrageenan (κ-CG) formulations but lower strength compared to mixed carrageenan systems (κ/ι-CG). This trend may be attributed to differences in polymer–mucin interactions and gel network characteristics. Gellan gum, being an anionic polysaccharide containing carboxyl groups, forms hydrogen bonds and electrostatic interactions with mucin, leading to stronger adhesion than κ-CG alone (A. Li et al., 2021). However, mixed carrageenan formulations demonstrated highest detachment forces (approx. 6–7 N), with statistically significant differences compared to most other formulations ($p < 0.001$). This enhanced mucoadhesion can be attributed to the combination of κ- and ι-carrageenan creating a denser, more elastic network with enhanced ionic crosslinking in the presence of cations (de Jong & van de Velde, 2007; Funami, 2011).

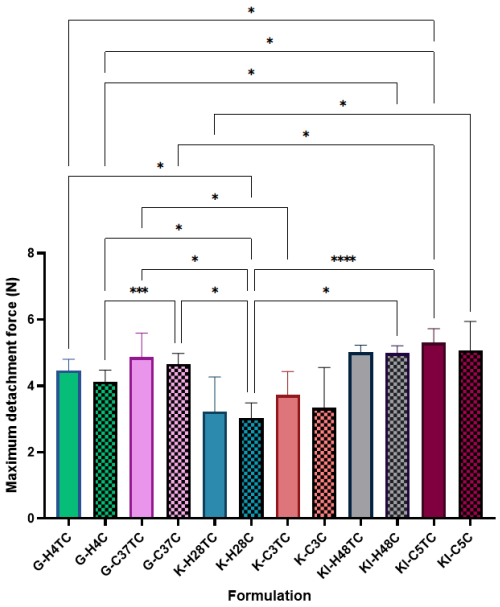

Figure 5.9 Comparison of mucoadhesive strength across optimized ion-induced gelling formulations (n = 3; mean ± SD). Statistically significant differences are denoted as *p < 0.05 and **p < 0.01, ***p < 0.001, ****p < 0.0001.

5.4.6 In-vitro drug release and release kinetics of ion induced gels.

The dissolution studies demonstrated distinct release behaviours depending on the polymer system and cannabinoid composition. Release of cannabinoids from optimized formulations are highlighted in Figure 5.10. Across all formulations, the release of CBD was consistently higher than THC, reflecting the lower aqueous solubility and hydrophobic nature of THC, which limits its diffusion through the gel matrices. Furthermore, with increased formulation viscosity hindering drug release (Ali & Al-Shohani, 2024; Zema et al., 2007), release from formulations with both CBD and THC were slower when compared to CBD-only formulations. Analysis of individual cannabinoid release from Formulations (G-H4TC, G-C37TC, K-H28TC, K-C3TC, KI-H48TC, KI-C5TC) (Figure 5.10 (B) to (G)) indicated comparable release rates for CBD and THC, with CBD showing a slightly higher overall cumulative release.

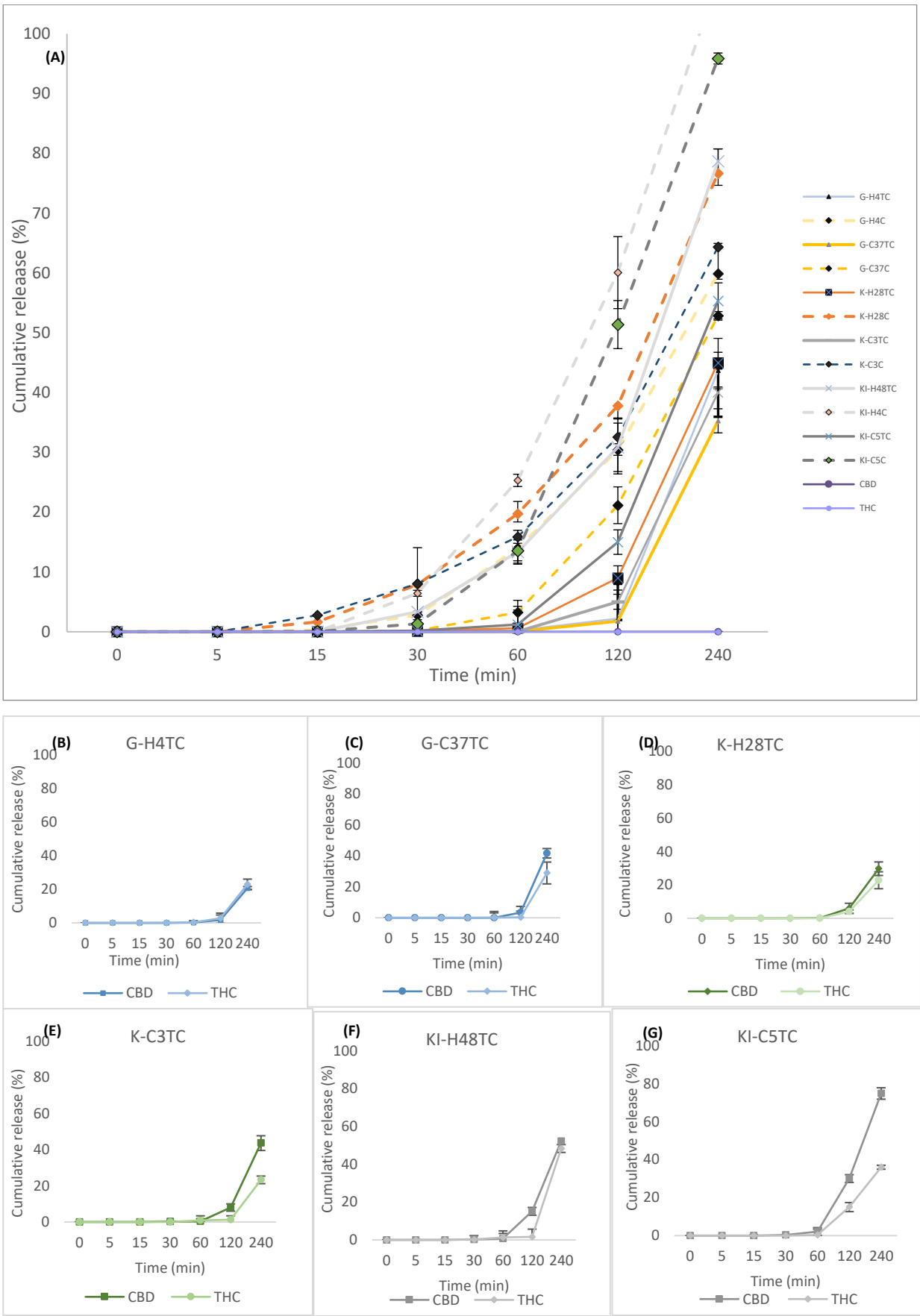

Figure 5.10 In-vitro release of cannabinoids from ion-induced in-situ gels; (A) Comparison of gel formulations with pure CBD and THC distillates, (B) Individual release profiles of CBD and THC from G-H4TC, (C) Individual release profiles of CBD and THC from G-C37TC, (D) Individual release profiles of CBD and THC from K-H28TC, (E) Individual release profiles of CBD and THC from K-C3TC, (F) Individual release profiles of CBD and THC from KI-H48TC, (G) Individual release profiles of CBD and THC from KI-C5TC (n = 3; mean ± SD).

Ion induced formulations containing HPMC (G-H4TC, G-H4C, K-H28TC, K-H28C, KI-H48TC, KI-H48C) showed higher drug release when compared with their Carbopol based counterparts (G-C37TC, G-C37C, K-C3TC, K-C3C, KI-C5TC, KI-C5C), which can be attributed to the lower viscosity of HPMC systems and the well-documented ability of Carbopol to sustain drug release over extended periods (E. D. Özyılmaz et al., 2024). Formulations containing mixed carrageenan exhibited the highest drug release profiles despite their high viscosity. This effect may be attributed to the synergistic gel network formed by κ- and ι-carrageenan, where the rigid and porous network contributed by κ-CG, combined with the enhanced swelling capacity of ι-CG, facilitates greater drug diffusion (Tavagnacco et al., 2023). Gellan gum formulations released cannabinoids more slowly than carrageenan formulations, which may be attributed to the stronger ionic crosslinking of gellan gum with divalent cations, resulting in a denser gel network impacting drug diffusion (Hazra et al., 2025).

The release data of cannabinoids from the optimized ion-induced in-situ gels were fitted to various kinetic models to elucidate the predominant release mechanisms (Table 5.13). The models included zero-order, first-order, Higuchi, Korsmeyer–Peppas, and Hixson–Crowell. The Korsmeyer–Peppas model provided the best overall fit, with high correlation coefficients (R^2 = 0.90–0.99) across all formulations. This indicating that release followed an anomalous (non-Fickian) transport mechanism, where drug diffusion is coupled with polymer relaxation or swelling, consistent with the behaviour of ion-induced gels where the polymer network undergoes structural changes upon hydration. Previous research suggest that gellan gum/carrageenan-based in situ gels often exhibit non-Fickian (anomalous) diffusion mechanisms, where drug release is influenced by both diffusion and polymer relaxation/swelling processes (Mohananaidu et al., 2022; Ren et al., 2025; Salunke & Patil, 2016).

Table 5.13 Kinetic modelling of cannabinoid release from ion-induced in-situ gel formulations fitted to zero-order, first-order, Higuchi, Korsmeyer–Peppas, and Hixson–Crowell models (R^2 values).

Formulation	Zero-order	First-order	Higuchi	Korsmeyer–Peppas	Hixson–Crowell
G-H4TC-CBD	0.7893	0.7367	-0.2031	0.9082	0.8076
G-H4TC-THC	0.7909	0.5939	-0.2045	0.9159	0.8596
G-H4C-CBD	0.9237	0.4778	-0.4437	0.9781	0.8065
G-C37TC-CBD	0.8418	0.6803	-0.2447	0.9909	0.7920
G-C37TC-THC	0.8664	0.5249	-0.2574	0.9981	0.8314
G-C37C-CBD	0.8256	0.2830	-0.6693	0.9796	0.6880
K-H28TC-CBD	0.7890	0.5902	-0.2100	0.9499	0.8651
K-H28TC-THC	0.7940	0.7437	-0.2061	0.9339	0.8134

K-H28C-CBD	0.8557	0.2435	-0.9056	0.9252	0.6364
K-C3TC-CBD	0.8933	0.4978	-0.2945	0.9860	0.8095
K-C3TC-THC	0.8292	0.6523	-0.2465	0.9612	0.7766
K-C3C-CBD	0.9254	0.2408	-0.7081	0.9928	0.6236
KI-H48TC-CBD	0.8168	0.4807	-0.2369	0.9559	0.7941
KI-H48TC-THC	0.8000	0.6869	-0.2134	0.9507	0.7903
KI-H48C-CBD	0.8581	0.3561	-0.3335	0.9669	0.7598
KI-C5TC-CBD	0.9404	0.4942	-0.3556	0.9666	0.8111
KI-C5TC-THC	0.8122	0.4848	-0.2330	0.9493	0.7960
KI-C5C-CBD	0.9141	0.3482	-0.6807	0.9990	0.7815

5.4.7 FTIR of ion-induced formulations

The FTIR spectra of the polymers (Gellan gum, κ-CG, and ι-CG) and cannabinoids (CBD and THC) incorporated in the formulations are depicted in Figure 5.11. The spectra corresponding to gellan gum formulations (G-H4TC, G-H4C, G-C37TC, G-C37C) are presented in Figure 5.12. Figure 5.13 and Figure 5.14 illustrate the spectra for κ-CG formulations (K-H28TC, K-H28C, K-C3TC, K-C3C) and mixed carrageenan formulations (KI-H48TC, KI-H48C, KI-C5TC, KI-C5C), respectively.

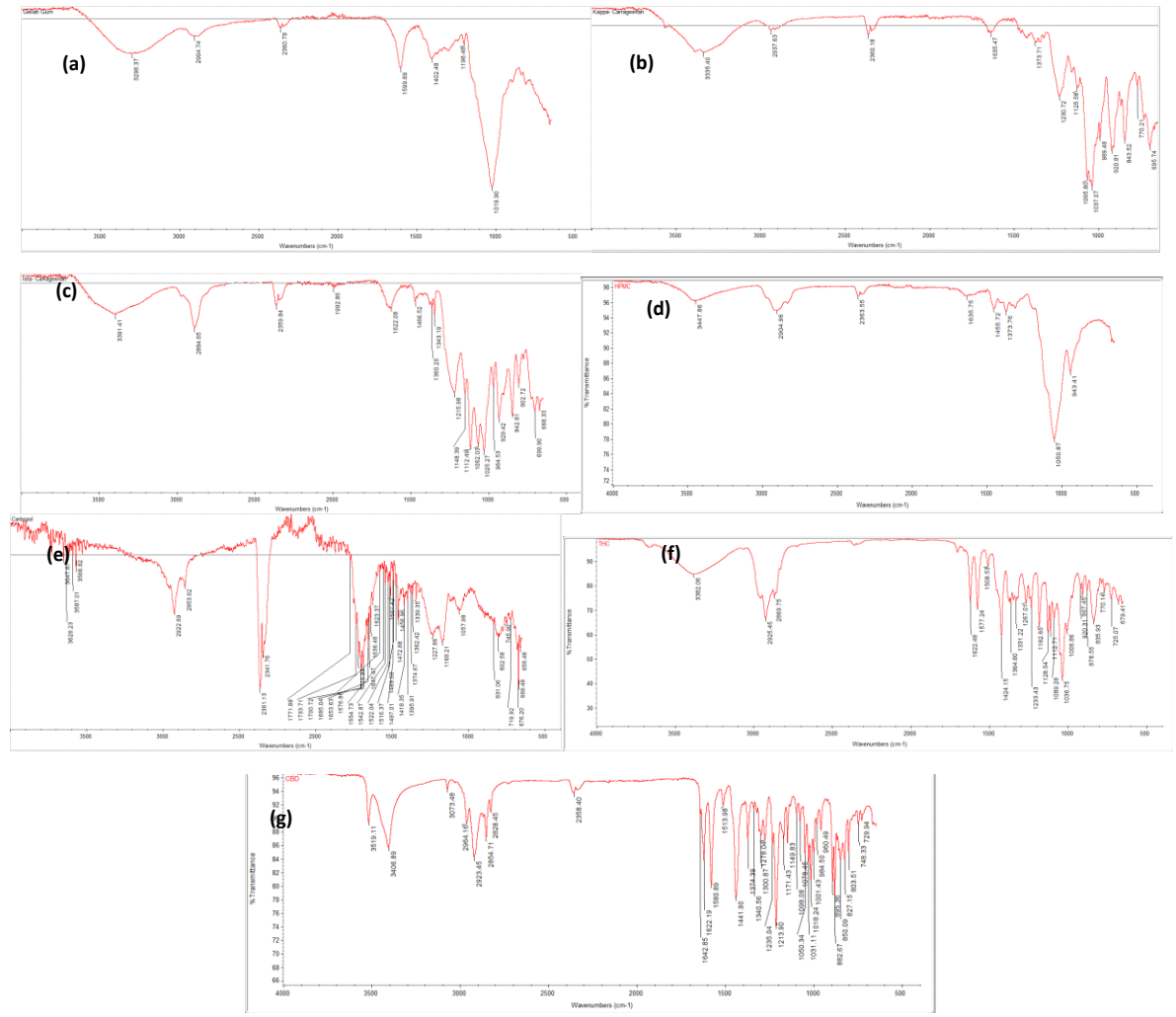

Figure 5.11 FTIR spectra of (a) Gellan gum (b) κ-CG, (c) ι-CG, (d) HPMC, (e) Carbopol, (f) THC, (g) CBD.

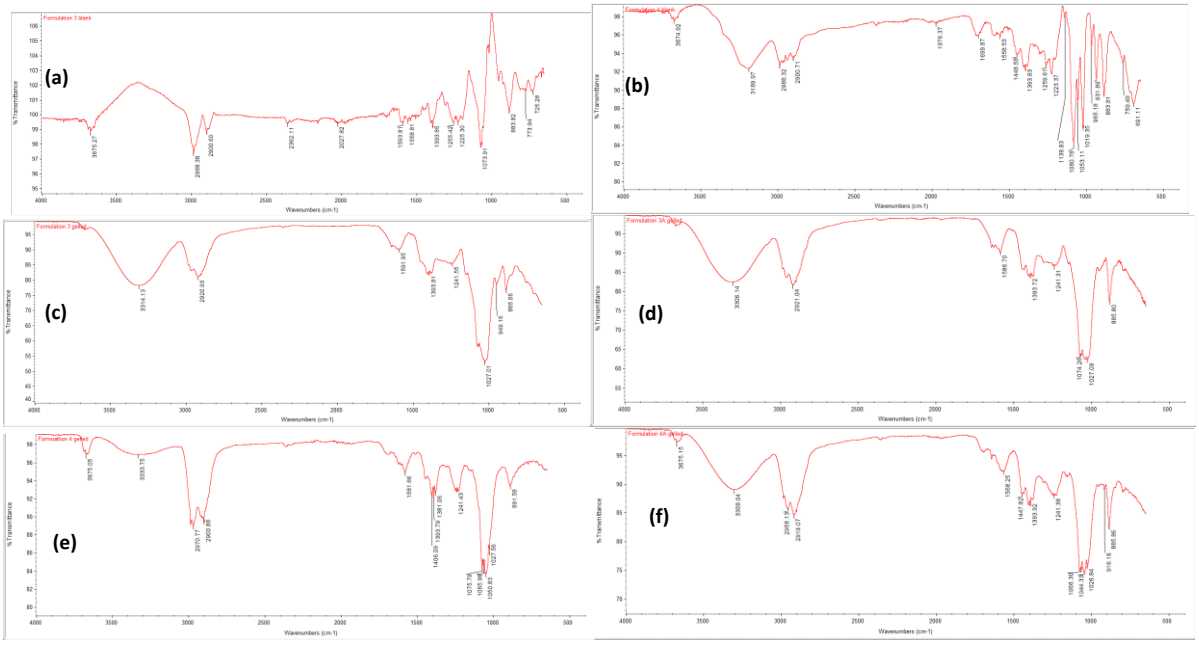

Figure 5.12 FTIR spectra of (a) blank HPMC gellan gum gel, (b) blank Carbopol gellan gum gel, (c) G-H4TC, (d) G-H4C (e) G-C37TC, and (f) G-C37C.

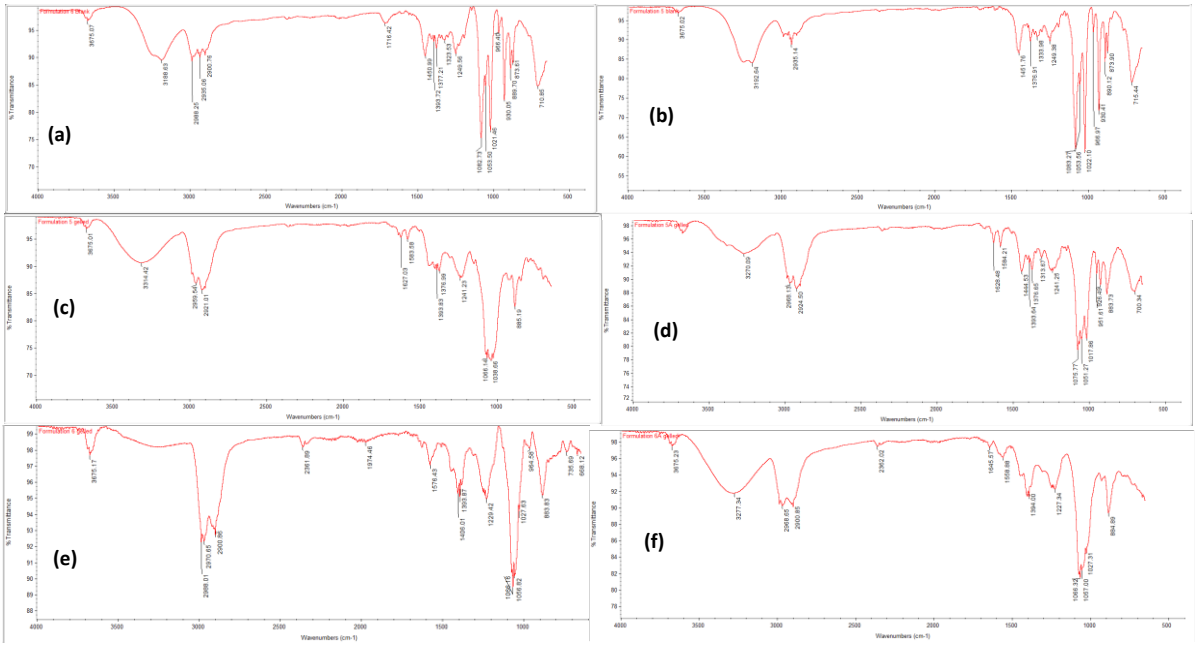

Figure 5.13 FTIR spectra of (a) blank HPMC κ-CG gel, (b) blank Carbopol κ-CG gel, (c) K-H28TC, (d) K-H28C, (e) K-C3TC, and (f) K-C3C.

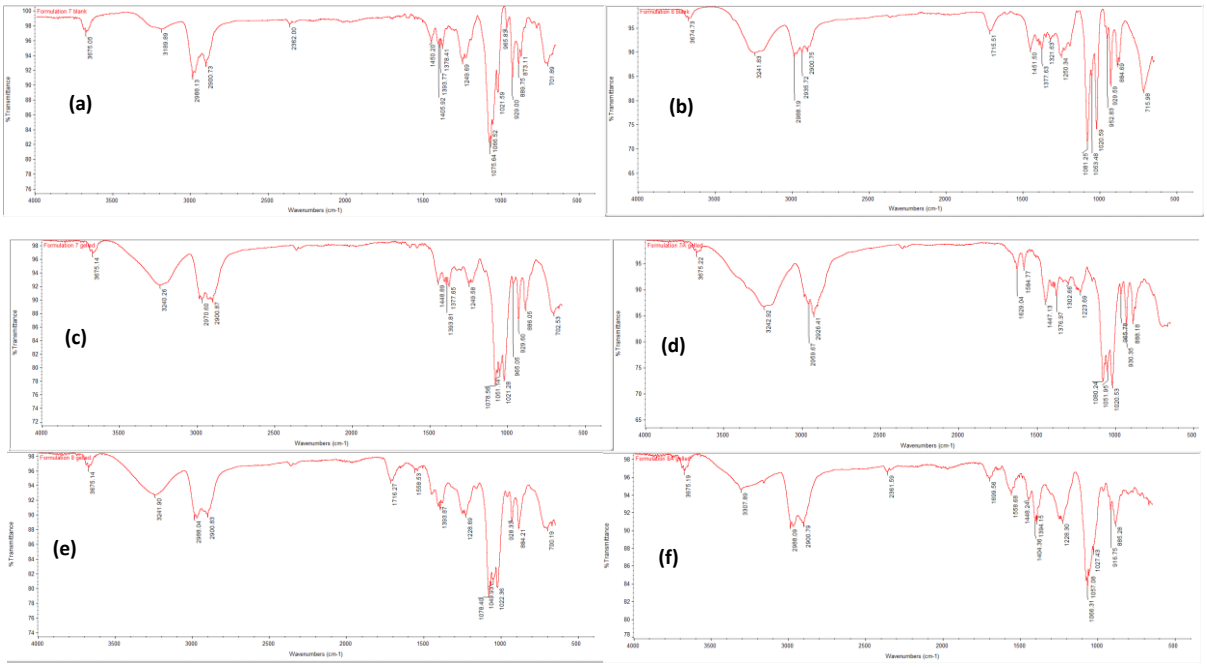

Figure 5.14 FTIR spectra of (a) blank HPMC mixed carrageenan gel, (b) blank Carbopol mix carrageenan gel, (c) KI-H48TC, (d) KI-H48C, (e) KI-C5TC, and (f) KI-C5C.

FTIR spectroscopy was used to confirm cannabinoid incorporation and assess potential drug and excipient interactions in the ion-induced in-situ gelling formulations. Across all formulations, the polymeric matrices displayed characteristic absorption bands consistent with gellan gum, carrageenan, HPMC, and Carbopol. A broad band between 3400–3200 cm^{-1} corresponded to O–H stretching vibrations, attributable to hydroxyl groups in polysaccharides and absorbed water, with variations in the peaks corresponding to the hydrogen bonding between the polymer chains and water molecules (Gómez-Ordóñez & Rupérez, 2011; Prasad et al., 2016; Verma et al., 2011). Absorptions around 2924 cm^{-1} corresponded to C–H stretching vibrations of $–CH_2$ and $–CH_3$ groups, commonly seen in cellulose derivatives such as HPMC (Akinosho et al., 2013). A distinct

band around 1720–1700 cm^{-1} was observed in Carbopol-containing formulations, representing C=O stretching of free carboxylic acid groups (Chalal et al., 2014).

In both blank and drug loaded formulations (K-H28TC, K-H28C, K-C3TC, K-C3C, KI-H48TC, KI-H48C, KI-C5TC, KI-C5C) with carrageenan's, highlighted in Figure 5.13 and Figure 5.14, additional bands were observed between 1250–1210 cm^{-1} and 850–800 cm^{-1} corresponding to absorptions associated with sulfate ester linkages and anomeric regions (Gómez-Ordóñez & Rupérez, 2011; Webber et al., 2012). Gellan gum formulations (G-H4TC, G-H4C, G-C37TC, G-C37C) in Figure 5.12 along with κ-CG and ι-CG formulations all displayed strong absorptions in the 1200–1000 cm^{-1} range representing C–O–C asymmetric stretching and C–O stretching of glycosidic linkages (Gómez-Ordóñez & Rupérez, 2011; Verma et al., 2011).

Drug-loaded formulations demonstrated additional peaks consistent with cannabinoid incorporation. Distinct absorptions at 2850 and 2950 cm^{-1} correspond to C-H stretching from the CBD-HP-β-CD complex and the THC-HP-β-CD complex, around 1645 cm^{-1} point towards H-O-H bending observed in HP-β-CD molecules, and around 1031 cm^{-1} referring to C-O or C-O-C vibrations (H. Li et al., 2021; Patil & Pandey, 2024; Upadhye et al., 2010). Overall, FTIR results confirmed the absence of chemical interaction between cannabinoids and excipients, while indicating physical entrapment of drugs CBD and THC (as inclusion complexes) within the polysaccharide matrices.

5.4.8 SEM analysis of cannabinoid-loaded ion-induced in situ gels

The surface morphology of cannabinoid-loaded ion induced in situ gelling formulations was examined using scanning electron microscopy (SEM) highlighted in Figure 5.15. Distinct differences were observed between gellan gum, κ-carrageenan (κ-CG), and mixed κ/ι-carrageenan (κ-CG/ι-CG) formulations, suggesting variation in interactions between the polymers and cannabinoids based on differences in surface morphology, pore structure, and network organisation observed.

CBD-only formulations G-H4C, G-C37C, G-H28C, G-C3C, G-H48TC, and G-C5C represented in Figure 5.15 B, D, F, H, J, and L, respectively were generally observed to possess a more textured surface with pores and aggregated domains compared to their dual cannabinoid (CBD, THC) counterparts. These findings indicate that the presence of THC promotes the development of a more compact and homogeneous microstructure, most likely through synergistic interactions with the polymeric network. This phenomenon may be attributed to reduced crosslinking density in the absence of THC, which otherwise provides additional hydrophobic interactions that support a more compact gel matrix. Lower crosslinking disrupts the hydrogel network, and during freeze-drying, the weaker polymeric framework is more prone to pore collapse and aggregate formation as water evaporates from the matrix. Such morphological features are consistent with previous studies (Cassanelli, Norton, et al., 2018; Diryak et al., 2018), where reduced or insufficient crosslinking led to irregular, porous, and aggregated microstructures upon drying. This might further explain the lower hardness

and cohesion, and higher drug release from CBD-only in-situ gels were observed when compared with gels with both CBD and THC.

Comparative SEM analysis between the formulations with different in situ gelling polymers revealed clear structural differences. Gellan gum-based formulations G-H4TC, G-H4C, G-C37TC, G-C37C highlighted in Figure 5.15 A, B, C, and D tended toward dense and relatively smooth surfaces. In contrast, κ-CG based formulations (K-H28TC, K-H28C, K-C3TC, K-C3C) in Figure 5.15 E, F, G and H exhibited more heterogeneous and fibrous surfaces. The mixed κ/ι-CG formulations (KI-H48TC, KI-H48C, KI-C5TC, KI-C5C) (Figure 5.15 I, J, K and L) demonstrated the greatest porosity and structural complexity, with ridges, voids, fibrous networks, and aggregates. This suggests synergistic effects of κ- and ι-helices forming interpenetrating networks, combined with the influence of the secondary polymer. Research has demonstrated that rheological investigations of κ/ι-carrageenan mixtures reveal distinct dual gelation processes, resulting in microstructures consistent with either interpenetrating or phase-separated network behaviour. This has been previously observed with freeze-dried gels (Nono et al., 2012; Ridout et al., 1996). The morphology of mixed systems further supports their enhanced drug diffusion.

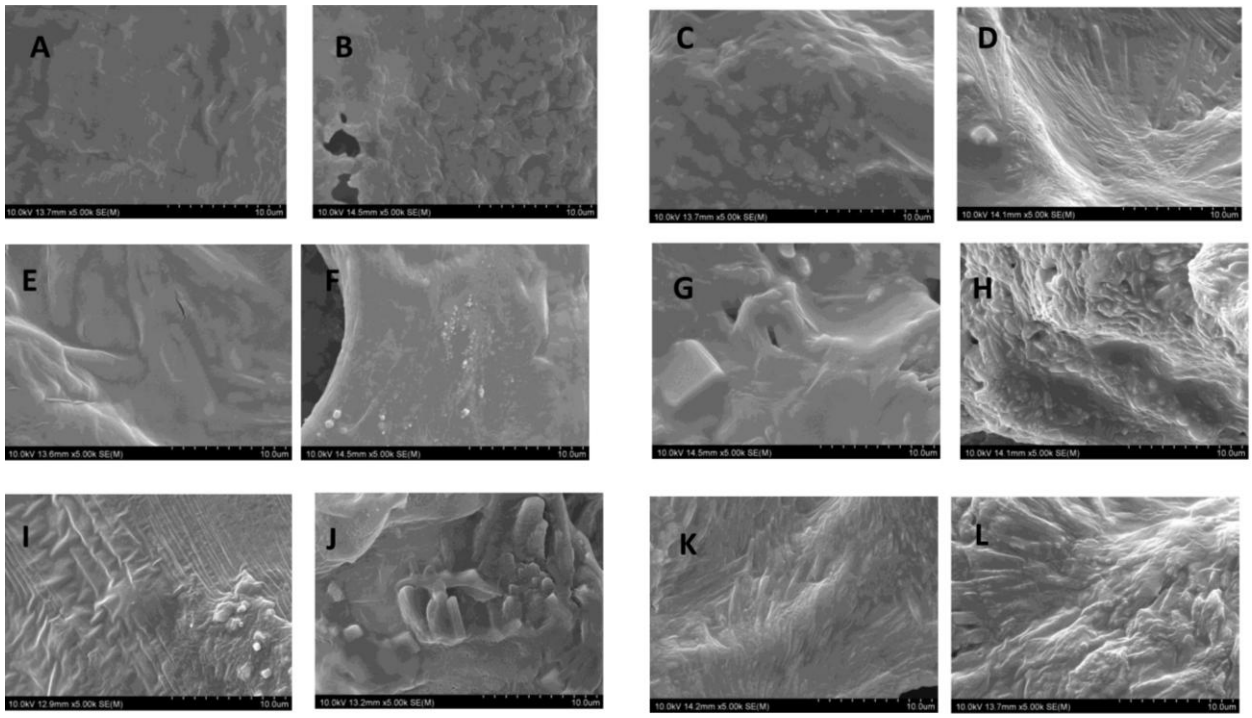

Figure 5.15 SEM captured at a magnification of ×5,000 with a scale bar representing 10 µm of optimized freeze-dried in-situ gels (A) G-H4TC, (B) G-H4C, (C) G-C37TC, (D) G-C37C (E) K-H28TC, (F) K-H28C, (G) K-C3TC, (H) K-C3C, (I) KI-H48TC, (J) KI-H48C, (K) KI-C5TC, and (L) KI-C5C.

5.4.9 Ex-vivo drug penetration

The ex vivo penetration profiles of cannabinoid-loaded ion induced in situ gels across porcine buccal mucosa are presented in Figure 5.16. All formulations exhibited measurable penetration of cannabinoids, with statistically significant differences between polymer systems ($p < 0.05$).

Formulations containing HPMC (G-H4TC, G-H4C, K-H28TC, K-H28C, KI-H48TC, KI-H48C) demonstrated significantly higher penetration compared to their Carbopol-based equivalents (G-C37TC, G-C37C, K-C3TC, K-C3C, KI-C5TC, KI-C5C). This trend is consistent with dissolution studies, where lower viscosity and weaker gel strength of HPMC matrices facilitated faster drug release and subsequent permeation. In contrast, Carbopol, while providing strong mucoadhesion, forms dense networks that restrict cannabinoid diffusion, resulting in lower permeation rates (Ali & Al-Shohani, 2024; Mohammad Hamdi, Azmi, Sabari, et al., 2023; Zema et al., 2007).

Ex vivo penetration results correlated with previously observed in-vitro drug release. Gellan gum-based systems (G-H4TC, G-H4C, G-C37TC, G-C37C) showed the lowest cannabinoid penetration among all formulations, attributable to the strong ionic crosslinking between gellan gum and divalent cations, which creates compact gel networks that hinder drug diffusion (Hazra et al., 2025). Conversely, mixed κ/ι-carrageenan-based formulations (KI-H48TC, KI-H48C, KI-C5TC, KI-C5C) exhibited the highest drug penetration. The enhanced transport is likely due to the synergistic gelation between κ- and ι-carrageenan, where κ-CG contributes a rigid but porous structure, while ι-CG enhances hydration and swelling, thereby improving drug release and mucosal diffusion (Tavagnacco et al., 2023).

The CBD-only formulations consistently showed slightly higher drug penetration than the dual cannabinoid (CBD, THC) counterparts. Furthermore, higher penetration of CBD was also observed in formulations with both the cannabinoids, as shown in Figure 5.16 (B), (C), and (D). This can be explained by previously demonstrated higher permeability of CBD in mucosal system, and the greater hydrophobicity and stronger interactions of THC with polymer matrices, which can hinder its penetration (C. J. Lucas et al., 2018; Varadi et al., 2023). Overall, these results demonstrate that polymer composition, viscosity, and cannabinoid type collectively influence ex vivo drug penetration.

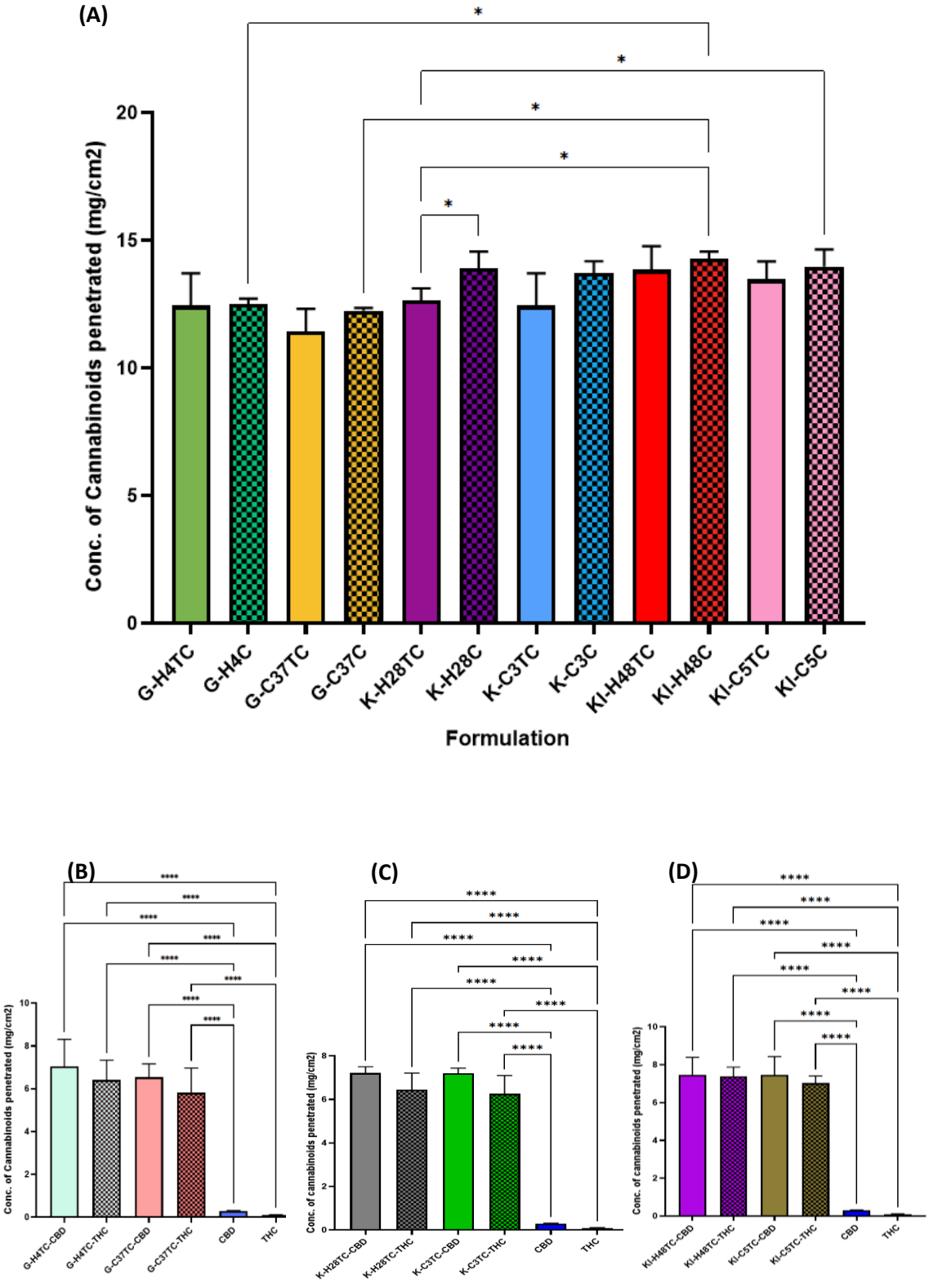

Figure 5.16 Ex-vivo penetration profiles of (A) Total cannabinoids from ion induced in-situ gelling formulations, (B) Individual penetration profiles of CBD and THC of gellan gum formulations, (C) Individual penetration profiles of CBD and THC of κ-CG formulations, (D) Individual penetration profiles of CBD and THC of mixed carrageenan formulations (n = 3; mean ± SD). Statistically significant differences are denoted as *p < 0.05 and **p < 0.01, ***p < 0.001, ****p < 0.0001.

5.4.10 Stability studies

Stability study results (pH, appearance, drug content, and gelling capacity over 6 months) are represented in Table 5.14. All formulations-maintained pH values within the range of 6.2–6.8 over six months, which falls within the acceptable buccal pH range (6.2–7.4). This suggests that the formulations are unlikely to cause mucosal irritation upon administration.

Appearance of formulations after 3 months is shown in Figure 5.17 and 6 months in Figure 5.18. Most formulations developed mild yellowing or yellowing after six months, which can be attributed to cannabinoid oxidation in aqueous environments. Jaidee et al. (2022) reported that cannabinoid degradation is accelerated at elevated temperatures and under strongly acidic conditions, whereas physiological temperature (37 °C) and near-neutral pH slow the process. Similarly, Jeong et al. (2023) demonstrated that while mildly acidic to neutral conditions reduce the rate of cannabinoid breakdown compared to harsher environments, prolonged exposure still results in gradual degradation over time. Formulations containing Carbopol (G-C37TC, G-C37C, K-C3TC, K-C3C, KI-C5TC, KI-C5C) appeared slightly resistant to discolouration, indicated by their mild yellowish colour, possibly due to stronger polymer and drug interactions stabilizing the cannabinoids against oxidative stress. Furthermore, Carbopol-based formulations showed higher drug stability compared to HPMC-based counterparts.

Carrageenan formulations with Carbopol (K-C3TC, K-C3C, KI-C5TC, KI-C5C) did not turn yellowish after 6 months. This greater resistance might have been due to synergistic stabilizing effects. Carrageenan, a sulfated polysaccharide, possesses inherent antioxidant properties that scavenge free radicals and reduce redox potential, thereby mitigating oxidation processes that lead to coloured degradation products (Kalsi et al., 2025). When combined with Carbopol, a high viscosity carbomer, this could have created a denser gel matrix that limits oxygen diffusion and enhances overall stability, preventing the gradual breakdown seen in other systems.

With dual drug formulations (G-H4TC, G-C37TC, K-H28TC, K-C3TC, KI-H48TC, KI-C5TC), both cannabinoids showed gradual reduction in content over time, with around 20–35% loss by 6 months. CBD-only formulations (G-H4C, G-C37C, K-H28C, K-C3C, KI-H48C, KI-C5C) demonstrated better retention of CBD (70–80%) compared to THC-containing counterparts. This aligns with reports that THC is more vulnerable to oxidative, thermal, and light-induced degradation pathways than CBD. Specifically, Peschel (2016) highlighted that THC oxidizes into CBN during storage and is particularly sensitive to light and oxygen exposure, whereas CBD shows relatively higher stability under similar conditions

All formulations retained strong gelling capacity (+++) across 6 months, indicating that the ion-activated in situ gelation mechanism remained robust despite drug degradation.

Table 5.14 Stability study of cannabinoid-loaded ion induced in situ gel formulations: changes in pH, appearance, drug content, and gelling capacity during 6 months of storage at room temperature (n = 3; mean ± SD).

Formulation	pH			Appearance			Drug content			Gelling capacity		
							% drug remaining					
	1m	3m	6m	1m	3m	6m	1m	3m	6m	1m	3m	6m
G-H4TC	6.4	6.33	6.32	Cream coloured	Cream coloured	Yellowish	CBD 98.33 ± 0.17 THC 93.99 ± 0.28	CBD 93.61 ± 0.61 THC 91.41 ± 0.24	CBD 79.99 ± 0.15 THC 78.58 ± 0.61	+++	+++	+++
G-H4C	6.79	6.63	6.54	Cream coloured	Cream coloured	Yellowish	CBD 99.49 ± 0.37	CBD 98.63 ± 0.11	CBD 80.48 ± 0.52	+++	+++	+++
G-C37TC	6.72	6.64	6.63	Cream coloured	Cream coloured	Mildly yellowish	CBD 88.58 ± 1.02 THC 89.88 ± 1.22	CBD 87.75 ± 0.13 THC 88.06 ± 0.19	CBD 65.44 ± 0.88 THC 66.48 ± 0.21	+++	+++	+++
G-C37C	6.62	6.55	6.54	Cream coloured	Cream coloured	Mildly yellowish	CBD 92.11 ± 0.27	CBD 91.11 ± 0.31	CBD 70.37 ± 0.11	+++	+++	+++
K-H28TC	6.68	6.56	6.54	Cream coloured	Cream coloured	Yellowish	98.28 ± 0.19 THC 95.22 ± 0.81	92.22 ± 0.77 THC 94.7 ± 0.17	78.67 ± 0.86 THC 70.58 ± 0.65	+++	+++	+++
K-H28C	6.48	6.4	6.36	Cream coloured	Cream coloured	Yellowish	CBD 96.45 ± 0.19	CBD 95.5 ± 0.92	CBD 71.23 ± 0.27	+++	+++	+++
K-C3TC	6.32	6.28	6.26	Cream coloured	Cream coloured	Mildly yellowish	CBD 97.57 ± 0.33 THC 97.35 ± 0.66	CBD 95.46 ± 0.31 THC 95.37 ± 0.22	CBD 76.45 ± 0.83 THC 75.92 ± 0.17	+++	+++	+++
K-C3C	6.34	6.3	6.28	Cream coloured	Cream coloured	Mildly yellowish	CBD 97.99 ± 0.34	CBD 96.01 ± 0.43	CBD 80.48 ± 0.32	+++	+++	+++
KI-H45TC	6.66	6.6	6.56	Cream coloured	Cream coloured	Yellowish	CBD 90.54 ± 0.13 THC 90.32 ± 0.99	CBD 90.12 ± 0.65 THC 90.02 ± 0.44	CBD 60.58 ± 0.72 THC 60.36 ± 0.54	+++	+++	+++
KI-H45C	6.68	6.62	6.6	Cream coloured	Cream coloured	Yellowish	CBD 98.54 ± 0.21	CBD 94.24 ± 0.72	CBD 76.78 ± 0.33	+++	+++	+++

KI-C5TC	6.67	6.62	6.58	Cream coloured	Cream coloured	Mildly yellowish	CBD 96.43 ± 0.26 THC 94.56 ± 0.53	CBD 94.24 ± 0.63 THC 93.05 ± 0.39	CBD 74.56 ± 0.55 THC 68.68 ± 0.74	+++	+++	+++
KI-C5C	6.42	6.4	6.38	Cream coloured	Cream coloured	Mildly yellowish	CBD 99.03 ± 0.43	CBD 98.84 ± 0.32	CBD 79.96 ± 0.31	+++	+++	+++

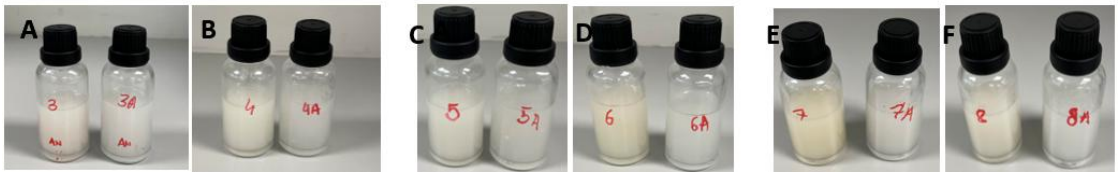

Figure 5.17 Appearance of formulations after 3 months, (A) L, G-H4TC and R, G-H4C, (B) L, G-C37TC and R, G-C37C (C) L, K-H28TC and R, K-H28C, (D) L, K-C3TC and R, K-C3C (E) L, KI-H48TC and R, KI-H48C, (F) L, KI-C5TC and R, KI-C5C.

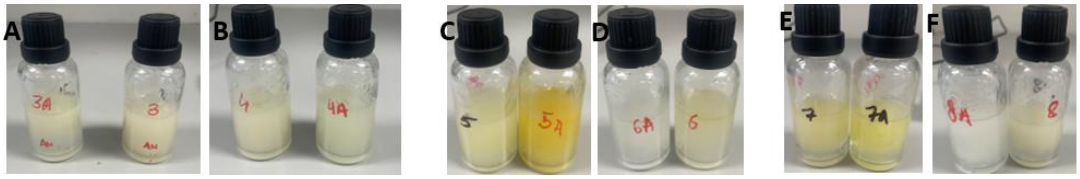

Figure 5.18 Appearance of formulations after 6 months, (A) L, G-H4TC and R, G-H4C, (B) L, G-C37TC and R, G-C37C (C) L, K-H28TC and R, K-H28C, (D) L, K-C3C and R, K-C3TC (E) L, KI-H48TC and R, KI-H48C, (F) L, KI-C5C and R, KI-C5TC.

5.4.10.1 Freeze dried ion induced in-situ gels with Carbopol.

Carbopol-based gels were found to exhibit superior mechanical strength, mucoadhesion, and sustained cannabinoid release, and were used for stability testing in their freeze-dried form (Figure 5.19), as an alternative approach to potentially prolong formulation stability. After 6 months and upon rehydration, their sol-to gel transitions were evaluated, as well as their pH, drug content and stability.

Sol-gel transitions

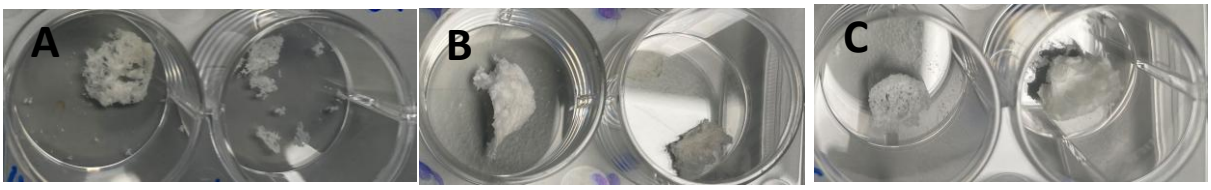

Figure 5.19. Freeze dried in-situ gels after 6 months, (A) L, G-C37TC and R, G-C37C, (B) L, K-C3TC and R, K-C3C (C) L, KI-C5TC and R, KI-C5C.

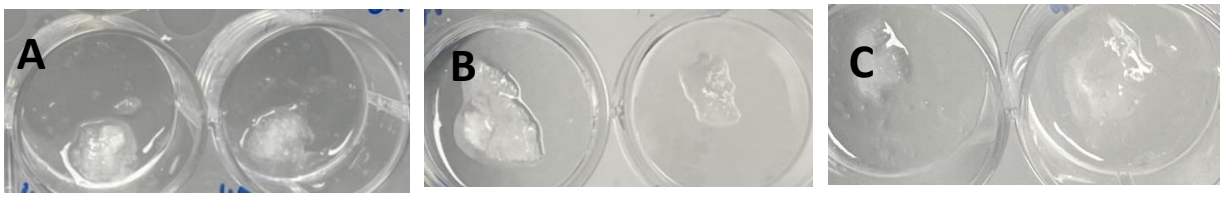

Figure 5.20. Sol-gel transition of rehydrated gels upon the addition of artificial saliva after 6 months, (A) L, G-C37TC and R, G-C37C, (B) L, K-C3TC and R, K-C3C (C) L, KI-C5TC and R, KI-C5C.

All the formulations were successfully rehydrated with distilled water, and gelled upon the addition of artificial saliva, as shown in Figure 5.20. Results of the sol-gel transition time are highlighted in Table 5.15. Across all formulations, freeze-dried gels demonstrated sol–gel transition times that were comparable to or slightly shorter than those of their in-situ counterparts. This pattern was supported by literature on similar polymeric systems. Studies have identified that freeze-drying method can introduce microstructural changes, which could influence gelation kinetics upon rehydration (Cassanelli, Norton, et al., 2018). Faster gelation time observed could be attributed to the porous structure of freeze dried gels that accelerate water uptake and potentially facilitate quicker gelation (Barbara Vigani et al., 2020).

Table 5.15. Sol–gel transition times of Carbopol-based in-situ gels compared with their corresponding freeze-dried and rehydrated gels in artificial saliva (n = 3; mean ± SD).

Formulation Code	Sol–gel transition time (s, ± SD) In-situ gels	Sol–gel transition time (s, ± SD) Freeze-dried gels
G-C37TC	33.0 ± 2.60	32 ± 1.2
G-C37C	32.0 ± 1.80	31.8 ± 2.10
K-C3TC	7.5 ± 1.30	7 ± 1.11
K-C3C	9.0 ± 2.00	8.8 ± 2.00
KI-C5TC	12.2 ± 1.10	12 ± 2.20
KI-C5C	19.6 ± 1.50	19 ± 0.95

pH, drug content, and gelling capacity of rehydrated in-situ gels.

The stability of freeze-dried Carbopol-based gels was assessed over six months at room temperature (25 °C), with evaluation of pH, drug content, and gelling capacity (Table 5.16). All formulations were found to maintain pH values between 6.4 and 6.7 after six months. Drug content analysis demonstrated high retention, with most formulations preserving a higher percentage of initial cannabinoid load after six months compared with in-situ gels that were not freeze dried. Formulations also retained strong gelling capacity, consistently scoring +++, confirming that the ion-responsive sol–gel transition behaviour was preserved following six months of storage.

Previous studies have demonstrated that lyophilization improves the stability of hydrophobic drugs and facilitates long-term storage by minimizing drug degradation. This is particularly relevant for formulations prone to hydrolytic, oxidative, or thermal degradation, as the removal of water during freeze-drying significantly slows these chemical processes. In addition to chemical stabilization, freeze-drying also preserves the physical structure of gels, maintaining the porous network and preventing collapse or aggregation that

could compromise gelation or drug release. By mitigating both chemical and physical instabilities that commonly occur during storage, freeze-drying not only enhances the shelf-life of pharmaceutical products but also helps retain their therapeutic efficacy upon reconstitution (Abla & Mehanna, 2022; Odziomek et al., 2024).

Table 5.16 Stability evaluation of freeze-dried Carbopol-based cannabinoid in-situ gels after six months of storage at 25 °C. Data are expressed as pH, percentage of drug remaining, and gelling capacity in artificial saliva (n = 3; mean ± SD).

Formulation	pH (6 m)	Drug content (% remaining)	Gelling capacity
G-C37TC	6.71	98.02 ± 0.66 CBD	+++
		96.33 ± 0.31 THC	
G-C37C	6.59	94.02 ± 0.52 CBD	+++
K-C3TC	6.61	98.12 ± 0.4 CBD	+++
		94.37 ± 0.73 THC	
K-C3C	6.40	95.34 ± 0.88 CBD	+++
KI-C5TC	6.45	98.34± 0.26 CBD	+++
		96.8 ± 0.36 THC	
KI-C5C	6.40	97.96 ± 0.08 CBD	+++

5.5 Conclusions

The evaluation of cannabinoid-loaded ion-induced in-situ gelling formulations underscores their potential as effective buccal delivery systems, with polymer composition exerting a profound influence on physicochemical properties. All formulations, comprising gellan gum, κ-carrageenan, or mixed κ/ι-carrageenan combined with HPMC or Carbopol, exhibited uniform appearance and consistent drug content, ensuring efficient cannabinoid incorporation without precipitation. pH profiling demonstrated compatibility with the buccal mucosa, minimizing irritation risk, supporting their suitability for clinical administration.

Gelation and rheological characterization revealed formulation-dependent distinctions. Carbopol-based systems displayed rapid gelation and elevated viscosity, indicative of stronger intermolecular interactions and enhanced gel strength, whereas HPMC-based gels showed slower gelation and lower viscosity. Mixed κ/ι-carrageenan formulations provided an optimal balance between rigidity and elasticity, with intermediate gelation times and superior viscosity. The co-presence of CBD and THC increased overall gel viscosity, suggesting a reinforcing effect of THC on the polymer network.

Mechanical and mucoadhesive evaluation highlighted that Carbopol-based gels exhibited superior hardness, cohesion, and mucoadhesive strength, with mixed κ/ι-carrageenan systems achieving the highest mucoadhesion through dense, elastic networks. Gellan gum formulations, although mechanically robust due to divalent cation crosslinking, demonstrated moderate mucoadhesion in comparison to the lower strength observed for κ-carrageenan based formulations. These findings indicate that Carbopol and mixed carrageenan systems are particularly effective in sustaining buccal contact, a critical determinant of prolonged drug absorption.

Drug release and penetration studies demonstrated that HPMC-based formulations facilitated faster cannabinoid release and higher mucosal permeation, attributable to their lower viscosity and less compact gel networks. In contrast, Carbopol-based formulations exhibited slower, more controlled release profiles, consistent with their denser networks, while mixed κ/ι-carrageenan systems supported enhanced release and penetration owing to their porous yet elastic structures. CBD consistently displayed faster release and penetration than THC, reflecting the hydrophobicity and limited diffusivity of THC. Stability studies confirmed maintenance of gelling properties and pH over time. However, cannabinoid degradation was observed after 6 months, highlighting the need for techniques to preserve cannabinoid integrity.

Freeze-drying emerged as an effective approach to improve the long-term stability of Carbopol-based gels. Upon rehydration, the formulations were found to maintain sol–gel transition times, pH, and gelling behaviour comparable to those of freshly prepared gels. Additionally, they exhibited higher drug retention after six months. These suggest that the structural integrity of the ion-responsive network is preserved during drying and rehydration, thereby enabling prolonged storage without compromising performance.

Overall, Carbopol-based mixed κ/ι-carrageenan formulations (KI-C5TC, KI-C5C) emerged as the most promising candidates for buccal cannabinoid delivery, combining rapid gelation, high viscosity, strong mechanical integrity, and robust mucoadhesive properties, thereby ensuring prolonged mucosal retention and sustained drug release. While HPMC-based gels offer faster release, their comparatively lower mucoadhesion and gel strength limit their potential for extended delivery. Collectively, these findings demonstrate that ion-induced in-situ gels can be strategically engineered to achieve controlled, stable, and effective buccal delivery of cannabinoids.

Chapter 6: Development and Characterization of 3D-Printed Mucoadhesive Buccal Films of Cannabinoids

Abstract

Three-dimensional (3D) printing has emerged as a versatile platform in pharmaceutical sciences, enabling precise fabrication of personalized dosage forms with controlled drug release and tailored properties. This study aimed to develop mucoadhesive buccal films for cannabinoid delivery using extrusion-based 3D bioprinting, incorporating cannabidiol (CBD) and tetrahydrocannabinol (THC) as cyclodextrin inclusion complexes, with HPMC or Carbopol as mucoadhesive polymers and terpenes as permeation enhancers. Bioinks were prepared and characterised for viscosity, pH, and drug content before printing films under optimized conditions. The 3D-printed films were evaluated for mechanical and physicochemical characteristics, as well as in vitro drug release and ex vivo buccal mucosal penetration of cannabinoids. HPMC-based films, with bioinks exhibiting good printability, demonstrated superior mechanical strength, cohesive and elastic matrices, and sustained, non-Fickian release of cannabinoids, while significantly enhancing ex vivo cannabinoid permeation compared to unformulated drugs. In contrast, Carbopol-based films, despite their higher mucoadhesive strength, showed weaker mechanical properties, faster erosion-driven release, and poorer printability of the corresponding bioinks. Overall, these findings highlight the potential of HPMC-based 3D-printed buccal films as an effective platform for transmucosal cannabinoid delivery.

6.1 Introduction

Three-dimensional (3D) printing has emerged as a transformative technology in pharmaceutical sciences, facilitating the rapid fabrication of complex, personalized therapeutics with high precision. This approach is particularly advantageous for a diverse range of drugs, as it allows meticulous control over drug loading, uniform distribution, and release kinetics, ensuring consistent and predictable therapeutic outcomes. Also referred to as additive manufacturing, 3D printing constructs dosage forms through a layer-by-layer deposition process, enabling intricate geometries and tailored drug delivery profiles. The practical applicability of 3D printing for producing personalized pharmaceutical dosage forms has been formally recognized, as demonstrated by the FDA's approval of Spritam (levetiracetam) in 2015. This 3D-printed orodispersible tablet highlighted the ability of additive manufacturing to create complex, patient-friendly dosage forms with precise drug content, rapid disintegration, and tailored release characteristics, opening opportunities in 3D-printed pharmaceuticals (Abdella et al., 2024; Fitzgerald, 2015; Kulkarni et al., 2024; Wang et al., 2023).

A variety of 3D printing technologies have been employed in pharmaceutical sciences to develop innovative dosage forms. Among the most established methods, fused deposition modelling (FDM) extrudes thermoplastic drug–polymer filaments layer by layer to produce tablets and implants, though its reliance on high temperatures limits application with thermolabile drugs (Elkanayati et al., 2022; Shipp et al., 2022). Semi-solid extrusion (SSE) overcomes this issue by extruding drug-loaded gels or pastes at ambient or slightly elevated temperatures, enabling incorporation of sensitive actives and excipients, and has been widely applied to fabricate oral dispersible films, chewable formulations, and personalized paediatric medicines (Aina et al., 2025; Cerveto et al., 2024). Other laser or light-based methods, including selective laser sintering (SLS) and stereolithography (SLA), offer excellent resolution and the ability to tailor porosity or microstructure, but are constrained by the need for pharmaceutically compatible photopolymers and heat-stable drugs (Afridi et al., 2024; Lakkala et al., 2023). Binder jetting and direct powder extrusion (DPE) represent additional approaches with lower thermal input, although challenges remain in these relatively new techniques and further studies are needed to determine their effectiveness in development of dosage forms with uniform drug distribution (Milliken et al., 2024). Such methods have enabled the creation of dosage forms ranging from fast-dissolving tablets to controlled-release systems, underscoring the versatility of additive manufacturing in advancing personalized medicine.

While these technologies demonstrate the feasibility of additive manufacturing for pharmaceuticals, their reliance on thermoplastics, resins, or powders presents challenges in incorporating mucoadhesive polymers and hydrophilic drug carriers. To address this, extrusion-based 3D bioprinting has emerged as a promising alternative (Aguilar-de-Leyva et al., 2020; Azad et al., 2020; Park et al., 2019). Bioprinting (extrusion-based) is an advanced form of 3D printing that is widely used for the fabrication of biomaterials and scaffolds and has also shown potential for developing drug delivery systems under mild conditions such as the absence of heat,

making it suitable for sensitive active pharmaceutical ingredients (APIs). This technique relies on bioinks, which are printable materials such as hydrogels or polymer solutions that can be extruded under mild conditions to form films, patches, or scaffolds suitable for drug delivery (Tejada Jacob et al., 2022).

Within mucosal drug delivery, particularly via the buccal route, extrusion bioprinting offers unique advantages by enabling the fabrication of mucoadhesive films, patches, or scaffolds with precise control over thickness, porosity, and drug loading. Buccal films are advantageous because they are thin, flexible, and discreet, which improves patient compliance across vulnerable populations such as paediatric, geriatric, and dysphagic patients. Their ease of administration, without the need for water, further enhances convenience and acceptability. Importantly, bioprinting allows the tailoring of these films to achieve either rapid drug release for immediate therapeutic action or sustained release for prolonged exposure, depending on the therapeutic requirements (de Carvalho et al., 2023). Several studies have demonstrated the potential of extrusion-based 3D printing and bioprinting for single or multi-layered buccal film fabrication, highlighting their utility in precise drug deposition and individualized therapy (Jovanović et al., 2021; Shipp et al., 2022; Erica Sjöholm & Niklas Sandler, 2019).

The incorporation of mucoadhesive polymers in buccal film formulations significantly enhances their performance by ensuring intimate contact with the buccal mucosa, thereby prolonging residence time and enabling controlled drug delivery. These polymers facilitate the adhesion of the film to the mucosal surface, allowing for sustained drug release and improved therapeutic efficacy. Various mucoadhesive polymers have been utilized as the backbone of buccal films, including natural, synthetic, and semi-synthetic polymers. Natural polymers such as chitosan and sodium alginate offer biocompatibility and biodegradability, while synthetic polymers like polyacrylic acid (Carbopol) and polyvinyl alcohol provide desired mechanical properties and mucoadhesive strength. Semi-synthetic polymers, such as hydroxypropyl methylcellulose (HPMC), combine the advantages of both natural and synthetic polymers, offering versatility in formulation design. Such polymers in addition with other excipients used can be used achieve optimal film characteristics tailored to specific drug delivery requirements (Karki et al., 2016; Landová et al., 2013; Shipp et al., 2022).

Additive manufacturing techniques have substantially advanced cannabinoid formulation strategies by enabling precise control over drug dosage, release kinetics, and structural design in pharmaceutical applications. Several studies have demonstrated the potential of 3D printing for cannabinoid delivery. Gościniak et al. (2024) fabricated bi-gel systems of cannabidiol (CBD)-rich hemp extracts with hyaluronic acid, while Antezana et al. (2022) developed gelatine-alginate scaffolds loaded with Cannabis sativa oil for enhanced wound repair, and Jennotte et al. (2023) used FDM to fabricate immediate-release oral CBD dosage forms with tailored solid dispersions. To address the poor solubility and limited bioavailability of cannabinoids, various strategies such as complexation with cyclodextrins or entrapment in nanoparticles have been explored. Andriotis et al. (2020) developed pectin-honey inks containing CBD–β-cyclodextrin complexes, which were printed using semi-solid extrusion-based printing for oral drug delivery. Similarly, P. K. Monou et

al. (2022) fabricated alginate films incorporating CBD/CBG nanoparticles to support wound healing due to their bioactive and mucoadhesive properties. Despite these advances, research on 3D-printed films for buccal cannabinoid delivery remains limited. Research by Abdella et al. (2024) addressed this by producing hydroxyethyl cellulose (HEC)-based gels loaded with CBD nanostructured lipid carriers (NLCs) using pressure-assisted micro-syringe extrusion, yielding thin, mucoadhesive films suitable for buccal administration.

Building on these previous findings, in this study, extrusion-based bioprinting was employed to fabricate mucoadhesive buccal films of cannabinoids. Cannabinoids were incorporated as cyclodextrin inclusion complexes to enhance solubility and stability, while HPMC or Carbopol served as mucoadhesive polymers to prolong residence time on the buccal mucosa. Additionally, terpenes (3.125% 1,8-cineole, 0.625% d-limonene, 0.625% L-menthol, and 0.625% α-pinene) were incorporated as permeation enhancers to improve drug absorption. This approach aims to combine the precision and versatility of 3D bioprinting with mucoadhesive polymeric matrices to achieve controlled release, sustained mucoadhesion, and improved bioavailability of cannabinoids via the buccal route, while also promoting high patient compliance.

6.2 Materials and methods

Hydroxypropyl methyl cellulose (HPMC) was purchased from Sigma-Aldrich, New Zealand. Carbopol 934P (Serva) from DKSH LabShop, New Zealand, D-Limonene from Thermo Fisher, New Zealand, 1,8- cineole, α-Pinene from Sigma-Aldrich, New Zealand, and l-Menthol from Chem express supplied by Focus Bioscience, Australia. Phosphate buffered saline (PBS) tablets (pH 7.4), Poly-ethylene glycol (PEG 400), HP-β-CD, and acetonitrile were purchased from Sigma-Aldrich, New Zealand. Pure isolated CBD and distilled oil of THC were provided by Helius Therapeutics Ltd, New Zealand. All other reagents used were of analytic grade.

Artificial saliva was prepared by dissolving 1.5% w/v potassium chloride (KCl), 0.43% w/v sodium chloride (NaCl), 0.22% w/v calcium chloride ($CaCl_2$), 0.42% w/v sodium bicarbonate ($NaHCO_3$), and an appropriate amount of sodium dihydrogen phosphate monohydrate ($NaH_2PO_4 \cdot H_2O$) in distilled water (B. Vigani, S. Rossi, et al., 2019).

6.2.1 Preparation of Mucoadhesive bioinks

HPMC or Carbopol (1-5 % w/v) were weighed and gradually dispersed in distilled water under continuous magnetic stirring at room temperature to prevent clumping, forming a homogenous polymeric solution. To this, polyethylene glycol 400 (PEG 400) was added as the plasticizer at 5/10% v/v. Cannabinoids, either CBD alone or a combination of CBD and THC in the form of inclusion complexes with HP-β-CD, were introduced into the solution at a final concentration of 20 mg/ml under gentle stirring. Then Mannitol (200 mg) was incorporated as a sweetener, and terpenes (D-limonene, L-menthol, α-pinene, and 1,8-cineole) were added as permeation enhancers. The complete mixture was homogenized using a magnetic stirrer for 30–45 minutes until a uniform bioinks were obtained. The prepared bioinks were loaded into syringe cartridges for

immediate printing or stored at 4 °C for further use. The procedure was developed based on modifying the methods reported in previous studies involving either cannabinoids or the fabrication of buccal films using mucoadhesive polymers (Abdella et al., 2024; Tagami et al., 2019). pH of the bioinks were adjusted to 6.4 using triethanolamine. The composition and concentration of the bioink components of cannabinoid-loaded mucoadhesive buccal films are summarized in Table 6.1.

Table 6.1. Composition of bioinks used for extrusion-based 3D bioprinting of cannabinoid-loaded mucoadhesive buccal films.

Component	Type / Description	Concentration / Amount
Mucoadhesive polymer(s)	HPMC	1–5% (w/v)
	Carbopol	1–5% (w/v)
Plasticizer	PEG 400	5, and 10% (v/v)
Sweetener	Mannitol	200 mg
Drug + Cyclodextrin	HP-β-CD with CBD, HP-β-CD with THC	20 mg/mL, 1:1 molar ratio
Permeation enhancer	D-Limonene, L-Menthol, α-Pinene, 1,8-Cineole	C: 3.125% (w/v); L, P, M: 0.625% (w/v) each

6.2.1.1 Viscosity of bioinks

The viscosity of the prepared bioinks was measured using a Brookfield RST-SST rheometer fitted with a rotating ramp measuring spindle. Viscosity values were recorded were at a constant shear rate of 100 s^{-1} to assess the flow properties and suitability of the bioinks for extrusion-based 3D bioprinting.

6.2.2 Bioprinting mucoadhesive films of cannabinoids

The design of the buccal films was created using SolidWorks software, establishing a film model with dimensions of 20 × 20 × 0.35 mm. The 3D computer-aided design (CAD) model was exported in STL file format and uploaded to Slice3r software, which converted the design into a layer-by-layer instructional format (G-code) required for printing. Repetier-Host software was employed to fine-tune printing parameters, including extrusion pressure, and printing speed, ensuring optimal deposition of the bioink. The generated G-code from Slice3r was used by the Allevi 3D bioprinter to fabricate the buccal films. Printing was performed on individual glass slides covered with adhesive tape to facilitate easy detachment post-printing. The bioinks were extruded using a previously optimized 25 G needle, selected based on the flow and rheological properties of the formulations. Following printing, all films were air-dried in the dark for 48 hours to achieve structural stability. The dried films were subsequently stored in a dark environment for further evaluations.

6.2.3 Determining pH, drug content, and weight of printed films.

The pH of the developed bioinks was measured using a calibrated bench-top pH meter (Interlab, New Zealand) to ensure compatibility of printed films with the buccal mucosa. The drug content of the films was quantified using the procedure described in Section 4.2.2, employing high-performance liquid chromatography (HPLC) to confirm accurate and uniform incorporation of the active cannabinoid compounds. Printed films were weighed using an electronic balance.

6.2.4 Mechanical properties of the films.

Mechanical properties of the films were determined using a texture analyser (Stable Micro Systems, UK) fitted with a 50 N load cell and using a stainless-steel spherical probe of 2mm diameter to compress each sample, as described previously in section 4.2.4.

6.2.5 Mucoadhesive strength of cannabinoid loaded films.

The mucoadhesive strength of the optimized 3D printed buccal films was assessed using freshly excised porcine buccal mucosa. A texture analyser (Stable Micro Systems, UK) was employed to measure the force required to detach the films from the mucosal surface, providing a quantitative assessment of their adhesion. The procedure followed the methodology outlined in Section 4.2.5.

6.2.6 Swelling ratio and dissolution time of printed films

The 3D printed buccal films were first weighed (W_1) and placed inside plastic tissue cassettes. The cassettes were then immersed in artificial saliva at 37°C for 1 hour. After incubation, the films were carefully removed, gently blotted with tissue paper to remove excess surface fluid, and weighed again using a digital balance (W_2). The degree of swelling, representing the fractional increase in weight of the films due to saliva absorption, known as the swelling ratio, was calculated using Equation 6.1 (Yildiz Pekoz et al., 2015).

Equation 6.1 $\text{Swelling ratio} = \frac{\text{Wt}-\text{W0}}{\text{W0}} \times 100$

Where, W_0 is the initial dry weight and W_t is the weight of the swollen sample at time t.

The dissolution time of the 3D printed buccal films was evaluated using simulated saliva (pH 6.8) at 37 ± 0.5 °C to mimic physiological conditions. A single film was carefully placed in a Petri dish containing 10 mL of the medium. The film was observed continuously for signs of softening, swelling, disintegration, or complete dissolution. Gentle agitation was applied intermittently to simulate oral movements. The time taken from initial contact with the medium until complete disintegration or dissolution of the film was recorded as the dissolution time. Each formulation was tested in triplicate, and the average dissolution time was calculated (J.-H. Lee et al., 2022).

6.2.7 In-vitro drug release and drug release kinetics

The in vitro release of cannabinoids from the 3D printed buccal films was evaluated using a Franz diffusion cell apparatus (Orchid Scientific, India) fitted with dialysis membranes (MWCO 14,000 Da). drug release kinetics was analysed using KinetDS software 3.0 (rev. 2010). These were conducted following the procedure described in Section 5.2.6.

6.2.8 FTIR of 3D printed cannabinoid films

FTIR analysis of the optimized 3D printed buccal films was performed using a Thermo Scientific FTIR spectrometer (Nicolet iS10, USA). The films were analysed to evaluate possible interactions between cannabinoids in inclusion complexes and mucoadhesive polymers, following the procedure outlined in Section 4.2.7.

6.2.9 SEM of 3D printed cannabinoid films

The surface morphology of the 3D printed films was examined using SEM. Samples were coated with a thin layer of platinum using an ion sputter coater (Hitachi E-1045) and imaged with a Schottky field emission scanning electron microscope (Thermo Scientific, HITACHI SU-70), as described in Section 5.2.8.

6.2.10 Ex-vivo penetration of cannabinoids from buccal films

Ex-vivo permeation of cannabinoids from the 3D printed films was evaluated using freshly excised porcine buccal mucosa mounted on a Franz diffusion cell apparatus (Orchid Scientific, India). The procedure followed the methodology outlined in Section 3, allowing assessment of drug penetration and absorption potential across the buccal mucosa.

6.3 Statistical analysis

Experimental data were processed and analysed using R programming and GraphPad Prism software (version 10.2.3). For datasets meeting the assumptions of normality and homogeneity of variances, statistical significance was determined using one-way analysis of variance (ANOVA). In cases where these assumptions were violated, the non-parametric Kruskal–Wallis test was employed. When significant differences were detected, post hoc comparisons were conducted using Tukey's multiple comparison test. A probability value of $P < 0.05$ was considered indicative of statistical significance.

6.4 Results and discussion

6.4.1 Viscosity of prepared bioinks

The viscosity of HPMC- and Carbopol-based bioinks (1-5% w/v) was evaluated at 100 s^{-1} shear rate to determine the influence of polymer concentration suitable for bioink preparation. In both polymer systems, viscosity increased in a concentration-dependent manner, shown in Figure 6.1. Carbopol-based bioinks

exhibited greater viscosity than HPMC-based bioinks, consistent with prior studies indicating that Carbopol is more viscous than HPMC at equivalent concentrations (E. Özyılmaz et al., 2024; Wu et al., 2007).

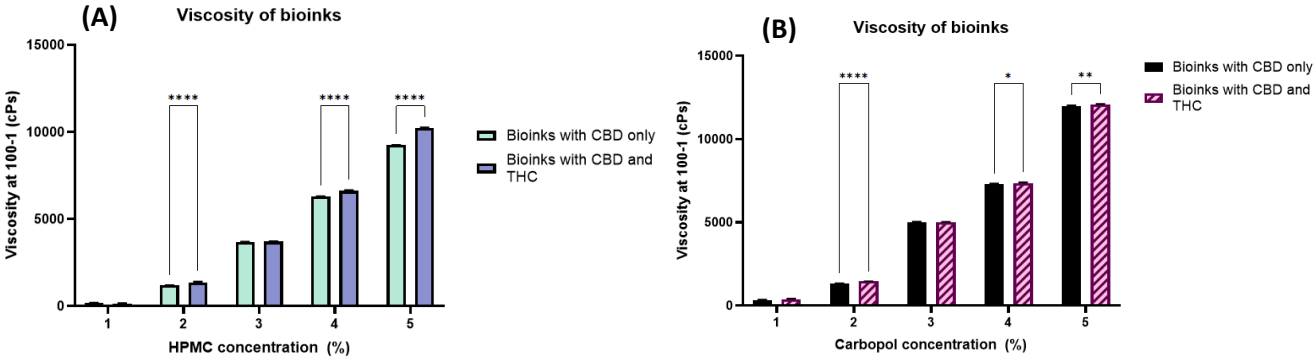

Figure 6.1 Viscosity profiles of bioinks containing either CBD-only or combined CBD and THC inclusion complexes at 100 s^{-1}; (A) HPMC-based and (B) Carbopol based bioinks (n = 3; mean ± SD). Statistical significance between CBD-only and CBD+THC formulations is indicated (*p < 0.05, **p < 0.01, ****p < 0.0001).

In both the bioinks, the addition of THC alongside CBD consistently increased viscosity compared to CBD-only formulations, indicating increased interactions from the added THC-cyclodextrin complex strengthening the polymer network in solution. These findings confirm that both polymer concentration and drug loading significantly influence rheological behaviour. From a formulation perspective, viscosity must be carefully optimized, as excessively low viscosity results in poor print fidelity and inadequate mucoadhesion, while overly high viscosity impairs extrusion, increases nozzle clogging risk, and may reduce patient acceptability or drug release rates (Tejada-Ortigoza & Cuan-Urquizo, 2022; Than et al., 2022). Based on these considerations, 3% and 4% concentrations of both the polymers were selected for printing buccal films. Selected polymer concentration and drug composition is presented in Table 6.2.

Table 6.2 Composition of 3D printing inks with different mucoadhesive polymers and cannabinoid inclusion complexes.

Code	Mucoadhesive Polymer	Drug in inclusion complex
H3C	3% HPMC	CBD (20 mg/ml)
H4C	4% HPMC	CBD (20 mg/ml)
H3TC	3% HPMC	THC + CBD (1:1, 20 mg/ml total)
H4TC	4% HPMC	THC + CBD (1:1, 20 mg/ml total)
C3C	3% Carbopol	CBD (20 mg/ml)
C4C	4% Carbopol	CBD (20 mg/ml)
C3TC	3% Carbopol	THC + CBD (1:1, 20 mg/ml total)
C4TC	4% Carbopol	THC + CBD (1:1, 20 mg/ml total)

6.4.2 Three-dimensional printing

6.4.2.1 Concentration of plasticizer (PEG) on printability of buccal films

The influence of PEG concentration on the printability and film quality of HPMC-based bioinks was investigated as shown in Table 6.3. Previous research has indicated that identifying that PEG levels are crucial to balance extrusion performance with final film stability (Saringat et al., 2005). At 10% PEG, HPMC-based inks printed well (Figure 6.2 A), but produced sticky films upon drying as shown in Figure 6.2 (B), suggesting excess plasticizer compromised structural stability. In contrast, as highlighted in Figure 6.2 (C) and (D), reducing the PEG concentration to 5% resulted in smooth, uniform prints with stable films after drying. Based on these findings, 5% PEG was selected as the optimal plasticizer concentration for further studies. This concentration was subsequently employed in both HPMC- and Carbopol-based bioinks to balance print fidelity, mechanical strength, and post-drying stability of the 3D-printed buccal films.

Table 6.3 Optimization of PEG concentration for extrusion-based 3D printing of buccal films (n = 3; mean ± SD).

Ink Composition	Temperature (°C)	Nozzle	Speed	Pressure (PSI)	Observations
HPMC 4% + PEG 10%	21.9–21.0	25G	6	24.6 ± 0.3	Good print (thin). Films sticky upon drying due to excess PEG.
HPMC 4% + PEG 5%	20.0–19.0	25G	6	37.8 ± 0.2	Perfect print (smooth, uniform lines). Stable films post-drying.

Figure 6.2**.** Effect of PEG concentration on the morphology of 3D-printed films before and after drying. (A) Film printed with 4% HPMC and 10% PEG before drying; (B) film printed with 4% HPMC and 10% PEG after drying; (C) film printed with 4% HPMC and 5% PEG before drying; (D) film printed with 4% HPMC and 5% PEG after drying.

All optimised printing parameters, including extrusion pressure, speed, temperature, and nozzle specifications, are summarised in Table 6.4.

Table 6.4 Printing parameters of different ink compositions, including temperature range, nozzle size, printing speed, and applied pressure during material extrusion 3D printing (n = 3; mean ± SD).

Ink Composition	Temperature (°C)	Nozzle	Speed (mm/s)	Pressure (PSI)
C3C	21.5–22.5	25G	6	10.1 ± 0.1
C4C	21.4–22.9	25G	6	11.6 ± 0.7
C3TC	21.3–22.8	25G	6	8 ± 0.6

C4TC	21.9–23.8	25G	6	9.9 ± 0.9
H3C	21.5–23.6	25G	6	31.4 ± 0.5
H4C	20.4–21.3	25G	6	39.7 ± 0.7
H3TC	21.4–21.7	25G	6	33.1 ± 0.8
H4TC	21.9	25G	6	40 ± 0.2

All inks were printed at ambient conditions (around 20–24 °C), with only minor variation across formulations. The narrow range indicates that temperature was well controlled and unlikely to have significantly influenced printability differences. A constant nozzle size (25G) and print speed (6 mm/s) were used for all formulations, meaning that differences in extrusion pressure directly reflect formulation-dependent viscosity and flowability. Increasing polymer concentration from 3% to 4% led to a marked rise in extrusion pressure, consistent with viscosity data. Carbopol inks (C3C, C4C, CT3, CT4) required low extrusion pressures of 8–11.6 PSI, while HPMC-based required substantially higher extrusion pressures of 31–40 PSI. This discrepancy can be attributed to their rheological behaviour, as Carbopol dispersions display strong shear-thinning, where the swollen microgel network collapses under shear and flows readily once the yield stress is overcome (Barreiro Carpio et al., 2023). However, upon drying, bioinks containing 3% or 4% w/v Carbopol with the dual drug combination (CBD and THC) exhibited structural instability, characterised by deformation, shrinkage, and loss of shape fidelity, while the CBD-only counterparts showed poor structural integrity due to low printability. Barreiro Carpio et al. (2023) have highlighted in their research that Carbopol inks, while easier to extrude due to strong shear-thinning behaviour, often exhibited poor dimensional stability post-printing due to insufficient structural recovery of the gel network.

As shown in Figure 6.3, Carbopol-based buccal films (C3C and C4C) failed to retain their shape, whereas HPMC-based films (H3C, H4C, H3TC, and H4TC) maintained their shape and consistency after drying. HPMC polymer has the ability to form a continuous and entangled chain network, which can resists alignment within the nozzle, resulting in higher flow resistance and greater extrusion pressures despite lower bulk viscosity values (Vlad et al., 2025). Resisting excessive chain alignment under shear reduces entanglement and compromises structural recovery after extrusion. Notably, the higher extrusion resistance of HPMC was accompanied by superior filament formation and print fidelity, with structures retaining their shape more effectively after deposition.

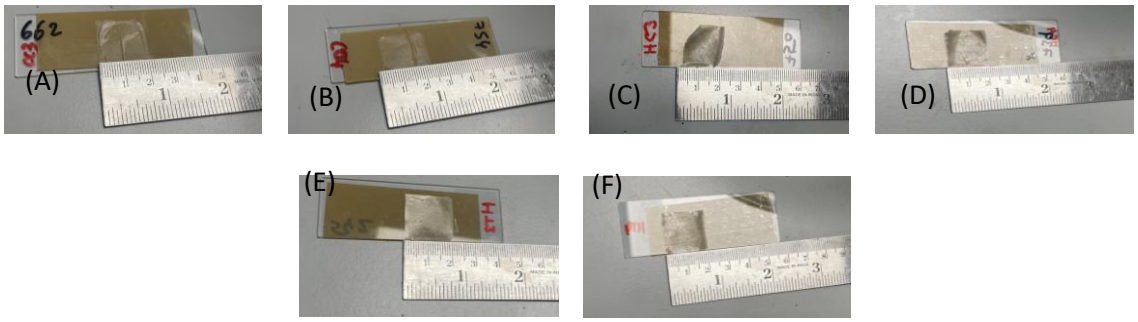

Figure 6.3. 3D-printed buccal cannabinoid films; (A) C3C, (B) C4C, (C) H3C, (D) H4C, (E) H3TC, and (F) H4TC.

6.4.3 pH, drug content, and weight of the buccal films

Drug content, dried film weight of the 3D printed films was determined, along with the pH of the bioinks. These are shown in Table 6.5. The pH of the bioinks ranged from 5.99 to 6.80, falling within or close to the physiological salivary pH range (6.2–7.4) (Aframian et al., 2006; He & Mu, 2023; Li & Castillo, 2020), upon adjusting using triethanolamine (TEA) as a neutralizing agent. Drug loading per 200 µL bioink was consistent across formulations. CBD-only systems showed approx. 4 mg CBD content, while dual cannabinoid systems (H3TC, H4TC) exhibited approx. 2 mg CBD and 2 mg THC each. The dried film weights ranged between 16.9 and 27.4 mg depending on polymer type and concentration. Carbopol-based films (C3C, C4C) had higher weights (26–27 mg) compared to HPMC-based films (17–23 mg). This difference can be attributed to Carbopol's higher water-binding capacity due to the presence of carboxylic groups, which absorbs high volume of water (George et al., 2025). This could have allowed Carbopol based films to retain more residual moisture even after drying, increasing the final weight. An increase in polymer concentration was associated with higher film weight, contributing to the development of more compact and densely printed structures. Similar findings have been reported by Panraksa et al. (2021), who also observed that higher polymer content results in greater solid mass of printed films.

Together, these findings show that both Carbopol and HPMC systems successfully produced films with physiologically acceptable pH, and consistent drug content, for buccal administration.

Table 6.5 pH, drug content, and weight of dried 3D-printed buccal cannabinoid films (n = 3; mean ± SD).

Ink Composition	pH	Drug Content (per 200 µL)	Weight of Dried Films (mg)
C3C	6.57 ± 0.36	4.06 ± 1.88 mg CBD	26.2 ± 0.3
C4C	6.34 ± 0.18	4.01 ± 1.05 mg CBD	27.4 ± 0.5
H3C	6.80 ± 0.01	4.05 ± 0.67 mg CBD	16.9 ± 0.8
H4C	6.40 ± 0.04	4.01 ± 0.029 mg CBD	22.8 ± 0.1
H3TC	6.10 ± 0.28	2.01 ± 0.82 mg CBD, 2.07 ± 0.32 mg THC	20.9 ± 0.9

H4TC	5.99 ± 0.07	2.03 ± 0.64 mg CBD, 2.00 ± 0.11 mg THC	26.5 ± 0.2

6.4.4 Mechanical properties of 3D printed films

Mechanical properties (hardness, springiness, and cohesion) of the 3D printed buccal films are represented in Table 6.6. HPMC films exhibited significantly higher hardness values (6.59–7.38 N) compared to Carbopol films (2.48–4.04 N). The greater hardness of HPMC matrices reflects their stronger polymer chain entanglement and denser film structure after drying, which improves mechanical robustness and handling, while Carbopol films (C3C and C4C) had reduced hardness. The improved structural integrity of HPMC-based films can be attributed to their inherent capacity to form dense, cohesive matrices during drying, driven by extensive polymer chain entanglement and tighter structural packing (Guo et al., 2022). In a study by Peh and Wong (1999), incorporation of Carbopol 934P into cellulose-based buccal films was found to reduce their mechanical strength, resulting in the formation of softer, more flexible films. Previous studies have shown that HPMC enhances the mechanical properties of films, with strength increasing in proportion to polymer concentration (Asatiani et al., 2023; Guo et al., 2022). A similar trend was observed in this study, where raising the HPMC concentration from 3% to 4% led to a general increase in hardness, indicating improved resistance to deformation.

Cohesion values reflect the internal bonding strength of the film matrix and its ability to resist structural breakdown under deformation. Cohesion values ranged from 0.824 to 0.999, with HPMC films displaying higher cohesiveness (0.88–1.00) than Carbopol films (0.82–0.90). This suggests that HPMC provides stronger internal bonding within the film matrix, allowing it to resist fracture during handling and buccal adhesion, consistent with previous studies highlighting the role of HPMC in enhancing film cohesiveness (Vlad et al., 2025). THC-containing formulations (H3TC, H4TC) also demonstrated improved cohesion, likely due to stabilizing interactions of dual cannabinoid–cyclodextrin complexes within the polymer network.

Springiness followed a clear trend with HPMC films were more elastic (99–100%) compared to Carbopol films (78–82%). Consistent with previous reports, HPMC was generally associated with the formation of more flexible films (Vlad et al., 2025). Carbopol, being a highly crosslinked poly (acrylic acid) (Shelke, 2016), might form a more brittle and rigid structure, limiting its elastic recovery. Overall, HPMC films outperformed Carbopol films in terms of mechanical strength, cohesion, and elasticity, making them more suitable for maintaining integrity during buccal placement and handling.

Table 6.6 Texture profile analysis of 3D-printed buccal cannabinoid films showing hardness, cohesion, and springiness (n = 3; mean ± SD). Values in each column bearing different superscript letters are significantly different ($p < 0.05$), whereas those sharing a common letter are not significantly different (one-way ANOVA with Tukey's post hoc test).

Formulation	Hardness (N)	Cohesion	Springiness (%)

H3C	6.92 ± 0.02 [ab]	0.982 ± 0.031 [a]	100.000 ± 0.11 [ab]
H4C	7.18 ± 0.011 [ac]	0.883 ± 0.029 [a]	99.418 ± 1.42 [a]
H3TC	6.59 ± 0.022 [ac]	0.973 ± 0.082 [ab]	99.976 ± 0.98 [b]
H4TC	7.38 ± 0.046 [bd]	0.999 ± 0.027 [bc]	99.284 ± 0.76 [c]
C3C	2.48 ± 0.018 [cde]	0.824 ± 0.062 [bc]	81.527 ± 0.18 [c]
C4C	4.04 ± 0.083 [e]	0.901 ± 0.04 [c]	78.671 ± 0.88 [d]

6.4.5 Mucoadhesive strength of the films

The ex vivo mucoadhesion of 3D-printed films, as depicted in Figure 6.4, reveals significant differences in maximum detachment force (N) across formulations. Carbopol based films (C3C and C3C) displayed higher mucoadhesiveness than HPMC based films (H3C, H4C, H3TC and H4TC). The superior mucoadhesive strength of Carbopol-based films (C3C and C4C) compared to HPMC-based films (H3C, H4C, H3TC, H4TC) can be attributed to the chemical and structural properties of Carbopol, a highly crosslinked poly (acrylic acid) polymer. The abundance of carboxyl groups in Carbopol facilitates strong hydrogen bonding and electrostatic interactions with mucin glycoproteins in the mucosal layer, enhancing adhesion despite the films' weaker mechanical properties, such as brittleness and reduced elasticity. In contrast, HPMC relies primarily on physical entanglement and hydrogen bonding, leading to relatively lower mucoadhesion (Dhawale et al., 2018; Smart, 2005).

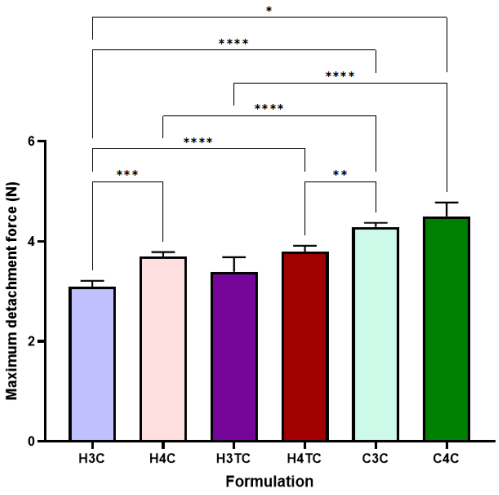

Figure 6.4 Mucoadhesive strength of 3D printed buccal films of cannabinoids (n = 3; mean ± SD). Statistically significant differences are denoted as *p < 0.05, **p < 0.01, ***p < 0.001 and ****p < 0.0001.

6.4.6 Swelling ratio and dissolution time

The swelling ratio (SR, %) of 3D-printed films is illustrated in Figure 6.5. HPMC-based films exhibited moderate swelling, with CBD-only formulations (H3C and H4C) and dual-cannabinoid films (H3TC and H4TC) showing slightly higher, though non-significant, values. An increase in polymer concentration in hydroxypropyl methylcellulose (HPMC)-based films led to a higher swelling ratio, with films containing 4% (w/v) HPMC exhibiting greater swelling than those with 3% (w/v). This might be due to the hydrophilic nature of HPMC, which contains numerous hydroxyl groups (-OH) that facilitate greater water absorption and matrix expansion. As the HPMC concentration rises more hydrophilic sites could have become available for hydrogen bonding with water molecules, enhancing the film's capacity to uptake fluids and swell (Bashir et al., 2020; Vlad et al., 2025). In contrast, Carbopol-based films (C3C and C4C) demonstrated significantly greater swelling, which can be attributed to Carbopol's high water-binding capacity due to its abundant carboxylic groups, allowing it to absorb a substantial volume of water (George et al., 2025).

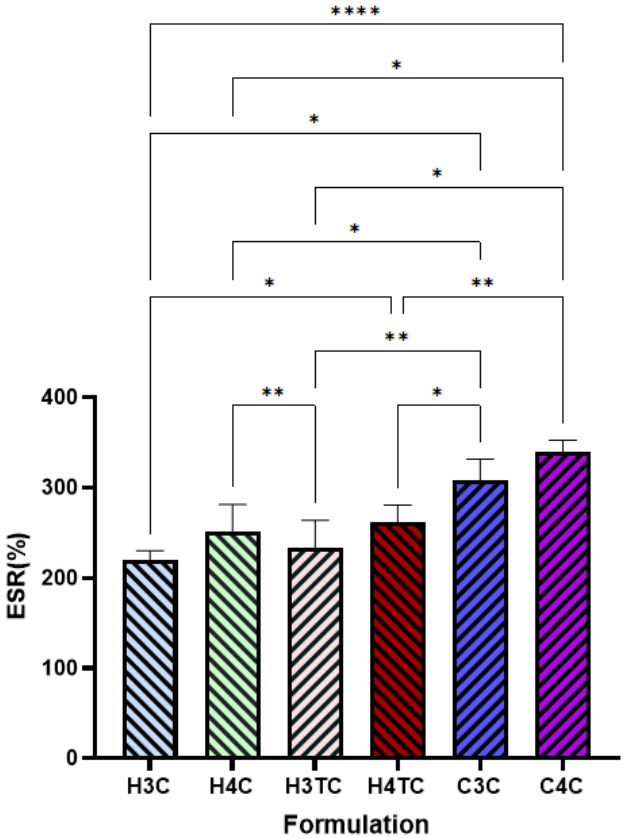

Figure 6.5 Equilibrium swelling ratio (ESR) % of 3D printed buccal films of cannabinoids (n = 3; mean ± SD). Statistically significant differences are denoted as *p < 0.05, **p < 0.01, ***p < 0.001 and ****p < 0.0001.

Buccal films incorporated with cannabinoids were also observed for their dissolution time in artificial saliva (Figure 6.6). HPMC-based films exhibited prolonged dissolution times, with H3C and H4C (CBD-only) formulations dissolving quicker than their dual-cannabinoid counterparts, H3TC and H4TC. The prolonged dissolution times observed in dual-cannabinoid HPMC-based films, despite their higher swelling ratios, can

be attributed to enhanced polymer–drug interactions and the role of cyclodextrins. In these dual formulations, both CBD and THC are individually complexed with cyclodextrins, resulting in a higher overall content of these anionic surfactants within the film. Cyclodextrins can form hydrogen bonds with the polymer matrix, strengthening the gel-like network during swelling. This more cohesive network impedes dissolution of the films. Previous research by Bagde and Rohera (2024) have reported that anionic surfactants can prolong the dissolution of gels prepared from hydrophilic polymers. In contrast, Carbopol-based films (C3C and C4C) displayed shorter dissolution times. This could be attributed to the high swelling capacity of Carbopol, as noted earlier, which could have accelerated water uptake and structural breakdown. Furthermore, their weaker mechanical properties could have influenced the dissolution of films by reducing their structural integrity and resistance to degradation in aqueous environments.

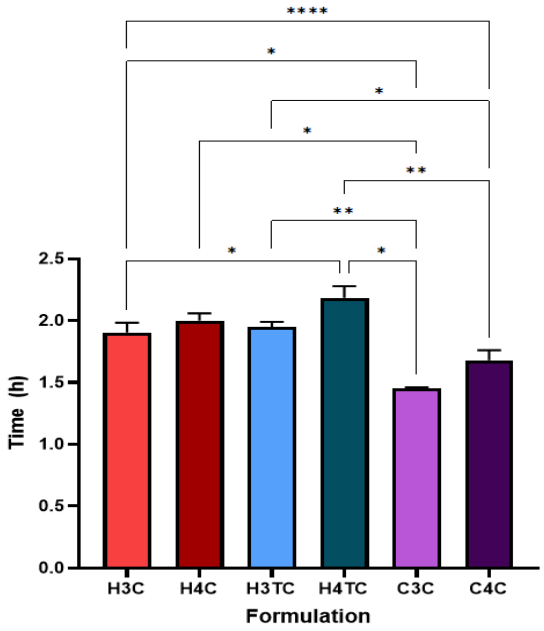

Figure 6.6 Dissolution time evaluation of cannabinoid loaded buccal films (n = 3; mean ± SD). Statistically significant differences are denoted as *p < 0.05, **p < 0.01, ***p < 0.001 and ****p < 0.0001.

6.4.7 In-vitro release of cannabinoids and release kinetics.

The in vitro release profiles of 3D-printed films are depicted in Figure 6.7. HPMC-based formulations (H3C, H4C, H3TC, H4TC) demonstrated a slower and more prolonged release of cannabinoids compared to Carbopol-based films (C3C, C4C). This difference can be attributed to the ability of HPMC to form a stable, cohesive gel network upon hydration (Vlad et al., 2025). Krese et al. (2016) demonstrated the influence of HPMC viscosity grade on controlled drug release by evaluating matrices prepared with different grades. Their findings confirmed that viscosity is a key factor in modulating release behaviour, with higher viscosity grades producing a more controlled and sustained release profile. In this study, the use of a high-viscosity grade HPMC (2,600–5,600 cP) likely contributed to the sustained release of cannabinoids. This is further supported by its superior structural integrity, as reflected in higher hardness and cohesiveness values. Additionally, the

lower swelling ratio observed in HPMC films relative to Carbopol suggests the formation of a denser hydrated matrix, which limited water penetration and slowed the outward diffusion of cannabinoids.

Increasing HPMC concentration from 3% to 4% (H4C, H4TC) further reinforced the gelling network, producing denser matrices and slower release rates. Comparable trends have been reported across different dosage forms, where higher HPMC concentrations consistently resulted in slower drug release (Khan et al., 2022; Mohamed et al., 2013). Moreover, drug composition significantly influenced release behaviour. Dual-cannabinoid films (H3TC, H4TC) exhibited slower cannabinoid release compared to the CBD-only films (H3C, H4C). This effect may be attributed to the presence of THC, as previous research have indicates that, even within inclusion complexes, THC tends to exhibit a slower release profile than CBD (Adriana Ribeiro et al., 2024). In the present study, film dissolution and cannabinoid release followed parallel trends, reflecting the fact that cannabinoids were dispersed within the polymer matrix rather than existing as separate crystalline phases.

The individual release profiles of CBD and THC from dual-cannabinoid HPMC films (H3TC and H4TC), highlighted in Figure 6.7 B and C, showed comparable patterns, with CBD exhibiting a slightly higher release than THC.

Overall, Carbopol films exhibited faster release, approx. 100% in 60 minutes, owing to extensive swelling and weaker matrix stability, whereas HPMC films provided a more sustained cannabinoid diffusion.

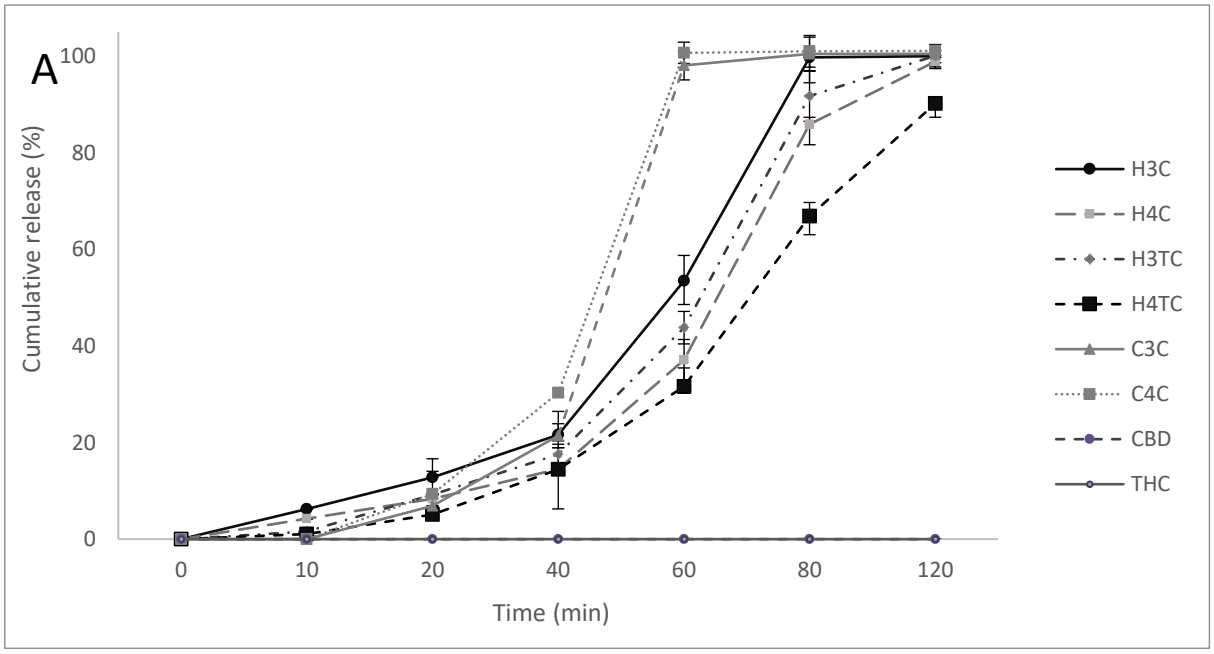

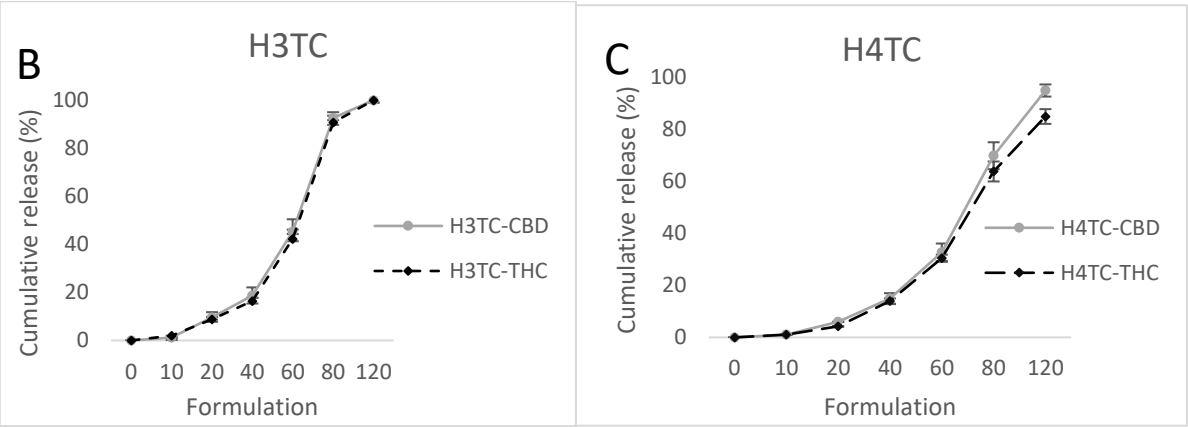

Figure 6.7. In vitro release profiles of (A) cannabinoid-loaded 3D printed films compared with pure CBD and THC distillates, (B) Individual release profiles of CBD and THC from film H3TC, (C) Individual release profiles of CBD and THC from film H4TC (n = 3; mean ± SD).

The release kinetics of cannabinoids from HPMC- and Carbopol-based buccal films were analysed using multiple kinetic models, and the corresponding correlation coefficients (R^2) are summarized in Table 6.7. For HPMC based formulations (H4C, H4C, H3TC, AND H4TC), Korsmeyer–Peppas analysis showed the highest correlation (R^2 = 0.952–0.992), suggesting that drug release occurs via a non-Fickian mechanism, driven by both diffusion through the hydrated HPMC matrix and polymer chain relaxation/swelling. This dual mechanism is well documented in the literature, as HPMC undergoes swelling upon contact with aqueous media to form a viscous gel layer that modulates diffusion (Siepmann & Peppas, 2001). Previous studies on HPMC-based films have similarly demonstrated that their drug release follows the Korsmeyer–Peppas model (Colucci & Rodrigues, 2022; Kondaveeti et al., 2017; Winarti et al., 2021). Furthermore, zero-order modelling yielded high correlation coefficients (R^2 = 0.888–0.962), indicating that drug release from HPMC films follows a near-constant release profiles. The Hixson–Crowell model also provided good fits (R^2 = 0.886–0.940), particularly for THC-containing films, indicating that matrix erosion contributes alongside diffusion (Askarizadeh et al., 2023).

Unlike HPMC-based films, Carbopol formulations showed weaker zero-order fits (R^2 ≈ 0.77) and lower Korsmeyer–Peppas R^2 values (around 0.64). Instead, they aligned strongly with the Hixson–Crowell model (R^2 = 0.926–0.928), suggesting that matrix erosion was the dominant mechanism of release (Askarizadeh et al., 2023). The burst-type release seen experimentally is therefore consistent with an erosion-driven mechanism.

Table 6.7 Kinetic modelling of cannabinoid release from 3D printed buccal films.

Formulations	Zero- order	First order	Higuchi	Korsmeyer-Peppas	Hixon-Crowell
			R^2		
H3C CBD	0.8879	0.8618	0.3605	0.9581	0.8899
H4C CBD	0.9154	0.9037	0.2274	0.9517	0.9288

H3TC CBD	0.9245	0.7675	0.0718	0.9575	0.8862
H3TC THC	0.9160	0.8317	0.1287	0.9736	0.9065
H4TC CBD	0.9614	0.8335	0.0509	0.9857	0.9402
H4TC THC	0.9623	0.8411	0.0266	0.9917	0.9382
C3C CBD	0.7717	0.3670	-1.3985	0.6478	0.9284
C4C CBD	0.7728	0.3557	-1.5885	0.6360	0.9257

6.4.8 FTIR of 3D printed cannabinoid films

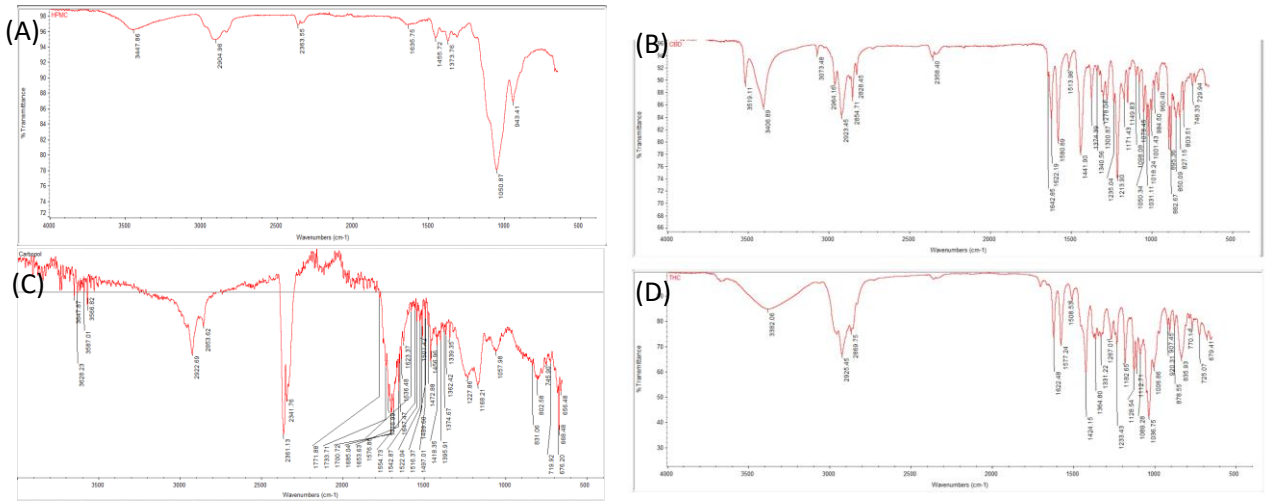

Figure 6.8 FTIR spectra of (A) HPMC, (B) CBD, (C) Carbopol, and (D) THC.

The FTIR spectra of the polymers (HPMC and Carbopol) and cannabinoids (CBD and THC) are depicted in Figure 6.8. The FTIR spectra of the 3D-printed buccal films, as shown in Figure 6.10, reveal characteristic absorption bands across the formulations in transmittance mode from 4000 to 600 cm^{-1}.

HPMC films (Figure 6.9 B and C) exhibited broad O–H stretching vibrations at 3417–3446 cm^{-1}, indicative of extensive hydrogen bonding from hydroxyl groups in the polymer (Gómez-Ordóñez & Rupérez, 2011; Prasad et al., 2016; Verma et al., 2011). Characteristic absorption bands were observed at 2870–2935 cm^{-1} (aliphatic C–H stretching, functional group region), and within the fingerprint region at 1369–1370 cm^{-1} (C–H bending) and 1050–1100 cm^{-1} (C–O stretching) (Takeuchi et al., 2025). The absence of significant shifts in C–O and other cellulose-related bands indicate homogeneous integration of the cannabinoid–cyclodextrin inclusion complexes without altering the polymer backbone.

Prominent bands around 2850 and 2950 cm^{-1} correspond to C–H stretching vibrations of the CBD–HP-β-CD and THC–HP-β-CD inclusion complexes. The absorption around 1031 cm^{-1} is assigned to C–O and C–O–C stretching vibrations within the cyclodextrin framework. In dual cannabinoid films, peaks for conjugated

carbonyl groups were observed around 1647 cm^{-1}, which may reflect contributions from both CBD and THC inclusion complexes (H. Li et al., 2021; Patil & Pandey, 2024; Upadhye et al., 2010).

Carbopol films (Figure 6.9 A) displayed broad O–H stretches around 3468–3473 cm^{-1} and C–H stretches at 2936–2938 cm^{-1}. A prominent carbonyl (C=O) band around 1716–1717 cm^{-1} confirmed the polyacrylic acid backbone, essential for maintaining acidic functionality that facilitates mucoadhesion via electrostatic interactions with mucosal surfaces. Additional bands at 1450–1457 cm^{-1} (C–H bending), 1240–1248 cm^{-1} (C–O–C and C–O stretching of ether linkages), and fingerprint region peaks at 1178 cm^{-1} (C–O–C asymmetric stretching) and 1078 cm^{-1} (C–O stretching) were consistent with polymer-specific vibrational modes (Chalal et al., 2014; Mahmood et al., 2023). The spectra revealed no significant shifts or disappearance of characteristic bands, indicating compatibility between Carbopol and cannabinoid complexes, with preservation of structural integrity during 3D printing and drying. No unexpected peaks or disappearances were observed, demonstrating excellent compatibility between cannabinoids in inclusion complexes and polymers.

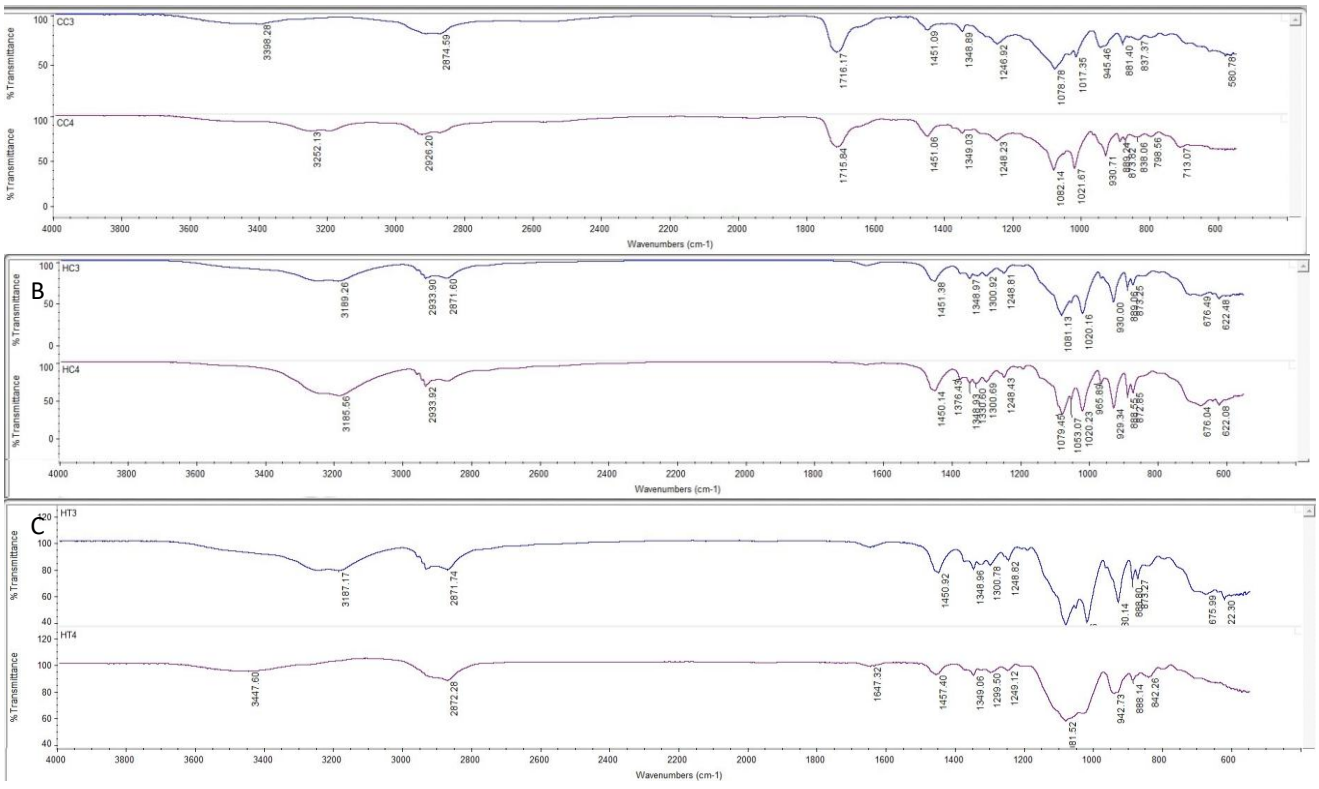

Figure 6.9 FTIR spectra of 3D printed buccal films; (A) C3C and C4C, (B) H3C and H4C, and (C) H3TC and H4TC.

6.4.9 SEM of 3D printed cannabinoid films

Scanning electron microscopy (SEM) images in Figure 6.10 illustrate the surface morphologies of the 3D-printed buccal films. Carbopol-based films (C3C, C4C) display rough, wavy surfaces with visible irregularities, indicative of a heterogeneous structure. The rough and wavy surface morphology observed in Carbopol-based films (C3C and C4C) can be attributed to the highly crosslinked poly(acrylic acid) structure of Carbopol, which

promotes uneven shrinkage and pore formation during drying, resulting in a brittle and heterogeneous matrix (Shelke, 2016).

In contrast, HPMC-based films (H3C, H4C, H3TC, and H4TC) exhibit smoother, more uniform surfaces. The smoother surfaces of HPMC based films might be due to the flexible, linear cellulose backbone of the polymer, which facilitates denser packing and homogeneous film formation through extensive hydrogen bonding (Guo et al., 2022). SEM observations from prior studies indicate that HPMC films maintain a uniform and smooth surface structure (Carvalho et al., 2023; Hay et al., 2018).

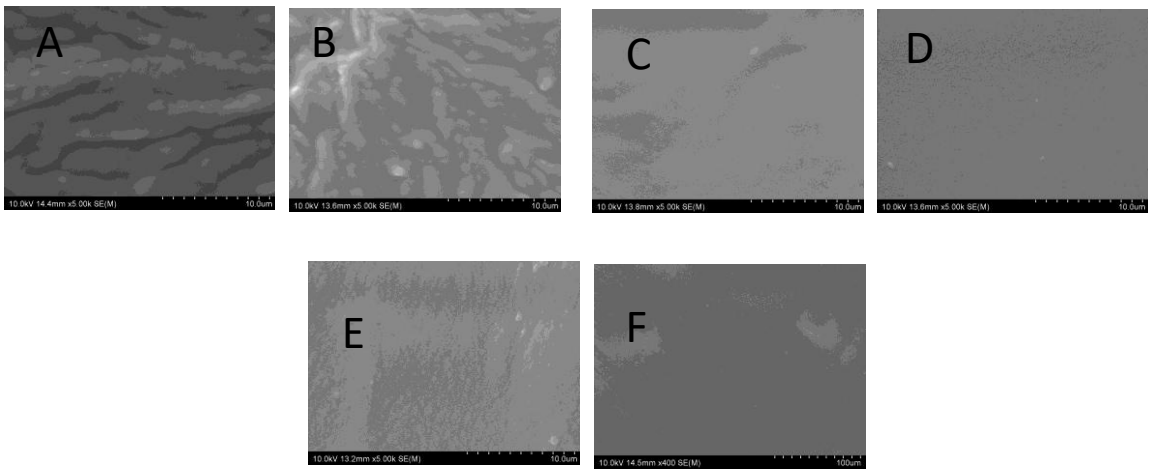

Figure 6.10 SEM captured at a magnification of ×5,000 with a scale bar representing 10 µm of 3D printed buccal films (A) C3C, (B) C4C, (C) H3C, (D) H4C, (E) H3TC, AND (F) H4TC.

6.4.10 Ex-vivo penetration of cannabinoids from printed films

The ex vivo penetration profiles demonstrated that all 3D-printed films markedly enhanced cannabinoid transport across the buccal mucosa compared with pure CBD and THC. As shown in Figure 6.11 A, both HPMC- and Carbopol-based films (H3C, H4C, H3TC, H4TC, C3C, C4C) achieved significantly higher penetration concentrations (around 3.0–3.3 mg/cm²) than pure cannabinoids (<0.5 mg/cm²). Statistical grouping confirmed that all polymeric formulations belonged to the same significance group (A), while unformulated cannabinoids were significantly lower (B). This highlights the critical role of polymeric carriers in improving cannabinoid solubility and permeability. Since the films dissolved within approximately 2 hours as observed from their dissolution time, the residence and release periods were comparable across formulations, which explains why cannabinoid penetration into the buccal mucosa was similar for both HPMC- and Carbopol-based films.

The enhanced permeation observed with the 3D-printed films can be explained by several complementary mechanisms. Firstly, the incorporation of a terpene combination likely played a major role, as terpenes have been widely reported to act as natural permeation enhancers by interacting with the lipid domains of the buccal mucosa and thereby improving cannabinoid penetration. This is consistent with previous findings (as identified in Chapter 3) and with earlier reports that terpenes such as limonene and menthol enhance the

buccal absorption of lipophilic drugs, including cannabinoids (Longgos et al., 2024; Prasanthi & Lakshmi, 2012). Furthermore, the mucoadhesive nature of HPMC and Carbopol prolonged the residence time of the films at the buccal surface, increasing mucosa contact period of the drug. This agrees with prior work showing that bioadhesive polymers enhance transmucosal delivery by preventing premature clearance and improving drug retention at the site of absorption (Asane et al., 2008; Chatterjee et al., 2017). Together, these factors explain the significantly greater cannabinoid transport achieved with the 3D-printed films compared to unformulated CBD and THC.

Figure 6.11 B, further compared CBD and THC permeation from dual-cannabinoid HPMC films (H3TC, H4TC). Both cannabinoids achieved comparable permeation (around 1.5–1.6 mg/cm²), significantly higher than their pure cannabinoid counterparts. No significant differences were observed between CBD and THC permeation within the same formulation.

Overall, these results demonstrate that 3D-printed buccal films dissolve within a clinically relevant timeframe and provide consistent, enhanced transmucosal delivery of cannabinoids compared with unformulated drugs.

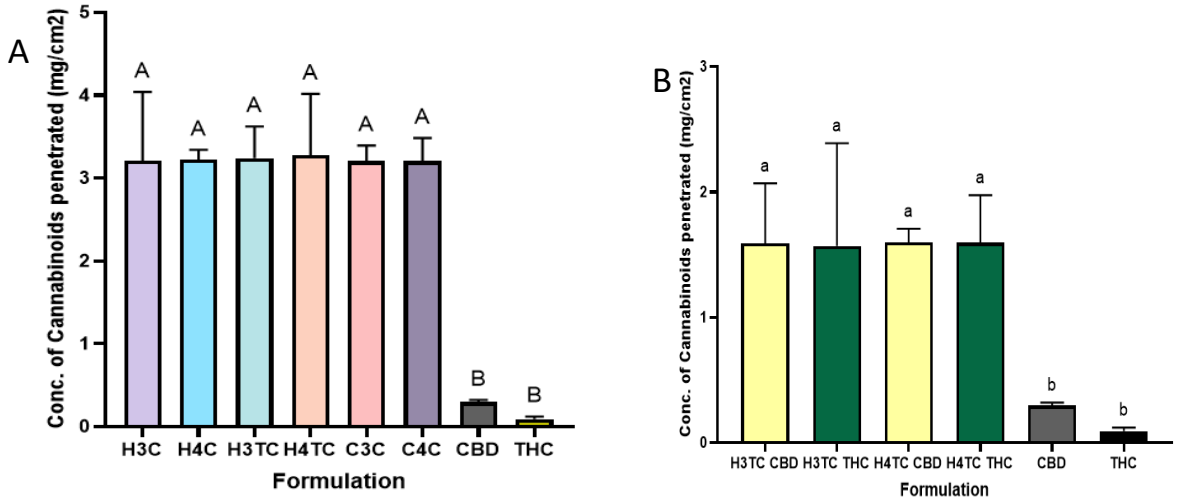

Figure 6.11 Ex-vivo penetration profiles of (A) Total cannabinoids from 3d printed films, (B) Individual permeation profiles of CBD and THC compared to pure CBD and THC distillate (n = 3; mean ± SD). Letters (A, B) above the bars indicate statistically significant differences between formulation and pure cannabinoids ($p < 0.05$); bars sharing the same letter indicate no significant difference.

6.5 Conclusions

This study successfully developed and characterised 3D-printed buccal films using HPMC and Carbopol polymers for cannabinoid delivery, demonstrating their potential as effective transmucosal drug delivery systems. Rheological assessment showed that polymer concentration and drug composition significantly influenced bioink viscosity, with Carbopol exhibiting higher viscosity but easier extrusion due to shear-thinning, whereas HPMC required higher extrusion pressures yet produced superior filament formation and print fidelity. All formulations maintained physiologically compatible pH and consistent cannabinoid content.

Mechanical testing revealed that HPMC-based films possessed greater hardness, cohesion, and elasticity, whereas Carbopol films, although softer and more brittle, displayed higher mucoadhesive strength through

carboxyl group-mediated hydrogen bonding with mucin. Swelling and dissolution studies indicated that Carbopol films absorbed more water and dissolved rapidly, whereas HPMC films, particularly dual-cannabinoid formulations, exhibited moderated swelling and prolonged dissolution due to cohesive polymer–drug–cyclodextrin networks.

In vitro release studies confirmed that HPMC films provided sustained cannabinoid release, with dual-cannabinoid systems releasing more slowly than CBD-only films. Carbopol films showed rapid release consistent with their higher swelling and weaker matrix stability. Kinetic analysis revealed that HPMC films followed a non-Fickian release mechanism, reflecting combined diffusion and polymer relaxation/swelling, whereas Carbopol films aligned with the Hixson–Crowell model, indicating matrix erosion-driven, burst-type release.

FTIR analysis confirmed compatibility between cannabinoids in inclusion complexes and both polymers, with no significant shifts or disappearance of characteristic bands, while SEM imaging revealed smooth, uniform surfaces in HPMC films and rough, heterogeneous surfaces in Carbopol films, reflecting differences in polymer chain flexibility and crosslinking. Ex vivo penetration studies further demonstrated that all 3D-printed films markedly enhanced cannabinoid transport across the buccal mucosa compared with unformulated CBD and THC.

Overall, HPMC-based films offered superior mechanical strength, structural integrity, controlled swelling, and sustained release, making them ideal for effective buccal delivery, whereas Carbopol films provided enhanced mucoadhesion but were limited by rapid dissolution and weaker mechanical properties. These findings highlight the critical role of polymer type, concentration, and drug composition in tailoring the physicochemical, mechanical, mucoadhesive, and release properties of 3D-printed cannabinoid buccal films, establishing a solid basis for the development of optimized transmucosal drug delivery systems.

Chapter 7: General discussion

7.1 Thesis overview

Cannabinoids such as CBD and THC represent a rapidly expanding area of therapeutic interest, with an increasing body of evidence highlighting their diverse pharmacological benefits. These naturally occurring phytochemicals have been investigated and, in some cases, approved for the management of several conditions, including chemotherapy-induced nausea and vomiting, spasticity associated with multiple sclerosis, anorexia and cachexia in patients with AIDS, chronic and neuropathic pain, and treatment-resistant epileptic disorders. Beyond these established uses, ongoing research continues to uncover their potential roles in neuroprotection, inflammation modulation, anxiety reduction, and metabolic regulation, thereby broadening their clinical relevance.

Despite the growing therapeutic interest in cannabinoids, only a few formulations have gained regulatory approval. Current marketed products face significant limitations, most notably poor oral bioavailability due to lipophilicity, extensive first-pass metabolism, and variable gastrointestinal absorption. Some rely on synthetic cannabinoids, which can produce undesirable side effects and reduce patient acceptance. Oromucosal sprays such as Sativex are further limited by partial swallowing of the dose, lowering mucosal absorption, and leading to variable efficacy. These shortcomings contribute to inefficient delivery, unpredictable outcomes, and frequent dosing requirements. Furthermore, cost and regulatory restrictions on cannabis-derived medicines remain barriers to accessibility, especially in healthcare systems with limited reimbursement pathways. Together, they highlight the need for innovative, patient-friendly platforms that improve bioavailability while reducing adverse effects.

The overarching objective of this thesis was to design, develop, and evaluate innovative transmucosal delivery systems for cannabinoids, with a focus on the buccal route. However, effective buccal delivery requires dosage forms with suitable mucoadhesion, mechanical integrity, drug solubilization strategies, and controlled release profiles. This research aimed to overcome the limitations of existing cannabinoid formulations by developing two complementary classes of buccal delivery systems. In both platforms, cannabinoid–cyclodextrin inclusion complexes were incorporated to enhance solubility, while terpene-based permeation enhancers were included to promote efficient transmucosal transport. The first approach focused on in-situ gelling systems, comprising thermoresponsive gels based on Poloxamer 407 and ion-responsive gels formulated with gellan gum (GG), κ-carrageenan (κ-CG), or mixed GG/ι-carrageenan systems. These gels were designed to undergo a sol-to-gel transition under physiological conditions, and when combined with mucoadhesive polymers, they offered ease of administration, improved mucosal residence time, and sustained drug release.

The second approach focused on the development of 3D-printed buccal films, fabricated through extrusion-based bioprinting of bioinks containing mucoadhesive polymers. Among these, films formulated with hydroxypropyl methylcellulose (HPMC) demonstrated particularly favourable properties, including sustained drug release, sufficient mechanical strength, adequate mucoadhesion to support prolonged residence, and

structural integrity suitable for buccal delivery. Beyond these functional attributes, the 3D printing strategy offered the advantage of ensuring consistent film quality while enabling the integration of formulation components such as solubilizers and permeation enhancers.

By integrating insights from both in-situ gelling systems and 3D-printed films, this work established a broad experimental platform to examine how polymer selection and formulation strategy influence the performance of buccal cannabinoid delivery systems. This discussion draws together findings across both delivery systems, emphasizing their suitability for clinical application.

7.2 Interpretations of thesis findings

Buccal drug delivery has gained considerable attention as an alternative to conventional routes due to its distinct advantages, including non-invasiveness, ease of administration, avoidance of first-pass metabolism, and suitability for patients with swallowing difficulties such as those experiencing dysphagia. This route also enables rapid onset of action and the potential for sustained therapeutic effects when combined with appropriate formulation strategies. Chapter 2 of this thesis provided a comprehensive review of buccal delivery systems for cannabinoids, with a particular emphasis on identifying polymers and excipients suitable for achieving prolonged and controlled drug release. Mucoadhesive polymers emerged as the foundation for mucosal formulations, as they adhere to the mucosal surface, thereby prolonging residence time and improving drug absorption. Their ability to form strong interactions with the mucosa makes them particularly advantageous for developing buccal dosage forms that can maintain consistent contact with the absorption site. The review also examined existing oromucosal cannabinoid formulations, such as Sativex, as well as other experimental systems under investigation. While these formulations have demonstrated therapeutic effectiveness, their limitations highlight the need for more efficient delivery strategies. Importantly, the review underscored the critical role of excipients, particularly solubility and permeation enhancers, in overcoming the intrinsic challenges of cannabinoid delivery. Cannabinoids are highly lipophilic and exhibit low aqueous solubility and poor permeability, necessitating the inclusion of functional excipients that improve dissolution, enhance transmucosal transport, and ensure ingredient compatibility. Equally vital is the selection of excipients that do not induce mucosal irritation, thereby supporting patient comfort and safety while preserving formulation stability. This chapter highlights that, novel buccal systems designed for systemic cannabinoid delivery, such as in situ gelling formulations or three dimensional printed mucoadhesive films with both cyclodextrin complexes and terpene permeation enhancers, have not been previously reported.

The identification of cyclodextrins as effective solubilizers and terpenes as permeation enhancers provided a strong rational foundation for the development of buccal cannabinoid delivery systems. Building on this, Chapter 3 focused on optimizing the type and concentration of cyclodextrins and terpenes to achieve efficient and stable delivery of cannabinoids. Among the cyclodextrins evaluated, hydroxypropyl-beta-cyclodextrin (HP-β-CD) proved particularly effective in encapsulating both CBD and THC, forming stable inclusion

complexes that significantly improved aqueous solubility and dissolution rates. Terpenes, natural phytoconstituents known for their permeation enhancing properties, were screened to identify those capable of facilitating transmucosal transport without causing local irritation or toxicity. Limonene, menthol, pinene, and cineole were tested individually and in combination at varying concentrations. The final optimized formulation employed a 5% terpene blend, which was found to maximize permeation while maintaining mucosal safety, providing a base for subsequent incorporation into drug-loaded dosage forms. In parallel, the methodology for evaluating in vitro release and ex vivo penetration was systematically optimized. Receptor media were selected to maintain sink conditions, ensuring accurate and reproducible measurement of drug release and permeation across the buccal mucosa. These optimizations not only ensured reliable evaluations but also established a framework for future studies. Collectively, these findings laid the groundwork for designing cannabinoid-loaded buccal dosage forms that combine enhanced solubility, controlled release, and efficient mucosal absorption.

Chapter 4 focused on the development of thermoresponsive in situ gels using Poloxamer 407 in combination with mucoadhesive polymers, HPMC or Carbopol, incorporating cannabinoids complexed with HP-β-CD. The terpene blend was not included in these gels, as it resulted in solutions that were excessively viscous at room temperature. Design by quality approach using Design-Expert was used to optimize the formulations. The performance of the in-situ gels was influenced by the choice of mucoadhesive polymer. Formulations containing HPMC gelled more rapidly upon exposure to physiological conditions and demonstrated faster release of cannabinoids, as evidenced by in vitro dissolution and ex vivo penetration studies, which showed strong correlation. In contrast, Carbopol-based formulations exhibited higher mechanical strength, greater mucoadhesive capacity, and superior long-term stability, suggesting their suitability for sustained buccal delivery where prolonged residence time and structural integrity are critical. Furthermore, comparative evaluation of single versus dual cannabinoid systems revealed that CBD-only formulations outperformed dual cannabinoid gels in terms of release rate and penetration efficiency. This observation may be attributed to differences in molecular interactions, solubility, or competitive transport effects when both cannabinoids are present in the gel matrix.

In Chapter 5, ion-induced in situ gels for buccal cannabinoid delivery were developed using gellan gum, κ-carrageenan, and combinations of κ-carrageenan and ι-carrageenan, with the addition of mucoadhesive polymers such as HPMC or Carbopol. Terpenes were incorporated as permeation enhancers, and formulation optimization was guided by a design of experiments approach to identify ideal polymer and excipient concentrations. Similar to the findings in Chapter 4, the choice of mucoadhesive polymer had a significant impact on the physicochemical and mechanical properties of the gels, but the presence of divalent cations introduced an additional modulatory factor by inducing gelation through ionic crosslinking. However, Carbopol-containing formulations exhibited faster gelation compared to their HPMC counterparts, likely due to stronger ionic interactions between Carbopol and the cations. Carbopol-based formulations also

demonstrated slower cannabinoid release and reduced permeation, while displaying enhanced mucoadhesive strength and mechanical integrity. Among the formulations studied, mixed κ/ι-carrageenan formulations with Carbopol emerged as the most promising candidates for buccal cannabinoid delivery, surpassing other ion-induced in situ gels developed. These formulations achieved a balance of rapid gelation, high viscosity, strong mechanical stability, and robust mucoadhesion, which together facilitated extended mucosal residence and controlled drug release. In both thermosensitive and ion-activated in-situ gels, a lag time of approximately 30 minutes was consistently observed for all formulations in the in-vitro drug release profiles. This is expected to be minimal or absent in vivo, where continuous salivary flow, and intimate contact with the buccal mucosa has the potential to accelerate gel hydration, network relaxation, and drug diffusion, allowing faster onset of release.

Stability studies revealed that these in-situ gels experienced some cannabinoid degradation and developed a yellowish appearance after six months, indicating limitations in long-term storage. To overcome these challenges, the gels were subjected to freeze-drying, resulting in formulations that retained their structural integrity upon rehydration. The freeze-dried gels maintained high drug content, and reproducible sol-gel transition behaviour. These findings indicate that freeze-dried ion-responsive gels represent a viable strategy to enhance the shelf-life of buccal cannabinoid formulations while preserving their functional performance, offering a practical alternative to conventional in-situ gels for long-term storage and clinical application.

In Chapter 6, 3D-printed buccal films were developed as an alternative platform for cannabinoid delivery, using extrusion-based printing of bioinks composed of mucoadhesive polymers (HPMC or Carbopol), terpene mixture, and cannabinoid–HP-β-CD inclusion complexes. HPMC-based films provided greater hardness, cohesion, and elasticity, with moderated swelling and sustained release, whereas Carbopol films, despite stronger mucoadhesion, exhibited softer and more brittle matrices and rapid water uptake leading to faster release. HPMC-based 3D-printed buccal films emerged as an effective platform for transmucosal cannabinoid delivery. The study also highlights the advantages of 3D printing as a formulation strategy, providing reproducibility, customizability, and the capacity to integrate solubility and permeation enhancers in the dosage forms developed. Overall, both the in-situ gels and 3D-printed films offer effective strategies for delivering cannabinoids via the buccal route, serving as promising alternatives to traditional oral/oromucosal formulations.

7.3 Thesis implications

7.3.1 Comparison of marketed/approved cannabinoid formulations with developed buccal formulations.

The findings of this thesis hold significant implications when evaluated against the backdrop of currently marketed cannabinoid formulations. Approved products such as Sativex® (oromucosal spray), Epidiolex® (oral

solution), and synthetic cannabinoids including dronabinol and nabilone have demonstrated therapeutic utility across various conditions. However, their clinical performance remains constrained by fundamental formulation limitations. Oral oils, capsules, and solutions suffer from poor aqueous solubility, erratic gastrointestinal absorption, and extensive first-pass metabolism, resulting in low and highly variable bioavailability (variable 9–13% for CBD and THC) (K. R. Hossain et al., 2023). This necessitates the use of very high doses of CBD in epilepsy studies, which can lead to increased risk of hepatotoxicity, gastrointestinal disturbances, and drug–drug interactions (Huestis et al., 2019; Thiele et al., 2018). Furthermore, oral dosing typically produces delayed onset (30 minutes to 2 hours) and short duration of effect, requiring multiple daily administrations that compromise patient adherence (K. R. Hossain et al., 2023).

Oromucosal sprays such as Sativex® were designed to bypass first-pass metabolism, but they too face limitations. A large fraction of the sprayed dose is washed into the gastrointestinal tract by saliva, thereby reintroducing variability associated with oral absorption. In addition, excipients such as ethanol and propylene glycol contribute to local irritation and burning sensations, which limit long-term acceptability. Spray delivery also restricts control over the precision of dose delivered, with inter- and intra-patient variability remaining high, particularly when multiple sprays are required to achieve therapeutic plasma levels (Karschner et al., 2011; Scully, 2007). Synthetic cannabinoids such as dronabinol and nabilone, are similarly hindered by slow onset, poor predictability, psychoactive side effects, and limited patient tolerability (Badowski, 2017; Ben Amar, 2006). Collectively, these shortcomings highlight the inadequacy of classical dosage forms in fully exploiting the therapeutic potential of cannabinoids.

In contrast, the buccal in-situ gels and 3D-printed films developed in this thesis were specifically designed to address these barriers. The incorporation of cyclodextrin inclusion complexes, such as hydroxypropyl-β-cyclodextrin (HP-β-CD), has been widely demonstrated in cannabinoid delivery systems to enhance solubility, stabilize cannabinoids, and improve dissolution rates, thereby have the potential to facilitate more consistent systemic absorption (Park et al., 2023; Srakhao et al., 2025). Similarly, terpene-based permeation enhancers have been successfully employed in buccal and transdermal formulations to transiently modulate epithelial barriers, increasing drug permeability without inducing mucosal irritation (Amaral et al., 2020; Chen et al., 2016; Peera Tabboon et al., 2022; Varman & Singh, 2012). Unlike sprays and oral solutions, which are prone to rapid washout or degradation, these systems employed mucoadhesive polymers (HPMC, Carbopol) to ensure intimate and prolonged contact with the buccal mucosa (Chen et al., 2023; Qi et al., 2007; F. Zahir-Jouzdani et al., 2018), thereby minimizing loss through swallowing and enabling sustained release at the absorption site. The developed thermoresponsive and ion-responsive gel systems, and 3D printed films provided favourable mechanical strength, flexibility, and mucoadhesion, ensuring ease of application and retention, while avoiding the irritation and instability associated with liquid formulations. Table 7.1 gives a comparative discussion of the situ gels and 3D-printed films developed against current cannabinoid products on the market.

Thus, by addressing the solubility, stability, and absorption limitations of existing products, the developed buccal formulations demonstrate a feasible pathway toward improved patient outcomes in cannabinoid therapy.

Table 7.1 Comparison of marketed cannabinoid dosage forms and developed buccal formulations.

	Products in the market	**In-Situ Gels & 3D-Printed Films**
Absorption	Approved oromucosal formulations may bypass some first-pass metabolism, but mostly are still partially swallowed, leading to GI absorption and metabolism (Karschner et al., 2011).	Buccal/gels & films target mucosal contact, mucoadhesion and sustained residence time to enhance direct transmucosal absorption, reduce swallowing/wash-out losses, and mitigate first-pass metabolism.
Bioavailability / Variability	Many approved products show low bioavailability and large inter- and intra-subject variability (Lorenzl et al., 2022; Catherine J Lucas et al., 2018; Millar et al., 2018).	Presence of solubility enhancers, permeation enhancers, and mucoadhesive polymers are expected to reduce variability and improve consistent drug exposure. In-vivo studies are required to confirm this.
Release Profile / Duration of Action	Many standard oral or orormucosal (sprays) formulations reach peak levels quickly then decline; often require frequent dosing to maintain therapeutic levels (Millar et al., 2018).	In-situ gels and films are designed for sustained release. This could translate into fewer doses per day, more stable plasma levels.
Stability	Existing sprays/oils are more susceptible to degradation (light, oxidation), possible instability of liquid formulations (Sitovs et al., 2024).	Studies show good stability (especially in freeze-dried in-situ gels) with maintained performance after storage; films generally more stable than liquids; better protection of cannabinoids via inclusion complexes.

7.3.2 Evidence from clinical studies and emerging research

Cannabinoids have been investigated for a wide range of clinical conditions due to their modulatory effects on the endocannabinoid system. The strongest clinical evidence supports their use in treatment-resistant epilepsy, management of spasticity associated with multiple sclerosis (MS), chemotherapy-induced nausea and vomiting (CINV), and AIDS-related anorexia. They have also been explored for chronic and neuropathic pain, although outcomes have been inconsistent, often due to poor pharmacokinetics and variable systemic exposure. Additional areas of investigation include anxiety disorders, sleep disturbances, neurodegenerative diseases, and palliative care. CBD, in particular, has attracted attention in emerging indications such as social anxiety disorder, with a phase 2 trial reporting significant improvements in anxiety scores (Bhuller et al., 2024). Studies have also suggested potential benefits in sleep disorders, including obstructive sleep apnoea and REM sleep behaviour disorder (Low et al., 2023). Preclinical research in neurodegenerative diseases indicates that cannabinoids may have neuroprotective effects, enhancing neurobehavioral function and reducing neurological deficits (Voicu et al., 2023).

Despite these promising findings, the clinical application of cannabinoids is often hindered by limitations inherent in traditional dosage forms. For instance, Epidiolex® has demonstrated efficacy in treatment-resistant epilepsies, but high doses required for therapeutic effect are often associated with adverse events,

raising concerns about long-term tolerability (O'Connell et al., 2017). Similarly, clinical studies with Sativex have shown favourable outcomes in managing multiple sclerosis related spasticity, particularly in patients who achieved little or no relief with conventional antispastic therapies (Haupts et al., 2024). However, Urits et al. (2021) reported that trials involving Sativex experienced higher dropout rates compared with placebo, largely attributable to treatment-related adverse effects. In chronic pain, traditional cannabinoid formulations have been limited by variable efficacy, inconsistent plasma concentrations, and the need for high doses that increase the risk of side effects ((Sic et al., 2025). These limitations underscore the need for more efficient and reliable delivery platforms.

In response, recent research has focused on innovative oro-mucosal delivery systems designed to overcome the shortcomings of conventional sprays and oral formulations. Nanoparticle based sprays, such as NanaBis™ and self-assembling cannabinoid nanoemulsions, have shown enhanced bioavailability and faster systemic absorption compared with approved sprays like Sativex®, while targeting mucosal tissues for improved therapeutic effect. These systems show promise in enhancing therapeutic effects, including pain relief and management of chronic conditions, though mild adverse effects such as drowsiness and nausea have been reported (Clarke et al., 2020; Provenzano et al., 2024). Solid dosage forms, including cyclodextrin-complexed tablets, fast-disintegrating wafers, and cannabinoid lozenges, have aimed to improve solubility, dissolution rate, and stability, enabling immediate release within the oral cavity (Crowley et al., 2018; Mannila et al., 2007; Monton et al., 2024). Despite these advances, these systems are still limited by low residence times, variable mucosal absorption, and the risk of accidental swallowing, which can reduce systemic exposure and therapeutic predictability. Mucoadhesive strategies, employing polymers such as Carbopol, HPMC, and hydroxypropyl cellulose, have been investigated to prolong residence time and facilitate controlled release, often with additional penetration enhancers like propylene glycol to improve drug permeability (Itin et al., 2020; Söpper et al., 2021). Early studies, including bi-layered films and 3D-printed mucoadhesive constructs, indicate the potential for sustained cannabinoid delivery, personalized dosing, and improved patient compliance, (Abdella et al., 2023; Laoasoke et al., 2024).

Although these novel formulations show promise in in-vitro and ex-vivo studies, clinical trials are essential to establish their safety, efficacy, and optimal dosing regimens in human populations. Ongoing and future clinical studies will provide critical insights into the potential of these advanced cannabinoid delivery systems.

7.3.3 Clinical implications

The translation of the buccal delivery platforms developed in this thesis into clinical practice carries important implications. By bypassing first-pass metabolism and enhancing transmucosal absorption, these systems have the potential to achieve therapeutic plasma concentrations at substantially lower doses compared with conventional oral solutions or capsules. This improvement in pharmacokinetics could reduce the need for high dosing, which is often associated with adverse effects and inter-patient variability, a limitation observed

in many clinical trials of oral and spray formulations (Haupts et al., 2024; Sic et al., 2025; Urits et al., 2021). Enhanced efficacy is another key advantage of these buccal platforms. More predictable absorption and sustained release profiles can reduce variability in clinical outcomes, providing a more reliable therapeutic effect (Ben Amar, 2006; Thiele et al., 2018). Patient compliance may also be significantly improved. Mucoadhesive in-situ gels and films offer convenient and non-invasive administration. This ease of use is particularly important in chronic conditions requiring long-term therapy, where adherence can strongly influence treatment success.

Condition-specific advantages are apparent across several indications. In epilepsy, lower and more stable CBD exposure could enhance seizure control while minimizing adverse effects (Thiele et al., 2018). In multiple sclerosis and chronic pain, sustained buccal delivery may provide more consistent symptom relief with fewer daily doses than sprays like Sativex (Karschner et al., 2011). For CINV and appetite stimulation for cachexia or AIDS-related anorexia, rapid buccal absorption could deliver effects with reduced psychoactive side effects (Catherine J Lucas et al., 2018; Rogers & Pacanowski, 2023). By addressing limitations of bioavailability, dosing variability, and patient usability, these buccal systems represent a clinically meaningful advancement in systemic cannabinoid therapeutics, offering the potential for safer, more effective, and patient-friendly treatment options.

Furthermore, the buccal formulations developed in this thesis hold significant potential for local therapeutic applications within the oral cavity. Emerging evidence indicates that cannabinoids can exert analgesic, anti-inflammatory, and wound-healing effects in oral tissues. Formulations developed have the potential as promising adjunctive strategy in oral healthcare, addressing conditions such as gingivitis, periodontitis, mucositis, and aphthous ulcers (Hu et al., 2024).

7.3.4 Dosing considerations

A critical challenge in cannabinoid therapy is establishing doses that achieve clinical efficacy while minimizing adverse effects. The dosing of cannabinoids in clinical practice is largely informed by product-specific regulatory approvals. Epidiolex, is recommended at 10–20 mg/kg/day for patients with epileptic disorders, with a starting dose of 2.5 mg/kg twice daily (Wechsler et al., 2024). Oromucosal sprays such as Sativex® deliver 2.7 mg THC and 2.5 mg CBD per spray, with multiple sclerosis patients requiring 6-8 sprays per day for symptom relief with maximum of 12 sprays per day (MacCallum & Russo, 2018). Synthetic THC formulations like dronabinol are typically dosed at 2.5–10 mg up to 4–6 times daily for nausea and emesis associated with chemotherapy, and a maximum of 10 mg twice daily for AIDS induced anorexia (Walsh et al., 2005).

In New Zealand, medicinal cannabis products that meet the minimum quality standard may be prescribed by medical practitioners without ministerial approval, but unlike fully approved medicines, they do not have standardized or regulator-endorsed dosing regimens. Instead, prescribers are expected to apply clinical judgment, often beginning with low doses and titrating upwards according to patient response and

tolerability, consistent with international recommendations of starting with low doses and increasing doses slowly and as required. Available dosage forms in New Zealand include oral liquids, sublingual solutions, controlled-drug oral liquids, and dried cannabis flower for inhalation, each of which requires individualized dosing considerations (Ministry of Health, 2025).

The buccal in-situ gels and 3D-printed films developed in this thesis offer versatile and patient-tailored dosing strategies. In-situ gels have the potential to enable precise titration of cannabinoid doses to achieve desired therapeutic effects. The flexibility to adjust either the administered volume or drug concentration provides a platform for individualized therapy, an application that has been highlighted as a promising avenue for in-situ gels (Patil et al., 2024). Similarly, 3D-printed buccal films utilize additive manufacturing to produce dosage forms with exact and reproducible drug loading. This approach enables precise control over film thickness, surface area, and geometry, which can be tailored to meet patient-specific needs, such as body weight, severity of symptoms, or sensitivity to cannabinoids (Auel et al., 2025). Such customization is particularly relevant in clinical settings where standard dosing is challenging due to variable bioavailability or sensitivity to psychoactive effects.

It is well established that bypassing hepatic metabolism can significantly improve the systemic bioavailability of cannabinoids, thereby enhancing absorption and therapeutic efficiency. This enhancement could theoretically reduce the required dose by half, thereby decreasing the risk of side effects and lowering overall treatment costs. Recent innovations in delivery systems have demonstrated bioavailability improvements. A clinical trial comparing a self-emulsifying cannabinoid powder formulation to traditional oil-based drops demonstrated a 2.9-fold increase in the relative bioavailability of tetrahydrocannabinol (THC) and a 2.3-fold increase for CBD, underscoring the importance of formulation design in improving absorption (Hermush et al., 2025). Similarly, 3D-printed cannabinoid microneedle patches have shown promising results in enhancing the bioavailability of CBD, highlighting the potential of advanced, patient-friendly delivery technologies to overcome the persistent limitations of conventional formulations (Bagde et al., 2024).

These developments highlight the importance of innovative delivery systems in optimizing cannabinoid therapy. Buccal in-situ gels and 3D-printed films represent significant advancements in the field of cannabinoid therapeutics.

7.4 Limitations and Future Perspectives of Developed Buccal Cannabinoid Delivery Systems

Thermoresponsive in-situ gels formulated with Poloxamer 407 in combination with mucoadhesive polymers such as HPMC and Carbopol represent a promising strategy for buccal cannabinoid delivery, owing to their ability to transition from liquid to gel at physiological temperatures. This sol-to-gel transition enables ease of administration and prolonged mucosal residence, facilitating sustained drug release. However, their clinical translation faces several limitations. A key concern lies in stability and storage. These gels rely heavily on the thermoresponsive nature of Poloxamer 407, with optimal gelation and viscosity occurring near 37 °C. Storage

at elevated temperatures can induce premature gelation, while room-temperature storage over time has been associated with shifts in sol–gel transition temperature, altered viscosity, and changes in drug release kinetics. Refrigerated storage maintains rheological stability and preserves cannabinoid integrity (Akash et al., 2014; Chen et al., 2021). In the studies conducted within this thesis, thermoresponsive gels were stored under refrigerated conditions to maintain stability over the study period. While refrigeration ensures consistency in physicochemical properties and preserves the integrity of cannabinoid inclusion complexes, it presents practical limitations for real-world use, particularly in contexts where cold-chain storage is unavailable or inconvenient for patients.

Another challenge encountered during this thesis was the inability to incorporate terpene as permeation enhancers. Terpenes such as limonene, menthol, and pinene have demonstrated efficacy in enhancing transmucosal permeation of cannabinoids (Amaral et al., 2020; Ceschel et al., 2000; Sharma et al., 2019); however, their addition destabilized the solution, rendering it less practical for in-situ administration. Study by Rhee et al. (2007) demonstrated that addition of terpenes to Poloxamer 407 solutions increases viscosity and lowers the sol–gel transition temperature, indicating that terpenes can significantly alter gel consistency and may complicate administration and drug release. This underscores the challenge in balancing formulation components, including achieving enhanced permeation while maintaining acceptable rheological and administration properties. Future work could explore the use of alternative permeation enhancer incorporation to maintain manageable viscosity while retaining permeation-enhancing effects.

Ion-responsive in-situ gels, based on gellan gum, κ-carrageenan, and mixed κ-CG/ι-CG matrices, offer the advantage of forming gels in the presence of physiological cations in saliva. The ionic interaction facilitates rapid gelation and provides strong mechanical integrity and mucoadhesive properties (Funami, 2011). However, these systems are inherently dependent on salivary composition and flow, which can vary considerably between individuals due to factors such as age, hydration status, medication use, and underlying medical conditions such as xerostomia. Such variability may directly impact gelation kinetics, drug release profiles, and overall therapeutic efficacy. Studies have confirmed that κ-carrageenan and gellan gum gels demonstrate distinct mechanical properties depending on ion type and concentration (Bui et al., 2019; Elfaruk et al., 2021; Huang et al., 2021; Liu et al., 2015). Patients with reduced salivary flow may experience delayed or incomplete gelation, potentially leading to premature loss of the formulation from the buccal cavity and inconsistent drug absorption. Conversely, individuals with high salivary flow might experience dilution effects that alter the gel's viscosity and reduce its residence time, potentially compromising sustained release. A formulation study on κ-carrageenan in-situ gels for oral mucosa demonstrated that gelation relies on salivary ions, indicating that insufficient ionic strength, as may occur in hyposalivation, can impair gel formation and compromise performance (B. Vigani, A. Faccendini, et al., 2019).

In addition, long-term stability is a critical concern for ion-responsive systems. Cannabinoid degradation, observed after six months of storage in initial formulations, resulted in discolouration and potential loss of

efficacy. While freeze-drying the gels preserved structural integrity, drug content, and rehydration properties (Abla & Mehanna, 2022; Odziomek et al., 2024), this approach introduces additional steps in manufacturing for clinical use. Therefore, scalability remains as a key challenge that must be addressed before these systems can be translated to clinical practice.

Similarly, 3D-printed buccal films, although offering precise dosing and design flexibility, require further evaluations. Long-term stability and storage of the printed films remain underexplored. While initial studies demonstrated consistent cannabinoid content, uniformity, and mechanical integrity, the stability of cannabinoids within the polymer matrix over prolonged periods, especially under variable environmental conditions such as humidity and temperature, requires thorough investigation. Research has demonstrated that HPMC based formulations are susceptible to moisture uptake, which compromises mechanical integrity, alters tensile strength, and modifies drug release kinetics. This effect is further accentuated in the presence of plasticizers such as PEG 400 (Kang et al., 2024; Saringat et al., 2005). Cannabinoids themselves are prone to degradation or crystallization, affecting efficacy over time (Peschel, 2016). Future research should focus on accelerated stability studies, moisture barrier packaging, and potential incorporation of stabilizers to maintain long-term formulation stability. Furthermore, while 3D printing enables precise dosing, the technology's scalability for large-scale production remains a practical challenge. High-throughput manufacturing processes will need to maintain accuracy, uniformity, and reproducibility while complying with good manufacturing practice (GMP) standards. Reviews on 3D-printed pharmaceuticals point out that many current 3D printers and workflows do not yet satisfy GMP requirements, particularly regarding uniformity and process validation (Mahmood, 2021). Regulatory approval pathways for 3D-printed drug products are still evolving. Although the FDA has approved one 3D-printed drug (Spritam®), there is still no fully established framework for 3D-printed medicines (Alzhrani et al., 2025).

Across all systems, a major limitation is the scarcity of in vivo data. Such studies would provide critical pharmacokinetic and pharmacodynamic data, allowing correlation between in vitro release/ex vivo penetration and actual systemic absorption, therapeutic efficacy, and safety. Early-phase clinical trials are required to assess tolerability, pharmacokinetics, and dose-response relationships in humans (Catherine J Lucas et al., 2018). Clinical trials evaluating buccal cannabinoid delivery systems should prioritize patient-centred outcomes, particularly focusing on comfort, ease of administration, taste, and adherence. Organoleptic testing plays a crucial role in assessing these factors, especially in paediatric and elderly populations. Unpleasant sensory attributes, such as bitterness, can significantly impact patient compliance, leading to incomplete dosing or avoidance of medication (Ranmal et al., 2025). Formulation acceptability can also influence dosing accuracy, as patients may inadvertently alter placement or retention time if the formulation is uncomfortable (S. Jacob et al., 2021; Shipp et al., 2022).

Packaging considerations are pivotal for the successful translation of novel buccal cannabinoid delivery systems into clinical practice. Ensuring the integrity, stability, and safety of these formulations requires

meticulous attention to packaging design and materials. In situ gels necessitate packaging solutions that maintain their structural integrity. Single-use syringes and prefilled applicators are commonly employed to facilitate accurate dosing and minimize contamination risks (B. Vigani et al., 2020). These systems should be constructed from materials compatible with the gel's composition to prevent interactions that could compromise the formulation's efficacy or safety. Additionally, temperature-stable containers are essential to preserve the gel's properties, as exposure to inappropriate temperatures can lead to phase transitions or degradation. Furthermore, amber-coloured glass bottles or vials and moisture-resistant packaging might be required for preservation of cannabinoid content (Fairbairn et al., 1976; Fraguas Sánchez et al., 2020; Jaidee et al., 2022). The integration of personalized medicine approaches represents a significant opportunity. 3D printing allows the production of individualized films with specific cannabinoid ratios, potentially enabling therapy tailored to patient-specific conditions, symptom severity, or metabolism.

Developed novel buccal delivery systems in this thesis show considerable promise; however, their widespread adoption depends on overcoming challenges related to storage stability, salivary variability, manufacturing scalability, and regulatory approval. Future advances in excipient design, stabilizer incorporation, packaging technologies, and personalization strategies, combined with rigorous in vivo validation, will be key in advancing these systems to clinically viable therapeutic options.

Collectively, these limitations highlight the next critical phase for translation, scaling manufacturing, ensuring stability, and validating performance in human subjects.

7.5 Conclusions

In this thesis, thermoresponsive in-situ gels, ion-responsive gels, and 3D-printed mucoadhesive films were designed to overcome the limitations of conventional formulations, including poor solubility, low and variable bioavailability, and short mucosal residence times. Incorporation of cyclodextrin inclusion complexes enhanced cannabinoid solubility and stability, while terpene-based permeation enhancers facilitated efficient transmucosal transport. Mucoadhesive polymers such as HPMC and Carbopol improved retention at the absorption site, enabling sustained and controlled drug release. Despite these advances, several challenges remain. Thermoresponsive gels require refrigerated storage to maintain stability, ion-responsive gels are sensitive to salivary composition and flow, and 3D-printed films face moisture-related degradation and regulatory hurdles for large-scale production. Furthermore, in vivo validation is necessary to confirm pharmacokinetics, pharmacodynamics, therapeutic efficacy, and patient usability, including organoleptic properties such as taste and comfort. Future directions include incorporation of stabilizers, optimized packaging to prevent environmental degradation, and personalized 3D-printed formulations for patient-specific dosing. Addressing these practical and translational challenges is critical for moving these platforms from laboratory studies to clinical applications. Beyond the major cannabinoids Δ^9-tetrahydrocannabinol (THC) and cannabidiol (CBD), growing research interest in minor cannabinoids such as cannabinol (CBN),

cannabigerol (CBG), and cannabichromene (CBC) highlights emerging therapeutic opportunities for neurodegenerative diseases, sleep disorders, inflammation, and skin conditions. The buccal delivery systems developed in this thesis have the potential to be tailored to encapsulate and deliver these minor cannabinoids, providing a versatile platform for future cannabinoid-based pharmacotherapy. Overall, the dosage forms developed provide a promising foundation for safer, more effective, and patient-friendly cannabinoid therapy. By overcoming pharmacokinetic barriers and enabling localized and systemic delivery, these innovative platforms hold promise not only for chronic pain management and multiple sclerosis but also for the emerging generation of cannabinoid-based therapeutics targeting diverse physiological pathways.

References

Abdella, S., Kim, S., Afinjuomo, F., Song, Y., Upton, R., & Garg, S. (2023). Harnessing the Synergistic Potential of 3D Printed Buccal Films and Nanostructured Lipid Carriers (NLCs) For Personalised Cannabidiol Delivery.

Abdella, S., Kim, S., Afinjuomo, F., Song, Y., Upton, R., & Garg, S. (2024). Combining the potential of 3D printed buccal films and nanostructured lipid carriers for personalised cannabidiol delivery. *Drug Delivery and Translational Research*, *14*(4), 984–1004. https://doi.org/10.1007/s13346-023-01446-0

Abdeltawab, H., Darren, S., & and Sharma, M. (2020). Formulation strategies to modulate drug release from poloxamer based in situ gelling systems. *Expert Opinion on Drug Delivery*, *17*(4), 495–509. https://doi.org/10.1080/17425247.2020.1731469

Abla, K. K., & Mehanna, M. M. (2022). Freeze-drying: A flourishing strategy to fabricate stable pharmaceutical and biological products. *International Journal of Pharmaceutics*, *628*, 122233. https://doi.org/https://doi.org/10.1016/j.ijpharm.2022.122233

Adelli, G. R., Bhagav, P., Taskar, P., Hingorani, T., Pettaway, S., Gul, W., ElSohly, M. A., Repka, M. A., & Majumdar, S. (2017). Development of a Δ9-Tetrahydrocannabinol Amino Acid-Dicarboxylate Prodrug With Improved Ocular Bioavailability. *Invest Ophthalmol Vis Sci*, *58*(4), 2167–2179. https://doi.org/10.1167/iovs.16-20757

Aframian, D., Davidowitz, T., & Benoliel, R. (2006). The distribution of oral mucosal pH values in healthy saliva secretors. *Oral Diseases*, *12*(4), 420–423. https://doi.org/https://doi.org/10.1111/j.1601-0825.2005.01217.x

Afridi, A., Al Rashid, A., & Koç, M. (2024). Recent advances in the development of stereolithography-based additive manufacturing processes: A review of applications and challenges. *Bioprinting*, *43*, e00360. https://doi.org/https://doi.org/10.1016/j.bprint.2024.e00360

Agabio, R., Sanna, F., Lobina, C., Monduzzi, M., Nairi, V., Cugia, F., Mameli, S., Pisanu, G., Gessa, G., & Melis, M. R. (2017). Is 2-Hydroxypropyl-β-cyclodextrin a Suitable Carrier for Central Administration of Δ9-Tetrahydrocannabinol? Preclinical Evidence. *Drug development research*, *78*(8), 411–419.

Agossa, K., Delepierre, A., Lizambard, M., Delcourt-Debruyne, E., Siepmann, J., Siepmann, F., & Neut, C. (2020). In-situ forming implants for dual controlled release of chlorhexidine and ibuprofen for periodontitis treatment: Microbiological and mechanical key properties. *Journal of Drug Delivery Science and Technology*, *60*, 101956. https://doi.org/https://doi.org/10.1016/j.jddst.2020.101956

Aguilar-de-Leyva, Á., Linares, V., Casas, M., & Caraballo, I. (2020). 3D Printed Drug Delivery Systems Based on Natural Products. *Pharmaceutics*, *12*(7), 620.

Ahmad Raus, R., Wan Nawawi, W. M. F., & Nasaruddin, R. R. (2021). Alginate and alginate composites for biomedical applications. *Asian J Pharm Sci*, *16*(3), 280–306. https://doi.org/10.1016/j.ajps.2020.10.001

Aina, M., Baillon, F., Sescousse, R., Sanchez-Ballester, N. M., Begu, S., Soulairol, I., & Sauceau, M. (2025). From conception to consumption: Applications of semi-solid extrusion 3D printing in oral drug delivery. *International Journal of Pharmaceutics*, *674*, 125436. https://doi.org/https://doi.org/10.1016/j.ijpharm.2025.125436

Aissou, M., Chemat-Djenni, Z., Yara-Varón, E., Fabiano-Tixier, A.-S., & Chemat, F. (2017). Limonene as an agro-chemical building block for the synthesis and extraction of bioactive compounds. *Comptes Rendus. Chimie*, *20*(4), 346–358.

Akash, M. S., Rehman, K., Sun, H., & Chen, S. (2014). Assessment of release kinetics, stability and polymer interaction of poloxamer 407-based thermosensitive gel of interleukin-1 receptor antagonist. *Pharm Dev Technol*, *19*(3), 278–284. https://doi.org/10.3109/10837450.2013.775158

Akinosho, H., Hawkins, S., & Wicker, L. (2013). Hydroxypropyl methylcellulose substituent analysis and rheological properties. *Carbohydrate Polymers*, *98*(1), 276–281. https://doi.org/https://doi.org/10.1016/j.carbpol.2013.05.081

Al-Ghananeem, A., Malkawi, H., & Crooks, P. (2011). Bioavailability of Δ 9 -tetrahydrocannabinol following intranasal administration of a mucoadhesive gel spray delivery system in conscious rabbits. *Drug development and industrial pharmacy*, *37*, 329–334. https://doi.org/10.3109/03639045.2010.513009

Al-Khazaleh, A. K., Jaye, K., Chang, D., Münch, G. W., & Bhuyan, D. J. (2024). Buds and Bugs: A Fascinating Tale of Gut Microbiota and Cannabis in the Fight against Cancer. *International Journal of Molecular Sciences*, *25*(2), 872.

Alberti, T., Didaran, F., Sharma, S., De Sarandy Raposo, R., Diatta, A. A., Maraschin, M., & Da Cunha Leme Filho, J. F. (2025). Bracts, Buds, and Biases: Uncovering Gaps in Trichome Density Quantification and Cannabinoid Concentration in Cannabis sativa L. *Plants*, *14*(14), 2220.

Aldrich, M. (1997). History of therapeutic cannabis. *Cannabis in medical practice. Jefferson, NC: Mc Farland*, 35–55.

Alhamdany, A., Yousif, N., & D. Salman, Z. (2020). An Innovative Mucoadhesive Thermosensitive In situ Gelling Liquid Suppository of Metoclopramide Hydrocloride for Treatment of Nausea and Vomiting Associated with Diseases. *Indian Journal of Pharmaceutical Sciences*, *82*, 650–664. https://doi.org/10.36468/pharmaceutical-sciences.691

Ali, F., & Al-Shohani, A. (2024). Preparation and Evaluation of in situ Ophthalmic Gel with a Dual Triggered Mechanism for the Delivery of Gatifloxacin and Betamethasone تحضير وتقييم جل العين الموضعي بآلية تحفيز مزدوجة لتوصيل جاتيفلوكساسين وبيتاميثازون فوسفات الصوديوم. *Al-Rafidain Journal of Medical Sciences (ISSN 2789-3219)*, *6*, 56–63. https://doi.org/10.54133/ajms.v6i2.597

Allam, A., & Fetih, G. (2016). Sublingual fast dissolving niosomal films for enhanced bioavailability and prolonged effect of metoprolol tartrate. *Drug design, development and therapy*, *10*, 2421–2433. https://doi.org/10.2147/DDDT.S113775

Alsalamat, H. A., Abuarab, S. F., Salamah, H. M., Ishqair, A. H., Dwikat, M. F., Nourelden, A. Z., Qandil, A. N., Barakat, Y., & Barakat, M. (2024). Cannabis and cancer: unveiling the potential of a green ally in breast, colorectal, and prostate cancer. *Journal of Cannabis Research*, *6*(1), 24. https://doi.org/10.1186/s42238-024-00233-z

Alzhrani, R. F., Fitahi, R. A., Majrashi, M. A., Zhang, Y., & Maniruzzaman, M. (2025). Toward a harmonized regulatory framework for 3D-printed pharmaceutical products: the role of critical feedstock materials and process parameters. *Drug Delivery and Translational Research*. https://doi.org/10.1007/s13346-025-01966-x

Amaral, B. R., Argenta, D. F., Kroth, R., & Caon, T. (2020). Transbuccal delivery of benznidazole associated with monoterpenes: permeation studies and mechanistic insights. *European Journal of Pharmaceutical Sciences*, *143*, 105177. https://doi.org/https://doi.org/10.1016/j.ejps.2019.105177

An, D., Peigneur, S., Hendrickx, L. A., & Tytgat, J. (2020). Targeting Cannabinoid Receptors: Current Status and Prospects of Natural Products. *International Journal of Molecular Sciences*, *21*(14), 5064.

Anand, U., Anand, P., & Sodergren, M. H. (2023). Terpenes in Cannabis sativa Inhibit Capsaicin Responses in Rat DRG Neurons via Na+/K+ ATPase Activation. *International Journal of Molecular Sciences*, *24*(22), 16340.

Andre, C. M., Hausman, J.-F., & Guerriero, G. (2016). Cannabis sativa: The Plant of the Thousand and One Molecules [Review]. *Frontiers in Plant Science*, *7*(19). https://doi.org/10.3389/fpls.2016.00019

Andriotis, E. G., Monou, P. K., Louka, A., Papaefstathiou, E., Eleftheriadis, G. K., & Fatouros, D. G. (2020). Development of food grade 3D printable ink based on pectin containing cannabidiol/cyclodextrin inclusion complexes. *Drug Dev Ind Pharm*, *46*(10), 1569–1577. https://doi.org/10.1080/03639045.2020.1791168

Antezana, P. E., Municoy, S., Orive, G., & Desimone, M. F. (2022). Design of a New 3D Gelatin—Alginate Scaffold Loaded with Cannabis sativa Oil. *Polymers*, *14*(21), 4506.

Aqil, M., Ahad, A., Sultana, Y., & Ali, A. (2007). Status of terpenes as skin penetration enhancers. *Drug Discovery Today*, *12*(23), 1061–1067. https://doi.org/https://doi.org/10.1016/j.drudis.2007.09.001

Arpa, M. D., Okur, N. Ü., Gök, M. K., Özgümüş, S., & Cevher, E. (2023). Chitosan-based buccal mucoadhesive patches to enhance the systemic bioavailability of tizanidine. *International Journal of Pharmaceutics*, *642*, 123168. https://doi.org/https://doi.org/10.1016/j.ijpharm.2023.123168

Asane, G. S., Nirmal, S. A., Rasal, K. B., Naik, A. A., Mahadik, M. S., & Rao, Y. M. (2008). Polymers for Mucoadhesive Drug Delivery System: A Current Status. *Drug development and industrial pharmacy*, *34*(11), 1246–1266. https://doi.org/10.1080/03639040802026012

Asatiani, N., Filipová, B., Pechočiaková, M., Kluk, A., Kunc, Š., & Mikeš, P. (2023). Electrospun HPMC/PEO-blend orodispersible films: how slight batch differences affect the crucial mechanical properties. *Cellulose*, *30*(7), 4527–4541. https://doi.org/10.1007/s10570-023-05137-4

Askarizadeh, M., Esfandiari, N., Honarvar, B., Sajadian, S. A., & Azdarpour, A. (2023). Kinetic Modeling to Explain the Release of Medicine from Drug Delivery Systems. *ChemBioEng Reviews*, *10*(6), 1006–1049. https://doi.org/https://doi.org/10.1002/cben.202300027

Auel, T., Mentrup, A. F. C., Oldfield, L. R., & Seidlitz, A. (2025). 3D printing of pharmaceutical dosage forms: Recent advances and applications. *Advanced Drug Delivery Reviews*, *217*, 115504. https://doi.org/https://doi.org/10.1016/j.addr.2024.115504

Azad, M. A., Olawuni, D., Kimbell, G., Badruddoza, A. Z. M., Hossain, M., & Sultana, T. (2020). Polymers for extrusion-based 3D printing of pharmaceuticals: A holistic materials–process perspective. *Pharmaceutics*, *12*(2), 124.

Badowski, M. E. (2017). A review of oral cannabinoids and medical marijuana for the treatment of chemotherapy-induced nausea and vomiting: a focus on pharmacokinetic variability and pharmacodynamics. *Cancer chemotherapy and pharmacology*, *80*(3), 441–449. https://doi.org/10.1007/s00280-017-3387-5

Badowski, M. E., & Yanful, P. K. (2018). Dronabinol oral solution in the management of anorexia and weight loss in AIDS and cancer. *Therapeutics and clinical risk management*, *14*, 643–651. https://doi.org/10.2147/TCRM.S126849

Bagde, A., Mosley-Kellum, K., Spencer, S., & Singh, M. (2024). 3D DLP-printed cannabinoid microneedles patch and its pharmacokinetic evaluation in rats. *J Pharm Pharmacol*, *76*(6), 616–626. https://doi.org/10.1093/jpp/rgae043

Bagde, S., & Rohera, B. D. (2024). Modification of the swelling behavior of a hydrophilic polymer as an approach to maintaining a constant gel layer thickness. *Journal of Drug Delivery Science and Technology*, *92*, 105294. https://doi.org/https://doi.org/10.1016/j.jddst.2023.105294

Baker, D., Pryce, G., Giovannoni, G., & Thompson, A. J. (2003). The therapeutic potential of cannabis. *The Lancet Neurology*, *2*(5), 291–298. https://doi.org/https://doi.org/10.1016/S1474-4422(03)00381-8

Bala, R., Pawar, P., Khanna, S., & Arora, S. (2013). Orally dissolving strips: A new approach to oral drug delivery system. *International journal of pharmaceutical investigation*, *3*(2), 67–76. https://doi.org/10.4103/2230-973X.114897

Balakrishnan, P., Park, E. K., Song, C. K., Ko, H. J., Hahn, T. W., Song, K. W., & Cho, H. J. (2015). Carbopol-incorporated thermoreversible gel for intranasal drug delivery. *Molecules*, *20*(3), 4124–4135. https://doi.org/10.3390/molecules20034124

Banerjee, S., Saharan, V. A., Banerjee, D., Ram, V., Kulhari, H., Pooja, D., & Singh, A. (2024). A comprehensive update on cannabidiol, its formulations and drug delivery systems. *Phytochemistry Reviews*. https://doi.org/10.1007/s11101-024-10001-9

Baron, E. P. (2015). Comprehensive Review of Medicinal Marijuana, Cannabinoids, and Therapeutic Implications in Medicine and Headache: What a Long Strange Trip It's Been …. *Headache: The Journal of Head and Face Pain*, *55*(6), 885–916. https://doi.org/https://doi.org/10.1111/head.12570

Barrales-Cureño, H. J., López-Valdez, L. G., Reyes, C., Cetina-Alcalá, V. M., Vasquez-García, I., Diaz-Lira, O. F., & Herrera-Cabrera, B. E. (2020). Chemical characteristics, therapeutic uses, and legal aspects of the cannabinoids of Cannabis sativa: a review. *Brazilian Archives of Biology and Technology*, *63*, e20190222.

Barreiro Carpio, M., Gonzalez Martinez, E., Dabaghi, M., Ungureanu, J., Arizpe Tafoya, A. V., Gonzalez Martinez, D. A., Hirota, J. A., & Moran-Mirabal, J. M. (2023). High-Fidelity Extrusion Bioprinting of Low-Printability Polymers Using Carbopol as a Rheology Modifier. *ACS Applied Materials & Interfaces*, *15*(47), 54234–54248. https://doi.org/10.1021/acsami.3c10092

Barua, S., Kim, H., Jo, K., Seo, C. W., Park, T. J., Lee, K. B., Yun, G., Oh, K., & Lee, J. (2016). Drug delivery techniques for buccal route: formulation strategies and recent advances in dosage form design. *Journal of Pharmaceutical Investigation*, *46*(7), 593–613. https://doi.org/10.1007/s40005-016-0281-9

Bashir, S., Zafar, N., Lebaz, N., Mahmood, A., & Elaissari, A. (2020). Hydroxypropyl methylcellulose-based hydrogel copolymeric for controlled delivery of galantamine hydrobromide in Dementia. *Processes*, *8*(11), 1350.

Bassi da Silva, J., Ferreira, S. B. d. S., Reis, A. V., Cook, M. T., & Bruschi, M. L. (2018). Assessing Mucoadhesion in Polymer Gels: The Effect of Method Type and Instrument Variables. *Polymers*, *10*(3), 254.

Bautista, J. L., Yu, S., & Tian, L. (2021). Flavonoids in Cannabis sativa: Biosynthesis, Bioactivities, and Biotechnology. *ACS Omega*, *6*(8), 5119–5123. https://doi.org/10.1021/acsomega.1c00318

Bedi, G., Cooper, Z. D., & Haney, M. (2013). Subjective, cognitive and cardiovascular dose-effect profile of nabilone and dronabinol in marijuana smokers. *Addiction biology*, *18*(5), 872–881. https://doi.org/10.1111/j.1369-1600.2011.00427.x

Belgamwar, V. S., Chauk, D. S., Mahajan, H. S., Jain, S. A., Gattani, S. G., & Surana, S. J. (2009). Formulation and evaluation of in situ gelling system of dimenhydrinate for nasal administration. *Pharmaceutical development and technology*, *14*(3), 240–248. https://doi.org/10.1080/10837450802498910

Ben Amar, M. (2006). Cannabinoids in medicine: A review of their therapeutic potential. *Journal of Ethnopharmacology*, *105*(1), 1–25. https://doi.org/https://doi.org/10.1016/j.jep.2006.02.001

Bethoux, F. A., Farrell, R., Checketts, D., Sahr, N., Berwaerts, J., Alexander, J. K., & Skobieranda, F. (2024). A Randomized, Double-Blind, Placebo-Controlled Trial to Evaluate the Effect of Nabiximols Oromucosal Spray on Clinical Measures of Spasticity in Patients With Multiple Sclerosis. *Multiple Sclerosis and Related Disorders*, 105740.

Bhuller, R., Schlage, W. K., & Hoeng, J. (2024). Review of the current ongoing clinical trials exploring the possible anti-anxiety effects of cannabidiol. *Journal of Cannabis Research*, *6*(1), 40. https://doi.org/10.1186/s42238-024-00250-y

Bi, X., & Liang, A. (2016). In situ-forming cross-linking hydrogel systems: Chemistry and biomedical applications. *Emerging concepts in analysis and applications of hydrogels*, *86*, 541–547.

Bifulco, M., & Pisanti, S. (2015). Medicinal use of cannabis in Europe. *EMBO reports*, *16*(2), 130–132. https://doi.org/https://doi.org/10.15252/embr.201439742

Blasco-Benito, S., Seijo-Vila, M., Caro-Villalobos, M., Tundidor, I., Andradas, C., García-Taboada, E., Wade, J., Smith, S., Guzmán, M., & Pérez-Gómez, E. (2018). Appraising the "entourage effect": Antitumor action of a pure cannabinoid versus a botanical drug preparation in preclinical models of breast cancer. *Biochemical pharmacology*, *157*, 285–293.

Bonn-Miller, M. O., Babson, K. A., & Vandrey, R. (2014). Using cannabis to help you sleep: Heightened frequency of medical cannabis use among those with PTSD. *Drug and Alcohol Dependence*, *136*, 162–165. https://doi.org/https://doi.org/10.1016/j.drugalcdep.2013.12.008

Bottorff, J. L., Bissell, L. J., Balneaves, L. G., Oliffe, J. L., Capler, N. R., & Buxton, J. (2013). Perceptions of cannabis as a stigmatized medicine: a qualitative descriptive study. *Harm Reduction Journal*, *10*(1), 1–10.

Bouhadir, K. H., Lee, K. Y., Alsberg, E., Damm, K. L., Anderson, K. W., & Mooney, D. J. (2001). Degradation of partially oxidized alginate and its potential application for tissue engineering. *Biotechnol Prog*, *17*(5), 945–950. https://doi.org/10.1021/bp010070p

Brunetti, P., Pichini, S., Pacifici, R., Busardò, F. P., & Del Rio, A. (2020). Herbal preparations of medical cannabis: a vademecum for prescribing doctors. *Medicina*, *56*(5), 237.

Bruni, N., Della Pepa, C., Oliaro-Bosso, S., Pessione, E., Gastaldi, D., & Dosio, F. (2018). Cannabinoid delivery systems for pain and inflammation treatment. *Molecules*, *23*(10), 2478.

Budumuru, P., Nagaraju, R., & Prasanth, D. (2020). A COMPREHENSIVE REVIEW ON IN SITU GELS. *International Journal of Applied Pharmaceutics*, 24–33. https://doi.org/10.22159/ijap.2020v12i6.38918

Bui, V. T. N. T., Nguyen, B. T., Nicolai, T., & Renou, F. (2019). Mixed iota and kappa carrageenan gels in the presence of both calcium and potassium ions. *Carbohydrate Polymers*, *223*, 115107. https://doi.org/https://doi.org/10.1016/j.carbpol.2019.115107

Campo, V. L., Kawano, D. F., Silva, D. B. d., & Carvalho, I. (2009). Carrageenans: Biological properties, chemical modifications and structural analysis – A review. *Carbohydrate Polymers*, *77*(2), 167–180. https://doi.org/https://doi.org/10.1016/j.carbpol.2009.01.020

Cao, S.-l., Zhang, Q.-z., & Jiang, X.-g. (2007). Preparation of ion-activated in situ gel systems of scopolamine hydrobromide and evaluation of its antimotion sickness efficacy. *Acta Pharmacologica Sinica*, *28*(4), 584–590. https://doi.org/10.1111/j.1745-7254.2007.00540.x

Carvalho, A. F. F. d., Caldeira, V. F., Oliveira, A. P., Gonsalves, J. K. M. d. C., & Araújo, E. C. d. C. (2023). Design and development of orally disintegrating films: A platform based on hydroxypropyl methylcellulose and guar gum. *Carbohydrate Polymers*, *299*, 120155. https://doi.org/https://doi.org/10.1016/j.carbpol.2022.120155

Casiraghi, A., Musazzi, U. M., Centin, G., Franzè, S., & Minghetti, P. (2020). Topical Administration of Cannabidiol: Influence of Vehicle-Related Aspects on Skin Permeation Process. *Pharmaceuticals (Basel)*, *13*(11). https://doi.org/10.3390/ph13110337

Cassanelli, M., Norton, I., & Mills, T. (2018). Role of gellan gum microstructure in freeze drying and rehydration mechanisms. *Food Hydrocolloids*, *75*, 51–61. https://doi.org/https://doi.org/10.1016/j.foodhyd.2017.09.013

Cassanelli, M., Prosapio, V., Norton, I., & Mills, T. (2018). Acidified/basified gellan gum gels: The role of the structure in drying/rehydration mechanisms. *Food Hydrocolloids*, *82*, 346–354. https://doi.org/https://doi.org/10.1016/j.foodhyd.2018.04.024

Çelik, B. (2017). Risperidone mucoadhesive buccal tablets: formulation design, optimization and evaluation. *Drug design, development and therapy*, *11*, 3355–3365. https://doi.org/10.2147/dddt.S150774

Cerveto, T., Denis, L., Stoops, M., Lechanteur, A., Jérôme, C., Leenhardt, J., Flynn, S., Goyanes, A., Mazet, R., Annereau, M., & Choisnard, L. (2024). The promising role of semi-solid extrusion technology in custom drug formulation for pediatric medicine. *IJB*, *10*(6). https://doi.org/10.36922/ijb.4063

Ceschel, G. C., Maffei, P., Moretti, M. D. L., Demontis, S., & Peana, A. T. (2000). In vitro permeation through porcine buccal mucosa of Salvia desoleana Atzei & Picci essential oil from topical formulations. *International Journal of Pharmaceutics*, *195*(1), 171–177. https://doi.org/https://doi.org/10.1016/S0378-5173(99)00381-6

Chalal, S., Haddadine, N., Bouslah, N., Souilah, S., Benaboura, A., Barille, R., & Haroun, A. (2014). Preparation Characterization and Thermal Behaviour of Carbopol-TiO₂ Nanocomposites. *Open Journal of Organic Polymer Materials*, *04*, 55–64. https://doi.org/10.4236/ojopm.2014.43008

Chalamaiah, M., & Sharma, P. (2016). Pre-Formulation and Formulation Approaches for Buccal Films. *J Bioequiv Availab*, *8*, 246–248.

Changsan, N., Sawatdee, S., Suedee, R., Chunhachaichana, C., & Srichana, T. (2023). Aqueous cannabidiol β-cyclodextrin complexed polymeric micelle nasal spray to attenuate in vitro and ex vivo SARS-CoV-2-induced cytokine storms. *Int J Pharm*, *640*, 123035. https://doi.org/10.1016/j.ijpharm.2023.123035

Chatterjee, B., Amalina, N., Sengupta, P., & Mandal, U. K. (2017). Mucoadhesive polymers and their mode of action: A recent update. *Journal of Applied Pharmaceutical Science*, *7*(5), 195–203.

Chaudhary, B., & Verma, S. (2014). Preparation and Evaluation of Novel In Situ Gels Containing Acyclovir for the Treatment of Oral Herpes Simplex Virus Infections. *The Scientific World Journal*, *2014*(1), 280928. https://doi.org/https://doi.org/10.1155/2014/280928

Chaurasia, G. (2016). A review on pharmaceutical preformulation studies in formulation and development of new drug molecules. *International Journal of Pharmaceutical Sciences and Research*, *7*(6), 2313.

Chen, J., Jiang, Q. D., Chai, Y. P., Zhang, H., Peng, P., & Yang, X. X. (2016). Natural Terpenes as Penetration Enhancers for Transdermal Drug Delivery. *Molecules*, *21*(12). https://doi.org/10.3390/molecules21121709

Chen, L. C., Lin, S. Y., Cheng, W. J., Sheu, M. T., Chung, C. Y., Hsu, C. H., & Lin, H. L. (2023). Poloxamer sols endowed with in-situ gelability and mucoadhesion by adding hypromellose and hyaluronan for prolonging corneal retention and drug delivery. *Drug Deliv*, *30*(1), 2158964. https://doi.org/10.1080/10717544.2022.2158964

Chen, Y., Lee, J.-H., Meng, M., Cui, N., Dai, C.-Y., Jia, Q., Lee, E.-S., & Jiang, H.-B. (2021). An Overview on Thermosensitive Oral Gel Based on Poloxamer 407. *Materials*, *14*(16), 4522.

Chen, Y., Liu, Y., Xie, J., Zheng, Q., Yue, P., Chen, L., Hu, P., & Yang, M. (2020). Nose-to-brain delivery by nanosuspensions-based in situ gel for breviscapine. *International Journal of Nanomedicine*, 10435–10451.

Cherniakov, I., Izgelov, D., Barasch, D., Davidson, E., Domb, A. J., & Hoffman, A. (2017). Piperine-pro-nanolipospheres as a novel oral delivery system of cannabinoids: Pharmacokinetic evaluation in healthy volunteers in comparison to buccal spray administration. *J Control Release*, *266*, 1–7. https://doi.org/10.1016/j.jconrel.2017.09.011

Chinna Reddy, P., Chaitanya, K. S. C., & Madhusudan Rao, Y. (2011). A review on bioadhesive buccal drug delivery systems: current status of formulation and evaluation methods. *Daru : journal of Faculty of Pharmacy, Tehran University of Medical Sciences*, *19*(6), 385–403.

Choi, S. G., Lee, S. E., Kang, B. S., Ng, C. L., Davaa, E., & Park, J. S. (2014). Thermosensitive and mucoadhesive sol-gel composites of paclitaxel/dimethyl-β-cyclodextrin for buccal delivery. *PLoS One*, *9*(9), e109090. https://doi.org/10.1371/journal.pone.0109090

Clarke, S., Butcher, B., McLachlan, A., Henson, J., Rutolo, D., Hall, S., & Vitetta, L. (2020). Pilot Clinical and Pharmacokinetic Study of Δ9-Tetrahydrocannabinol and Cannabidiol Oro-Buccal Spray in Advanced Cancer with Uncontrolled Pain. *Authorea Preprints*.

Colucci, L. A., & Rodrigues, L. N. C. (2022). Development of Orally Disintegrating Films HPMC-Based Containing Captopril: Mechanical, Optical and Physicochemical Studies. *Brazilian Archives of Biology and Technology*, *65*, e22220073.

Costa, J. S. R., de Oliveira Cruvinel, K., & Oliveira-Nascimento, L. (2019). A mini-review on drug delivery through wafer technology: Formulation and manufacturing of buccal and oral lyophilizates. *Journal of Advanced Research*, *20*, 33–41. https://doi.org/https://doi.org/10.1016/j.jare.2019.04.010

Coutinho, D. F., Sant, S. V., Shin, H., Oliveira, J. T., Gomes, M. E., Neves, N. M., Khademhosseini, A., & Reis, R. L. (2010). Modified Gellan Gum hydrogels with tunable physical and mechanical properties. *Biomaterials*, *31*(29), 7494–7502. https://doi.org/10.1016/j.biomaterials.2010.06.035

Crowley, K., de Vries, S. T., & Moreno-Sanz, G. (2018). Self-Reported Effectiveness and Safety of Trokie(®) Lozenges: A Standardized Formulation for the Buccal Delivery of Cannabis Extracts. *Frontiers in neuroscience*, *12*, 564–564. https://doi.org/10.3389/fnins.2018.00564

Czégény, Z., Nagy, G., Babinszki, B., Bajtel, Á., Sebestyén, Z., Kiss, T., Csupor-Löffler, B., Tóth, B., & Csupor, D. (2021). CBD, a precursor of THC in e-cigarettes. *Scientific Reports*, *11*(1), 8951. https://doi.org/10.1038/s41598-021-88389-z

Dash, S., Murthy, P. N., Nath, L., & Chowdhury, P. (2010). Kinetic modeling on drug release from controlled drug delivery systems. *Acta Pol Pharm*, *67*(3), 217–223.

De Caro, V., Giandalia, G., Siragusa, M. G., Sutera, F. M., & Giannola, L. I. (2012). New prospective in treatment of Parkinson's disease: Studies on permeation of ropinirole through buccal mucosa. *International Journal of Pharmaceutics*, *429*(1), 78–83. https://doi.org/https://doi.org/10.1016/j.ijpharm.2012.03.022

de Carvalho, A. C. W., Paiva, N. F., Demonari, I. K., Duarte, M. P. F., do Couto, R. O., de Freitas, O., & Vicentini, F. (2023). The Potential of Films as Transmucosal Drug Delivery Systems. *Pharmaceutics*, *15*(11). https://doi.org/10.3390/pharmaceutics15112583

de Jong, S., & van de Velde, F. (2007). Charge density of polysaccharide controls microstructure and large deformation properties of mixed gels. *Food Hydrocolloids*, *21*(7), 1172–1187. https://doi.org/https://doi.org/10.1016/j.foodhyd.2006.09.004

De Petrocellis, L., & Di Marzo, V. (2009). An introduction to the endocannabinoid system: from the early to the latest concepts. *Best Practice & Research Clinical Endocrinology & Metabolism*, *23*(1), 1–15. https://doi.org/https://doi.org/10.1016/j.beem.2008.10.013

De Souza Ferreira, S. B., Da Silva, J. B., Borghi-Pangoni, F. B., Junqueira, M. V., & Bruschi, M. L. (2017). Linear correlation between rheological, mechanical and mucoadhesive properties of polycarbophil

polymer blends for biomedical applications. *Journal of the Mechanical Behavior of Biomedical Materials*, *68*, 265–275. https://doi.org/https://doi.org/10.1016/j.jmbbm.2017.02.016

Deiringer, N., Fischer, F., Hofsäss, M., Ranft, M., & Ebert, S. (2025). Alteration of gel point of poloxamer 338 induced by pharmaceutical actives and excipients. *European Journal of Pharmaceutics and Biopharmaceutics*, *207*, 114628. https://doi.org/https://doi.org/10.1016/j.ejpb.2025.114628

Dhawale, P., Mahajan, N. M., Mahapatra, D. K., Mahajan, U. N., & Gangane, P. S. (2018). HPMC K15M and Carbopol 940 mediated fabrication of ondansetron hydrochloride intranasal mucoadhesive microspheres. *Journal of Applied Pharmaceutical Science*, *8*(8), 075–083.

Diaz-Salmeron, R., Toussaint, B., Huang, N., Bourgeois Ducournau, E., Alviset, G., Goulay Dufaÿ, S., Hillaireau, H., Dufaÿ Wojcicki, A., & Boudy, V. (2021). Mucoadhesive Poloxamer-Based Hydrogels for the Release of HP-β-CD-Complexed Dexamethasone in the Treatment of Buccal Diseases. *Pharmaceutics*, *13*(1), 117.

Diryak, R., Kontogiorgos, V., Ghori, M. U., Bills, P., Tawfik, A., Morris, G. A., & Smith, A. M. (2018). Behavior of In Situ Cross-Linked Hydrogels with Rapid Gelation Kinetics on Contact with Physiological Fluids. *Macromolecular Chemistry and Physics*, *219*(8), 1700584.

Duran, M., Pérez, E., Abanades, S., Vidal, X., Saura, C., Majem, M., Arriola, E., Rabanal, M., Pastor, A., & Farré, M. (2010). Preliminary efficacy and safety of an oromucosal standardized cannabis extract in chemotherapy-induced nausea and vomiting. *British journal of clinical pharmacology*, *70*(5), 656–663.

Durgun, M. E., Mesut, B., Hacıoğlu, M., Güngör, S., & Özsoy, Y. (2022). Optimization of the Micellar-Based In Situ Gelling Systems Posaconazole with Quality by Design (QbD) Approach and Characterization by In Vitro Studies. *Pharmaceutics*, *14*(3). https://doi.org/10.3390/pharmaceutics14030526

Eisenberg, E., Ogintz, M., & Almog, S. (2014). The Pharmacokinetics, Efficacy, Safety, and Ease of Use of a Novel Portable Metered-Dose Cannabis Inhaler in Patients With Chronic Neuropathic Pain: A Phase 1a Study. *Journal of Pain & Palliative Care Pharmacotherapy*, *28*(3), 216–225. https://doi.org/10.3109/15360288.2014.941130

El Oihabi, M., Soultana, M., Ammari, M., Ben Allal, L., & Fakih Lanjri, A. (2024). Diversity and variability of bioactive compounds in Cannabis sativa: Effects on therapeutic and environmental uses and orientations for future research. *Case Studies in Chemical and Environmental Engineering*, *9*, 100732. https://doi.org/https://doi.org/10.1016/j.cscee.2024.100732

Elfaruk, M. S., Wen, C., Chi, C., Li, X., & Janaswamy, S. (2021). Effect of salt addition on iota-carrageenan solution properties. *Food Hydrocolloids*, *113*, 106491. https://doi.org/https://doi.org/10.1016/j.foodhyd.2020.106491

Elkanayati, R. M., Chambliss, W. G., Omari, S., Almutairi, M., Repka, M. A., & Ashour, E. A. (2022). Mucoadhesive buccal films for treatment of xerostomia prepared by coupling HME and 3D printing technologies. *Journal of Drug Delivery Science and Technology*, *75*, 103660. https://doi.org/https://doi.org/10.1016/j.jddst.2022.103660

Elmowafy, E., Cespi, M., Bonacucina, G., & Soliman, M. E. (2019). In situ composite ion-triggered gellan gum gel incorporating amino methacrylate copolymer microparticles: a therapeutic modality for buccal applicability. *Pharmaceutical development and technology*, *24*(10), 1258–1271.

ElSohly, M. A., & Slade, D. (2005). Chemical constituents of marijuana: The complex mixture of natural cannabinoids. *Life Sciences*, *78*(5), 539–548. https://doi.org/https://doi.org/10.1016/j.lfs.2005.09.011

Esteso, M. A., & Romero, C. M. (2024). Cyclodextrins: Properties and Applications. *Int J Mol Sci*, *25*(8). https://doi.org/10.3390/ijms25084547

Fairbairn, J. W., Liebmann, J. A., & Rowan, M. G. (1976). The stability of cannabis and its preparations on storage. *J Pharm Pharmacol*, *28*(1), 1–7. https://doi.org/10.1111/j.2042-7158.1976.tb04014.x

Fairman, B. J. (2015). Cannabis problem experiences among users of the tobacco–cannabis combination known as blunts. *Drug and Alcohol Dependence*, *150*, 77–84.

Fakhari, A., Corcoran, M., & Schwarz, A. (2017). Thermogelling properties of purified poloxamer 407. *Heliyon*, *3*(8), e00390. https://doi.org/10.1016/j.heliyon.2017.e00390

Fathalla, Z., Mustafa, W. W., Abdelkader, H., Moharram, H., Sabry, A. M., & Alany, R. G. (2022). Hybrid thermosensitive-mucoadhesive in situ forming gels for enhanced corneal wound healing effect of L-carnosine. *Drug Deliv*, *29*(1), 374–385. https://doi.org/10.1080/10717544.2021.2023236

Fava, A. L. M., Souza, C. M. d., Santos, É. M. d., Silvério, L. A. L., Ataide, J. A., Paiva-Santos, A. C., Costa, J. L., Melo, D. O. d., & Mazzola, P. G. (2024). Evidence of Cannabidiol Effectiveness Associated or Not with Tetrahydrocannabinol in Topical Administration: A Scope Review. *Pharmaceuticals*, *17*(6), 748.

FDA, U. S. (2021). *FDA Regulation of Cannabis and Cannabis-Derived Products, Including Cannabidiol (CBD)*. https://www.fda.gov/news-events/public-health-focus/fda-regulation-cannabis-and-cannabis-derived-products-including-cannabidiol-cbd

Ferreira, S. B. S., Braga, G., Oliveira É, L., da Silva, J. B., Rosseto, H. C., de Castro Hoshino, L. V., Baesso, M. L., Caetano, W., Murdoch, C., Colley, H. E., & Bruschi, M. L. (2019). Design of a nanostructured mucoadhesive system containing curcumin for buccal application: from physicochemical to biological aspects. *Beilstein J Nanotechnol*, *10*, 2304–2328. https://doi.org/10.3762/bjnano.10.222

Finnin, B., Walters, K. A., & Franz, T. J. (2012). In vitro skin permeation methodology. In *Transdermal and topical drug delivery: principles and practice* (pp. 85–108). John Wiley & Sons.

Fitzgerald, S. (2015). FDA Approves First 3D-printed epilepsy drug experts assess the benefits and caveats. *Neurology Today*, *15*(18), 26–27.

Fordjour, E., Manful, C. F., Sey, A. A., Javed, R., Pham, T. H., Thomas, R., & Cheema, M. (2023). Cannabis: a multifaceted plant with endless potentials. *Front Pharmacol*, *14*, 1200269. https://doi.org/10.3389/fphar.2023.1200269

Fordjour, E., Manful, C. F., Sey, A. A., Javed, R., Pham, T. H., Thomas, R., & Cheema, M. (2023). Cannabis: a multifaceted plant with endless potentials [Review]. *Frontiers in Pharmacology*, *14*. https://doi.org/10.3389/fphar.2023.1200269

Fraguas Sánchez, A., Fernández-Carballido, A., Sabroso, C., & Torres-Suarez, A. (2020). Stability characteristics of Cannabidiol for the design of pharmacological, biochemical and pharmaceutical studies. *Journal of Chromatography B*, *1150*, 122188. https://doi.org/10.1016/j.jchromb.2020.122188

Franz-Montan, M., Serpe, L., Martinelli, C. C. M., da Silva, C. B., Santos, C. P. d., Novaes, P. D., Volpato, M. C., de Paula, E., Lopez, R. F. V., & Groppo, F. C. (2016). Evaluation of different pig oral mucosa sites as permeability barrier models for drug permeation studies. *European Journal of Pharmaceutical Sciences*, *81*, 52–59. https://doi.org/https://doi.org/10.1016/j.ejps.2015.09.021

Funami, T. (2011). Next target for food hydrocolloid studies: Texture design of foods using hydrocolloid technology. *Food Hydrocolloids*, *25*(8), 1904–1914. https://doi.org/https://doi.org/10.1016/j.foodhyd.2011.03.010

Furqan, M., Iqbal, F., & Tulain, U. R. (2017). Microwave radiation induced synthesis of hydroxypropyl methylcellulose-graft-(polyvinylalcohal-co-acrylic acid) polymeric network and its in vitro evaluation. *Acta Poloniae Pharmaceutica - Drug Research*, *74*, 527–541.

Furuishi, T., Kato, Y., Fukami, T., Suzuki, T., Endo, T., Nagase, H., Ueda, H., & Tomono, K. (2013). Effect of Terpenes on the Skin Permeation of Lomerizine Dihydrochloride. *Journal of pharmacy & pharmaceutical sciences : a publication of the Canadian Society for Pharmaceutical Sciences, Societe canadienne des sciences pharmaceutiques*, *16*, 551–563. https://doi.org/10.18433/J36890

Gábor, K., Sipos, B., Budai-Szűcs, M., Balogh, G., Veszelka, S., Grof, I., Deli, M., Volk, B., Szabó-Révész, P., & Csoka, I. (2021). Development of In Situ Gelling Meloxicam-Human Serum Albumin Nanoparticle Formulation for Nose-to-Brain Application. *Pharmaceutics*, *13*. https://doi.org/10.3390/pharmaceutics13050646

Gallardo, A. A., Gutierrez, M. R., Gomez, L. A. J., Reyes, P. A. O. D., Dones, S. A. A., Dumbrique, M. M. U., Lim, H. E., Liquido, M. I. H., Macawile, M. M. L., & Maglaqui, E. D. A. B. (2024). A Comparative Analysis on the Potential Anticancer Properties of Tetrahydrocannabinol, Cannabidiol, and Tetrahydrocannabivarin Compounds Through In Silico Approach. *Asian Pacific Journal of Cancer Prevention: APJCP*, *25*(3), 839.

Galocha-León, C., Antich, C., Voltes-Martínez, A., Marchal, J. A., Mallandrich, M., Halbaut, L., Rodríguez-Lagunas, M. J., Souto, E. B., Clares-Naveros, B., & Gálvez-Martín, P. (2023). Development and characterization of a poloxamer hydrogel composed of human mesenchymal stromal cells (hMSCs) for reepithelization of skin injuries. *International Journal of Pharmaceutics*, *647*, 123535. https://doi.org/https://doi.org/10.1016/j.ijpharm.2023.123535

Gandhi, S., & Shende, P. (2021). Cyclodextrins-modified metallic nanoparticles for effective cancer therapy. *Journal of Controlled Release*, *339*, 41–50. https://doi.org/https://doi.org/10.1016/j.jconrel.2021.09.025

Garala, K., Joshi, P., Shah, M., Ramkishan, A., & Patel, J. (2013). Formulation and evaluation of periodontal in situ gel. *International journal of pharmaceutical investigation*, *3*, 29–41. https://doi.org/10.4103/2230-973X.108961

Garala, K., Joshi, P., Shah, M., Ramkishan, A., & Patel, J. (2013). Formulation and evaluation of periodontal in situ gel. *International journal of pharmaceutical investigation*, *3*(1), 29–41. https://doi.org/10.4103/2230-973x.108961

Garcia, M. T., Carmo, P., Figueiredo-Godoi, L. M. A., Gonçalves, N. I., Lima, P. M. N., Ramos, L. P., Oliveira, L. D., Borges, A. L. S., Shukla, A., & Junqueira, J. C. (2024). Gellan-Based Hydrogel as a Drug Delivery System for Caffeic Acid Phenethyl Ester in the Treatment of Oral Candida albicans Infections. *Pharmaceutics*, *16*(3). https://doi.org/10.3390/pharmaceutics16030298

Gaston, T. E., & Szaflarski, J. P. (2018). Cannabis for the Treatment of Epilepsy: an Update. *Current Neurology and Neuroscience Reports*, *18*(11), 73. https://doi.org/10.1007/s11910-018-0882-y

George, A., Limbachiya, V., & Shrivastav, P. S. (2025). Current status and role of carbopols in oral, nasal, transdermal, topical and ophthalmic drug delivery systems. *Next Materials*, *9*, 100848. https://doi.org/https://doi.org/10.1016/j.nxmate.2025.100848

Geshtakovska, G., & Stefkov, G. (2016). Routes of cannabis administration: a brief review. *Your hosts Macedonian Pharmaceutical Association and Faculty of Pharmacy, Ss Cyril and Methodius University in Skopje*, *515*.

Giardina, A., Palmieri, R., Ponticelli, M., Antonelli, C., Carlucci, V., Colangelo, M., Benedetto, N., Di Fazio, A., & Milella, L. (2024). Is a Low Dosage of Medical Cannabis Effective for Treating Pain Related to Fibromyalgia? A Pilot Study and Systematic Review. *Journal of Clinical Medicine*, *13*(14), 4088.

Gilhotra, R. M., Ikram, M., Srivastava, S., & Gilhotra, N. (2014). A clinical perspective on mucoadhesive buccal drug delivery systems. *Journal of biomedical research*, *28*(2), 81–97. https://doi.org/10.7555/JBR.27.20120136

Giroud, C., De Cesare, M., Berthet, A., Varlet, V., Concha-Lozano, N., & Favrat, B. (2015). E-cigarettes: a review of new trends in cannabis use. *International journal of environmental research and public health*, *12*(8), 9988–10008.

Giuliano, E., Paolino, D., Fresta, M., & Cosco, D. (2018). Mucosal Applications of Poloxamer 407-Based Hydrogels: An Overview. *Pharmaceutics*, *10*(3). https://doi.org/10.3390/pharmaceutics10030159

Gomes, D., Batista-Silva, J. P., Sousa, A., & Passarinha, L. A. (2023). Progress and opportunities in Gellan gum-based materials: A review of preparation, characterization and emerging applications. *Carbohydrate Polymers*, *311*, 120782. https://doi.org/https://doi.org/10.1016/j.carbpol.2023.120782

Gómez-Ordóñez, E., & Rupérez, P. (2011). FTIR-ATR spectroscopy as a tool for polysaccharide identification in edible brown and red seaweeds. *Food Hydrocolloids*, *25*(6), 1514–1520. https://doi.org/https://doi.org/10.1016/j.foodhyd.2011.02.009

Gościniak, A., Kocaj, F., Stasiłowicz-Krzemień, A., Szymański, M., Karpiński, T. M., & Cielecka-Piontek, J. (2024). 3D Printed Bigel: A Novel Delivery System for Cannabidiol-Rich Hemp Extract. *Gels*, *10*(12). https://doi.org/10.3390/gels10120770

Goyal, A. K., Singh, R., Chauhan, G., & Rath, G. (2018). Non-invasive systemic drug delivery through mucosal routes. *Artificial Cells, Nanomedicine, and Biotechnology*, *46*(sup2), 539–551. https://doi.org/10.1080/21691401.2018.1463230

Gratieri, T., Gelfuso, G. M., Rocha, E. M., Sarmento, V. H., de Freitas, O., & Lopez, R. F. V. (2010). A poloxamer/chitosan in situ forming gel with prolonged retention time for ocular delivery. *European Journal of Pharmaceutics and Biopharmaceutics*, *75*(2), 186–193. https://doi.org/https://doi.org/10.1016/j.ejpb.2010.02.011

Greer, G. R., Grob, C. S., & Halberstadt, A. L. (2014). PTSD Symptom Reports of Patients Evaluated for the New Mexico Medical Cannabis Program. *Journal of Psychoactive Drugs*, *46*(1), 73–77. https://doi.org/10.1080/02791072.2013.873843

Grijó, D. R., Rocha, E. M. T. d., Almeida, V. d. C., Amado, C. A. B., Olivo, J. E., & Lima, O. C. d. M. (2023). Experimental acute anti-inflammatory activity of preparations with complexed cannabidiol in carriers. *Brazilian Journal of Pharmaceutical Sciences*, *59*, e221000.

Guo, J., Dong, S., Ye, M., Wu, X., Lv, X., Xu, H., & Li, M. (2022). Effects of Hydroxypropyl Methylcellulose on Physicochemical Properties and Microstructure of κ-Carrageenan Film. *Foods*, *11*, 3023. https://doi.org/10.3390/foods11193023

Haller, J. (2024). Herbal Cannabis and Depression: A Review of Findings Published over the Last Three Years. *Pharmaceuticals*, *17*(6), 689.

Hanuš, L. O., & Hod, Y. (2020). Terpenes/Terpenoids in Cannabis: Are They Important? *Med Cannabis Cannabinoids*, *3*(1), 25–60. https://doi.org/10.1159/000509733

Harish, N. M., Prabhu, P., Charyulu, R. N., Gulzar, M. A., & Subrahmanyam, E. V. (2009). Formulation and Evaluation of in situ Gels Containing Clotrimazole for Oral Candidiasis. *Indian J Pharm Sci*, *71*(4), 421–427. https://doi.org/10.4103/0250-474x.57291

Haupts, M. R., Essner, U., & Mäurer, M. (2024). Patient-reported benefits from nabiximols treatment in multiple sclerosis-related spasticity exceed conventional measures. *Neurodegener Dis Manag*, *14*(1), 11–20. https://doi.org/10.2217/nmt-2023-0040

Hay, W. T., Fanta, G. F., Peterson, S. C., Thomas, A., Utt, K. D., Walsh, K. A., Boddu, V. M., & Selling, G. W. (2018). Improved hydroxypropyl methylcellulose (HPMC) films through incorporation of amylose-sodium palmitate inclusion complexes. *Carbohydrate Polymers*, *188*, 76–84.

Hazra, R., Alam, M. S. S., Malakar, A., Rakshit, P., Giri, T. K., Samanta, A., & Mukherjee, K. (2025). Metal ion crosslinked polysaccharide hydrogels: A review on their potential for therapeutic delivery and tissue engineering. *International Journal of Biological Macromolecules*, *310*, 143467. https://doi.org/https://doi.org/10.1016/j.ijbiomac.2025.143467

HB N, B. S., & Pawar, S. (2010). In-situ gel: new trends in controlled and sustained drug delivery system. *International Journal of PharmTech Research*, *2*(2), 1398–1408.

He, S., & Mu, H. (2023). Microenvironmental pH Modification in Buccal/Sublingual Dosage Forms for Systemic Drug Delivery. *Pharmaceutics*, *15*(2). https://doi.org/10.3390/pharmaceutics15020637

Hermush, V., Mizrahi, N., Brodezky, T., & Ezra, R. (2025). Enhancing cannabinoid bioavailability: a crossover study comparing a novel self-nanoemulsifying drug delivery system and a commercial oil-based formulation. *Journal of Cannabis Research*, *7*(1), 35. https://doi.org/10.1186/s42238-025-00294-8

Hossain, K. R., Alghalayini, A., & Valenzuela, S. M. (2023). Current Challenges and Opportunities for Improved Cannabidiol Solubility. *Int J Mol Sci*, *24*(19). https://doi.org/10.3390/ijms241914514

Hossain, M. L., Nguyen, M., Benington, L., Lim, L. Y., Hammer, K., Hettiarachchi, D., & Locher, C. (2023). Application of a Customised Franz-Type Cell Coupled with HPTLC to Monitor the Timed Release of Bioactive Components in Complex Honey Matrices. *Methods Protoc*, *6*(4). https://doi.org/10.3390/mps6040070

Howlett, A. C., Barth, F., Bonner, T. I., Cabral, G., Casellas, P., Devane, W. A., Felder, C. C., Herkenham, M., Mackie, K., Martin, B. R., Mechoulam, R., & Pertwee, R. G. (2002). International Union of Pharmacology. XXVII. Classification of cannabinoid receptors. *Pharmacol Rev*, *54*(2), 161–202. https://doi.org/10.1124/pr.54.2.161

Hu, Z., Qin, Z., Xie, J., Qu, Y., & Yin, L. (2024). Cannabidiol and its application in the treatment of oral diseases: therapeutic potentials, routes of administration and prospects. *Biomedicine & Pharmacotherapy*, *176*, 116271. https://doi.org/https://doi.org/10.1016/j.biopha.2024.116271

Hua, S. (2019). Advances in Nanoparticulate Drug Delivery Approaches for Sublingual and Buccal Administration [Mini Review]. *Frontiers in Pharmacology*, *10*(1328). https://doi.org/10.3389/fphar.2019.01328

Huang, H., Qi, X., Chen, Y., & Wu, Z. (2019). Thermo-sensitive hydrogels for delivering biotherapeutic molecules: A review. *Saudi Pharmaceutical Journal*, *27*(7), 990–999. https://doi.org/https://doi.org/10.1016/j.jsps.2019.08.001

Huang, Y., Yang, N., Zhang, Y., Hou, J., Gao, Y., Tian, L., Jin, Z., Shen, Y., & Guo, S. (2021). The gelling behavior of gellan in the presence of different sodium salts. *International Journal of Biological Macromolecules*, *193*, 768–777. https://doi.org/https://doi.org/10.1016/j.ijbiomac.2021.10.173

Huestis, M. A. (2007). Human cannabinoid pharmacokinetics. *Chemistry & biodiversity*, *4*(8), 1770.

Huestis, M. A., Solimini, R., Pichini, S., Pacifici, R., Carlier, J., & Busardò, F. P. (2019). Cannabidiol Adverse Effects and Toxicity. *Curr Neuropharmacol*, *17*(10), 974–989. https://doi.org/10.2174/1570159x17666190603171901

Israni, D. K., Raghani, N. R., Soni, J., Shah, M., Prajapati, B. G., Chorawala, M. R., Mangmool, S., Singh, S., & Chittasupho, C. (2024). Harnessing Cannabis sativa Oil for Enhanced Skin Wound Healing: The Role of Reactive Oxygen Species Regulation. *Pharmaceutics*, *16*(10), 1277.

Itin, C., Barasch, D., Domb, A. J., & Hoffman, A. (2020). Prolonged oral transmucosal delivery of highly lipophilic drug cannabidiol. *International Journal of Pharmaceutics*, *581*, 119276. https://doi.org/https://doi.org/10.1016/j.ijpharm.2020.119276

Itin, C., Domb, A. J., & Hoffman, A. (2019). A meta-opinion: cannabinoids delivered to oral mucosa by a spray for systemic absorption are rather ingested into gastro-intestinal tract: the influences of fed / fasting states. *Expert Opinion on Drug Delivery*, *16*(10), 1031–1035. https://doi.org/10.1080/17425247.2019.1653852

Jabeen, F., Zil, E. A., Ahmad, R., Mir, S., Awwad, N. S., & Ibrahium, H. A. (2025). Carrageenan: structure, properties and applications with special emphasis on food science. *RSC Adv*, *15*(27), 22035–22062. https://doi.org/10.1039/d5ra03296b

Jacob, S., Nair, A. B., Boddu, S. H., Gorain, B., Sreeharsha, N., & Shah, J. (2021). An Updated Overview of the Emerging Role of Patch and Film-Based Buccal Delivery Systems. *Pharmaceutics*, *13*(8), 1206.

Jacob, S., Nair, A. B., Boddu, S. H. S., Gorain, B., Sreeharsha, N., & Shah, J. (2021). An Updated Overview of the Emerging Role of Patch and Film-Based Buccal Delivery Systems. *Pharmaceutics*, *13*(8). https://doi.org/10.3390/pharmaceutics13081206

Jaidee, W., Siridechakorn, I., Nessopa, S., Wisuitiprot, V., Chaiwangrach, N., Ingkaninan, K., & Waranuch, N. (2022). Kinetics of CBD, Δ9-THC Degradation and Cannabinol Formation in Cannabis Resin at Various Temperature and pH Conditions. *Cannabis and Cannabinoid Research*, *7*(4), 537–547. https://doi.org/10.1089/can.2021.0004

Jain, D., Kumar, V., Singh, S., Mullertz, A., & Bar-Shalom, D. (2016). Newer trends in in situ gelling systems for controlled ocular drug delivery. *J Anal Pharm Res*, *2*(3), 00022.

Jaipal, A., Pandey, M. M., Charde, S. Y., Raut, P. P., Prasanth, K. V., & Prasad, R. G. (2015). Effect of HPMC and mannitol on drug release and bioadhesion behavior of buccal discs of buspirone hydrochloride: In-vitro and in-vivo pharmacokinetic studies. *Saudi Pharm J*, *23*(3), 315–326. https://doi.org/10.1016/j.jsps.2014.11.012

Jarho, P., Pate, D. W., Brenneisen, R., & Järvinen, T. (1998). Hydroxypropyl-β-cyclodextrin and its combination with hydroxypropyl-methylcellulose increases aqueous solubility of Δ9-tetrahydrocannabinol. *Life Sciences*, *63*(26), PL381–PL384.

Jelvehgari, M., Valizadeh, H., Ziapour, S., Rahmani, M., Montazam, S. H., & Soltani, S. (2016). Comparative study of different combinational mucoadhesive formulations of sumatriptan-metoclopramide. *Advanced pharmaceutical bulletin*, *6*(1), 119.

Jennotte, O., Koch, N., Lechanteur, A., & Evrard, B. (2023). Formulation and quality consideration of cannabidiol printed forms produced by fused-deposition modeling. *Journal of Drug Delivery Science and Technology*, *87*, 104837. https://doi.org/https://doi.org/10.1016/j.jddst.2023.104837

Jeong, M., Lee, S., Seo, C., Kwon, E., Rho, S., Cho, M., Kim, M. Y., Lee, W., Lee, Y. S., & Hong, J. (2023). Chemical transformation of cannabidiol into psychotropic cannabinoids under acidic reaction conditions: Identification of transformed products by GC-MS. *J Food Drug Anal*, *31*(1), 165–176. https://doi.org/10.38212/2224-6614.3452

Johal, H., Devji, T., Chang, Y., Simone, J., Vannabouathong, C., & Bhandari, M. (2020). Cannabinoids in chronic non-cancer pain: a systematic review and meta-analysis. *Clinical Medicine Insights: Arthritis and Musculoskeletal Disorders*, *13*, 1179544120906461.

Johnson, D. A., Funnell, M. P., Heaney, L. M., Cable, T. G., Wheeler, P. C., Bailey, S. J., Clifford, T., & James, L. J. (2024). Cannabidiol Oil Ingested as Sublingual Drops or Within Gelatin Capsules Shows Similar Pharmacokinetic Profiles in Healthy Males. *Cannabis and Cannabinoid Research*, *9*(5), e1423–e1432. https://doi.org/10.1089/can.2023.0117

Jones, D. S., Bruschi, M. L., de Freitas, O., Gremião, M. P. D., Lara, E. H. G., & Andrews, G. P. (2009). Rheological, mechanical and mucoadhesive properties of thermoresponsive, bioadhesive binary mixtures composed of poloxamer 407 and carbopol 974P designed as platforms for implantable

drug delivery systems for use in the oral cavity. *International Journal of Pharmaceutics*, *372*(1), 49–58. https://doi.org/https://doi.org/10.1016/j.ijpharm.2009.01.006

Joshi, N., Mariam, H., & Kamath, A. (2024). Cannabinoids for the treatment of glaucoma: a review. *Medical Cannabis and Cannabinoids*, 1–21. https://doi.org/10.1159/000541461

Jovanović, M., Petrović, M., Cvijić, S., Tomić, N., Stojanović, D., Ibrić, S., & Uskoković, P. (2021). 3D Printed Buccal Films for Prolonged-Release of Propranolol Hydrochloride: Development, Characterization and Bioavailability Prediction. *Pharmaceutics*, *13*(12). https://doi.org/10.3390/pharmaceutics13122143

Kailash, A., & Rahul, S. (2023). Preformulation Studies: A Versatile Tool in Formulation Design. In S. Rahul, K. Aleksey, & A. Akbar (Eds.), *Drug Formulation Design* (pp. Ch. 1). IntechOpen. https://doi.org/10.5772/intechopen.110346

Kalant, H. (2001). Medicinal Use of Cannabis: History and Current Status. *Pain Research and Management*, *6*(2), 469629. https://doi.org/https://doi.org/10.1155/2001/469629

Kalsi, G., Hazarika, U., Baruah, L. D., Bordoloi, P. L., & Gogoi, M. (2025). Comprehensive review of carrageenan's multifaceted role in health and food systems. *Discover Food*, *5*(1), 115. https://doi.org/10.1007/s44187-025-00405-7

Kamatou, G. P. P., Vermaak, I., Viljoen, A. M., & Lawrence, B. M. (2013). Menthol: A simple monoterpene with remarkable biological properties. *Phytochemistry*, *96*, 15–25. https://doi.org/https://doi.org/10.1016/j.phytochem.2013.08.005

Kang, C. Y. X., Chow, K. T., Lui, Y. S., Salome, A., Boit, B., Lefevre, P., Hiew, T. N., Gokhale, R., & Heng, P. W. S. (2024). Mannitol-Coated Hydroxypropyl Methylcellulose as a Directly Compressible Controlled Release Excipient for Moisture-Sensitive Drugs: A Stability Perspective. *Pharmaceuticals (Basel)*, *17*(9). https://doi.org/10.3390/ph17091167

Kang, L., Kumar, V. H., Lim, P. F. C., Cheong, H. H., & Chan, S. Y. (2013). Terpenes and Improvement of Transdermal Drug Delivery. In K. G. Ramawat & J.-M. Mérillon (Eds.), *Natural Products: Phytochemistry, Botany and Metabolism of Alkaloids, Phenolics and Terpenes* (pp. 3757–3774). Springer Berlin Heidelberg. https://doi.org/10.1007/978-3-642-22144-6_160

Karavasili, C., & Fatouros, D. G. (2016). Smart materials: in situ gel-forming systems for nasal delivery. *Drug Discovery Today*, *21*(1), 157–166. https://doi.org/https://doi.org/10.1016/j.drudis.2015.10.016

Karki, S., Kim, H., Na, S.-J., Shin, D., Jo, K., & Lee, J. (2016). Thin films as an emerging platform for drug delivery. *Asian Journal of Pharmaceutical Sciences*, *11*(5), 559–574. https://doi.org/https://doi.org/10.1016/j.ajps.2016.05.004

Karschner, E. L., Darwin, W. D., Goodwin, R. S., Wright, S., & Huestis, M. A. (2011). Plasma cannabinoid pharmacokinetics following controlled oral delta9-tetrahydrocannabinol and oromucosal cannabis extract administration. *Clinical chemistry*, *57*(1), 66–75. https://doi.org/10.1373/clinchem.2010.152439

Kaszyńska, A. A. (2024). Cannabinoids: Potential for Modulation and Enhancement When Combined with Vitamin B12 in Case of Neurodegenerative Disorders. *Pharmaceuticals*, *17*(6), 813.

Khan, N. A., Khan, A., Ullah, R., Ullah, M., Alotaibi, A., Ullah, R., & Haider, A. (2022). Preparation and Characterization of Hydrophilic Polymer Based Sustained-Release Matrix Tablets of a High Dose Hydrophobic Drug. *Polymers (Basel)*, *14*(10). https://doi.org/10.3390/polym14101985

Khutoryanskiy, V. V. (2011). Advances in mucoadhesion and mucoadhesive polymers. *Macromol Biosci*, *11*(6), 748–764. https://doi.org/10.1002/mabi.201000388

Kianfar, F., Antonijevic, M., Chowdhry, B., & Boateng, J. S. (2013). Lyophilized wafers comprising carrageenan and pluronic acid for buccal drug delivery using model soluble and insoluble drugs. *Colloids Surf B Biointerfaces*, *103*, 99–106. https://doi.org/10.1016/j.colsurfb.2012.10.006

Kirk, R. D., Akanji, T., Li, H., Shen, J., Allababidi, S., Seeram, N. P., Bertin, M. J., & Ma, H. (2022). Evaluations of Skin Permeability of Cannabidiol and Its Topical Formulations by Skin Membrane-Based Parallel Artificial Membrane Permeability Assay and Franz Cell Diffusion Assay. *Med Cannabis Cannabinoids*, *5*(1), 129–137. https://doi.org/10.1159/000526769

Knaub, K., Sartorius, T., Dharsono, T., Wacker, R., Wilhelm, M., & Schön, C. (2019). A Novel Self-Emulsifying Drug Delivery System (SEDDS) Based on VESIsorb(®) Formulation Technology Improving the Oral Bioavailability of Cannabidiol in Healthy Subjects. *Molecules (Basel, Switzerland)*, *24*(16), 2967. https://doi.org/10.3390/molecules24162967

Kocis, P. T., & Vrana, K. E. (2020). Delta-9-Tetrahydrocannabinol and Cannabidiol Drug-Drug Interactions. *Medical Cannabis and Cannabinoids*, *3*(1), 61–73. https://doi.org/10.1159/000507998

Kolawole, O. M., & Cook, M. T. (2023). In situ gelling drug delivery systems for topical drug delivery. *European Journal of Pharmaceutics and Biopharmaceutics*, *184*, 36–49. https://doi.org/https://doi.org/10.1016/j.ejpb.2023.01.007

Kondaveeti, S., Damato, T. C., Carmona-Ribeiro, A. M., Sierakowski, M. R., & Petri, D. F. (2017). Sustainable hydroxypropyl methylcellulose/xyloglucan/gentamicin films with antimicrobial properties. *Carbohydr Polym*, *165*, 285–293. https://doi.org/10.1016/j.carbpol.2017.02.066

Krese, A., Kovačič, N. N., Kapele, T., Mrhar, A., & Bogataj, M. (2016). Influence of ionic strength and HPMC viscosity grade on drug release and swelling behavior of HPMC matrix tablets. *Journal of Applied Polymer Science*, *133*(26). https://doi.org/https://doi.org/10.1002/app.43604

Kulkarni, V. R., Saha, T., Raj Giri, B., Lu, A., Das, S. C., & Maniruzzaman, M. (2024). Recent Advancements in Pharmaceutical 3D Printing Industry. *Journal of Drug Delivery Science and Technology*, *100*, 106072. https://doi.org/https://doi.org/10.1016/j.jddst.2024.106072

Kuzumi, A., Yamashita, T., Fukasawa, T., Yoshizaki-Ogawa, A., Sato, S., & Yoshizaki, A. (2024). Cannabinoids for the treatment of autoimmune and inflammatory skin diseases: A systematic review. *Experimental Dermatology*, *33*(3), e15064. https://doi.org/https://doi.org/10.1111/exd.15064

Laffleur, F., & Keckeis, V. (2020). Advances in drug delivery systems: Work in progress still needed? *International Journal of Pharmaceutics*, *590*, 119912. https://doi.org/https://doi.org/10.1016/j.ijpharm.2020.119912

Lakkala, P., Munnangi, S. R., Bandari, S., & Repka, M. (2023). Additive manufacturing technologies with emphasis on stereolithography 3D printing in pharmaceutical and medical applications: A review. *International Journal of Pharmaceutics: X*, *5*, 100159. https://doi.org/https://doi.org/10.1016/j.ijpx.2023.100159

Lam, J. K. W., Cheung, C. C. K., Chow, M. Y. T., Harrop, E., Lapwood, S., Barclay, S. I. G., & Wong, I. C. K. (2020). Transmucosal drug administration as an alternative route in palliative and end-of-life care during the COVID-19 pandemic. *Advanced drug delivery reviews*, *160*, 234–243. https://doi.org/10.1016/j.addr.2020.10.018

Landová, H., Daněk, Z., Gajdziok, J., Vetchý, D., & Stembírek, J. (2013). Mucoadhesive films as perspective oral dosage form. *Ceska Slov Farm*, *62*(1), 4–11.

Laoasoke, W., Choipang, C., Chaiarwut, S., Suwantong, O., Chuysinuan, P., Techasakul, S., Sangsanoh, P., & Supaphol, P. (2024). Preparation and Characterization of Hydroxypropyl Methylcellulose/Polyvinyl Alcohol Mucoadhesive Buccal Film of Cannabidiol. *Journal of Polymers and the Environment*, *32*(7), 3061–3070. https://doi.org/10.1007/s10924-023-03160-x

Laprairie, R., Bagher, A., Kelly, M., & Denovan-Wright, E. (2015). Cannabidiol is a negative allosteric modulator of the cannabinoid CB1 receptor. *British journal of pharmacology*, *172*(20), 4790–4805.

Lazarjani, M., Seyfoddin, A., Le, T. T., & Chen, T. (2024). Development and validation of HPLC and GC methods for quantification of cannabinoids and terpenes extracted by ultrasound assisted extraction technique. *Drug Analytical Research*, *8*(1), 33–45.

Lee, H.-S., Tamia, G., Song, H.-J., Amarakoon, D., Wei, C.-I., & Lee, S.-H. (2022). Cannabidiol exerts anti-proliferative activity via a cannabinoid receptor 2-dependent mechanism in human colorectal cancer cells. *International immunopharmacology*, *108*, 108865.

Lee, J.-H., Park, C., Song, I.-O., Lee, B.-J., Kang, C.-Y., & Park, J.-B. (2022). Investigation of Patient-Centric 3D-Printed Orodispersible Films Containing Amorphous Aripiprazole. *Pharmaceuticals*, *15*(7), 895.

Li, A., Khan, I. N., Khan, I. U., Yousaf, A. M., & Shahzad, Y. (2021). Gellan Gum-Based Bilayer Mucoadhesive Films Loaded with Moxifloxacin Hydrochloride and Clove Oil for Possible Treatment of Periodontitis. *Drug design, development and therapy*, *15*, 3937–3952. https://doi.org/10.2147/dddt.S328722

Li, H., Chang, S.-L., Chang, T.-R., You, Y., Wang, X.-D., Wang, L.-W., Yuan, X.-F., Tan, M.-H., Wang, P.-D., Xu, P.-W., Gao, W.-B., Zhao, Q.-S., & Zhao, B. (2021). Inclusion complexes of cannabidiol with β-cyclodextrin and its derivative: Physicochemical properties, water solubility, and antioxidant activity. *Journal of Molecular Liquids*, *334*, 116070. https://doi.org/https://doi.org/10.1016/j.molliq.2021.116070

Li, H., Zhao, Q.-S., Chang, S.-L., Chang, T.-R., Tan, M.-H., & Zhao, B. (2022). Development of cannabidiol full-spectrum oil/2,6-di-O-methyl-β-cyclodextrin inclusion complex with enhanced water solubility, bioactivity, and thermal stability. *Journal of Molecular Liquids*, *347*, 118318. https://doi.org/https://doi.org/10.1016/j.molliq.2021.118318

Li, K. L., & Castillo, A. L. (2020). Formulation and evaluation of a mucoadhesive buccal tablet of mefenamic acid. *Brazilian Journal of Pharmaceutical Sciences*, *56*, e18575.

Li, T., Bao, Q., Shen, J., Lalla, R. V., & Burgess, D. J. (2020). Mucoadhesive in situ forming gel for oral mucositis pain control. *International Journal of Pharmaceutics*, *580*, 119238. https://doi.org/https://doi.org/10.1016/j.ijpharm.2020.119238

Liang, J., Peng, X., Zhou, X., Zou, J., & Cheng, L. (2020). Emerging Applications of Drug Delivery Systems in Oral Infectious Diseases Prevention and Treatment. *Molecules (Basel, Switzerland)*, *25*(3), 516. https://doi.org/10.3390/molecules25030516

Liu, J., Zhan, X., Wan, J., Wang, Y., & Wang, C. (2015). Review for carrageenan-based pharmaceutical biomaterials: Favourable physical features versus adverse biological effects. *Carbohydrate Polymers*, *121*, 27–36. https://doi.org/https://doi.org/10.1016/j.carbpol.2014.11.063

Longgos, L. D., Pequiro, E. B., Liston, L. S. B., Flores, K. A. M., Ecoy, G. A. U., Sakdiset, P., See, G. L. L., & Arce, F. V., Jr. (2024). Effect of Terpenes on the Enhancement of Skin Permeation of Lipophilic Drugs: A Systematic Review. *Acta Med Philipp*, *58*(4), 59–71. https://doi.org/10.47895/amp.vi0.6505

Lorenzl, S., Gottwald, F., Nistler, A., Brehm, L., Grötsch, R., Haber, G., Bremm, C., Weck, C., Trummer, C., & Brand, W. (2022). A Phase I Trial to Determine the Pharmacokinetics, Psychotropic Effects, and Safety Profile of a Novel Nanoparticle-Based Cannabinoid Spray for Oromucosal Delivery. *Med Cannabis Cannabinoids*, *5*(1), 9–19. https://doi.org/10.1159/000521352

Low, Z. X. B., Lee, X. R., Soga, T., Goh, B. H., Alex, D., & Kumari, Y. (2023). Cannabinoids: Emerging sleep modulator. *Biomedicine & Pharmacotherapy*, *165*, 115102. https://doi.org/https://doi.org/10.1016/j.biopha.2023.115102

Lowe, H., Steele, B., Bryant, J., Toyang, N., & Ngwa, W. (2021). Non-Cannabinoid Metabolites of Cannabis sativa L. with Therapeutic Potential. *Plants (Basel)*, *10*(2). https://doi.org/10.3390/plants10020400

Lu, H.-C., & Mackie, K. (2016). An Introduction to the Endogenous Cannabinoid System. *Biological psychiatry*, *79*(7), 516–525. https://doi.org/10.1016/j.biopsych.2015.07.028

Lucas, C. J., Galettis, P., & Schneider, J. (2018). The pharmacokinetics and the pharmacodynamics of cannabinoids. *British journal of clinical pharmacology*, *84*(11), 2477–2482.

Lucas, C. J., Galettis, P., & Schneider, J. (2018). The pharmacokinetics and the pharmacodynamics of cannabinoids. *Br J Clin Pharmacol*, *84*(11), 2477–2482. https://doi.org/10.1111/bcp.13710

Lucas, P., Walsh, Z., Crosby, K., Callaway, R., Belle-Isle, L., Kay, R., Capler, R., & Holtzman, S. (2016). Substituting cannabis for prescription drugs, alcohol and other substances among medical cannabis patients: The impact of contextual factors. *Drug and alcohol review*, *35*(3), 326–333.

Łyszczarz, E., Brniak, W., Szafraniec-Szczęsny, J., Majka, T. M., Majda, D., Zych, M., Pielichowski, K., & Jachowicz, R. (2021). The Impact of the Preparation Method on the Properties of Orodispersible Films with Aripiprazole: Electrospinning vs. Casting and 3D Printing Methods. *Pharmaceutics*, *13*(8). https://doi.org/10.3390/pharmaceutics13081122

M.A. Fathalla, Z., Vangala, A., Longman, M., Khaled, K. A., Hussein, A. K., El-Garhy, O. H., & Alany, R. G. (2017). Poloxamer-based thermoresponsive ketorolac tromethamine in situ gel preparations: Design, characterisation, toxicity and transcorneal permeation studies. *European Journal of Pharmaceutics and Biopharmaceutics*, *114*, 119–134. https://doi.org/https://doi.org/10.1016/j.ejpb.2017.01.008

Ma, L., Liu, M., Liu, C., Zhang, H., Yang, S., An, J., Qu, G., Song, S., & Cao, Q. (2024). Research Progress on the Mechanism of the Antitumor Effects of Cannabidiol. *Molecules*, *29*(9), 1943.

MacCallum, C. A., & Russo, E. B. (2018). Practical considerations in medical cannabis administration and dosing. *European Journal of Internal Medicine*, *49*, 12–19. https://doi.org/https://doi.org/10.1016/j.ejim.2018.01.004

Mahajan, A., Chhabra, N., & Aggarwal, G. (2011). Formulation and characterization of fast dissolving buccal films: A review. *Der Pharmacia Lettre*, *3*(1), 152–165.

Mahajan, H. S., & Gattani, S. (2010). In situ gels of Metoclopramide Hydrochloride for intranasal delivery: In vitro evaluation and in vivo pharmacokinetic study in rabbits. *Drug delivery*, *17*(1), 19–27. https://doi.org/10.3109/10717540903447194

Mahajan, N., Shende, S., Dumore, N., & Nasare, L. (2019). Development and evaluation of ion induced in situ gelling system of opoid analgesic for nose to brain delivery. *Research Journal of Pharmacy and Technology*, *12*(10), 4741–4746.

Mahdi, M. H., Conway, B. R., & Smith, A. M. (2014). Evaluation of gellan gum fluid gels as modified release oral liquids. *International Journal of Pharmaceutics*, *475*(1-2), 335–343.

Mahmood, A., Mahmood, A., Ibrahim, M. A., Hussain, Z., Ashraf, M. U., Salem-Bekhit, M. M., & Elbagory, I. (2023). Development and Evaluation of Sodium Alginate/Carbopol 934P-Co-Poly (Methacrylate) Hydrogels for Localized Drug Delivery. *Polymers (Basel)*, *15*(2). https://doi.org/10.3390/polym15020311

Mahmood, M. A. (2021). 3D Printing in Drug Delivery and Biomedical Applications: A State-of-the-Art Review. *Compounds*, *1*(3), 94–115.

Makharadze, D., del Valle, L. J., Katsarava, R., & Puiggalí, J. (2025). The Art of PEGylation: From Simple Polymer to Sophisticated Drug Delivery System. *International Journal of Molecular Sciences*, *26*(7), 3102.

Mannila, J., Järvinen, T., Järvinen, K., & Jarho, P. (2007). Precipitation complexation method produces cannabidiol/β-cyclodextrin inclusion complex suitable for sublingual administration of cannabidiol.

Journal of Pharmaceutical Sciences, *96*(2), 312–319. https://doi.org/https://doi.org/10.1002/jps.20766

Mannila, J., Järvinen, T., Järvinen, K., Tarvainen, M., & Jarho, P. (2005). Effects of RM-β-CD on sublingual bioavailability of Δ9-tetrahydrocannabinol in rabbits. *European Journal of Pharmaceutical Sciences*, *26*(1), 71–77. https://doi.org/https://doi.org/10.1016/j.ejps.2005.04.020

Mannila, J., Järvinen, T., Järvinen, K., Tervonen, J., & Jarho, P. (2006). Sublingual administration of Δ9-tetrahydrocannabinol/β-cyclodextrin complex increases the bioavailability of Δ9-tetrahydrocannabinol in rabbits. *Life Sciences*, *78*, 1911–1914. https://doi.org/10.1016/j.lfs.2005.08.025

Marques, B. L., & Campos, A. C. (2024). Chapter Six - Cannabidiol and Alzheimer's disease. In E. Del-Bel, F. V. Gomes, & S. F. Lisboa (Eds.), *International Review of Neurobiology* (Vol. 177, pp. 121–134). Academic Press. https://doi.org/https://doi.org/10.1016/bs.irn.2024.04.014

Matarazzo, A. P., Elisei, L. M. S., Carvalho, F. C., Bonfílio, R., Ruela, A. L. M., Galdino, G., & Pereira, G. R. (2021). Mucoadhesive nanostructured lipid carriers as a cannabidiol nasal delivery system for the treatment of neuropathic pain. *European Journal of Pharmaceutical Sciences*, *159*, 105698. https://doi.org/https://doi.org/10.1016/j.ejps.2020.105698

Maver, U., & Maver, T. (2022). The importance of the correct choice of Franz diffusion cell volume for in vitro drug release testing of wound dressings. *Acta Medico-Biotechnica*, *15*(2), 41–48.

Mayol, L., Quaglia, F., Borzacchiello, A., Ambrosio, L., & La Rotonda, M. I. (2008). A novel poloxamers/hyaluronic acid in situ forming hydrogel for drug delivery: Rheological, mucoadhesive and in vitro release properties. *European Journal of Pharmaceutics and Biopharmaceutics*, *70*(1), 199–206.

Mechoulam, R., & Parker, L. A. (2013). The endocannabinoid system and the brain. *Annual review of psychology*, *64*(1), 21–47.

Meher, J., Yadav, N., Yadav, K., & Rai, V. (2012). Buccal Drug Delivery System and Penetration Enhancer: A Review. *The Pharma Review*, *10*, 113–117.

Mendyk, A., Jachowicz, R., Fijorek, K., Dorożyński, P., Kulinowski, P. P., & Polak, S. (2012). KinetDS: An Open Source Software for Dissolution Test Data Analysis. *Dissolution Technologies*, *19*. https://doi.org/10.14227/DT190112P6

Mikuriya, T. H. (1969). Marijuana in medicine: past, present and future. *Calif Med*, *110*(1), 34–40.

Millar, S. A., Stone, N. L., Yates, A. S., & O'Sullivan, S. E. (2018). A Systematic Review on the Pharmacokinetics of Cannabidiol in Humans [Original Research]. *Frontiers in Pharmacology*, *9*(1365). https://doi.org/10.3389/fphar.2018.01365

Milliken, R. L., Quinten, T., Andersen, S. K., & Lamprou, D. A. (2024). Application of 3D printing in early phase development of pharmaceutical solid dosage forms. *International Journal of Pharmaceutics*, *653*, 123902. https://doi.org/https://doi.org/10.1016/j.ijpharm.2024.123902

Ministry of Health. (2025). Medicinal cannabis products that meet the minimum quality standard.

Mohamed, F. A., Roberts, M., Seton, L., Ford, J. L., Levina, M., & Rajabi-Siahboomi, A. R. (2013). The influence of HPMC concentration on release of theophylline or hydrocortisone from extended release mini-tablets. *Drug Dev Ind Pharm*, *39*(8), 1167–1174. https://doi.org/10.3109/03639045.2012.681053

Mohammad Hamdi, N. A., Azmi, N., Sabari, N., Harun Ismail, A. F., & Haris, M. S. (2023). An insight into the use and advantages of Carbopol in topical mucoadhesive drug delivery system: A systematic review. *Journal of Pharmacy*, *3*, 53–65. https://doi.org/10.31436/jop.v3i1.156

Mohammad Hamdi, N. A., Azmi, N. A., Mohd Sabari, N. H., Harun, A. F., & Haris, M. S. (2023). An insight into the use and advantages of Carbopol in topical mucoadhesive drug delivery system: A systematic review. *Journal of Pharmacy*, *3*(1), 53–65. https://doi.org/10.31436/jop.v3i1.156

Mohananaidu, K., Chatterjee, B., Mohamed, F., Mahmood, S., & Hamed Almurisi, S. (2022). Thermoreversible Carbamazepine In Situ Gel for Intranasal Delivery: Development and In Vitro, Ex Vivo Evaluation. *AAPS PharmSciTech*, *23*(8), 288. https://doi.org/10.1208/s12249-022-02439-x

Mokhtari, H., Tavakoli, S., Safarpour, F., Kharaziha, M., Bakhsheshi-Rad, H. R., Ramakrishna, S., & Berto, F. (2021). Recent Advances in Chemically-Modified and Hybrid Carrageenan-Based Platforms for Drug Delivery, Wound Healing, and Tissue Engineering. *Polymers (Basel)*, *13*(11). https://doi.org/10.3390/polym13111744

Monou, P. K., Mamaligka, A. M., Tzimtzimis, E. K., Tzetzis, D., Vergkizi-Nikolakaki, S., Vizirianakis, I. S., Andriotis, E. G., Eleftheriadis, G. K., & Fatouros, D. G. (2022). Fabrication and Preliminary In Vitro Evaluation of 3D-Printed Alginate Films with Cannabidiol (CBD) and Cannabigerol (CBG) Nanoparticles for Potential Wound-Healing Applications. *Pharmaceutics*, *14*(8). https://doi.org/10.3390/pharmaceutics14081637

Monou, P. K., Mamaligka, A. M., Tzimtzimis, E. K., Tzetzis, D., Vergkizi-Nikolakaki, S., Vizirianakis, I. S., Andriotis, E. G., Eleftheriadis, G. K., & Fatouros, D. G. (2022). Fabrication and Preliminary In Vitro Evaluation of 3D-Printed Alginate Films with Cannabidiol (CBD) and Cannabigerol (CBG) Nanoparticles for Potential Wound-Healing Applications. *Pharmaceutics*, *14*(8), 1637.

Montero-Padilla, S., Velaga, S., & Morales, J. O. (2017). Buccal Dosage Forms: General Considerations for Pediatric Patients. *AAPS PharmSciTech*, *18*(2), 273–282. https://doi.org/10.1208/s12249-016-0567-2

Montgomery, D., & St, C. (2022). *Design and Analysis of Experiments, 9th Edition*.

Monton, C., Kulvanich, P., Chankana, N., Suksaeree, J., & Songsak, T. (2024). Fabrication of Orally Fast-Disintegrating Wafer Tablets Containing Cannabis Extract Using Freeze-Drying Method. *Medical Cannabis and Cannabinoids*, *7*(1), 51.

Morano, A., Fanella, M., Albini, M., Cifelli, P., Palma, E., Giallonardo, A. T., & Di Bonaventura, C. (2020). Cannabinoids in the Treatment of Epilepsy: Current Status and Future Prospects. *Neuropsychiatric Disease and Treatment*, *16*(null), 381–396. https://doi.org/10.2147/NDT.S203782

Morris, E. R., Nishinari, K., & Rinaudo, M. (2012). Gelation of gellan – A review. *Food Hydrocolloids*, *28*(2), 373–411. https://doi.org/https://doi.org/10.1016/j.foodhyd.2012.01.004

Narang, N., & Sharma, J. (2011). Sublingual mucosa as a route for systemic drug delivery. *Int J Pharm Pharm Sci*, *3*(Suppl 2), 18–22.

Necas, J., & Bartosikova, L. (2013). Carrageenan: a review [journal article]. *Veterinární medicína*, *58*(4), 187–205.

Ng, S. F., Rouse, J. J., Sanderson, F. D., Meidan, V., & Eccleston, G. M. (2010). Validation of a static Franz diffusion cell system for in vitro permeation studies. *AAPS PharmSciTech*, *11*(3), 1432–1441. https://doi.org/10.1208/s12249-010-9522-9

Nicolazzo, J. A., Reed, B. L., & Finnin, B. C. (2005). Buccal penetration enhancers—How do they really work? *Journal of Controlled Release*, *105*(1), 1–15. https://doi.org/https://doi.org/10.1016/j.jconrel.2005.01.024

Nono, M., Durand, D., & Nicolai, T. (2012). Rheology and structure of mixtures of ι-carrageenan and sodium caseinate. *Food Hydrocolloids*, *27*(1), 235–241. https://doi.org/https://doi.org/10.1016/j.foodhyd.2011.07.002

O'Connell, B. K., Gloss, D., & Devinsky, O. (2017). Cannabinoids in treatment-resistant epilepsy: A review. *Epilepsy & Behavior*, *70*, 341–348. https://doi.org/https://doi.org/10.1016/j.yebeh.2016.11.012

O'Sullivan, S. E., Jensen, S. S., Kolli, A. R., Nikolajsen, G. N., Bruun, H. Z., & Hoeng, J. (2024). Strategies to Improve Cannabidiol Bioavailability and Drug Delivery. *Pharmaceuticals*, *17*(2), 244.

Odziomek, K., Drabczyk, A. K., Kościelniak, P., Konieczny, P., Barczewski, M., & Bialik-Wąs, K. (2024). The Role of Freeze-Drying as a Multifunctional Process in Improving the Properties of Hydrogels for Medical Use. *Pharmaceuticals (Basel)*, *17*(11). https://doi.org/10.3390/ph17111512

Özyılmaz, E., Mavideniz, A., & Nobavar, Z. (2024). Comparison of In Vitro Ibuprofen Release Rates from HPMC and Carbopol® Gels. *EMU Journal of Pharmaceutical Sciences*, *7*. https://doi.org/10.54994/emujpharmsci.1530626

Özyılmaz, E. D., Mavideniz, A., & Nobavar, Z. (2024). Comparison of In Vitro Ibuprofen Release Rates from HPMC and Carbopol® Gels. *EMU Journal of Pharmaceutical Sciences*, *7*(2), 40–47.

Paccione, N., Guarnizo-Herrero, V., Ramalingam, M., Larrarte, E., & Pedraz, J. L. (2024). Application of 3D printing on the design and development of pharmaceutical oral dosage forms. *Journal of Controlled Release*, *373*, 463–480. https://doi.org/https://doi.org/10.1016/j.jconrel.2024.07.035

Pacheco-Quito, E. M., Ruiz-Caro, R., & Veiga, M. D. (2020). Carrageenan: Drug Delivery Systems and Other Biomedical Applications. *Mar Drugs*, *18*(11). https://doi.org/10.3390/md18110583

Panraksa, P., Qi, S., Udomsom, S., Tipduangta, P., Rachtanapun, P., Jantanasakulwong, K., & Jantrawut, P. (2021). Characterization of Hydrophilic Polymers as a Syringe Extrusion 3D Printing Material for Orodispersible Film. *Polymers*, *13*(20), 3454.

Park, B. J., Choi, H. J., Moon, S. J., Kim, S. J., Bajracharya, R., Min, J. Y., & Han, H.-K. (2019). Pharmaceutical applications of 3D printing technology: current understanding and future perspectives. *Journal of Pharmaceutical Investigation*, *49*(6), 575–585. https://doi.org/10.1007/s40005-018-00414-y

Park, C., Zuo, J., Gil, M. C., Löbenberg, R., & Lee, B. J. (2023). Investigation of Cannabinoid Acid/Cyclodextrin Inclusion Complex for Improving Physicochemical and Biological Performance. *Pharmaceutics*, *15*(11). https://doi.org/10.3390/pharmaceutics15112533

Park, S., Mun, S., & Kim, Y. R. (2020). Influences of added surfactants on the water solubility and antibacterial activity of rosemary extract. *Food Sci Biotechnol*, *29*(10), 1373–1380. https://doi.org/10.1007/s10068-020-00792-w

Patel, V. F., Liu, F., & Brown, M. B. (2011). Advances in oral transmucosal drug delivery. *J Control Release*, *153*(2), 106–116. https://doi.org/10.1016/j.jconrel.2011.01.027

Patel, V. M., Prajapati, B. G., & Patel, M. M. (2007). Formulation, evaluation, and comparison of bilayered and multilayered mucoadhesive buccal devices of propranolol hydrochloride. *AAPS PharmSciTech*, *8*(1), E147–E154.

Pather, S. I., Rathbone, M. J., & Şenel, S. (2008). Current status and the future of buccal drug delivery systems. *Expert Opinion on Drug Delivery*, *5*(5), 531–542. https://doi.org/10.1517/17425247.5.5.531

Patil, K., & Pandey, A. (2024). A Simple and Rapid Spectro-Electrochemical Analysis of Delta-9 Tetrahydrocannabinol (δ9-thc) using Carbon and Platinum Screen Printed Electrodes. *Oriental Journal Of Chemistry*, *40*, 681–688. https://doi.org/10.13005/ojc/400307

Patil, R. R., Patil, A. S., Chougule, K., Patil, A. S., Ugare, P., & Masareddy, R. S. (2024). Exploring the Transformative Potential of In Situ Gels: An Overview of Thermosensitive and pH-Sensitive Gel Systems for Biomedical Applications. Macromolecular Symposia,

Patilea-Vrana, G. I., & Unadkat, J. D. (2019). Quantifying Hepatic Enzyme Kinetics of (-)-Δ⁹-Tetrahydrocannabinol (THC) and Its Psychoactive Metabolite, 11-OH-THC, through In Vitro Modeling. *Drug Metabolism and Disposition*, *47*(7), 743–752. https://doi.org/10.1124/dmd.119.086470

Patlolla, V. G. R., Holbrook, W. P., Gizurarson, S., & Kristmundsdottir, P. (2020). Evaluation of in vitro mucoadhesiveness and texture profile analysis of doxycycline in situ hydrogels. *Pharmazie*, *75*(1), 7–12. https://doi.org/10.1691/ph.2020.9122

Paul, S., Majumdar, S., Chakraborty, M., Mukherjee, S., Sarkar, N., Prajapati, B., Ali, N., AlAsmari, A. F., & Nishat, S. (2025). In-situ gel bases ocular delivery system of Ganciclovir, in-vivo and in-vitro investigation. *BMC Pharmacol Toxicol*, *26*(1), 102. https://doi.org/10.1186/s40360-025-00934-y

Peh, K. K., & Wong, C. F. (1999). Polymeric films as vehicle for buccal delivery: swelling, mechanical, and bioadhesive properties. *J Pharm Pharm Sci*, *2*(2), 53–61.

Peppas, N. A., & Sahlin, J. J. (1996). Hydrogels as mucoadhesive and bioadhesive materials: a review. *Biomaterials*, *17*(16), 1553–1561. https://doi.org/10.1016/0142-9612(95)00307-x

Pertwee, R. G. (2008). The diverse CB1 and CB2 receptor pharmacology of three plant cannabinoids: delta9-tetrahydrocannabinol, cannabidiol and delta9-tetrahydrocannabivarin. *British journal of pharmacology*, *153*(2), 199–215. https://doi.org/10.1038/sj.bjp.0707442

Perucca, E. (2017). Cannabinoids in the Treatment of Epilepsy: Hard Evidence at Last? *J Epilepsy Res*, *7*(2), 61–76. https://doi.org/10.14581/jer.17012

Peschel, W. (2016). Quality Control of Traditional Cannabis Tinctures: Pattern, Markers, and Stability. *Sci Pharm*, *84*(3), 567–584. https://doi.org/10.3390/scipharm84030567

Peters, J., & Chien, J. (2018). Contemporary Routes of Cannabis Consumption: A Primer for Clinicians. *Journal of Osteopathic Medicine*, *118*(2), 67–70. https://doi.org/doi:10.7556/jaoa.2018.020

Pinto, S., Pintado, M. E., & Sarmento, B. (2020). In vivo, ex vivo and in vitro assessment of buccal permeation of drugs from delivery systems. *Expert Opinion on Drug Delivery*, *17*(1), 33–48. https://doi.org/10.1080/17425247.2020.1699913

Pourseyed Lazarjani, M., Torres, S., Hooker, T., Fowlie, C., Young, O., & Seyfoddin, A. (2020). Methods for quantification of cannabinoids: a narrative review. *Journal of Cannabis Research*, *2*(1), 35. https://doi.org/10.1186/s42238-020-00040-2

Poyatos, L., Pérez-Acevedo, A. P., Papaseit, E., Pérez-Mañá, C., Martin, S., Hladun, O., Siles, A., Torrens, M., Busardo, F. P., & Farré, M. (2020). Oral Administration of Cannabis and Δ-9-tetrahydrocannabinol (THC) Preparations: A Systematic Review. *Medicina*, *56*(6), 309.

Prasad, A., Prasanthi, N., Durga, K., & Rao, M. (2016). FORMULATION AND EVALUATION OF GASTRORETENSIVE FLOATING TABLETS OF VENLAFAXINE HCl. *Indo American Journal of Pharmaceutical Research*, *6*, 6171–6181.

Prasannan, A., Joseph, S., & Abraham, E. (2018). Oral In Situ Gel; A Novel Drug Delivery System for Oral Diseases. *American Journal of PharmTech Research*, *8*, 1–8. https://doi.org/10.46624/ajptr.2018.v8.i3.001

Prasannan, A. M., Joseph, S., & Abraham, E. (2018). Oral In Situ Gel; A Novel Drug Delivery System for Oral Diseases.

Prasanthi, D., & Lakshmi, P. K. (2012). Terpenes: Effect of lipophilicity in enhancing transdermal delivery of alfuzosin hydrochloride. *J Adv Pharm Technol Res*, *3*(4), 216–223. https://doi.org/10.4103/2231-4040.104712

Provenzano, R., De Caro, C., Vitiello, A., Izzo, L., Ritieni, A., Ungaro, F., Quaglia, F., Russo, E., Miro, A., & d'Angelo, I. (2024). Enhancing transmucosal delivery of CBD through nanoemulsion: in vitro and in vivo studies. *Drug Delivery and Translational Research*, *14*(6), 1648–1659. https://doi.org/10.1007/s13346-023-01481-x

Qi, H., Chen, W., Huang, C., Li, L., Chen, C., Li, W., & Wu, C. (2007). Development of a poloxamer analogs/carbopol-based in situ gelling and mucoadhesive ophthalmic delivery system for puerarin. *International Journal of Pharmaceutics*, *337*(1), 178–187. https://doi.org/https://doi.org/10.1016/j.ijpharm.2006.12.038

Qian, L., Beers, J. L., Jackson, K. D., & Zhou, Z. (2024). CBD and THC in Special Populations: Pharmacokinetics and Drug–Drug Interactions. *Pharmaceutics*, *16*(4), 484.

Qian, L., Cook, M. T., & Dreiss, C. A. (2025). In Situ Gels for Nasal Delivery: Formulation, Characterization and Applications. *Macromolecular Materials and Engineering*, *310*(6), 2400356. https://doi.org/https://doi.org/10.1002/mame.202400356

Radwan, M. M., Chandra, S., Gul, S., & ElSohly, M. A. (2021). Cannabinoids, Phenolics, Terpenes and Alkaloids of Cannabis. *Molecules*, *26*(9). https://doi.org/10.3390/molecules26092774

Raja Kumar, J., E.Jayachandran, Umadevi, S., Ch.Mallikarjuna, & Jameel, S. G. (2011). *GELLAN GUM BASED pH INDUCED IN SITU GELS CONTAINING CICLOPRIOX OLAMINE FOR ORAL THRUSH AGAINST CANDIDA STRAINS*. https://doi.org/10.13140/2.1.1035.7768

Raknam, P., Balekar, N., Teanpaisan, R., & Amnuaikit, T. (2022). Thermoresponsive sol-gel containing probiotic's cell free supernatant for dental caries prophylaxis. *J Oral Microbiol*, *14*(1), 2012390. https://doi.org/10.1080/20002297.2021.2012390

Rana, P., & Murthy, R. (2013). Formulation and evaluation of mucoadhesive buccal films impregnated with carvedilol nanosuspension: a potential approach for delivery of drugs having high first-pass metabolism. *Drug delivery*, *20*(5), 224–235.

Ranmal, S. R., Walsh, J., & Tuleu, C. (2025). Poor-tasting pediatric medicines: Part 1. A scoping review of their impact on patient acceptability, medication adherence, and treatment outcomes. *Frontiers in Drug Delivery*, *5*, 1553286.

Rao, N. R., Shravani, B., & Reddy, M. S. (2013). Overview on buccal drug delivery systems. *Journal of Pharmaceutical Sciences and Research*, *5*(4), 80.

Ravi, P., Aditya, N., Patil, S., & Cherian, L. (2015). Nasal in-situ gels for delivery of rasagiline mesylate: improvement in bioavailability and brain localization. *Drug delivery*, *22*(7), 903–910.

Ravi, P. R., Aditya, N., Patil, S., & Cherian, L. (2015). Nasal in-situ gels for delivery of rasagiline mesylate: improvement in bioavailability and brain localization. *Drug Deliv*, *22*(7), 903–910. https://doi.org/10.3109/10717544.2013.860501

Ren, J., Jin, J., Wang, Y., Liu, Y., & Qi, H. (2025). Preparation and drug release behavior study of intelligent pH-Responsive sodium alginate/κ-carrageenan polysaccharide-based hydrogels. *Food Bioscience*, *64*, 105975.

Rençber, S., & Karavana, S. Y. (2020). Formulation and optimization of gellan gum-poloxamer based dexamethasone mucoadhesive in situ gel. *J. Res. Pharm*, *201*, 529–538.

Rhee, Y.-S., Shin, Y.-H., Park, C.-W., Chi, S.-C., & Park, E.-S. (2007). Effect of flavors on the viscosity and gelling point of aqueous poloxamer solution. *Archives of pharmacal research*, *29*, 1171–1178. https://doi.org/10.1007/BF02969310

Ribeiro, A., Loureiro, R., & Cabral-Marques, H. (2024). Enhancing Cannabinoid Bioavailability in Pain Management: The Role of Cyclodextrins. *Molecules*, *29*(22). https://doi.org/10.3390/molecules29225340

Ribeiro, A., Loureiro, R., & Cabral-Marques, H. (2024). Enhancing Cannabinoid Bioavailability in Pain Management: The Role of Cyclodextrins. *Molecules*, *29*(22), 5340.

Ridout, M. J., Garza, S., Brownsey, G. J., & Morris, V. J. (1996). Mixed iota-kappa carrageenan gels. *International Journal of Biological Macromolecules*, *18*(1), 5–8. https://doi.org/https://doi.org/10.1016/0141-8130(95)01037-8

Robson, P. (2001). Therapeutic aspects of cannabis and cannabinoids. *British Journal of Psychiatry*, *178*(2), 107–115. https://doi.org/10.1192/bjp.178.2.107

Rodríguez de Fonseca, F., Del Arco, I., Bermudez-Silva, F. J., Bilbao, A., Cippitelli, A., & Navarro, M. (2005). The endocannabinoid system: physiology and pharmacology. *Alcohol and Alcoholism*, *40*(1), 2–14.

Rogers, C. I., & Pacanowski, C. R. (2023). The relationship between cannabis and anorexia nervosa: a scoping review. *Journal of Eating Disorders*, *11*(1), 186. https://doi.org/10.1186/s40337-023-00887-9

Ruel-Gariépy, E., & Leroux, J.-C. (2004). In situ-forming hydrogels—review of temperature-sensitive systems. *European Journal of Pharmaceutics and Biopharmaceutics*, *58*(2), 409–426. https://doi.org/https://doi.org/10.1016/j.ejpb.2004.03.019

Rungpetchanan, T., Krathumkhet, N., Sirivat, A., & Paradee, N. (2023). Electrically controlled transdermal drug release of ionic and non-ionic drug from kappa-iota carrageenan cryogel. *Materials Chemistry and Physics*, *309*, 128391. https://doi.org/10.1016/j.matchemphys.2023.128391

Russo, E., Selmin, F., Baldassari, S., Gennari, C. G. M., Caviglioli, G., Cilurzo, F., Minghetti, P., & Parodi, B. (2016). A focus on mucoadhesive polymers and their application in buccal dosage forms. *Journal of Drug Delivery Science and Technology*, *32*, 113–125. https://doi.org/https://doi.org/10.1016/j.jddst.2015.06.016

Ružić Zečević, D., Folić, M., Tantoush, Z., Radovanović, M., Babić, G., & Janković, S. M. (2018). Investigational cannabinoids in seizure disorders, what have we learned thus far? *Expert Opinion on Investigational Drugs*, *27*(6), 535–541. https://doi.org/10.1080/13543784.2018.1482275

S M, S., Priya, S., & Maxwell, A. (2018). FORMULATION AND EVALUATION OF NOVEL IN SITU GEL OF LAFUTIDINE FOR GASTRO RETENTIVE DRUG DELIVERY. *Asian Journal of Pharmaceutical and Clinical Research*, *11*, 88. https://doi.org/10.22159/ajpcr.2018.v11i8.25582

Safi, K., Sobieraj, J., Błaszkiewicz, M., Żyła, J., Salata, B., & Dzierżanowski, T. (2024). Tetrahydrocannabinol and Cannabidiol for Pain Treatment—An Update on the Evidence. *Biomedicines*, *12*(2), 307.

Salunke, S. R., & Patil, S. B. (2016). Ion activated in situ gel of gellan gum containing salbutamol sulphate for nasal administration. *International Journal of Biological Macromolecules*, *87*, 41–47. https://doi.org/https://doi.org/10.1016/j.ijbiomac.2016.02.044

Samineni, R., Chimakurthy, J., & Konidala, S. (2022). Emerging Role of Biopharmaceutical Classification and Biopharmaceutical Drug Disposition System in Dosage form Development: A Systematic Review. *Turk J Pharm Sci*, *19*(6), 706–713. https://doi.org/10.4274/tjps.galenos.2021.73554

Sampson, P. B. (2021). Phytocannabinoid Pharmacology: Medicinal Properties of Cannabis sativa Constituents Aside from the "Big Two". *Journal of Natural Products*, *84*(1), 142–160. https://doi.org/10.1021/acs.jnatprod.0c00965

Santos Akkari, A. C., Ramos Campos, E. V., Keppler, A. F., Fraceto, L. F., de Paula, E., Tófoli, G. R., & de Araujo, D. R. (2016). Budesonide-hydroxypropyl-β-cyclodextrin inclusion complex in binary poloxamer 407/403 system for ulcerative colitis treatment: A physico-chemical study from micelles to

hydrogels. *Colloids and Surfaces B: Biointerfaces*, *138*, 138–147. https://doi.org/https://doi.org/10.1016/j.colsurfb.2015.11.048

Sapra, B., Jain, S., & Tiwary, A. K. (2008). Percutaneous permeation enhancement by terpenes: mechanistic view. *Aaps j*, *10*(1), 120–132. https://doi.org/10.1208/s12248-008-9012-0

Saringat, H., Alfadol, K., & Khan, G. M. (2005). The influence of different plasticizers on some physical and mechanical properties of hydroxypropyl methylcellulose free films. *Pakistan journal of pharmaceutical sciences*, *18*, 25–38.

Savjani, K. T., Gajjar, A. K., & Savjani, J. K. (2012). Drug solubility: importance and enhancement techniques. *ISRN Pharm*, *2012*, 195727. https://doi.org/10.5402/2012/195727

Schmidt, A. P. (2024). The role of cannabinoids in chronic pain management: clinical insights and challenges. *Brazilian Journal of Anesthesiology (English Edition)*, *74*(4), 844523. https://doi.org/https://doi.org/10.1016/j.bjane.2024.844523

Schrot, R. J., & Hubbard, J. R. (2016). Cannabinoids: Medical implications. *Annals of Medicine*, *48*(3), 128–141. https://doi.org/10.3109/07853890.2016.1145794

Scully, C. (2007). Cannabis; adverse effects from an oromucosal spray. *British dental journal*, *203*(6), E12–E12.

Seyfoddin, A., Shaw, J., & Al-Kassas, R. (2010). Solid lipid nanoparticles for ocular drug delivery. *Drug delivery*, *17*(7), 467–489. https://doi.org/10.3109/10717544.2010.483257

Seymour-Jackson, E., Laird, B. J. A., Sayers, J., Fallon, M., Solheim, T. S., & Skipworth, R. (2023). Cannabinoids in the treatment of cancer anorexia and cachexia: Where have we been, where are we going? *Asia-Pacific Journal of Oncology Nursing*, *10*, 100292. https://doi.org/https://doi.org/10.1016/j.apjon.2023.100292

Shahbazi, F., Grandi, V., Banerjee, A., & Trant, J. F. (2020). Cannabinoids and cannabinoid receptors: the story so far. *Iscience*, *23*(7), 101301.

Shakya, P., Madhav, N. V. S., Shakya, A. K., & Singh, K. (2011). Palatal mucosa as a route for systemic drug delivery: A review. *Journal of Controlled Release*, *151*(1), 2–9. https://doi.org/https://doi.org/10.1016/j.jconrel.2010.11.003

Shalata, W., Abu Saleh, O., Tourkey, L., Shalata, S., Neime, A. E., Abu Juma'a, A., Soklakova, A., Tourkey, L., Jama, A. A., & Yakobson, A. (2024). The Efficacy of Cannabis in Oncology Patient Care and Its Anti-Tumor Effects. *Cancers*, *16*(16), 2909.

Sharma, N., Kurmi, B. D., Singh, D., Mehan, S., Khanna, K., Karwasra, R., Kumar, S., Chaudhary, A., Jakhmola, V., Sharma, A., Singh, S. K., Dua, K., & Kakkar, D. (2024). Nanoparticles toxicity: an overview of its mechanism and plausible mitigation strategies. *Journal of Drug Targeting*, *32*(5), 457–469. https://doi.org/10.1080/1061186X.2024.2316785

Sharma, N., Sharma, S., & Kaushik, R. (2019). Formulation and evaluation of lornoxicam transdermal patches using various permeation enhancers. *International Journal of Drug Delivery Technology*, *9*(4), 597–607.

Sharon, N., Yarmolinsky, L., Khalfin, B., Fleisher-Berkovich, S., & Ben-Shabat, S. (2024). Cannabinoids' Role in Modulating Central and Peripheral Immunity in Neurodegenerative Diseases. *International Journal of Molecular Sciences*, *25*(12), 6402.

Shelke, O. (2016). Carbomer A comprehensive review. *2016*, 1–8.

Shipp, L., Liu, F., Kerai-Varsani, L., & Okwuosa, T. C. (2022). Buccal films: A review of therapeutic opportunities, formulations & relevant evaluation approaches. *Journal of Controlled Release*, *352*, 1071–1092. https://doi.org/https://doi.org/10.1016/j.jconrel.2022.10.058

Shivam U, U., Siddhi K, C., Devarshi U, G., Umeshkumar M, U., & Jayvadan K, P. (2020). Nanoparticles laden In situ gel for sustained drug release after topical ocular administration. *Journal of Drug Delivery Science and Technology*, *57*, 101736. https://doi.org/https://doi.org/10.1016/j.jddst.2020.101736

Shojaei, A. H., Khan, M., Lim, G., & Khosravan, R. (1999). Transbuccal permeation of a nucleoside analog, dideoxycytidine: effects of menthol as a permeation enhancer. *International Journal of Pharmaceutics*, *192*(2), 139–146. https://doi.org/https://doi.org/10.1016/S0378-5173(99)00301-4

Shrivastava, A. (2011). Methods for the determination of limit of detection and limit of quantitation of the analytical methods. *Chronicles of Young Scientists*, *2*, 21–25. https://doi.org/10.4103/2229-5186.79345

Siamidi, A., Tsintavi, E., Rekkas, D. M., & Vlachou, M. (2020). 3D-Printed Modified-Release Tablets: A Review of the Recent Advances. *Molecular Pharmacology*.

Sic, A., George, C., Gonzalez, D. F., Tseriotis, V.-S., & Knezevic, N. N. (2025). Cannabinoids in Chronic Pain: Clinical Outcomes, Adverse Effects and Legal Challenges. *Neurology International*, *17*(9), 141.

Siemiradzka, W., Dolińska, B., & Ryszka, F. (2020). Development and Study of Semi-Solid Preparations Containing the Model Substance Corticotropin (ACTH): Convenience Application in Neurodegenerative Diseases. *Molecules*, *25*(8). https://doi.org/10.3390/molecules25081824

Siepmann, J., & Peppas, N. A. (2001). Modeling of drug release from delivery systems based on hydroxypropyl methylcellulose (HPMC). *Advanced Drug Delivery Reviews*, *48*(2), 139–157. https://doi.org/https://doi.org/10.1016/S0169-409X(01)00112-0

Siepmann, J., & Siepmann, F. (2020). Sink conditions do not guarantee the absence of saturation effects. *Int J Pharm*, *577*, 119009. https://doi.org/10.1016/j.ijpharm.2019.119009

Silva, J., Cook, M., & Bruschi, M. (2020). Thermoresponsive systems composed of poloxamer 407 and HPMC or NaCMC: mechanical, rheological and sol-gel transition analysis. *Carbohydrate Polymers*, *240*, 116268. https://doi.org/10.1016/j.carbpol.2020.116268

Singh, V., Khullar, P., Dave, P. N., & Kaur, N. (2013). Micelles, mixed micelles, and applications of polyoxypropylene (PPO)-polyoxyethylene (PEO)-polyoxypropylene (PPO) triblock polymers. *International Journal of Industrial Chemistry*, *4*(1), 12. https://doi.org/10.1186/2228-5547-4-12

Sitovs, A., Logviss, K., Lauberte, L., & Mohylyuk, V. (2024). Oral delivery of cannabidiol: Revealing the formulation and absorption challenges. *Journal of Drug Delivery Science and Technology*, *92*, 105316. https://doi.org/https://doi.org/10.1016/j.jddst.2023.105316

Sjöholm, E., & Sandler, N. (2019). Additive manufacturing of personalized orodispersible warfarin films. *International Journal of Pharmaceutics*, *564*, 117–123. https://doi.org/https://doi.org/10.1016/j.ijpharm.2019.04.018

Sjöholm, E., & Sandler, N. (2019). Additive manufacturing of personalized orodispersible warfarin films. *Int J Pharm*, *564*, 117–123. https://doi.org/10.1016/j.ijpharm.2019.04.018

Smart, J. D. (2005). The basics and underlying mechanisms of mucoadhesion. *Advanced drug delivery reviews*, *57*(11), 1556–1568. https://doi.org/https://doi.org/10.1016/j.addr.2005.07.001

Smith, C. J., Vergara, D., Keegan, B., & Jikomes, N. (2022). The phytochemical diversity of commercial Cannabis in the United States. *PLoS One*, *17*(5), e0267498. https://doi.org/10.1371/journal.pone.0267498

Smith, L. A., Azariah, F., Lavender, V. T., Stoner, N. S., & Bettiol, S. (2015). Cannabinoids for nausea and vomiting in adults with cancer receiving chemotherapy. *Cochrane Database Syst Rev*, *2015*(11), Cd009464. https://doi.org/10.1002/14651858.CD009464.pub2

Sohi, H., Ahuja, A., Ahmad, F. J., & Khar, R. K. (2010). Critical evaluation of permeation enhancers for oral mucosal drug delivery. *Drug Dev Ind Pharm*, *36*(3), 254–282. https://doi.org/10.1080/03639040903117348

Soliman, K. A., Ullah, K., Shah, A., Jones, D. S., & Singh, T. R. R. (2019). Poloxamer-based in situ gelling thermoresponsive systems for ocular drug delivery applications. *Drug Discovery Today*, *24*(8), 1575–1586. https://doi.org/https://doi.org/10.1016/j.drudis.2019.05.036

Som, I., Bhatia, K., & Yasir, M. (2012). Status of surfactants as penetration enhancers in transdermal drug delivery. *J Pharm Bioallied Sci*, *4*(1), 2–9. https://doi.org/10.4103/0975-7406.92724

Söpper, U., Hoffmann, A., & Daniels, R. (2021). Mucoadhesion and Mucopenetration of Cannabidiol (CBD)-Loaded Mesoporous Carrier Systems for Buccal Drug Delivery. *Scientia Pharmaceutica*, *89*(3), 35.

Spindle, T. R., Bonn-Miller, M. O., & Vandrey, R. (2019). Changing landscape of cannabis: novel products, formulations, and methods of administration. *Current Opinion in Psychology*, *30*, 98–102. https://doi.org/https://doi.org/10.1016/j.copsyc.2019.04.002

Srakhao, W., Nakpheng, T., Mohd Amin, M. C. I., & Srichana, T. (2025). Therapeutic Potential of Cannabidiol Cyclodextrin Complex in Polymeric Micelle and Tetrahydrocurcumin Cyclodextrin Complex Loaded in Hydrogel to Treat Lymphedema. *International Journal of Molecular Sciences*, *26*(7), 3428.

Stasiłowicz-Krzemień, A., Nogalska, W., Maszewska, Z., Maleszka, M., Dobroń, M., Szary, A., Kępa, A., Żarowski, M., Hojan, K., Lukowicz, M., & Cielecka-Piontek, J. (2024). The Use of Compounds Derived from Cannabis sativa in the Treatment of Epilepsy, Painful Conditions, and Neuropsychiatric and Neurodegenerative Disorders. *International Journal of Molecular Sciences*, *25*(11), 5749.

Stella, B., Baratta, F., Della Pepa, C., Arpicco, S., Gastaldi, D., & Dosio, F. (2021). Cannabinoid Formulations and Delivery Systems: Current and Future Options to Treat Pain. *Drugs*, *81*(13), 1513–1557. https://doi.org/10.1007/s40265-021-01579-x

Stockings, E., Zagic, D., Campbell, G., Weier, M., Hall, W. D., Nielsen, S., Herkes, G. K., Farrell, M., & Degenhardt, L. (2018). Evidence for cannabis and cannabinoids for epilepsy: a systematic review of controlled and observational evidence. *Journal of Neurology, Neurosurgery & Psychiatry*, *89*(7), 741–753. https://doi.org/10.1136/jnnp-2017-317168

Sundararaj, S. C., Al-Sabbagh, M., Rabek, C. L., Dziubla, T. D., Thomas, M. V., & Puleo, D. A. (2016). Comparison of sequential drug release in vitro and in vivo. *J Biomed Mater Res B Appl Biomater*, *104*(7), 1302–1310. https://doi.org/10.1002/jbm.b.33472

Swain, G. P., Patel, S., Gandhi, J., & Shah, P. (2019). Development of Moxifloxacin Hydrochloride loaded in-situ gel for the treatment of periodontitis: In-vitro drug release study and antibacterial activity. *J Oral Biol Craniofac Res*, *9*(3), 190–200. https://doi.org/10.1016/j.jobcr.2019.04.001

Szekalska, M., Czajkowska-Kośnik, A., Maciejewski, B., Misztalewska-Turkowicz, I., Wilczewska, A. Z., Bernatoniene, J., & Winnicka, K. (2023). Mucoadhesive Alginate/Pectin Films Crosslinked by Calcium Carbonate as Carriers of a Model Antifungal Drug-Posaconazole. *Pharmaceutics*, *15*(10). https://doi.org/10.3390/pharmaceutics15102415

Tabboon, P., Pongjanyakul, T., Limpongsa, E., & Jaipakdee, N. (2022). Mucosal Delivery of Cannabidiol: Influence of Vehicles and Enhancers. *Pharmaceutics*, *14*(8), 1687.

Tabboon, P., Pongjanyakul, T., Limpongsa, E., & Jaipakdee, N. (2022). Mucosal Delivery of Cannabidiol: Influence of Vehicles and Enhancers. *Pharmaceutics*, *14*(8). https://doi.org/10.3390/pharmaceutics14081687

Tagami, T., Yoshimura, N., Goto, E., Noda, T., & Ozeki, T. (2019). Fabrication of muco-adhesive oral films by the 3D printing of hydroxypropyl methylcellulose-based catechin-loaded formulations. *Biological and Pharmaceutical Bulletin*, *42*(11), 1898–1905.

Taha, I. E., ElSohly, M. A., Radwan, M. M., Omari, S., Repka, M. A., & Ashour, E. A. (2024). Development and in vitro Evaluation of Cannabidiol Mucoadhesive Buccal Film Formulations Using Hot-Melt Extrusion Technology. *Medical Cannabis and Cannabinoids*, *7*(1), 171–182. https://doi.org/10.1159/000540353

Takeuchi, Y., Hayakawa, F., & Takeuchi, H. (2025). Formulation Design of Orally Disintegrating Film Using Two Cellulose Derivatives as a Blend Polymer. *Pharmaceutics*, *17*(1). https://doi.org/10.3390/pharmaceutics17010084

Tanasescu, R., & Constantinescu, C. S. (2013). Pharmacokinetic evaluation of nabiximols for the treatment of multiple sclerosis pain. *Expert Opinion on Drug Metabolism & Toxicology*, *9*(9), 1219–1228. https://doi.org/10.1517/17425255.2013.795542

Tavagnacco, L., Chiessi, E., Severini, L., Franco, S., Buratti, E., Capocefalo, A., Brasili, F., Mosca Conte, A., Missori, M., Angelini, R., Sennato, S., Mazzuca, C., & Zaccarelli, E. (2023). Molecular origin of the two-step mechanism of gellan aggregation. *Sci Adv*, *9*(10), eadg4392. https://doi.org/10.1126/sciadv.adg4392

Taylor, M. J., Tomlins, P., & Sahota, T. S. (2017). Thermoresponsive Gels. *Gels*, *3*(1), 4.

Tejada-Ortigoza, V., & Cuan-Urquizo, E. (2022). Towards the Development of 3D-Printed Food: A Rheological and Mechanical Approach. *Foods*, *11*(9). https://doi.org/10.3390/foods11091191

Tejada Jacob, G., Passamai, V. E., Katz, S., Castro, G. R., & Alvarez, V. (2022). Hydrogels for extrusion-based bioprinting: General considerations. *Bioprinting*, *27*, e00212. https://doi.org/https://doi.org/10.1016/j.bprint.2022.e00212

Than, Y. M., Suriyarak, S., & Titapiwatanakun, V. (2022). Rheological Investigation of Hydroxypropyl Cellulose–Based Filaments for Material Extrusion 3D Printing. *Polymers*, *14*(6), 1108.

Thapa, R., Pandey, P., Parat, M.-O., Gurung, S., & Parekh, H. S. (2024). Phase transforming in situ gels for sustained and controlled transmucosal drug delivery via the intravaginal route. *International Journal of Pharmaceutics*, *655*, 124054. https://doi.org/https://doi.org/10.1016/j.ijpharm.2024.124054

Thiele, E. A., Marsh, E. D., French, J. A., Mazurkiewicz-Beldzinska, M., Benbadis, S. R., Joshi, C., Lyons, P. D., Taylor, A., Roberts, C., & Sommerville, K. (2018). Cannabidiol in patients with seizures associated with Lennox-Gastaut syndrome (GWPCARE4): a randomised, double-blind, placebo-controlled phase 3 trial. *Lancet*, *391*(10125), 1085–1096. https://doi.org/10.1016/s0140-6736(18)30136-3

Thomas, B. F., & Pollard, G. T. (2016). Preparation and Distribution of Cannabis and Cannabis-Derived Dosage Formulations for Investigational and Therapeutic Use in the United States [Perspective]. *Frontiers in Pharmacology*, *7*(285). https://doi.org/10.3389/fphar.2016.00285

Thrimawithana, T. R., Young, S. A., Bunt, C. R., Green, C. R., & Alany, R. G. (2011). In-vitro and in-vivo evaluation of carrageenan/methylcellulose polymeric systems for transscleral delivery of macromolecules. *European Journal of Pharmaceutical Sciences*, *44*(3), 399–409. https://doi.org/https://doi.org/10.1016/j.ejps.2011.08.026

Tiago, F. J., Paiva, A., Matias, A. A., & Duarte, A. R. C. (2022). Extraction of Bioactive Compounds From Cannabis sativa L. Flowers and/or Leaves Using Deep Eutectic Solvents. *Front Nutr*, *9*, 892314. https://doi.org/10.3389/fnut.2022.892314

Tian, Y., Orlu, M., Woerdenbag, H. J., Scarpa, M., Kiefer, O., Kottke, D., Sjöholm, E., Öblom, H., Sandler, N., Hinrichs, W. L. J., Frijlink, H. W., Breitkreutz, J., & Visser, J. C. (2019). Oromucosal films: from patient centricity to production by printing techniques. *Expert Opinion on Drug Delivery*, *16*(9), 981–993. https://doi.org/10.1080/17425247.2019.1652595

Tijani, A. O., Thakur, D., Mishra, D., Frempong, D., Chukwunyere, U. I., & Puri, A. (2021). Delivering therapeutic cannabinoids via skin: Current state and future perspectives. *Journal of Controlled Release*, *334*, 427–451. https://doi.org/https://doi.org/10.1016/j.jconrel.2021.05.005

Trzaskowski, B., Latek, D., Yuan, S., Ghoshdastider, U., Debinski, A., & Filipek, S. (2012). Action of molecular switches in GPCRs--theoretical and experimental studies. *Current medicinal chemistry*, *19*(8), 1090–1109. https://doi.org/10.2174/092986712799320556

Tsang, C. C., & Giudice, M. G. (2016). Nabilone for the Management of Pain. *Pharmacotherapy: The Journal of Human Pharmacology and Drug Therapy*, *36*(3), 273–286. https://doi.org/https://doi.org/10.1002/phar.1709

Turcotte, C., Blanchet, M.-R., Laviolette, M., & Flamand, N. (2016). The CB(2) receptor and its role as a regulator of inflammation. *Cellular and molecular life sciences : CMLS*, *73*(23), 4449–4470. https://doi.org/10.1007/s00018-016-2300-4

Turcotte, D., Dorze, J.-A. L., Esfahani, F., Frost, E., Gomori, A., & Namaka, M. (2010). Examining the roles of cannabinoids in pain and other therapeutic indications: a review. *Expert Opinion on Pharmacotherapy*, *11*(1), 17–31. https://doi.org/10.1517/14656560903413534

Upadhye, S., Kulkarni, S., Majumdar, S., Avery, M., Gul, W., Elsohly, M., & Repka, M. (2010). Preparation and Characterization of Inclusion Complexes of a Hemisuccinate Ester Prodrug of Δ9-Tetrahydrocannabinol with Modified Beta-Cyclodextrins. *AAPS PharmSciTech*, *11*, 509–517. https://doi.org/10.1208/s12249-010-9401-4

Urits, I., Charipova, K., Gress, K., Li, N., Berger, A. A., Cornett, E. M., Kassem, H., Ngo, A. L., Kaye, A. D., & Viswanath, O. (2021). Adverse Effects of Recreational and Medical Cannabis. *Psychopharmacol Bull*, *51*(1), 94–109.

Valiveti, S., Agu, R. U., Hammell, D. C., Paudel, K. S., Caroline Earles, D., Wermeling, D. P., & Stinchcomb, A. L. (2007). Intranasal absorption of Δ9-tetrahydrocannabinol and WIN55,212-2 mesylate in rats. *European Journal of Pharmaceutics and Biopharmaceutics*, *65*(2), 247–252. https://doi.org/https://doi.org/10.1016/j.ejpb.2006.08.009

Vandrey, R., Herrmann, E. S., Mitchell, J. M., Bigelow, G. E., Flegel, R., LoDico, C., & Cone, E. J. (2017). Pharmacokinetic Profile of Oral Cannabis in Humans: Blood and Oral Fluid Disposition and Relation to Pharmacodynamic Outcomes. *Journal of Analytical Toxicology*, *41*(2), 83–99. https://doi.org/10.1093/jat/bkx012

Varadi, G., Zhu, Z., Crowley, H. D., Moulin, M., Dey, R., Lewis, E. D., & Evans, M. (2023). Examining the Systemic Bioavailability of Cannabidiol and Tetrahydrocannabinol from a Novel Transdermal Delivery System in Healthy Adults: A Single-Arm, Open-Label, Exploratory Study. *Adv Ther*, *40*(1), 282–293. https://doi.org/10.1007/s12325-022-02345-5

Varman, R. M., & Singh, S. (2012). Investigation of effects of terpene skin penetration enhancers on stability and biological activity of lysozyme. *AAPS PharmSciTech*, *13*(4), 1084–1090. https://doi.org/10.1208/s12249-012-9840-1

Vemuri, V. K., & Makriyannis, A. (2015). Medicinal chemistry of cannabinoids. *Clinical Pharmacology & Therapeutics*, *97*(6), 553–558. https://doi.org/https://doi.org/10.1002/cpt.115

Verma, A., Dixit, R., Singh, U., Soni, S., Mishra, A., Bansal, A., & Pandit, J. (2011). Preparation and Characterization of Gellan-Chitosan Polyelectrolyte Complex Beads. *LATIN AMERICAN JOURNAL OF PHARMACY*, *30*, 1186–1195.

Vigani, B., Faccendini, A., Rossi, S., Sandri, G., Bonferoni, M. C., Gentile, M., & Ferrari, F. (2019). Development of a Mucoadhesive and In Situ Gelling Formulation Based on κ-Carrageenan for Application on Oral Mucosa and Esophagus Walls. I. A Functional In Vitro Characterization. *Mar Drugs*, *17*(2). https://doi.org/10.3390/md17020112

Vigani, B., Rossi, S., Gentile, M., Sandri, G., Bonferoni, M. C., Cavalloro, V., Martino, E., Collina, S., & Ferrari, F. (2019). Development of a mucoadhesive and an in situ gelling formulation based on κ-carrageenan for application on oral mucosa and esophagus walls. II. Loading of a bioactive hydroalcoholic extract. *Marine drugs*, *17*(3), 153.

Vigani, B., Rossi, S., Gentile, M., Sandri, G., Bonferoni, M. C., Cavalloro, V., Martino, E., Collina, S., & Ferrari, F. (2019). Development of a Mucoadhesive and an in Situ Gelling Formulation Based on κ-Carrageenan for Application on Oral Mucosa and Esophagus Walls. II. Loading of a Bioactive Hydroalcoholic Extract. *Mar Drugs*, *17*(3). https://doi.org/10.3390/md17030153

Vigani, B., Rossi, S., Sandri, G., Bonferoni, M. C., Caramella, C. M., & Ferrari, F. (2020). Recent Advances in the Development of In Situ Gelling Drug Delivery Systems for Non-Parenteral Administration Routes. *Pharmaceutics*, *12*(9), 859.

Vigani, B., Rossi, S., Sandri, G., Bonferoni, M. C., Caramella, C. M., & Ferrari, F. (2020). Recent Advances in the Development of In Situ Gelling Drug Delivery Systems for Non-Parenteral Administration Routes. *Pharmaceutics*, *12*(9). https://doi.org/10.3390/pharmaceutics12090859

Vlachou, M., Tragou, K., Siamidi, A., Kikionis, S., Chatzianagnostou, A.-L., Mitsopoulos, A., Ioannou, E., Roussis, V., & Tsotinis, A. (2018). Modified in vitro release of the chronobiotic hormone melatonin from matrix tablets based on the marine sulfated polysaccharide ulvan. *Journal of Drug Delivery Science and Technology*, *44*, 41–48.

Vlad, R.-A., Pintea, A., Pintea, C., Rédai, E.-M., Antonoaea, P., Bîrsan, M., & Ciurba, A. (2025). Hydroxypropyl Methylcellulose—A Key Excipient in Pharmaceutical Drug Delivery Systems. *Pharmaceutics*, *17*(6), 784.

Vlaia, L., Olariu, I., Georgeta, C., Vlaia, V., Popoiu, C., Corina, S., Muţ, A. M., Szabadai, Z., & Lupuleasa, D. (2014). Percutaneous penetration enhancement of propranolol hydrochloride from HPMC-Based hydroethanolic gels containing terpenes. *Farmacia*, *62*, 992–1008.

Voicu, V., Brehar, F.-M., Toader, C., Covache-Busuioc, R.-A., Corlatescu, A. D., Bordeianu, A., Costin, H. P., Bratu, B.-G., Glavan, L.-A., & Ciurea, A. V. (2023). Cannabinoids in Medicine: A Multifaceted Exploration of Types, Therapeutic Applications, and Emerging Opportunities in Neurodegenerative Diseases and Cancer Therapy. *Biomolecules*, *13*(9), 1388.

Vučković, S., Srebro, D., Vujović, K. S., Vučetić, Č., & Prostran, M. (2018). Cannabinoids and Pain: New Insights From Old Molecules [Review]. *Frontiers in Pharmacology*, *9*. https://doi.org/10.3389/fphar.2018.01259

Walsh, D., Kirkova, J., & Davis, M. P. (2005). The Efficacy and Tolerability of Long-Term Use of Dronabinol in Cancer-Related Anorexia: A Case Series. *Journal of Pain and Symptom Management*, *30*(6), 493–495. https://doi.org/10.1016/j.jpainsymman.2005.11.007

Walsh, Z., Gonzalez, R., Crosby, K., S. Thiessen, M., Carroll, C., & Bonn-Miller, M. O. (2017). Medical cannabis and mental health: A guided systematic review. *Clinical Psychology Review*, *51*, 15–29. https://doi.org/https://doi.org/10.1016/j.cpr.2016.10.002

Wang, C., Erridge, S., & Sodergren, M. H. (2024). Medical cannabis and fibromyalgia: a narrative review of current evidence. *British Journal of Neuroscience Nursing*, *20*(3), 108–113. https://doi.org/10.12968/bjnn.2024.0028

Wang, S., Chen, X., Han, X., Hong, X., Li, X., Zhang, H., Li, M., Wang, Z., & Zheng, A. (2023). A Review of 3D Printing Technology in Pharmaceutics: Technology and Applications, Now and Future. *Pharmaceutics*, *15*(2). https://doi.org/10.3390/pharmaceutics15020416

Wang, S., Gao, Z., Liu, L., Li, M., Zuo, A., & Guo, J. (2022). Preparation, in vitro and in vivo evaluation of chitosan-sodium alginate-ethyl cellulose polyelectrolyte film as a novel buccal mucosal delivery

vehicle. *European Journal of Pharmaceutical Sciences*, *168*, 106085. https://doi.org/https://doi.org/10.1016/j.ejps.2021.106085

Wang, S., Zuo, A., & Guo, J. (2021). Types and evaluation of in vitro penetration models for buccal mucosal delivery. *Journal of Drug Delivery Science and Technology*, *61*, 102122.

Wardill, H. R., Wooley, L. T., Bellas, O. M., Cao, K., Cross, C. B., van Dyk, M., Kichenadasse, G., Bowen, J. M., Zannettino, A. C. W., Shakib, S., Crawford, G. B., Boublik, J., Davis, M. M., Smid, S. D., & Price, T. J. (2024). Supporting gut health with medicinal cannabis in people with advanced cancer: potential benefits and challenges. *British Journal of Cancer*, *130*(1), 19–30. https://doi.org/10.1038/s41416-023-02466-w

Webber, V., Carvalho, S., Ogliari, P., Hayashi, L., & Luiz Manique Barreto, P. (2012). Optimization of the extraction of carrageenan from Kappaphycus alvarezii using response surface methodology. *Food Science and Technology (Campinas)*, *32*, 812–818. https://doi.org/10.1590/S0101-20612012005000111

Wechsler, R. T., Burdette, D. E., Gidal, B. E., Hyslop, A., McGoldrick, P. E., Thiele, E. A., & Valeriano, J. (2024). Consensus panel recommendations for the optimization of EPIDIOLEX® treatment for seizures associated with Lennox-Gastaut syndrome, Dravet syndrome, and tuberous sclerosis complex. *Epilepsia Open*, *9*(5), 1632–1642. https://doi.org/10.1002/epi4.12956

Williams, N. N. B., Ewell, T. R., Abbotts, K. S. S., Harms, K. J., Woelfel, K. A., Dooley, G. P., Weir, T. L., & Bell, C. (2021). Comparison of Five Oral Cannabidiol Preparations in Adult Humans: Pharmacokinetics, Body Composition, and Heart Rate Variability. *Pharmaceuticals*, *14*(1), 35.

Winarti, L., Laksono, B. T., & Sari, L. O. R. K. (2021). Optimization of hydroxy propyl methyl cellulose and carbomer in diltiazem hydrochloride mucoadhesive buccal film. *Indonesian Journal of Pharmacy*, 43–51.

Wojtyłko, M., Froelich, A., & Jadach, B. (2024). Hypromellose-, Gelatin- and Gellan Gum-Based Gel Films with Chlorhexidine for Potential Application in Oral Inflammatory Diseases. *Gels*, *10*(4), 265.

Wu, C., Qi, H., Chen, W., Huang, C., Su, C., Li, W., & Hou, S. (2007). Preparation and evaluation of a Carbopol/HPMC-based in situ gelling ophthalmic system for puerarin. *Yakugaku Zasshi*, *127*(1), 183–191. https://doi.org/10.1248/yakushi.127.183

Wu, Y., Liu, Y., Li, X., Kebebe, D., Zhang, B., Ren, J., Lu, J., Li, J., Du, S., & Liu, Z. (2019). Research progress of in-situ gelling ophthalmic drug delivery system. *Asian Journal of Pharmaceutical Sciences*, *14*(1), 1–15. https://doi.org/https://doi.org/10.1016/j.ajps.2018.04.008

Xia, H., Jin, H., Cheng, Y., Cheng, Z., & Xu, Y. (2019). The Controlled Release and Anti-Inflammatory Activity of a Tetramethylpyrazine-Loaded Thermosensitive Poloxamer Hydrogel. *Pharmaceutical Research*, *36*(4), 52. https://doi.org/10.1007/s11095-019-2580-0

Xu, H., Shi, M., liu, Y., Jiang, J., & Ma, T. (2014). A Novel <italic>In Situ</italic> Gel Formulation of Ranitidine for Oral Sustained Delivery. *Biomolecules & Therapeutics*, *22*(2), 161–165. https://doi.org/10.4062/biomolther.2013.109

Yadav, S. P. S., Kafle, M., Ghimire, N. P., Shah, N. K., Dahal, P., & Pokhrel, S. (2023). An overview of phytochemical constituents and pharmacological implications of Cannabis sativa L. *Journal of Herbal Medicine*, *42*, 100798. https://doi.org/https://doi.org/10.1016/j.hermed.2023.100798

Yang, Z., Mao, X., Cui, J., Wang, Y., & Zhang, Y. (2021). Enhancement and analysis of Anthracene degradation by Tween 80 in LMS-HOBt. *Scientific Reports*, *11*(1), 13121. https://doi.org/10.1038/s41598-021-90609-5

Yasser, M., Teaima, M., El-Nabarawi, M., & El-Monem, R. (2019). Cubosomal based Oral Tablet for controlled Drug Delivery of Telmisartan: Formulation, in-vitro Evaluation and in-vivo Comparative

Pharmacokinetic Study in Rabbits. *Drug development and industrial pharmacy*, *45*, 1–45. https://doi.org/10.1080/03639045.2019.1590392

Yildiz Pekoz, A., Erdal, M., Okyar, A., Ocak, M., Tekeli, F., Kaptan, E., Sagirli, O., & Araman, A. (2015). Preparation and in-vivo evaluation of dimenhydrinate buccal mucoadhesive films with enhanced bioavailability. *Drug development and industrial pharmacy*, *42*, 1–10. https://doi.org/10.3109/03639045.2015.1091470

Zahir-Jouzdani, F., Wolf, J. D., Atyabi, F., & Bernkop-Schnürch, A. (2018). In situ gelling and mucoadhesive polymers: why do they need each other? *Expert Opin Drug Deliv*, *15*(10), 1007–1019. https://doi.org/10.1080/17425247.2018.1517741

Zahir-Jouzdani, F., Wolf, J. D., Atyabi, F., & Bernkop-Schnürch, A. (2018). In situ gelling and mucoadhesive polymers: why do they need each other? *Expert Opinion on Drug Delivery*, *15*(10), 1007–1019.

Zarrintaj, P., Ramsey, J. D., Samadi, A., Atoufi, Z., Yazdi, M. K., Ganjali, M. R., Amirabad, L. M., Zangene, E., Farokhi, M., Formela, K., Saeb, M. R., Mozafari, M., & Thomas, S. (2020). Poloxamer: A versatile tri-block copolymer for biomedical applications. *Acta Biomaterialia*, *110*, 37–67. https://doi.org/https://doi.org/10.1016/j.actbio.2020.04.028

Zema, L., Maroni, A., Foppoli, A., Palugan, L., Sangalli, M. E., & Gazzaniga, A. (2007). Different HPMC viscosity grades as coating agents for an oral time and/or site-controlled delivery system: an investigation into the mechanisms governing drug release. *J Pharm Sci*, *96*(6), 1527–1536. https://doi.org/10.1002/jps.20802

Zeng, N., Dumortier, G., Maury, M., Mignet, N., & Boudy, V. (2014). Influence of additives on a thermosensitive hydrogel for buccal delivery of salbutamol: relation between micellization, gelation, mechanic and release properties. *Int J Pharm*, *467*(1-2), 70–83. https://doi.org/10.1016/j.ijpharm.2014.03.055

Zhang, H., Zhang, J., & Streisand, J. B. (2002). Oral mucosal drug delivery: clinical pharmacokinetics and therapeutic applications. *Clin Pharmacokinet*, *41*(9), 661–680. https://doi.org/10.2165/00003088-200241090-00003

Zhou, J., Jia, J., He, J., Li, J., & Cai, J. (2022). Cyclodextrin Inclusion Complexes and Their Application in Food Safety Analysis: Recent Developments and Future Prospects. *Foods*, *11*(23), 3871.

Zhu, X., Li, H., Huang, L., Zhang, M., Fan, W., & Cui, L. (2020). 3D printing promotes the development of drugs. *Biomedicine & Pharmacotherapy*, *131*, 110644. https://doi.org/https://doi.org/10.1016/j.biopha.2020.110644

Zia, K. M., Tabasum, S., Khan, M. F., Akram, N., Akhter, N., Noreen, A., & Zuber, M. (2018). Recent trends on gellan gum blends with natural and synthetic polymers: A review. *International Journal of Biological Macromolecules*, *109*, 1068–1087. https://doi.org/https://doi.org/10.1016/j.ijbiomac.2017.11.099

Zuardi, A. W. (2006). History of cannabis as a medicine: a review. *Brazilian Journal of Psychiatry*, *28*, 153–157.